The Regulation and Consequences of Type-2 Helper T Cells During Pulmonary Cryptococcal Infection

A DOCTORAL THESIS
SUBMITTED TO THE FACULTY OF
UNIVERSITY OF MINNESOTA
BY

Darin Lawrence Wiesner

IN PARTIAL FULFILLMENT OF THE REQUIREMENTS
FOR THE DEGREE OF
DOCTOR OF PHILOSOPHY

Kirsten Nielsen (Primary Advisor), Paul Bohjanen (Co-adviser)

September 2015

Acknowledgements

First and foremost, I would like to thank my primary mentor, Dr. Kirsten Nielsen. Her continuous generosity and curiosity fostered my intellectual growth. Science could not have been more fun under her guidance. Next, I would like to offer gratitude to my co-advisor, Dr. Paul Bohjanen. I owe my passion for science to his enduring support and direction. I am greatly appreciative to Dr. Marc Jenkins for allowing me to be a part of a *bona fide* immunology lab. Wednesday lab meetings were often the highlight of my week. I would like to give special acknowledgment to my thesis committee chair, Dr. Peter Southern. The hallway/stairwell discussions we had will always be fond memories. I am grateful for Dr. David Masopust for serving on my preliminary examination and thesis committees, as well as being an exemplary scientist. I would like to acknowledge the help and camaraderie of my lab mate, Kyle Smith. Arguing sports was, at times, a welcome distraction. I would like to thank the MICAB program personnel, including Louise Shand, Dr. Christopher Pennell, and Dr. Stephen Jameson for flawlessly managing the program. I am grateful for the fellowship funding I received during my traning from the following sources: NIH T32 training grant AI007313, University of Minnesota Doctoral Dissertation Fellowship, and Dennis W. Watson Fellowship. Finally, I deeply appreciate my fellow graduate students. They are not only esteemed colleagues, but they are also unforgettable friends.

Dedication

This thesis is dedicated to my mother, father, and brother for making the sacrifices that have allowed me to chase my dreams.

Abstract

Pathogens are microbes that infect hosts and cause disease. There are many forms of pathogens, including: bacteria, viruses, parasites, and fungi. In particular, fungi are found throughout the environment, and as a result, humans are continuously exposed to these organisms. While in many cases our immune system provides protection against lethal disease, individuals with immune deficiencies are dramatically more susceptible to fungal disease. Conversely, fungal exposure causes over half of the pulmonary allergies and asthma experienced by otherwise healthy humans with normal immune function.

The immune system is comprised of innate and adaptive components. The innate arm provides rapid and generalized protection to pathogen invasion, whereas the adaptive arm acquires specialized functions to combat specific microbes. T cells of the adaptive immune system express receptors that recognize molecules (i.e. antigens) uniquely produced by the pathogen. This allows T cells to mount highly potent responses against invading microbes while avoiding responses directed towards the host. T cells are particularly important in response to fungal infection. A selective elimination of T cells due to HIV infection results in more frequent and severe fungal disease. However, the allergy and asthma symptoms associated with fungal exposure in healthy individuals are also a direct result of inappropriate T cell responses.

T cells come in many flavors and each T cell subset coordinates unique components of the immune response. Type-1 Helper (Th1) and Type-17 Helper (Th17) T cells generally contribute to protective anti-fungal immunity, whereas Type-2 Helper T (Th2) cells produced in response to many fungal infections positively correlate with disease severity and allergy symptoms. Another lineage of T cells, regulatory T (Treg) cells can inhibit the function of the helper T cells upon resolution of the infection. Mechanisms describing Th2 and Treg cell responses underlying fungal disease are ill defined. Thus, my thesis research aims to understand the induction, suppression, and downstream consequences of Th2 cells using a mouse model of pulmonary infection with the fungus, *Cryptococcus neoformans*.

Table of Contents

List of Tables

List of Figures

FOREWORD

The work presented herein is a compilation of published, to be published, and unpublished works. Moreover, these chapters contain data collected as a collaborative effort of many individuals. Thus, it is necessary to explain the publication status of each chapter, as well as indicate my contribution to these sections.

Chapter 1 – Wiesner DL, Moskalenko O, Corcoran JM, McDonald T, Rolfes MA, Meya DB, Kajambula H, Kambugu A, Bohjanen PR, Knight JF, Boulware DR, Nielsen K. "Cryptococcal Genotype Influences Immunologic Response and Human Clinical Outcome after Meningitis." *mBio*. 2012;3(5).

> I shared first author of this publication. I performed ex vivo antigen stimulations of human whole blood and measured cytokine responses. I analyzed a portion of the data and wrote the manuscript.

Chapter 2 – Wiesner DL, Specht CA, Lee CK, Smith KD, Mukaremera L, Lee ST, Lee CG, Elias JA, Nielsen JN, Boulware DR, Bohjanen PR, Jenkins MK, Levitz SM, Nielsen K. "Chitin Promotes Type-2 Helper T Cell Responses During Pulmonary Cryptococcal Infection." *PLoS Pathogens*. 2015; 11(3):e1004701.

> As leading author of this publication, I designed and performed nearly all experiments, analyzed all data, and wrote the manuscript.

Chapter 3 – Wiesner DL, Smith KD, Kotov DI, Nielsen JN, Bohjanen PR, Nielsen K. "Regulatory T Cell Induction and Retention in the Lungs Drives Suppression of Detrimental Type-2 Helper T Cells During Pulmonary Cryptococcal Infection." Under Review at *The Journal of Immunology*.

I designed and performed nearly all experiments, analyzed all data, and wrote the entire manuscript.

Chapter 4 – Wiesner DL, Bohjanen PR, Jenkins MK, Nielsen K. "Lymphocyte Competition Determines Granulocyte Response to Pulmonary Fungal Infection." In Submission to *Mucosal Immunology*.

I designed and performed nearly all experiments, analyzed all data, and wrote the manuscript.

INTRODUCTION

Cryptococcus – a significant human pathogen

Cryptococcosis is a mycotic disease caused by the basidiomycete, *Cryptococcus*. The saprophytic fungus thrives in the environment by feeding on decaying organic matter. *Cryptococcus* can be isolated from animal excreta and superficial surfaces of trees and soil (1-3). When these surfaces are disturbed, aerosolized cryptococcal yeasts or spores are inhaled into the lower respiratory tract of terrestrial vertebrates where they can cause symptomatic disease.

Two established cryptococcal species typically cause disease: *C. neoformans* and *C. gattii,* although recent nomenclature recommendations further sub-divide these into 7 species (4). Exposure to *C. neoformans* is quite common in humans, as most individuals produce cryptococcal antibodies by school age (5), indicating a history of cryptococcal infection and further supporting the ubiquity of *C. neoformans* in the environment. Disease onset after *C. neoformans* exposure is mainly determined by the competence of the adaptive host immune response, while the spectrum of disease severity can be additionally ascribed to strain-dependent cryptococcal virulence (6, 7). Consequently, due to the high incidence of HIV infections, cryptococcosis is the leading cause of death in persons living with AIDS in Sub-Saharan Africa (8). In contrast to *C. neoformans*, *C. gattii* causes disease in otherwise healthy individuals (9). *C. gattii* was previously thought to be sequestered in tropical or sub-tropical regions of the world but an outbreak and subsequent spread in North America has prompted additional analysis of the prevalence of this species throughout the Americas, Europe, and Asia (10). The mechanism by which *C. gattii* causes disease in apparently healthy individuals is still under investigation, but disease threshold may be driven, in part, by rare exposure to this highly virulent fungus. With both species, if the pulmonary immune response does not sufficiently limit fungal replication, *Cryptococcus* eventually escapes into the peripheral circulation, accumulates in the brain, and results in semi-occult pneumonia and clinically apparent meningoencephalitis.

Evolution of cryptococcal virulence

C. neoformans is remarkably well suited to survive in a human host. Despite the moniker, "opportunistic pathogen," an immaculate conception of random traits does not faithfully explain cryptococcal acrimony in the context of human disease. Rather, its virulence is more likely a culmination of traits that evolved in a multilayered process in both environmental and animal niches (**Figure 1**).

The first layer of evidence for evolved virulence is the capacity of *C. neoformans* to subsist in the environment while also avoiding uptake and killing by organisms (i.e. amoeba, nematodes, and insect larvae) with ancestral components of our innate immune system (11-13). A unique characteristic among medically important fungi is the thick polysaccharide capsule that surrounds *C. neoformans*. The capsule protects against environmental dehydration (14), as well as allowing *C. neoformans* to resist oxidative damage of primordial lysosomal conditions (15). Furthermore, melanin produced by *C. neoformans* absorbs damaging radiation (16) and inhibits the effect of reactive oxygen species produced in the lysosome (17). Natural selection driven by primitive features of human physiology has likely played a significant role of the evolution of cryptococcal virulence.

Several enzymes and secreted factors produced by *C. neoformans* also alter the adaptive immune response, modulate the lung epithelium, and compromise the blood-brain barrier (18-21). These actions are required for the establishment of pulmonary infection, systemic dissemination, and accumulation in the central nervous system (CNS). Only higher vertebrates have analogous anatomy or adaptive immune systems, and consequently, *C. neoformans* probably evolved these properties under the selective pressures of reptilian/avian/mammalian hosts within the environment. Further evidence supporting non-human mammals as a natural host and reservoir for virulence trait selection and maintenance comes from the identification of various animals - from aquatic mammals to companion animals - as emergent species affected by the *C. gattii* outbreak (22-24).

T cell-mediated immunity is effective at preventing invasive cryptococcal disease. Yet, *C. neoformans* circumvent effector mechanisms of adaptive immunity. As a result, the fungus is not always completely cleared from healthy human hosts following exposure, resulting in latent infections (25, 26). Perhaps the ability to remain latent without perturbing its host is the strongest evidence for host adaptation by *C. neoformans*. Taken together, these observations suggest that interactions with both soil microorganisms and vertebrates within the environment likely play a critical role in the virulence potential of *C. neoformans* (**Figure 1**).

Cryptococcal morphology: spores, yeasts, and titan cells

C. neoformans has a diverse repertoire of morphologies that impact its ability to establish pulmonary infection. Cryptococcal yeasts and spores are capable of generating robust pulmonary infections in animal models of experimental cryptococcosis (27, 28). Recent studies in mouse models of cryptococcosis revealed that spores and yeast cells interact with the host immune system differently and these differences can promote development of disease. Giles et al. showed spores were phagocytized more efficiently than yeast cells, and these infections readily disseminate to the brain (27, 29). Although both forms commonly exist in the environment, the infectious propagule of *C. neoformans* that humans naturally encounter is not empirically testable and consequently, remains speculative.

Whether derived from spores or yeast cells, upon inhalation into a mammalian host, all *C. neoformans* transition to or maintain a yeast form. Recent studies have highlighted the unique diversity of cryptococcal yeast cells within the host. When grown under laboratory conditions, *C. neoformans* is a round, budding yeast 5-7 microns in diameter. Yet in the host, the cells show dramatic variation in their cell size, structure, and characteristics (30, 31). The best studied atypical morphology occurs in the form of cryptococcal titan cells (32). Titan cells are greater than 12 microns in diameter (excluding capsule), are polyploid instead of haploid, have highly crosslinked capsules and a thickened cell wall (33, 34). Titan cell formation is regulated by pheromone-sensing and G-protein-coupled receptor signaling (35), which is functionally analogous to

virulence conferred by quorum sensing in pathogenic bacteria (36). The transcription factor, Rim101, controls titan cell production along with many other cryptococcal virulence factors, suggesting titan cell formation intersects with a generalized virulence program of *C. neoformans* (35, 37, 38). Finally, infection with *C. neoformans* mutants that are incapable of generating titan cells, yet retain an otherwise normal virulence phenotype, results in extended survival of mice (39). Therefore, the collective traits associated with titan cell formation enhance cryptococcal virulence. How each of the aforementioned titan cell characteristics influence *C. neoformans* pathogenesis remains under active investigation (39).

Pulmonary immune response to cryptococcal infection

The lung is a primary interface with the external environment and is under constant assault from infectious microbes. As a result, innate and adaptive immune cells must efficiently coordinate protection against invading pathogens in the lungs (**Figure 2, Top**). Airway resident phagocytes, known as alveolar macrophages, are among the first to respond to pulmonary cryptococcal infection (40). In addition, monocytes and neutrophils are quickly recruited after infection to the lung mucosa (41, 42). Pathogen associated molecular patterns (PAMPs) unique to fungi are found on the fungal cell surface. These PAMPs are recognized by receptors on innate immune cells, leading to a cascade of innate immune cell activation (43). Despite pattern recognition of fungal cell wall carbohydrates, innate immunity may not be sufficient to eliminate *C. neoformans* from the lungs.

A profound capacity to resist phagocytic killing lies at the core of cryptococcal virulence. Several well-studied cryptococcal traits allow the fungus to avoid phagocytosis, as well evade destruction within phagocytes. Specifically, the polysaccharide capsule blocks complement from opsonizing cryptococcal cells (44) and inhibits maturation of dendritic cells and macrophages (45). Anti-phagocytic protein-1 produced by *C. neoformans* antagonizes complement receptors on pulmonary phagocytes, which prevents *C. neoformans* uptake (46). Melanin and capsule also act as redox sinks to prevent oxidative damage within the phagolysosome, thereby promoting

the survival of internalized cryptococcal cells (15, 17). *C. neoformans* employs potent phagocyte evasion strategies and the immune system must rely on additional methods to eliminate cryptococcal infection

The selective depletion of T cells due to HIV/AIDS dramatically enhances susceptibility to invasive cryptococcosis (8). This experiment of nature indicates that the immune system requires additional help from Th cells to prevent cryptococcal disease. Before Th cells can enact their functions, naïve Th cells must undergo priming. Th cells are incapable of coordinating their own activation and differentiation. This task is performed by professional antigen presenting cells (APC). Microbial peptides are bound by major histocompatibility II (MHCII) molecules and presented on the surface of the APC. Rare naïve Th cells survey APC, usually within lymphoid tissues, searching for a peptide-MHCII complex with high avidity for peptide-specific T cell receptors on the Th cell surface. Upon finding the cognate peptide-MHCII, the Th cell undergoes rapid proliferation. The APC also provides secondary cues that further promote Th cell activation and instruct the Th cell to acquire a stable effector function (e.g. Th1/2/17).

"The Th1/Th2 Paradigm" has been a useful framework for understanding cell-mediated immunity, where Th1 cell responses provide protection against intracellular microbes and Th2 cell responses confer resistance to protozoan and helminth parasites (47). However, the discovery of additional Th cell subsets has forced the revision of this idea (e.g. Th9, Th17 and regulatory T cells) (48-52). These Th cell subsets may play an important but hitherto incompletely understood role in immunity to *C. neoformans* (53, 54).

Despite the lack of more contemporary knowledge of Th cell subsets pertaining to cryptococcal pathogenesis, current evidence suggests Th1 responses are protective and Th2 responses are pathologic. The Th1 cytokine, interferon gamma (IFN-γ), positively correlates with patient survival and fungal clearance from the cerebrospinal fluid when used as adjunct therapy in cryptococcal meningitis patients (55, 56). Conversely, excess Th2 cell cytokines, IL-4, and IL-13, as well as a lack of IFN-γ in the peripheral blood and CSF are associated with poor clinical outcome in a separate cohort of patients (57, 58). In mouse models of cryptococcosis, Th2 cell polarized responses promote disseminated

disease (59-62), whereas infection with a modified strain of *C. neoformans* that produces recombinant IFN-γ results in sterilizing primary immunity and protection from fully virulent rechallenge. However, the capacity of *C. neoformans* to modulate the host response during human infection is still unknown. Furthermore, the molecular and cellular mechanisms underlying Th2 cell differentiation are poorly understood.

Activated, fully differentiated Th cells instruct several fundamental processes during the immune response to pulmonary fungal infection. First, Th cells form an immunological synapse with macrophages and exchange signals via co-receptors and cytokines. In the case of Th1 cells, IFN-γ instigates a series of changes in macrophages, including: phagolysosome fusion, nitric oxide synthase expression, and reactive oxygen species production (63). This "classical" activation allows the macrophage to eliminate the intracellular cryptococcal cells (**Figure 2, Top**). Th2 cells similarly interact with macrophages, yet the production of IL-5 and IL-13 causes "alternative" activation of macrophages and the failure to control intracellular cryptococcal replication (63) (**Figure 2, Top**).

Th cells, along with other lymphocytes, produce cytokines with wide ranging effects. More specifically, IL-5 produced by Th2 cells and IL-17A produced by Th17 cells lead to the differentiation and recruitment of eosinophil and neutrophil granulocytes, respectively (**Figure 2, Top**). There is conflicting evidence showing eosinophils and neutrophils are beneficial, detrimental, and dispensable to cryptococcal immunity (64-68). Perhaps, the discrepancy in the role of granulocytes in response to cryptococcal infection arises from a recent but still poorly understood observation of eosinophil/neutrophil compensation, where the loss of eosinophils often promotes neutrophil accumulation and *vice versa* (69, 70). In addition to the Th cell subsets, several other lymphocytes produce Th cell cytokines, such as: innate lymphoid cells (ILC), CD8 T (Tc17) cells, and γδ T cells. Thus, the study of granulocytes is further complicated by the existence of an array of lymphocytes with the capacity to coordinate granulocyte responses during cryptococcal infection.

Exit from the lung and dissemination to the central nervous system

C. neoformans encapsulation, melanin production, and titan cell formation discussed above have clear indications for promoting the establishment of infection. However, an important characteristic of cryptococcosis involves the exit of *C. neoformans* from the lungs into peripheral blood circulation and entry into the CNS compartment.

C. neoformans produces several enzymes that modulate the respiratory epithelium and promote escape into the periphery. Mannoproteins have been implicated in the attachment of cryptococcal cells to the unidentified receptors on pulmonary epithelial cells (71). This affords an opportunity for *C. neoformans* to exert highly localized manipulations of epithelial cells. Phospholipase B hydrolyzes phospholipids in epithelial membranes and airway surfactants (72, 73), which compromises the integrity of the physical barrier defenses in the lung. Finally, urease catalyzes the conversion of urea into ammonia, and increased ammonia concentration in the lung could cause epithelial cell cytotoxicity, as is the case in other instances of pathogen-derived urease activity (74). *C. neoformans* has well adapted traits that allow it to penetrate the mucosal barrier of the lungs.

Most fungi that resist immune control at the mucosae readily disseminate to distal regions of the body, yet very few fungi accumulate in the brain (75). Due to the potentially devastating consequences of collateral damage to nervous tissue during a robust immune response in the brain, the CNS is both an immune privileged site and a highly sterile environment (76). Therefore, *C. neoformans* must have evolved potent methods to traverse the blood-brain barrier (BBB) and subsist in the CNS. There are three proposed mechanisms that *C. neoformans* could utilize to penetrate this impervious palisade: paracytosis, transcytosis, and intracellular transport via a "Trojan horse" uptake system.

First, the yeasts could force their way between the tight junctions of the endothelial cells in a process known as paracytosis (**Figure 2, bottom**). This feat is not easily accomplished due to the highly regulated claudins and other proteins that impede transfer of even small molecules and proteins (77). Recent evidence from Vu et al.

indicates *C. neoformans* produces a metalloprotease, Mpr1 that could disrupt endothelial cell junctions to promote transmigration across the BBB (78). Impressively, when the *mpr1* gene was introduced into *S. cerevisiae*, a fungus not normally able to penetrate the BBB, it gained the ability to cross endothelial cells in an *in vitro* transwell assay. Additional studies utilizing powerful intravital imaging demonstrated that *C. neoformans* crosses the BBB by inducing an embolic event in the microvaculature that lines the brain, and this process is dependent on a secreted cryptococcal enzyme, urease (21, 79).

The second mechanism of BBB penetration is transcytosis (**Figure 2, bottom**). Hyaluronic acid situated on the surface of *C. neoformans* binds to CD44 on the luminal endothelium, allowing the fungus to affix to the host cell, enter the cytoplasm, and escape from the basolateral side into the CNS (80-83).

Finally, *C. neoformans* is thought to cross the BBB in host phagocytes, analogous to the "Trojan Horse" entry mechanism from mythology (**Figure 2, bottom**). Phagocytosis and intracellular killing is central to controlling *C. neoformans* replication, yet depletion of alveolar macrophages significantly reduces cryptococcal dissemination to the CNS (84). Furthermore, infecting monocytes *in vitro* and transferring the cells into naïve hosts substantially increased cryptococcal accumulation in the brain compared to transferring *C. neoformans* directly, supporting the role of monocytes as carriers for breaching the BBB (85). While paracytosis, transcytosis, and the Trojan Horse models all fundamentally differ, elements of each of these models are readily observed and likely occur in concert.

Not much is known about the behavior of *C. neoformans* once it has traversed the BBB. However, a study of the transcriptome of cryptococcal yeasts isolated from clinical cerebrospinal fluid samples offers a brief view into this window (86). Most notably, *C. neoformans* is remarkably metabolically active considering CSF is a relatively nutrient deplete medium, and this increased activity correlated with elevated expression of virulence genes. Prospective studies across independent patient cohorts employing similar methods will undoubtedly yield important information regarding the lifestyle of *C. neoformans* within the CNS.

The accumulation of *C. neoformans* in the brain causes meningoencephalitis, also referred to as cryptococcal meningitis (CM). The fever, headache, altered mental state, and death that accompany CM are direct results of increased intracranial pressure (87). Unfortunately, lumbar punctures to reduce intracranial pressure are among the few treatment options at this stage of disease (88). If *C. neoformans* is allowed to disseminate to the brain, the ensuing meningitis is often fatal, even with standard anti-fungal therapy (57, 58). Advances in early cryptococcal antigen detection (89) afford an opportunity to treat infections in the lung before they cause lethal CNS disease. Therefore, my dissertation research focused on the early immune response to pulmonary infection before the onset of meningitis.

Allergic airway disease

Another thrust of my thesis research aims to unify the clinical observations of Th2 cell responses that correlate with invasive disease in immunocompromised individuals and the type-2 driven allergic asthma in otherwise healthy individuals.

Allergic bronchopulmonary Aspergillosis, severe asthma with fungal sensitization, and allergic fungal rhinosinusitis account for over half of the 50 million people that experience asthma and pulmonary allergy and >10 billion dollars that the United States spends annually for treatment of these diseases (90-95). An association between fungal exposure and allergic Th2 inflammation is well established (96). Hallmarks of these allergic pulmonary diseases include Th2 cytokine secretion, eosinophilia, mucus and IgE production, and airway obstruction (97). Undoubtedly, these hallmarks reflect induced activation in both the innate and adaptive immune arms of the immune system. Protease activity from exogenous and endogenous sources has profound impact on innate immune responses underlying allergic inflammation (98, 99). Likewise, pulmonary inoculation with purified chitin has been implicated in eosinophil recruitment, alternative macrophage polarization, and lung epithelium activation (100, 101). However, durable recall responses to allergen challenge and IgE isotype switching both require CD4+ T cell help, underscoring the importance of CD4+ T cells in mediating fungal pathology (102).

The cellular and molecular events underlying Th2 cell fate determination during fungal infection are incompletely known. This information is critically important for the development of novel pharmaceuticals that block immunopathologic responses and/or promote beneficial immune responses (103, 104).

Thesis summary

Pulmonary mycoses, including invasive fungal infections and allergic asthma, affect millions of people worldwide. Fungi inhabit a multitude of ecological niches, and consequently, humans continuously inhale potentially pathogenic fungi. Adaptive immune cells, and in particular, Th cells, are critical to the immune response to fungal infection. While Th1 subsets contribute to protective antifungal immunity, Th2 cell responses to many fungal infections correlate with increased invasive disease severity and allergy symptoms. Yet the cellular and molecular basis for Th2 cell responses is poorly known.

My thesis project aims to understand the fundamental, yet unanswered, question of how fungal-intrinsic properties and host determinants influence Th2 cell differentiation. Through multilocus sequence typing of clinical isolates from humans with cryptococcal disease, I noted a genetic clustering of *C. neoformans*. Genetically related clusters of *C. neoformans* isolates were associated with differential mortality in the patients. Representative isolates from certain clades provoked type-2 cytokine responses to *ex vivo* stimulation of human blood, and this type-2 response directly correlated with *in vivo* virulence. These data suggested pathogen-derived signals altered the host immune response to infection. To further define how the host generates this type-2 response, I developed novel tools and strategies to analyze Th cell production in a mouse model of pulmonary infection. I found that *C. neoformans* influences detrimental Th2 cell generation through the production of chitin. The host additionally contributes to this harmful response by promoting chitin recognition via the chitinase, Chit1. Furthermore, I elucidated a detailed mechanism that the host employs to resist Th2 cell-mediated disease by inducing suppressive Treg cells in the lungs. Lastly, Th2 cells and other lymphocytes engage in a competition to drive neutrophil and eosinophil development in the bone

marrow and accumulation in the lungs of infected mice. Biasing granulocytes towards eosinophil- or neutrophil-dominated responses significantly worsen lethal disease.

These investigations into both fungal intrinsic factors and host responses may eventually guide novel anti-fungal therapies by interrupting the deleterious chitin recognition pathway, leveraging Treg cell suppression of Th2 cells, or skewing lymphocyte competition to prompt favorable, balanced granulocyte responses.

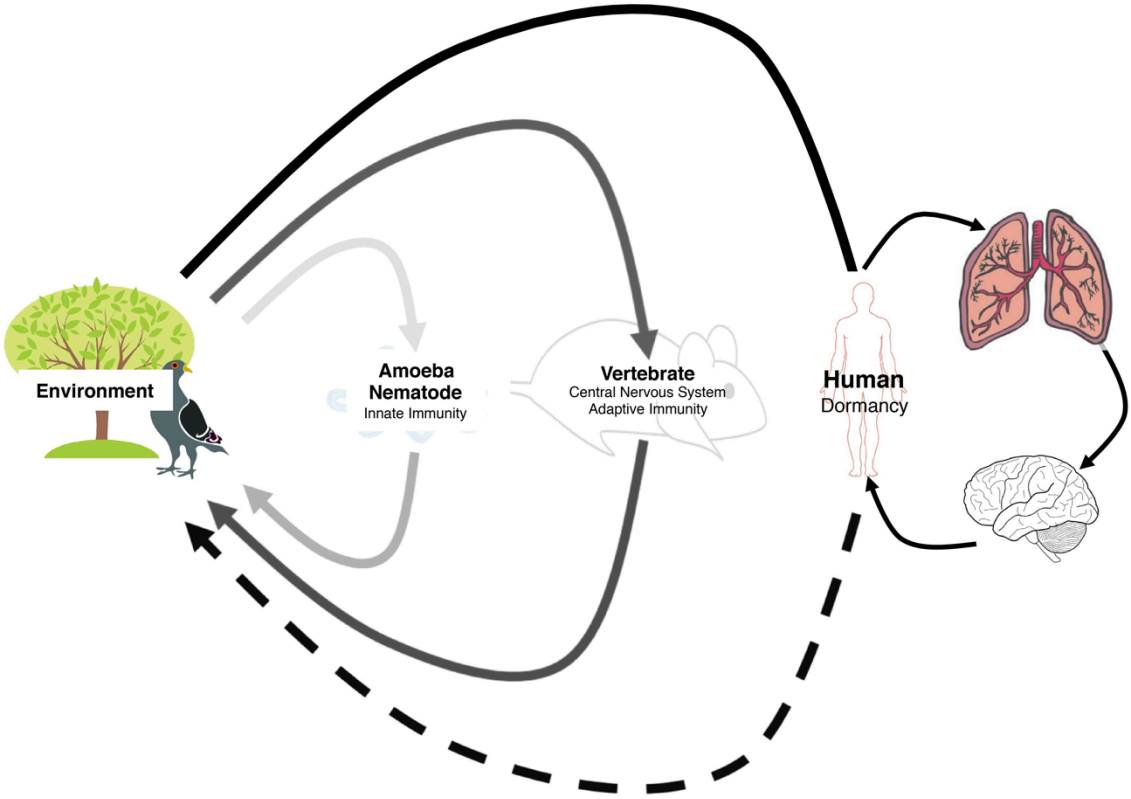

Figure 1. Virulence Evolution of an "Opportunist."

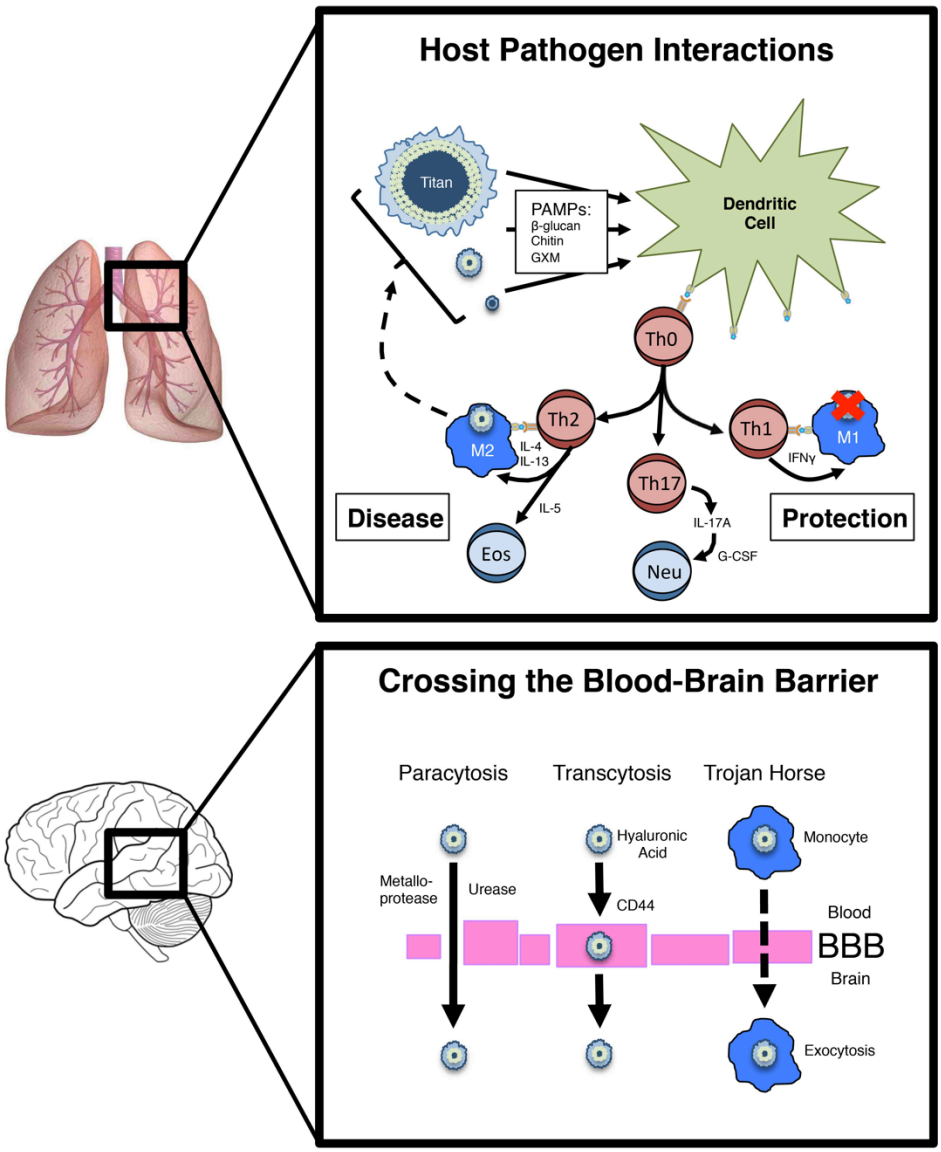

Figure 2. Cryptococcal Behavior and Host Response in the Lung and Brain. BBB, blood-brain barrier; Eos, eosinophil; G-CSF, granulocyte-colony stimulating factor; GXM, glucoronoxylomannan; Th, helper T cell; IFN, Interferon; IL, Interleukin; M1, classically activated macrophage; M2, alternatively activated macrophage, Neu, neutrophil;

CHAPTER 1

Cryptococcal Genotype Influences Immunologic Response and Human Clinical Outcome after Meningitis

Darin L. Wiesner, Oleksandr Moskalenko, Jennifer M. Corcoran, Tami McDonald, Melissa A. Rolfes, David B. Meya, Henry Kajumbula, Andrew Kambugu, Paul R. Bohjanen, Joseph F. Knight, David R. Boulware, and Kirsten Nielsen

Previously published in *mBio*. 2012;3(5)

SUMMARY

In sub-Saharan Africa, cryptococcal meningitis (CM) continues to be a predominant cause of AIDS-related mortality. Understanding virulence and improving clinical treatments remain important. To characterize the role of strain genotype in clinical disease, we analyzed 140 *Cryptococcus* isolates from 111 Ugandans with AIDS and CM. Isolates consisted of 107 non-redundant *Cryptococcus neoformans* var. *grubii* strains and 8 *C. grubii/neoformans* hybrid strains. Multi-locus Sequence Typing (MLST) was used to characterize genotypes, yielding 15 sequence types and 4 clonal clusters. The largest clonal cluster consisted of 74 isolates. Burst and phylogenetic analysis suggested the var. *grubii* strains could be separated into three non-redundant evolutionary groups (Burst group 1 to group 3). Patient mortality was differentially associated with the different evolutionary groups (P=0.04), with highest mortality observed among Burst group 1, Burst group 2, and hybrid strains. Compared to Burst group 3 strains, Burst group 1 strains were associated with higher mortality (P=0.02), exhibited increased capsule shedding (P=0.02), and elicited a more pronounced Th_2 response during *ex vivo* cytokine release assays with strain-specific capsule stimulation (P=0.02). These analyses suggest that cryptococcal strain variation can be an important determinant of human immune responses and mortality.

IMPORTANCE

Cryptococcus neoformans is a common life-threatening human fungal pathogen that is responsible for an estimated 1 million cases of meningitis in HIV-infected patients annually. Virulence factors important for human disease have been identified, yet the impact of strain genotype on virulence and outcomes of human infection remains poorly understood. Using an analysis of strain variation based on *in vitro* assays and clinical data from Ugandans living with AIDS and cryptococcal infection, we report that strain genotype predicts the type of immune response and mortality risk. These studies suggest that knowledge of the strain genotype during human infections could be used to predict outcomes and lead to improved treatment approaches aimed at targeting the specific combination of pathogen virulence and host response.

INTRODUCTION

More than 2.7 million new HIV infections and 1.8 million AIDS-related deaths occurred in 2010, despite the roll out of antiretroviral therapy (105). Based on community cohorts, 13–44% of HIV/AIDS deaths are due to *Cryptococcus* infections (8). Consequently, cryptococcal meningitis (CM) may be the fourth leading cause of death due to infectious disease in Africa with estimates of a half million deaths annually (8). Even with antiretroviral therapy (ART) access, the 6-month survival remains >40% (8, 58, 106). Efforts to improve survival of HIV/AIDS patients in sub-Saharan Africa must focus on the development of effective treatments for opportunistic infections such as CM.

One possible approach to improving clinical outcome is to customize the treatment based on specific pathogen virulence and host response. A healthy immune response to *Cryptococcus* depends on coordinated interactions between antigen presenting cells (APCs) and effector T-cells to generate a type-1 helper T-cell (Th_1) response that stimulates classical activation of macrophages and destruction of internalized cryptococcal cells (44, 107-110). IFNγ induces protective Th_1 responses and human studies have shown that IFNγ in the CSF is associated with increased fungal clearance (111). In contrast, Th_2 biased responses to *Cryptococcus* are not protective and result in disseminated, uncontrolled infections in mice (60, 61). IL-10 produced by Th_2 and regulatory T-cells inhibits synthesis of pro-inflammatory cytokines such as IFNγ and is generated in response to purified cryptococcal capsule (112, 113). Finally, IL-4 is a powerful inducer of Th_2 development, suppresses Th_1 development, and compromises the ability of IFN-γ to drive protective Th_1 responses (112). Therefore, patients exhibiting Th_2-biased immune responses to cryptococcal infections could be at higher risk for poor clinical outcomes.

Numerous relationships between pathogen genotypes and virulence have been demonstrated in bacterial pathogens (114-117) as well as between *Cryptococcus gattii* genotypes and virulence in the Vancouver Island outbreak (118), suggesting that cryptococcal strain variation could play a role in determining clinical outcomes. However, clinical outcomes in cryptococcosis are multi-factorial – both the pathogen and

the host contribute to disease. Epidemiologic characteristics of *Cryptococcus neoformans*, virulence-associated phenotypic traits, and host immune responses have been studied as individual factors influencing cryptococcosis outcomes but none of these studies have found associations between cryptococcal strain variation and human disease (119, 120). We propose that exogenous (pathogen) and endogenous (host) factors contribute concurrently to the pathophysiology of cryptococcosis. Consequently, an integrated investigation of cryptococcal strain coupled with host immune response could provide valuable insight into cryptococcal pathogenesis and potentially lead to custom therapies that target the host-pathogen interface. Thus, we hypothesize that differences in strain genotype, as determined by Multi-locus sequence typing (MLST), and strain phenotype could be responsible for disease severity and clinical outcome in patients. To test these hypotheses, we analyzed cryptococcal strains and clinical data from a cohort of ART-naive Ugandans with AIDS and CM. We report that the genotype of the infecting strain is associated with the type of immune response and clinical outcome.

RESULTS

Cohort Demographic Characteristics

A prospective cohort of 199 HIV-infected, ART-naive Ugandans with a first episode of CM was recruited at Mulago Hospital, Kampala, Uganda, over a 26-month enrollment period between 2006 to 2009 in order to study immune reconstitution inflammatory syndrome and other clinical outcomes after ART initiation (58). Of these, 111 patients had culture-positive CSF samples stored for subsequent genotypic analysis. Detailed clinical and demographic information from 98 of these patients were used for comparison of strain genotype to clinical outcome (Table 1).

Cryptococcal Strain Genotypes

Cryptococcal strains were colony purified from a total of 140 CSF specimens from the 111 patients. Genotypes of the Ugandan clinical (UgCl) strains were determined by MLST according to a consensus scheme that included eight loci: CAP59, GPD1, IGS1, LAC1, PLB1, SOD1, URA5, and TEF1 (121).

Eight isolates could not be fully genotyped as some loci were recalcitrant to PCR amplification upon sequencing with either legacy (122) or consensus (121) MLST primers at >1 MLST locus. Loci from these non-genotyped strains showed highest similarity to *Cryptococcus neoformans* var. *neoformans* (n=4) or var. *grubii* (n=4) (data not shown). None of the strains were *C. gattii* based on sequencing or CGB agar screening. PCR serotyping showed combinations of both var. *grubii* and *neoformans* gene alleles in the strains (data not shown). Taken together, these data suggest the eight strains are *grubii/neoformans* "hybrids".

Colony purification allowed us to analyze the greatest number of clinical isolates from the broadest spectrum of patients, but co-infection of patients with multiple strains could confound this approach (123). Thus, multiple isolates were collected from 24 patients. In 20 of 24 persons, no differences in MLST alleles between isolate pairs were observed; however, multiple genotypically distinct isolates were identified in four patients (17%) suggesting co-infection with ≥2 strains. Subsequent analyses included

single isolates from clonally infected patients as well as both isolates from patients infected with two genotypes.

Sequences for each MLST locus were compared, reduced to non-redundant clonal sets, and a maximum parsimony analysis of the sequences at individual loci was performed (Supplemental Figure 1). Only one strain showed a polymorphism at the URA5 locus. The SOD1 locus was completely clonal in our population. Locus allele identifiers for each strain were combined to produce a strain sequence type that serves as a representation of the strain genotype. A total of 15 sequence types (ST) were identified (Table 2). The sequence types consisted of four clonal clusters and 11 singleton sequence types (Figure 1A). The largest clonal cluster (UgCl001) contained 74 isolates. The other clonal clusters contained n=14, n=5, and n=3 isolates (represented in Table 2 by UgCl021, UgCl011, and UgCl057, respectively).

A single representative strain for each sequence type was used to analyze evolutionary relationships between the UgCl strains and further stratify the isolates into distinct groups. Phylogenetic analyses including maximum parsimony, maximum likelihood, and bootstrap were performed on the concatenated sequences of MLST loci for the 15 identified sequence types. Maximum parsimony analysis was performed with inclusion of reference strain sequences for the major *C. neoformans* var. *grubii* VNI, VNII, and VNB clades to place the resulting tree in the context of previously established evolutionary relationships (Figure 1B) (122). Maximum parsimony and maximum likelihood analyses produced comparable results (not shown). To further stratify the isolates, an MLST-specific Burst clustering analysis was performed (124). The Burst clustering hypothesized a division of the 15 sequence types into three non-redundant Burst groups and four more distant singleton strains (Figure 1C). The more highly stratified three Burst groups were used in subsequent clinical and phenotypic analyses. For the 4 patients with multiple infections, 2 patients had infections with strains in the same Burst group and thus the demographic and clinical comparisons were not repeated. Two of the patients had infections with strains in different Burst groups. In these instances, the clinical and geographic data were analyzed as part of each respective Burst group.

Patient Clinical Outcome

Having identified three distinct Burst groups and a hybrid group, we next asked whether cryptococcal genotype could predict disease severity. Patient 1-year clinical outcome was available for 98 of the 111 culture-positive patients (Table 1). The overall 1-year mortality rate was 78%. Patients infected with Burst group 1 & 2 strains had higher mortality than Burst group 3 strains (79% (68/86) vs. 38% (3/8), chi-square: p=0.05). Survival curves showed patients infected with Burst group 3 strains lived longer than patients infected with the other genotypes (Figure 2, log-rank: p = 0.009). None of the six patients infected with hybrid strains survived the infection. No other clinical or demographic parameter monitored, including CD4 count and HIV-1 viral load, was associated with genotype.

Environmental exposure to specific cryptococcal strains in particular geographic regions is a possible explanation for the association between isolate genotype and patient death. The majority of patients lived in parishes within the Kampala district but no geographic clusters of patients infected with similar genotypes was observed (Supplemental Figure 2).

Cryptococcal Strain Phenotypes

At least three major virulence factors are important for cryptococcal pathogenesis: mating type, melanin, and polysaccharide capsule (119, 120). Mating type determination and *in vitro* assays of melanin and capsule production were performed to identify association with genotype that could explain differences in lethality.

Strain mating type was determined by PCR using *STE20* primers specific for mating type and serotype. The vast majority of the *C. neoformans* var. *grubii* strains were mating type α (αA); only two were mating type **a** (**a**A). Because only 2 out of 132 var. *grubii* strains were mating type **a**, sufficient variation was not present to allow for comparison of mating type to genotype, phenotypes, or patient outcome.

Melanin production by the clinical isolates was analyzed using media containing niger seeds or L-DOPA (L-3,4-dihydroxyphenylalanine). These media provide biphenolic

precursors for melanin production along distinct pathways (125). A relative scoring method based on similarity to reference strains with weak (JEC20) and strong (KN99α) melanization was employed to analyze melanin production over 48 hours (Supplemental Figure 3A). K-means clustering analysis for both media types showed separation of the melanin production into 10 major clusters on niger seed and 7 major clusters on L-DOPA media (Supplemental Figure 3B). The Burst and hybrid groups did not differ significantly in their ability to produce melanin on niger seed media (Figure 3A). In contrast, while no association between genotype and melanin production on L-DOPA was observed for the Burst groups, the hybrid group had significantly higher melanin production on L-DOPA media (Tukey-adjusted T-test: p=0.001) (Figure 3B).

Capsule production by the UgCl isolates was monitored in two ways for comparison to isolate genotype. First, *in vivo* capsule release into patient CSF at the time of presentation with meningitis was measured using a qualitative CRAG agglutination assay. No association between clinical CRAG titer and Burst genotype was observed (ANOVA, $p \geq 0.32$). This result could be confounded by differences in fungal burden between patients resulting in inaccurate measures of capsule production. Consequently, an *in vitro* quantitative CRAG assay was performed to more precisely determine the capacity of each strain to produce and shed capsule. Burst group 1 strains had the highest capacity to produce and secrete capsule (Figure 3C). Importantly, Burst group 1 showed elevated capsule release compared to Burst group 3 (Tukey-adjusted t-test: p=0.02) and higher (but not statistically significant) capsule release compared to Burst group 2 strains. These data implicate elevated capsule production as one potential mechanism by which Burst group 1 isolates could cause increased lethality in patients.

Patient/Host Immune Response

The observation that Burst group 1 isolates were associated with higher mortality and shed more capsule than the other Burst groups led us to hypothesize that the capsule from these strains could influence the type of immune response during infection. To directly test this hypothesis we developed an *ex vivo* cytokine release assay to measure responses to capsule and cell wall preparations obtained from representative Burst group

1 and 3 isolates. Blood samples from 18 healthy volunteers were incubated with Burst group 1 and 3 antigens, cytokine production was quantified by multiplex assay, and differences between each volunteer's response to the Burst group 1 and 3 antigens was determined by paired t-test.

Release of the Th_1 cytokine, IFNγ, was similar between the Burst group 1 and 3 capsule antigens (paired *t*-test: p=0.08) (Figure 4A). In contrast, production of the Th_2 cytokines, IL-4 and IL-10, was significantly higher in response to capsule antigens from Burst group 1 strains compared to Burst group 3 strains (paired T-test: p=0.02, p=0.003, respectively) (Figure 4B,C). The amount of capsule antigen (measured by CRAG assay) was standardized in these assays, and both capsule antigens elicited equivalent dose-dependent IL-8 chemokine responses (paired *t*-test: p=0.99) (Figure 4D, Supplemental Figure 4B). Thus, the observed differences in immune response to capsule antigen were due to intrinsic properties of the capsule and not the quantity of capsule generated by the Burst group 1 and 3 isolates.

The cell wall antigen preparations did not elicit robust cytokine responses, but dose-dependent IL-8 chemokine responses equivalent to those observed with the capsule antigens were still detected (Supplemental Figure 4). These data show that capsule, but not cell wall, from Burst group 1 isolates elicits a stronger Th_2 cytokine response than capsule from Burst group 3 isolates.

DISCUSSION

We report the association between cryptococcal genotype and clinical outcome with further determination of the effect of virulence potential on disease severity in a cohort of Ugandans with AIDS and culture-positive CM. Our investigation revealed that different genotypes are associated with differences in patient survival. Cryptococcal genotypes associated with high patient mortality exhibited increased capsule (Burst group 1) or melanin (hybrid strains) production, which are two known virulence factors. We showed that capsule differences between genotypes also may have affected the host immune response, because capsule from genotypes associated with high mortality elicited a greater Th_2 cytokine response.

Previous studies noted genotypic diversity in clinical isolates from Southern Africa (e.g. Botswana, South Africa) predominantly in the VNI and VNB clades that show evidence of recombination (122, 126, 127). In contrast, clinical isolates from other regions of the world show significant clonality and are typically members of the VNI and VNII clades (127). The UgCl strains had the same SOD1 locus observed in other African cohorts [15, 24]. Yet, the Ugandan cohort had significant clonality and the predominant clade has diverged from the VNI, VNII, and VNB reference alleles. These data suggest that cryptococcal populations in Uganda are isolated, highly clonal, and that the unique Burst group 1 genotypes may be responsible for the unusually high mortality rates observed in Ugandan patient cohorts found several sequence types associated with specific regions in South Africa (126). Our data showing no geographic distribution of the UgCl strains in the Ugandan patient population suggest that patient geographic location within Uganda cannot be used to predict infection with the different Ugandan genotypes.

MLST has been used extensively to analyze both global and regional population structures in both *C. neoformans* and *C. gattii* (121-123). Yet the ability of MLST to resolve clinically relevant differences between strains remained unclear. The data presented here show that MLST can be used to distinguish differences in clinical outcome and provide insight into factors affecting disease development. The Ugandan

isolates were relatively homogenous with extensive clonality by MLST genotyping and with few polymorphisms between genotypes. Because of this homogeneity, most var. *grubii* isolates in the cohort could be stratified into one of three sub-populations based on Burst analysis. Each Burst group had multiple patients with identical MLST genotypes that could be compared. This clustering of the data revealed connections between genotype, clinical outcome, and virulence factor production that may not be readily apparent in more genotypically diverse populations.

Coinfection with multiple strains of *C. neoformans* has been observed (128). Previous studies identified coinfections based on phenotypic traits (128), mating type (123), or genotype of serial isolates (129). Desnos-Ollivier estimated coinfections could account for 20% of cryptococcal disease based on studies of a French cohort (123). Similarly, 17% of the Ugandan patients screened for coinfection were infected with multiple strains. The effect of coinfection on clinical presentation and patient outcome remains to be determined. In this study only 4 patients had confirmed coinfections and only two of the patients had infections with evolutionarily distinct strains in different Burst groups. Unfortunately, because the vast majority of the clinical isolates used here were colony purified before storage, coinfection could not be controlled in this study and the effect of coinfection on clinical outcome remains unknown. If coinfection rates are almost 20%, as the available data suggests, then coinfection could lead to a 20% error rate in accurately predicting the host response to infection. In this case, our results showing associations between genotype and clinical outcome could underestimate the differences between genotypes. The differences might be more pronounced if coinfections were identified and excluded from the analysis. Future studies in which coinfections and single infections are analyzed for their clinical outcome and host response will be necessary to define the effect coinfection has and whether the host response is cumulative, associated with the predominant strain, or associated with the most antigenic strain. Yet, the high prevalence of coinfection suggests single colony purified isolates may not accurately represent *C. neoformans* infections. This has broad implications for many types of studies, including assessing anti-fungal susceptibility.

Genotype was associated with differences in clinical outcome. Patients infected

with Burst group 1 or 2 isolates had higher mortality rates and shorter survival times than patients infected with Burst group 3 isolates (p=0.02); though, admittedly, there were few subjects with Burst group 3 isolates. One possible explanation for the low prevalence of Burst group 3 isolates is that they may be poor pathogens and do not cause severe meningitis as frequently. This hypothesis is consistent with our results showing reduced capsule production and stimulation of a protective immune response by Burst group 3 strains that would limit disease progression.

To understand the connection between cryptococcal genotype and patient outcome, we analyzed virulence factor production by the different genotypes. We focused on three widely acknowledged virulence factors of *Cryptococcus*: mating type, melanin, and capsule. While global populations of *C. neoformans* var. *grubii* are predominantly α mating type, a high prevalence of **a** mating type strains were observed in strains from Botswana (130). Most of the Ugandan isolates were α mating type, consistent with global populations, with only 2% **a** mating type in the Ugandan cohort. Thus, differences in mating type are unlikely to explain the higher lethality associated with Burst groups 1/2 relative to Burst group 3 strains.

Our findings suggested that Ugandan hybrid strains were associated with increased mortality. Hybrid strains have attenuated virulence in mouse models of cryptococcal infection (131) and often produce less severe infections in humans (119). Thus, the 100% mortality observed with the Ugandan hybrid strains was surprising. A larger cohort of patients infected with hybrid strains compared to *C. neoformans* var. *grubii* strains is needed to further explore differences between the infections.

In assessing melanin production, we found no differences between genotypes when cultured on niger seed medium. However, the hybrid strains produced significantly more melanin when L-DOPA was provided as the biphenolic precursor. Although we found increased melanin production by hybrid strains when growing these isolates on L-DOPA-containing media *in vitro*, we cannot draw conclusions about melanin production by these strains in human infections *in vivo*. L-DOPA, however, is prevalent in the central nervous system (119); thus, the increased melanin production of the hybrid strains in response to L-DOPA could potentially occur *in vivo* and promote virulence, leading to increased

mortality.

Capsule production was measured both *in vivo* and *in vitro*. The *in vitro* data proved superior for a number of reasons. First, the high degree of variability in the *in vivo* CRAG titers and small cohort made the statistical comparisons underpowered. Second, many uncontrolled factors, including duration of infection and amount of fungal proliferation, affect the amount of capsule present in the *in vivo* samples. These factors likely resulted in the high variability of the *in vivo* CRAG titers. Cell number and duration of culture were controlled more rigorously in the *in vitro* assay. Consequently, we were able to precisely stratify the Burst groups and hybrids based on capsule shedding. Notably, the high lethality Burst group 1/2 strains shed the greatest amount of capsule whereas the less lethal Burst group 3 strains shed significantly less capsule. The observation that capsule differences between genotypes are statistically associated with differences in patient mortality suggests that genetic diversity of the cryptococcal capsule may directly influence clinical outcome and immune response in humans.

The current study demonstrates that strain genotype may be a significant factor in determining the immune response in patients with AIDS and CM. Protective immunity to *Cryptococcus* requires several elements. Innate cells such as macrophages, monocytes, and dendritic cells produce TNFα, CCL2 (MCP-1), CCL3 (MIP-1α), and IL-12 to recruit and license additional leukocytes to the site of infection (132-134). The innate immune system alone is not sufficient to clear cryptococcal infections, as assistance is required from adaptive immunity with helper T cells. The priming and differentiation of CD4+ T cells to the Th_1 lineage is crucial for a protective immune response to cryptococcal infection (135). IFNγ produced by Th_1 cells not only acts in a positive feedback loop to stimulate the production of more Th_1 cells, but also classically activates macrophages to increase reactive oxygen production and kill internalized cryptococcal cells (136-138). Conversely, an IL-4 driven Th_2 adaptive response generates alternatively activated macrophages, is non-protective, results in greater fungal burden, and allows dissemination (62, 126). The Th_1/Th_2 balance paradigm used to define interactions between *Mycobacterium tuberculosis* and the human host (139, 140) may also apply to *Cryptococcus*. The pathogen competes against the host to shift a protective Th_1 response

to a pathogenic Th_2 response. How *Cryptococcus* affects this balance is an active area of research and capsule production is one potential strategy.

An *ex vivo* antigen stimulation assay was used to determine the effect of genetic diversity within the cryptococcal capsule on the Th_1/Th_2 balance in humans. High lethality Burst group 1 isolates stimulated greater IL-4 and IL-10 production compared to less lethal Burst group 3 isolates. IL-4 is a powerful inducer of Th_2 development, serving as a positive feedback signal for more IL-4 production as well as a negative feedback for Th_1 responses. Similarly, IL-10 is a suppressive cytokine that has antagonistic effects on Th_1 responses and development (112). These data suggest that the high lethality Burst group 1 isolates shift the Th_1/Th_2 balance in favor of the pathogenic Th_2 response. In contrast, the less lethal Burst group 3 isolates are unable to elicit a robust Th_2 response allowing for a Th_1/Th_2 balance shifted to the more protective Th_1 response.

The capsule antigen preparations used in this study were a heterogeneous mix of microvessicles, proteins, immunogenic lipids, and capsule polysaccharide. Therefore, it is likely that T cell antigens, mainly proteins, present in the preparation were processed and presented by APCs to generate the Th_1 protective immune response observed in all of the preparations. In contrast, capsule polysaccharide is widely implicated in host immune evasion and can influence host responses in several ways. Capsule can directly inhibit opsonization, phagocytosis, and lysosomal degradation within phagosomes (141-143). In addition, shed capsule can disrupt cytokine signaling and lymphocytes (108, 144, 145). The major component of capsule polysaccharide, glucuronoxylomannan (GXM), can also promote secretion of Th_2 cytokines by monocytes (146). Burst group 1 strains produce more polysaccharide than Burst group 3 strains, yet the amount of polysaccharide used in the *ex vivo* assay was held constant. Thus, the differences in immune response to the capsule preparations observed in the *ex vivo* assay were due solely to genetic differences between the Burst group 1 and 3 strains that affect the structure, function, and/or composition of the capsule polysaccharide or other components of the preparation. The fact that Burst group 1 strains also produce more capsule polysaccharide suggests that the actual affect on the Th_1/Th_2 balance is even greater than observed in the *ex vivo* antigen stimulation assay. A shift of the Th_1/Th_2 balance in favor of a pathogenic Th_2 response

results in greater fungal burden, dissemination, and ultimately death in mouse models of cryptococcosis (59, 147). Our data show strains capable of shifting the Th_1/Th_2 balance toward a Th_2 cytokine response in humans are also associated with high mortality rates.

The studies presented here were designed to analyze the effect of two parameters on the immune response and clinical outcome: capsule and cell wall. The capsule data – both the amount of capsule and the type of capsule – differed between genotypes and affected the immune response. In contrast, while melanin production was found to differ in the hybrids, no effect of cell wall components on the immune response was observed. Thus, the combination of the melanin and cell wall cytokine induction experiments suggest that alterations in cell wall and melanin production can differ between strains, but the role, if any, cell wall components play in disease outcome remains unclear.

The high overall mortality rate in the Ugandan culture-positive cohort resulted in too few surviving patients to analyze the effect of strain genotype on subsequent development of immune reconstitution inflammatory syndrome following anti-retroviral therapy (ART). A larger cohort of culture-positive patients that initiate ART will be needed to examine associations between strain genotype and risk for IRIS. IRIS patients have an aberrant immune response following reconstitution of their CD4+ T cell population. Current theories suggest this aberrant response is due to uncontrolled reconstitution of the immune system or continued prevalence of a highly reactive antigen (148). Our data show that Burst group 1 strains produce abundant, Th_2 reactive, capsule antigen. Thus, Burst group 1 strains may also be more likely to elicit IRIS in patients who survive the initial infection compared to Burst group 3 strains with lower and less reactive antigen.

Taken together, the data presented show that strain genotype is associated with disease outcome. The observation that strain genotype affects the immune response to cryptococcal infections suggests that genotype can be clinically informative and leads to interesting possibilities for new treatment strategies in patients with AIDS and CM. Treatment regiments targeted at the unique combination of pathogen and host may improve clinical outcomes. For example, new treatments such as IFNg (55) or other approaches that increase Th_1 cytokines in patients infected with those *Cryptococcus*

strains that elicit predominant Th_2 responses may restore proper Th_1/Th_2 balance and allow better control of the infection.

MATERIALS AND METHODS

Ethical Statement and Data. Clinical samples were collected during an observational, prospective study of Ugandan AIDS patients with CM designed to study immune reconstitution inflammatory syndrome following ART initiation (57, 58, 149). Each patient contributed only one episode of CM. This study was reviewed and approved by the institutional review board of the University of Minnesota, Makerere University, and the Uganda National Council of Science and Technology. Written informed consent was obtained from all subjects, and all data were de-identified.

Strains and Media. *C. neoformans* clinical isolates (UgCl) collected from cerebrospinal fluid (CSF) were colony purified and stored as glycerol stocks. *Cryptococcus* and *Candida albicans* reference strains (Supplemental Table 1) were also stored as glycerol stocks. All strains were grown on yeast peptone dextrose (YPD) medium prior to subsequent analysis. Complete Dulbecco's modified Eagle's medium (DMEM+C), Niger seed, L-DOPA, canavanine glycine bromothymol blue (CGB), and Christensen's urea media were used as previously described (150, 151).

Multi-locus Sequence Typing (MLST). Genomic DNA extraction was performed as described previously (152). Eight loci were amplified and sequenced - seven ISHAM consensus loci CAP59, GPD1, IGS1, LAC1, PLB1, SOD1, URA5 (121) and the optional highly-polymorphic TEF1 locus (122). An additional LAC1Ra primer was developed to replace the consensus primer, which was not sufficiently specific for LAC1 amplification in our samples. All primers are listed in Supplemental Table 2. MLST PCR products were resolved by agarose gel electrophoresis, excised, purified, and sequenced. Sequence assembly was performed with Sequencher 4.9 software (Genecodes, Ann Arbor, MI). Exported sequences were truncated to the consensus MLST ends (121). Sequences for each locus were aligned using ClustalW software (153). All polymorphisms were verified using the sequence chromatograms and alignments were manually edited to resolve ambiguities. Manual indel coding was performed by collapsing gaps to a single

nucleotide gap at the 5' end. Multiple alignments were processed with PAUP4.0b10 software to produce maximum parsimony trees using a heuristic algorithm with 1000 random sequence additions and gaps treated as the fifth base (154). 4430 characters were analyzed: 4315 characters were constant, 71 variable characters were parsimony-uninformative, and 44 characters were parsimony-informative. Sequences for all loci for each UgCl sample were concatenated and subjected to maximum parsimony, maximum likelihood and bootstrap analyses using PAUP4.0b10 software (Sinauer Associates, Sunderland, MA). Non-redundant allelic sets were compiled using the Non-redundant databases (NRDB) web tool (http://pubmlst.org). Novel allele sequences were deposited in MLST.net, BioloMICS Net, and BLAST public databases. Sequence types were identified as combinations of allelic types for individual loci based on NRDB data. Sequence types were subjected to Burst analysis (124) to produce a putative evolutionary relationship between clusters of closely related sequence types. A minimum spanning tree was produced from the sequence types with Prim's algorithm combined with Burst clustering.

Phenotypic analyses. Cryptococcal yeasts were plated onto either Christensen's urea or CGB plates and incubated concurrently with control strains at room temperature for 24-48 hours. Plates were visually inspected for color changes. *Cryptococcus gattii* strains were used as positive controls for the CGB test and KN99α was used as a positive control for Christensen's urea and a negative control for CGB test. Bright field microscopy with a Zeiss Axioplan microscope with an attached AxioCam camera (Carl Zeiss, Germany) was used for analysis of cellular morphology.

Melanin production was measured by comparing pigmentation of UgCl strains grown on Niger Seed and L-DOPA media (17) to reference strains with strong (KN99α) and weak (JEC20) melanization. Cell suspensions were adjusted to 10^6 and 10^7 yeasts/mL using a hemocytometer, plated onto YPD, grown at 25^{o}C in the dark, and examined at 12, 18, 36, and 48 hours. Melanin assays were performed in triplicate. Absolute production of melanin was variable between replicates, but relative amounts of melanin were highly reproducible. Relative melanization scores of zero (no

pigmentation), one (equal to JEC20), two (between JEC20 and KN99α), three (equal to KN99α), or four (more than KN99α) were assigned to UgCl strains based on comparison with the reference strains grown on the same plate. *C. albicans* strain SC5314 was used as a negative melanization control.

Cryptococcal antigen assay (CRAG) was performed at time of diagnosis using the Murex *Cryptococcus* latex agglutination assay (Murex Diagnostics, Norcross, GA) according to manufacturer's specifications or following *in vitro* culture with the Premier Cryptococcal Antigen Kit (Meridian Bioscience, Cincinnati, OH) according to manufacturer's specifications with a modified procedure for sample preparation. Briefly, DMEM+C was inoculated and incubated at 30^{o}C. Cultures with an optical density $(OD)_{600}$ of 0.90-1.10 were centrifuged at 10,000 rpm and the supernatant serially diluted from 1:10 to 1:6,250 with the provided "DIL" solution to obtain an absorbance at 450 nm of 0.14 to 1.50. Enzyme Immunoassay value for each sample was calculated from the A_{450} value according to manufacturer's instructions and normalized to OD_{600} of 1.0. PCR with differential PAK1, GPA1, and Ste20 primers was used for determination of serotype and mating type as previously described (155).

***Ex vivo* Antigen stimulation.** Antigens were prepared from the cell wall and culture supernatants of six strains that included the control H99 strain and five strains representative of the mean CRAG data points within each of the MLST clonal cluster genotypic groups. A capsule antigen preparation was prepared from culture supernatant from each strain grown in DMEM+C. The supernatant was decanted, frozen at -80^{o}C, and lyophilized. The lyophilized sample was reconstituted in phosphate buffered saline (PBS), and the CRAG titer measured. A cell wall antigen preparation was prepared from the yeasts. Cells were flash-frozen in liquid nitrogen, combined with glass beads, and vortexed vigorously for two hours at 4^{o}C to disrupt the cells. The insoluble fraction (i.e. cell wall) was analyzed for CRAG and for protein (BCA Protein Assay, Thermo Fisher Scientific, Rockford, IL) concentrations. Endotoxin levels in all antigen preparations were undetectable (<0.06 U/mL) by *Limulus* Amebocyte Lysate assay (Associates of Cape Cod, MA).

Whole blood samples for the cryptococcal cytokine release assay were obtained from healthy individuals in North America. Peripheral blood from each subject was drawn into lithium heparin tubes, diluted 2-fold with PBS, and dispensed into a tissue culture plate. Cell wall and capsule antigens were added to each well to yield a physiologically comparable glucuronoxylomannan (GXM) CRAG titer of 1:256. PBS was used as the negative control. Plates were incubated at 37°C in 5% CO_2 for 20 hours. After incubation, the plasma was separated from the cells and stored at 4^oC until cytokine analysis. Cytokines were quantified in duplicate for Interleukin (IL)-2, IL-4, IL-6, IL-8, IL-10, granulocyte macrophage colony stimulating factor (GM-CSF), interferon-gamma (IFN-γ), and tumor necrosis factor-alpha (TNF-α) using a Luminex 100 instrument (Bio-Rad, Hercules, CA). Negative controls incubated in PBS were subtracted from the raw data to determine the net response.

Statistics. Means were compared across groups of isolates using ANOVA and *t*-tests, and medians were compared using Kruskal-Wallis rank sum tests and Mann-Whitney U tests. Chi-square and Fishers Exact tests were used to evaluate frequencies of categorical variables. Tukey adjustments were made to correct for multiple comparisons. Mantel-Cox logrank test was used for the survival anaylsys. All analyses were performed with SAS (SAS Institute Inc, Cary, NC).

ACKNOWLEDGEMENTS

This work was supported by NIH grants AI070152, AI089244, AI073192, AI078750, and AI096925; the University of Minnesota (UMN) Office of International Programs; UMN Center for Infectious Diseases and Microbiology Translational Research; UMN Academic Health Center Collaborative and Tibotec REACH Initiative grants; and the Minnesota Medical Foundation Robert and Mabel Bohjanen Immune Reconstitution Research Fund.

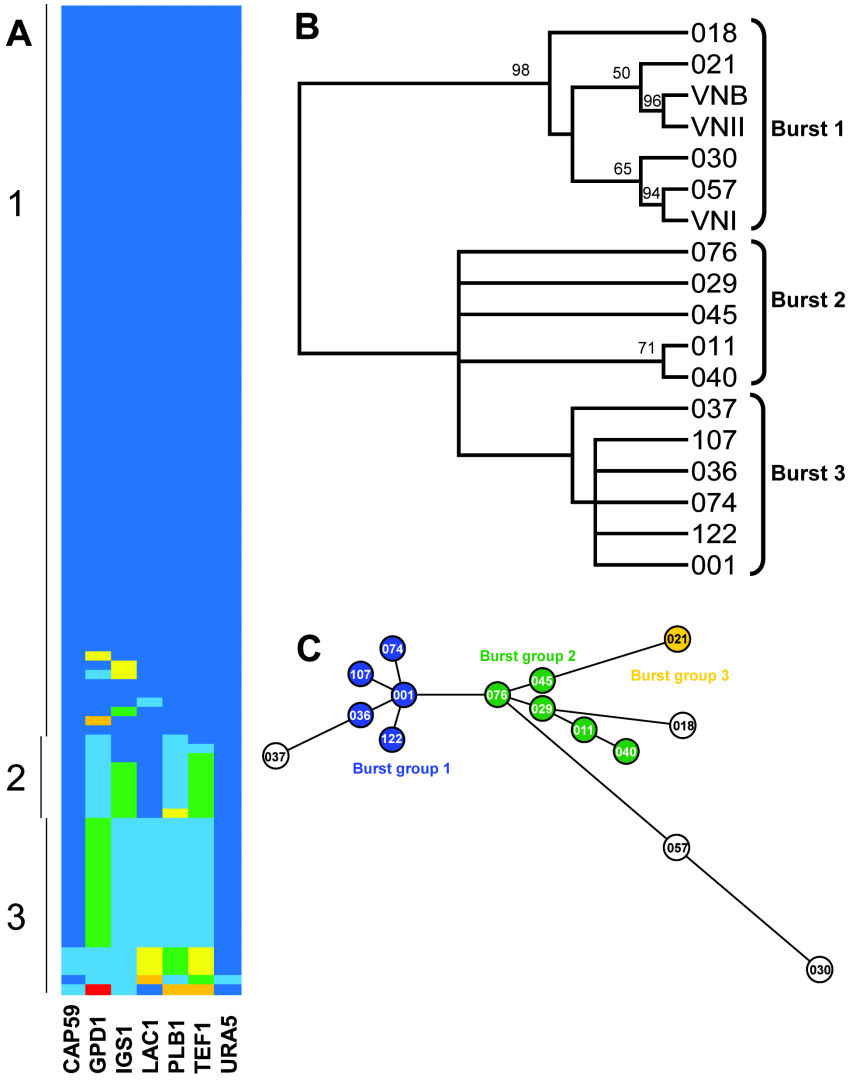

Figure 1. Multilocus sequence typing of Ugandan clinical isolates. (**A**) Pseudo-color representation of the allelic structure of the UgCl strain population. Alleles at each locus are indicated by different colors. Each row indicates a single strain. Vertical lines on the left represent Burst groups. (**B**) Consensus tree from 1000 bootstrapped replicates of a maximum parsimony analysis of the concatenated sequences of all informative loci. Bootstrap values over 50% are shown. (**C**) Analytical separation of UgCl strains into non-redundant evolutionary groups based on Burst analysis of the sequence types. Fill color represents the 3 Burst groups. Singleton strains are not shaded.

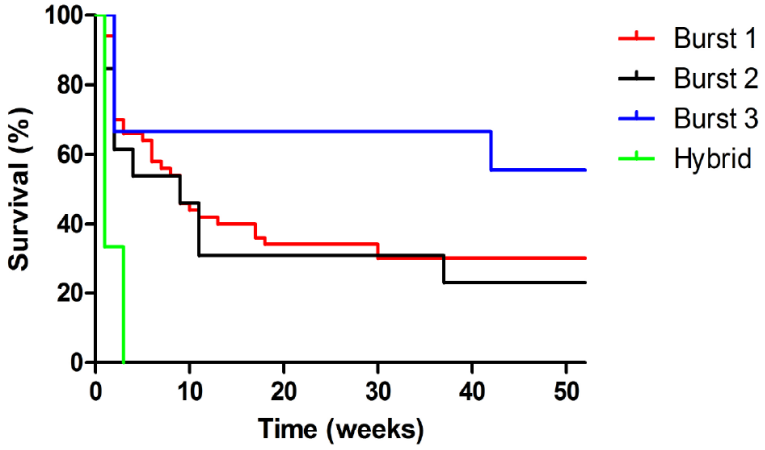

Figure 2. One-year survival of culture-positive patients presenting at Mulago hospital in Kampala, Uganda based on strain genotype. Patients infected with Burst group 3 strains lived longer than patients infected with other genotypes (p=0.007, Logrank test). No patients infected with hybrid strains survived the infection.

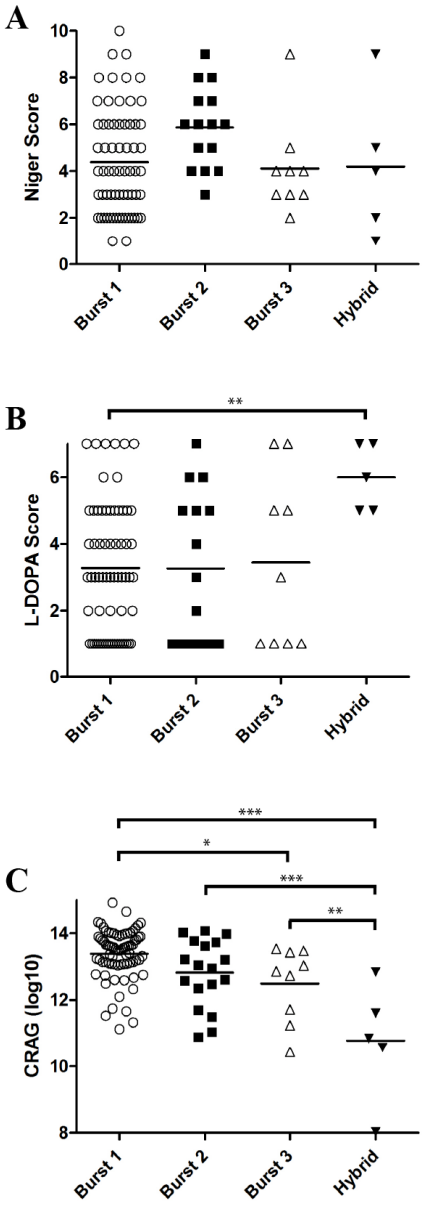

Figure 3. Cryptococcal virulence factors and genotype. (**A/B**) Association between Burst groups and temporal melanization as indicated by K-means cluster rank on niger seed (**A**) or L-DOPA (**B**) medium. (**C**) Association between Burst groups and shed capsule as measured by Cryptococcal Antigen titer. Asterix represents degree of statistical significance with * for $p<0.05$, ** for $p<0.005$, *** for $p<0.0005$.

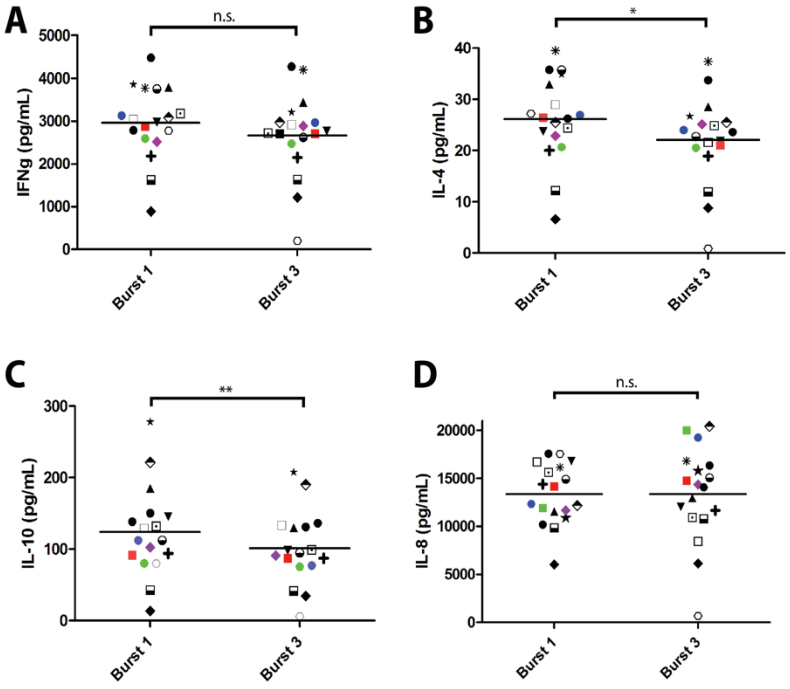

Figure 4. Immune response of healthy volunteers to *ex vivo* stimulation with capsule antigens from genetically distinct strains. Production of IFNγ (**A**), IL-4 (**B**), IL-10 (**C**), and IL-8 (**D**) cytokines in response to shed capsule antigen from a representative clonal cluster strain within each Burst group. Antigens were standardized to a physiologically relevant final assay CRAG titer of 1:1024 as determined by cryptococcal antigen agglutination assay. Data are representative of assays from 6 independent strains. Asterix represents degree of statistical significance with * for $p<0.05$, ** for $p<0.005$, and "n.s." for non-significant with $p=0.08$, 0.99 for A & D, respectively.

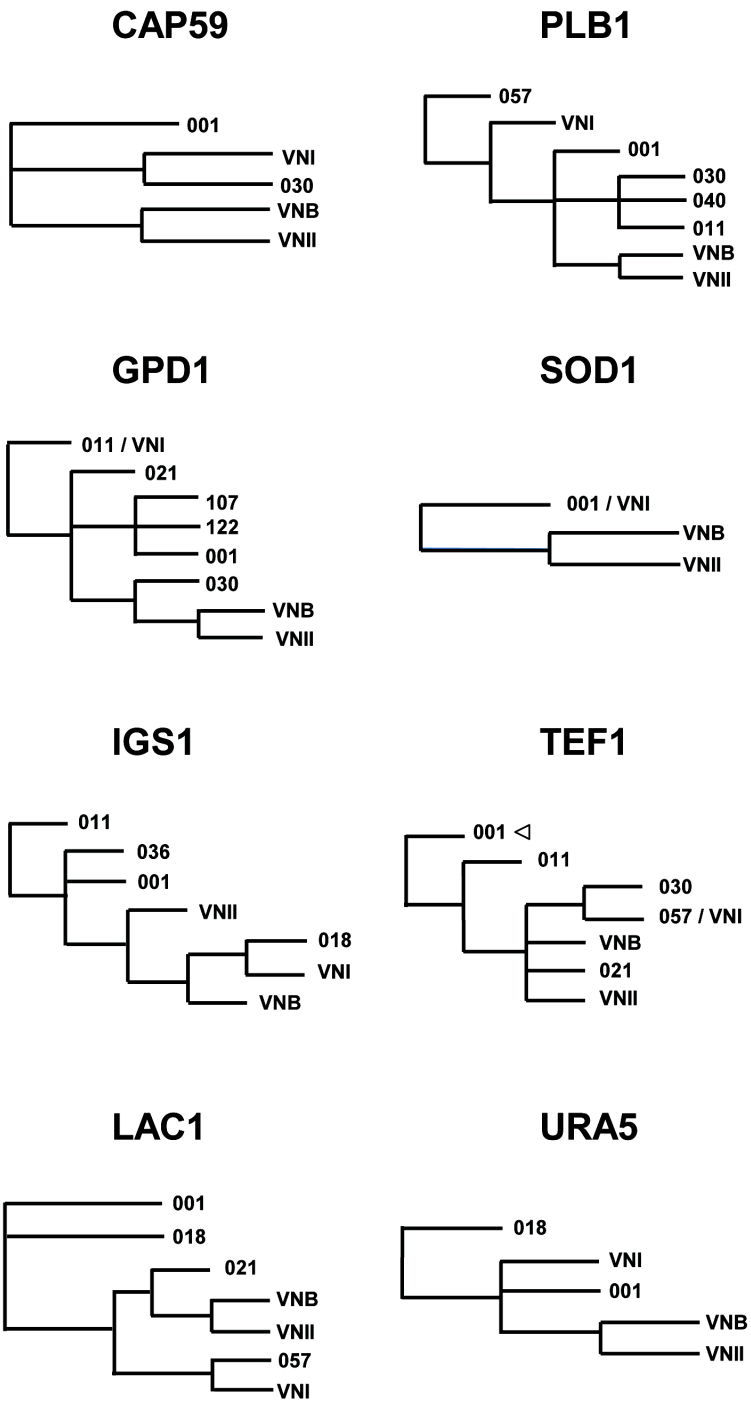

Supplemental Figure S1. Maximum parsimony trees of individual MLST loci.

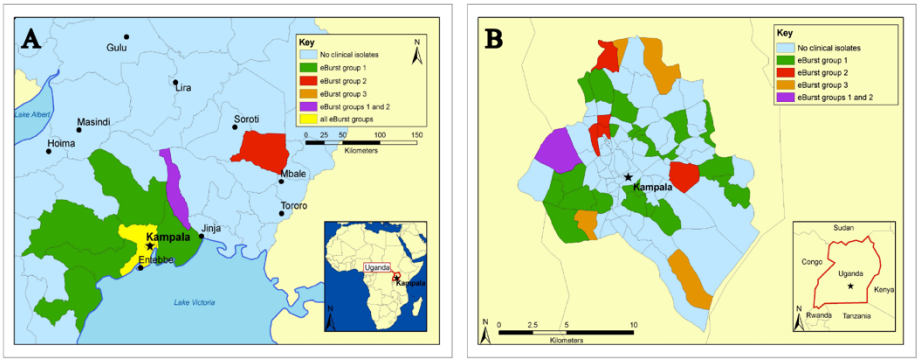

Supplemental Figure S2. **Geographical distribution of culture-positive patients presenting at Mulago hospital in Kampala, Uganda**. No association between geographic location and strain genotype was observed. (A) Districts within Uganda with culture-positive patients. (B) Parishes within the Kampala district with culture-positive patients.

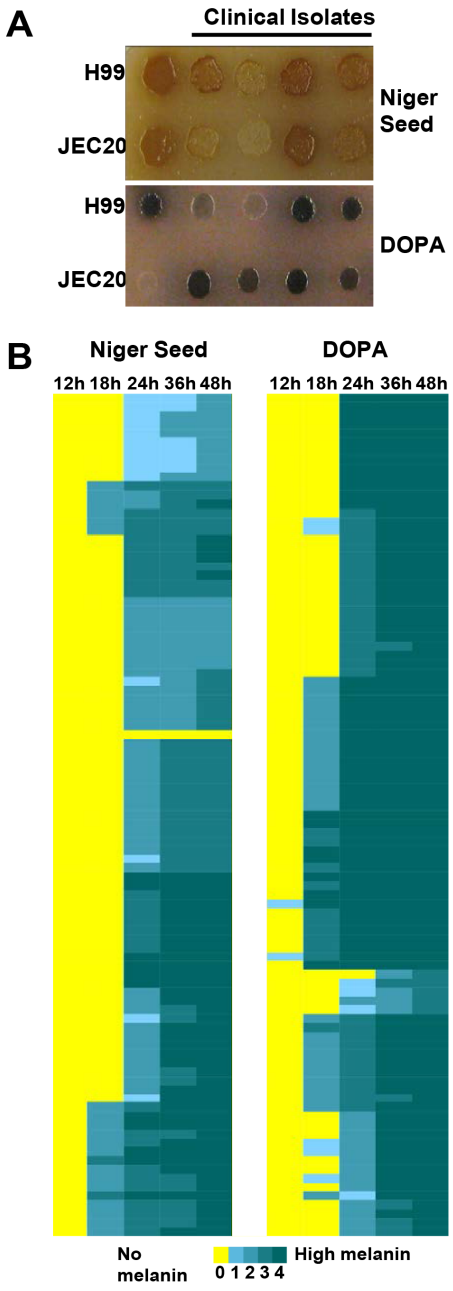

Supplemental Figure S3. **Melanin production**. (**A**) Melanization of representative UgCl strains relative to controls on niger seed and L-DOPA media. (**B**) Temporal representation of strain melanization on niger seed and L-DOPA media using K-means clustering of melanin production from 12 to 48 hours.

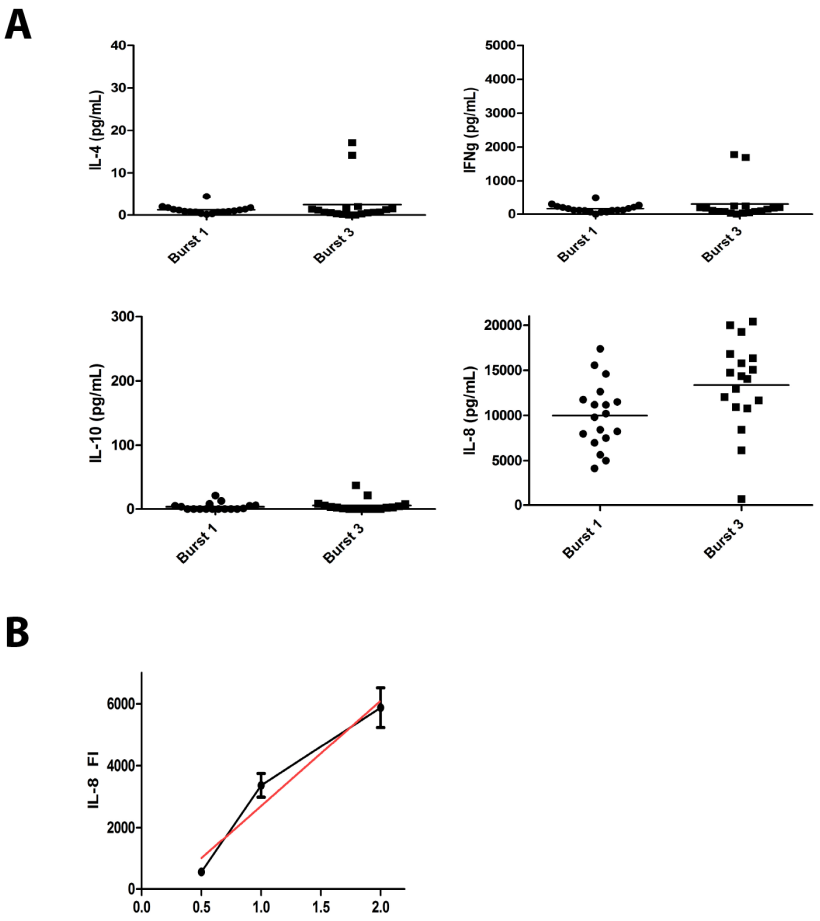

Supplemental Figure S4. Immune response of healthy volunteers to *ex vivo* stimulation with cell wall antigens. (**A**) Production of IL-4, IL-10, IFNγ, and IL-8 cytokines in response to cell wall extract antigen from a representative clonal cluster strain within each Burst group. Antigens were standardized to a final assay concentration of 5ug of protein per well as determined by Bradford protein assay. (**B**) IL-8 Dose-response curve to diluted (0.5), undiluted (1.0) and concentrated (2.0) capsule antigen. Best-fit linear regression line is red ($p<0.0001$, $R^2=0.79$, beta=3401). Units are fluorescence intensity (FI) as reported by the Luminex multiplex instrument.

CHAPTER 2

Chitin Recognition via Chitotriosidase Promotes Pathologic Type-2 Helper T Cell Responses to Cryptococcal Infection

Darin L. Wiesner, Charles A. Specht, Chrono K. Lee, Kyle D. Smith, Liliane Mukaremera, S. Thera Lee, Chun G. Lee, Jack A. Elias, Judith N. Nielsen, David R. Boulware, Paul R. Bohjanen, Marc K. Jenkins, Stuart M. Levitz, Kirsten Nielsen

Previously published in *PLoS Pathogens*. 2015; 11(3):e1004701

SUMMARY

Pulmonary mycoses are often associated with type-2 helper T (Th2) cell responses. However, mechanisms of Th2 cell accumulation are multifactorial and incompletely known. To investigate Th2 cell responses to pulmonary fungal infection, we developed a peptide-MHCII tetramer to track antigen-specific CD4+ T cells produced in response to infection with the fungal pathogen *Cryptococcus neoformans*. We noted massive accruement of pathologic cryptococcal antigen-specific Th2 cells in the lungs following infection that was coordinated by lung-resident CD11b+ IRF4-dependent conventional dendritic cells. Other researchers have demonstrated that this dendritic cell subset is also capable of priming protective Th17 cell responses to another pulmonary fungal infection, *Aspergillus fumigatus*. Thus, higher order detection of specific features of fungal infection by these dendritic cells must direct Th2 cell lineage commitment. Since chitin-containing parasites commonly elicit Th2 responses, we hypothesized that recognition of fungal chitin is an important determinant of Th2 cell-mediated mycosis. Using *C. neoformans* mutants or purified chitin, we found that chitin abundance impacted Th2 cell accumulation and disease. Importantly, we determined Th2 cell induction depended on cleavage of chitin via the mammalian chitinase, chitotriosidase, an enzyme that was also prevalent in humans experiencing overt cryptococcosis. The data presented herein offers a new perspective on fungal disease susceptibility, whereby chitin recognition via chitotriosidase leads to the initiation of harmful Th2 cell differentiation by CD11b+ conventional dendritic cells in response to pulmonary fungal infection.

AUTHOR SUMMARY

Humans often inhale potentially pathogenic fungi in the environment. While CD4+ helper T (Th) cells are required for protection against invasive disease, a subset of Th cells, called Th2 cells, are associated with increased mortality and allergy/asthma morbidity. Our study aimed to unravel the cellular and molecular basis of pulmonary Th2 cell induction in response to lethal infection with *Cryptococcus neoformans*. Antigen-presenting cells coordinate naïve Th cell priming and differentiation, but the precise leukocyte responsible for Th2 cell expansion to pulmonary cryptococcal infection has not been determined. Using an experimental mouse model of pulmonary cryptococcosis, we show that a subset of lung-resident dendritic cells is uniquely required for Th2 cell induction. We additionally sought to identify the molecular signal received by the host that allows dendritic cells to selectively induce Th2 cells. Since parasites and fungi elicit Th2 cell responses and both produce chitin, a molecule not found in vertebrates, we hypothesized that recognition of fungal chitin is a determinant of fungal disease. Here, we demonstrate that *C. neoformans* chitin and the host-derived chitinase, chitotriosidase, promote Th2 cell accumulation and disease. These findings highlight a promising target of next generation therapies aimed at limiting immunopathology caused by pulmonary fungal infection.

INTRODUCTION

Pulmonary mycoses, ranging from invasive fungal infection to severe asthma with fungal sensitization, affect millions of people worldwide (75, 90). Fungi inhabit a multitude of ecological niches, and consequently, humans continuously encounter potentially pathogenic fungi in the environment. Subsequent disease is determined by the size of the innoculum, virulence of the microbe, and immune status of the host. In particular, CD4+ helper T (Th) cell subsets are critical mediators of the immune response to fungal exposure. Interferon-γ from Th1 cells and interleukin (IL)-17 from Th17 cells contribute to protective immunity via classical activation of macrophages and neutrophil recruitment, respectively (53). Conversely, Th2 cell production of IL-4, IL-5, and IL-13 impels eosinophilia, alternative macrophage activation, mucus and IgE production, and airway obstruction (97). These type-2 responses drive fungal-associated allergies and positively correlate with invasive fungal disease severity (97). Although a fair amount is known about type-2 responses and their downstream consequences, the basis of Th2 cell induction associated with pulmonary mycosis is less well defined.

Antigen presentation by an immune cell bearing major histocompatibility II (MHCII) is required for naïve Th cell priming and differentiation. Thus, a cellular intermediate must coordinate Th2 cell induction. Professional antigen presenting cells direct Th cell fate, and inflamed lungs contain several ontologically distinct immune cells with this potential capability (156). The precise leukocyte subset responsible for priming Th2 cells, as well as the location that this event occurs, whether at the site of infection or within secondary lymphoid tissue, has not been comprehensively investigated. Furthermore, specific features of the infection that lead to Th2 cell lineage commitment remain largely unexplored in the context of pulmonary fungal infection.

While some models attribute induction of type-2 responses to protease cleavage of host proteins and wound repair of lung injury (157), many microbes that elicit Th2 cell responses produce chitin (158). Chitin is a polysaccharide composed of polymeric *N*-acetylglucosamine. The rigidity of chitin is utilized in the cell wall of fungi as well as the exoskeleton of arthropods and filarial sheath of parasitic worms. Higher organisms rely

on keratin for similar structural purposes, and as a result, vertebrates do not synthesize or store chitin. These differences allow an opportunity for the vertebrate immune system to detect chitin-containing pathogens as foreign (159, 160). While chitin detection may prove beneficial to the host in the context of parasitic infection (161), we hypothesize that inappropriate or dysregulated Th2 responses instigated by recognition of chitin promotes fungal pathogenesis.

Chitinases are a pivotal component of the host response to chitinous organisms (162). Chitin is positioned beneath layers of mannans and glucans in the fungal cell wall, thus secreted host chitinases are needed to penetrate the wall matrix and make chitin fragments available to host surveillance (163). Mammals encode two functional chitinases, chitotriosidase (Chit1) and acidic mammalian chitinase (AMCase) (162). A naturally occurring allele of *CHIT1* renders the enzyme inactive (164), and these mutations have been associated with susceptibility to parasitic worm infection in humans (165). Likewise, AMCase has been linked to eosinophilia (98) and alternative macrophage activation (100) in mouse models of pulmonary allergy. Consequently, we reasoned that mammalian chitinases could be necessary for efficient host recognition of fungal chitin and subsequent Th2 cell priming.

Using an inhalation model of *Cryptococcus neoformans* infection and novel reagents to detect *Cryptococcus*-specific Th cells, we unravel the basis for Th2 cell induction in response to pulmonary fungal infection. We report profound accumulation of detrimental Th2 cells in the lungs of infected mice. We additionally show that lung-resident CD11b+ interferon regulatory factor (IRF) 4-dependent conventional dendritic cells present antigen to Th cells and drive potent Th2 differentiation at the site of infection in the lungs. Surprisingly, our results demonstrate that an excess of fungal chitin, as well as digestion of chitin via Chit1, and not AMCase, lead to chitin detection, Th2 cell accumulation, and enhanced disease. Lastly, we observed increased Chit1 activity in humans with confirmed fungal infections, reinforcing the relevance of Chit1 in human disease. This study offers novel insights into the cellular source of antigen presentation and molecular basis of chitin recognition via Chit1 that underlies deleterious Th2 cell formation during pulmonary mycosis.

RESULTS

Pulmonary cryptococcal infection results in profound accumulation of antigen-specific Th2 cells.

We utilized a murine model of pulmonary cryptococcosis to investigate Th cell priming during fungal infection. Upon inhalation, *Cryptococcus neoformans* establishes a robust lower respiratory tract infection that causes tissue damage and ultimately leads to mortality from pulmonary complications and dissemination resulting in meningoencephalitis. To distinguish Th cell responses to infection from non-specific wound healing Th2 cell responses, we generated a recombinant peptide-major histocompatibility class II (pMHCII) tetramer that enabled identification of *C. neoformans* antigen-specific Th cells. The pMHCII tetramer contains a 13 amino acid peptide from an immunodominant cryptococcal protein, chitin deacetylase 2 (Cda2) **(Table 1)** (166). The Cda2-MHCII tetramer labeled a population of antigen-experienced (i.e. CD44+) Th cells, but it did not stain non-activated (i.e. CD44-) Th cells from *C. neoformans* infected mice or CD44+ Th cells from naive mice **(Fig. 1A, S1 Fig.** for flow cytometry gating). In addition, mice infected with a *C. neoformans* mutant (*cda2Δ*) that lacks Cda2 protein expression (167) had marked reductions in Cda2-MHCII tetramer binding cells **(Fig. 1A)**. Though Cda2 contains a dominant CD4+ T cell epitope, cross-reactivity to other closely related cryptococcal proteins likely account for the remaining tetramer binding Th cells generated during infection with *cda2Δ* **(Table 1)**. Taken together, these studies show the Cda2-MHCII tetramer reliably identified antigen-specific CD4+ T cells produced in response to *C. neoformans* infection.

We characterized the immune response in the lung and lung-draining mediastinal lymph node (MLN) to determine the relative contributions of each site to CD4+ T cell subset differentiation. Pulmonary cryptococcal infection resulted in a progressive accumulation of Cda2-MHCII-specific T cells in the lungs that predominately expressed the Th2 cytokines IL-5 and/or IL-13 **(Fig. 1B-D)**. In addition, Th2 cytokines IL-5, IL-13, and CCL5 were among the most abundant cytokines present in infected lung homogenates **(Fig. 1E),** and eosinophils, a downstream correlate of type-2 cytokines,

represented an overwhelming majority of the bulk leukocyte population in the lungs **(S2 Fig.** for flow cytometry gating, **S3A Fig.)**. In contrast, the Cda2-MHCII-specific Th2 cell response within the MLN **(Fig. 1F-H)** was significantly lower than the response observed in the lungs**,** and eosinophils comprised an insubstantial component of the lymph node resident leukocytes **(S3 Fig.)**. These findings collectively suggest the local inflammatory environment in the lung may shape the differentiation and/or promote the selective expansion of Th2 cells.

Interleukin-2 cytokine/antibody complexes enhance Th2 cell expansion and disease.

Due to the seemingly contradictory roles of Th2 cells in beneficial wound healing responses and harmful allergic disease (168), it is not entirely clear whether Th2 cells simply correlate with or cause disease associated with fungal infection. To test the causal relationship of Th2 cells with disease severity in this model, we augmented the endogenous Th2 cell response to fungal infection using IL-2 cytokine/antibody complex treatment. IL-2 can be targeted to the high affinity IL-2 receptor to enhance Th cell proliferation by conjugating IL-2 cytokine with anti-IL-2 antibody to form IL-2 cytokine/antibody complexes (169, 170). Since Th2 cells generated during pulmonary cryptococcal infection expressed high levels of the alpha chain of the high affinity IL-2 receptor (CD25) **(Fig. 2A)**, we sought to use IL-2 complexes to boost the Th2 cell response.

The wildtype strain of *C. neoformans*, KN99α, induces an extremely aggressive infection that leaves little room to increase the Th2 cell response. Consequently, we used an attenuated strain of *C. neoformans, gpr4Δgpr5Δ* (attenuation explained below/Figure 5; deficient in production of large, chitinous cells). Treatment with IL-2 complexes increased Th2 cell numbers compared with similarly infected mice receiving antibody or cytokine alone **(Fig. 2B)**. Th2 cells and cytokines were also elevated in lung homogenates from infected mice treated with IL-2 complexes **(Fig. 2C&D)**. In addition to Th2 cells, Regulatory T (Treg) cells can be expanded by IL-2 complex treatment (169, 170) (**S4A Fig.**). This increase of Treg cells in mice treated with the IL-2 complex could theoretically suppress protective Th cell responses and allow Th2 cells to predominate the

response. However, IL-2 complex treatment did not affect Th1 or Th17 cell numbers **(Fig. 2B)** and only minimal changes in IFNγ cytokine (**Fig. 2C**) and monocyte accumulation (**Fig. 2D**) were observed, showing IL-2 complex treatment did not eliminate the effector activity of protective Th1 cells **(Fig. 2D)**. Instead, Schulze et al. (171) showed Treg cells suppress Th2 cells during cryptococcal infection **(S4B&C Fig.)**, suggesting the increase in Treg cells due to IL-2 complex treatment would actually limit Th2 cell accumulation in this system. Hence, IL-2 complexes can be used to augment the Th2 cell response during pulmonary fungal infection and assess the relationship between Th2 cells and fungal disease.

If Th2 cells promote disease, we hypothesized that increasing the Th2 response should accelerate death during infection with the virulence-attenuated strain, *gpr4Δgpr5Δ*. IL-2 complex treatment increased the Th2 cell response to levels even higher than the fully virulent KN99α infection **(Fig. 2E)**. Treatment with IL-2 complexes also greatly reduced the survival time of infected mice **(Fig. 2F)** without affecting pulmonary fungal burden **(Fig. 2G)**. Uninfected mice treated with the same regimen of IL-2 complexes survived more than 30 days and remained healthy (**Fig. 2F**), indicating the IL-2 complex treatment targeted detrimental cells that were only present during infection. IL-2 treatment of infected mice also induced obvious lung pathology consistent with increased Th2 activity, noted by increased metaplasia of the bronchiolar epithelium and mucous obstruction of the airways **(Fig. 2H).** En masse, these data indicate that Th2 cells exacerbate pulmonary disease during fungal infection.

Th2 cells are primed at the site of infection by IRF4-dependent conventional dendritic cells.

The diminished Th2 response in the MLN compared to the lung led us to question whether lymphoid priming was required for Th2 cell induction during pulmonary fungal infection. Fms-like tyrosine kinase 3 ligand (Flt3L) is a differentiation factor for several hematopoietic cell subsets, and genetic deletion of Flt3L causes defects in antigen presenting cell traffic between the site of infection and secondary lymphoid organs (172). Flt3L deficient mice infected with *C. neoformans* neither experienced mediastinal

lymphadenopathy (**Fig. 3A**) nor elicited a polyclonal Th2 response in the MLN **(Fig. 3B)**. Surprisingly, the Th2 cell response in the lungs after *C. neoformans* infection was unaffected by Flt3L deficiency compared to wildtype animals **(Fig. 3C)**, indicating lymphoid priming is not required for pulmonary Th2 cell accumulation.

To determine the immune cell intermediate that primes Th2 cells in the lungs, we relied on the fact that Th cells are MHCII restricted. Three leukocyte subsets that express MHCII exist in the lungs of mice infected with *C. neoformans*: monocytes, CD11c+ cells, and B cells **(Fig. 4A)**. Of these, CD11c+ cells are the most abundant in the lungs during cryptococcal infection **(Fig. 4A)**. Consequently, we interrupted the specific interaction between CD11c+ cells and Th cells by generating mice with conditional deletion of MHCII in cells that express CD11c (CD11c-cre MHCII fl/fl) **(Fig. 4B)**. Unlike NOD/SCID/Rag mice that fail to generate mature Th cells, naïve CD11c-cre MHCII fl/fl mice produced an equivalent number of Th cells as naïve wildtype mice **(Fig. 4C)**, showing the peripheral Th cell compartment remained intact in CD11c-cre MHII fl/fl mice. Thus, conditional deletion of MHCII on CD11c+ dendritic cells allowed specific disruption of the interaction between the dendritic cells and the Th cells in the periphery. Pulmonary Th cell expansion during cryptococcal infection was completely abolished in CD11c-cre MHCII fl/fl mice **(Fig. 4C-D)**. Consequently, MHCII-bearing CD11c+ cells prime antigen-specific Th cells in the lungs of mice infected with *C. neoformans*.

CD11c+ cells are a heterogeneous group of macrophages and several dendritic cells (DC) subsets in the lungs (173). Therefore, we sought to discern the specific lineage of the CD11c+ antigen presenting cell that is responsible for pulmonary Th2 cell induction using an unbiased forward genetic screen of mouse lines genetically deficient in various CD11c+ subsets or their ability to interact with Th cells via MHCII (**S5A Fig.**). Lysozyme M (LysM)-cre MHCII fl/fl (macrophages and granulocytes (174)), BATF3-/- (CD103+ conventional dendritic cells (156)), and CCR2-/- (monocytes and monocyte-derived dendritic cells (175)) mice generated robust antigen-specific Th2 responses during cryptococcal infection **(S5-6 Fig.)**. Only mice deficient in CD11b+ conventional dendritic cells, abrogated using CD11c-cre IRF4 fl/fl mice, experienced blunted Th2 cell

accumulation with cryptococcal infection **(Fig. 4E-H)**. Therefore, our exhaustive search revealed lung-resident CDllc+ CDllb+ IRF4-dependent conventional DC (referred to as CD11b+ conventional DC) are uniquely required for Th2 cell induction in response to pulmonary cryptococcal infection.

Fungal chitin correlates with Th2 cell induction and subsequent disease.

Existing evidence and our data show CD11b+ conventional dendritic cells are capable of inducing both Th17 and Th2 cell responses to pulmonary fungal infection (176); therefore, these DC are not inherently programmed to specify a single Th cell lineage. Determination of Th2 cell fate by these lung resident DC must require higher order detection of specific features of the fungal infection. Many chitin-containing pathogens, as well as asthma/allergy models using purified chitin, evoke type-2 immunity (69, 100, 160). Consequently, the striking Th2 cell response to pulmonary fungal infection prompted us to explore the role of chitin as a Th2 cell adjuvant.

Maintaining chitin homeostasis is critical for cell wall integrity and microbe vigor. Chitin synthases that regulate cell wall chitin deposition are often essential for fungal viability or are part of a redundant pathway (177). As a result, studies that attempt to correlate loss-of-function mutations in chitin synthesis genes with modulation of the host response and attenuation of virulence would be challenging to interpret. Whether loss of Th2 cells and alterations in disease were due to a decrease in chitin, a loss of cryptococcal fitness/growth, or unmasking of other antigens due to modifications of the fungal cell wall or capsule would not be easily distinguishable (178).

In lieu of testing the requirement of chitin in Th2 cell induction, we exploited a natural property of *C. neoformans* to determine if increased fungal chitin was sufficient to expand Th2 cell formation. Approximately 20% of wildtype cryptococcal cells (KN99α) recovered from the lungs of infected mice increase in diameter from <10 μm to 15-100 μm (32-34). Previous studies have shown these enlarged cells, known as titan cells, exhibit increased thickness of the fungal cell wall (33). Using the fluorescent dye calcofluor white to measure chitin content in individual cells by epifluorescence microscopy **(Fig. 5A-B),** or at the population level with flow cytometry **(S7A Fig.)**, we

found the large *C. neoformans* titan cells contained more chitin, at a higher density, than the typical sized cells. *C. neoformans* produces several enzymes that deacetylate chitin to form chitosan (167, 178). Biochemical analyses additionally revealed that the amount of chitosan produced by titan cells and typical size cells did not differ, whereas chitin was significantly more abundant in the titan cells (**Fig. 5C**). Therefore, enhanced chitin content accompanied cell size increases during formation of cryptococcal titan cells.

To control for the relative effects of cell size and chitin content on Th2-mediated disease, we utilized several mutants of *C. neoformans*. A strain with targeted deletions in G protein-coupled receptor (*gpr*) 4 & *gpr*5 produces >95% typical sized cells *in vivo* (35), and these cells retain normal amounts of chitin **(Fig. 5A)**. Deletion of the transcription factor Rim101 (*rim101Δ*) abolishes titan cell production (35, 38), yet the typical sized cells have increased expression of chitin synthesis genes and elevated chitin content (179, 180) **(Fig. 5A).** Using these mutants, we were able to dissociate cryptococcal cell size from cell wall chitin as well as manipulate the total amount of chitin present during infection (**Table 2**).

We examined the impact of alterations in chitin content in *C. neoformans* on Th2 cell accumulation in the lungs. Antigen-specific Th cell priming and Th2 cell differentiation were reduced in mice infected with the low chitin *gpr4Δgpr5Δ* strain compared to infections with both the high chitin KN99α (due to titan cell production) and *rim101Δ* strains **(Fig. 5D-E)**. The Cda2-independent polyclonal Th2 cell response to *gpr4Δgpr5Δ* infection was also significantly lower than the responses to KN99α and *rim101Δ* infections **(S7B Fig.)**, indicating the defect in antigen-specific Th2 cell accumulation to *gpr4Δgpr5Δ* infection was not due to differential expression of *cda2* between the strains. Finally, the secreted Th2 cytokines IL-5, IL-13, and CCL5 present in lung homogenates from mice infected with *gpr4Δgpr5Δ* were significantly reduced compared to KN99α and *rim101Δ* infections **(Fig. 5F)**. Of note, secreted Th1 and Th17 cytokines, interferon-γ and IL-17A, did not concomitantly increase in response to *gpr4Δgpr5Δ* infection **(Fig. 5F)**. Thus, Th cells not receiving strongly polarizing Th2 signals in the *gpr4Δgpr5Δ* infection failed to acquire an alternate Th1 or Th17 cell differentiation fate. Since KN99α and *rim101Δ* strains contribute more total chitin to the

infection than the *gpr4Δgpr5Δ* strain **(Table 2, S7A Fig.)**, these data demonstrate that chitin abundance and not cell size positively correlated with Th2 cell response intensity.

Uncontrolled factors affected by the *gpr4Δgpr5Δ* or *rim101Δ* mutations could correlate with chitin levels and independently contribute to Th2 cell accumulation. To directly test if purified chitin can increase Th2 cell numbers, mice were infected with *gpr4Δgpr5Δ*, and <10 μm chitin particles were co-administered into the lungs. Chitin treatments partially rescued the attenuated Th2 cell response **(Fig. 5G)**. Importantly, this effect was observed in the clonal population of antigen-specific cells, and therefore, chitin increased the potency of Th2 cell induction during *C. neoformans* infection.

We examined the correlation between chitin, Th2 cell accumulation, and disease severity in our experimental model of cryptococcal infection. Infections with the high chitin strains, KN99α and *rim101Δ*, significantly hastened the time to death relative to mice infected with *gpr4Δgpr5Δ* **(Fig. 5H)**. Interestingly, all strains had equivalent pulmonary colony forming units at 14-days post-infection, indicating the differences in disease were not simply due to a failure to control the infection **(Fig. 5I)**, but rather paralleled the total amount of chitin present during infection **(Table 2)**. In summary, both chitin production by *C. neoformans* and Th2 cell accumulation directly correlated with exacerbation of lethal fungal disease.

Chitotriosidase deficiency confers resistance to Th2-mediated fungal disease.

We next investigated host intrinsic factors that could influence detrimental Th2 cell responses to chitin - specifically the mammalian chitinases, AMCase and Chit1. pH-sensitive differences in enzyme activity allow for an assessment of the contribution of each enzyme to chitin cleavage. Consistent with published reports, recombinant AMCase cleaved 4-methlylumbelliferone chitotriose across a broad pH range, whereas recombinant Chit1 was only active at less acidic pH **(Fig. 6A)** (181). Chitinase activity in lung homogenates from infected mice was significantly elevated compared with uninfected animals at pH 2 and pH 5 **(Fig. 6A).** Furthermore, lung homogenates from infected mice genetically deficient in Chit1 or AMCase both showed decreased cleavage of the fluorescent chitin substrate **(Fig. 6A).** These data indicate both chitinase enzymes

are active during pulmonary fungal infection, and genetic abolishment of these enzymes can be used to understand the effect of chitin degradation on Th2-mediated fungal pathogenesis.

To test the hypothesis that Th2 cell-associated disease depends on chitinases, we infected wildtype, Chit1-/-, and AMCase-/- mice with *C. neoformans* and quantified the Th2 cell response. Despite no differences in pulmonary fungal burden at 14-days post-infection **(S8A Fig.)**, Th2 cells were 10-fold less abundant in the lungs of infected Chit1-/- mice compared with wildtype controls **(Fig. 6B-C)**, and this trend was consistent with all the strains of *C. neoformans* tested **(S8B Fig.)**. Conversely, AMCase deficiency did not impact Th2 cell quantities after cryptococcal infection **(Fig. 6B-C)**. Furthermore, Chit1 deficiency and not AMCase deficiency also significantly extended the survival of mice infected with *C. neoformans* relative to age matched, wildtype animals **(Fig. 6D-E)**. The loss of Th2 cell accumulation with Chit1 deficiency was responsible for attenuation of disease, because the use of IL-2 complexes to boost Th2 cell numbers **(Fig. 6C)** and associated cytokines **(Fig. 6F)** also hastened lethal disease in Chit1-/- mice compared with infection-matched, untreated Chit1-/- controls **(Fig. 6D)**. Similar to our previous studies using the IL-2 complex, Th1 cytokine production in the Chit1-/- mice was only minimally affected by the IL-2 complex treatment (**Fig. 6F**). Thus, the presence of Chit1, and not AMCase, positively influences Th2 induction and subsequent disease.

Digestion of chitin via chitotriosidase promotes Th2 cell accumulation.

Chitin receptors in plants bind chitin oligomers (182), and chitin polymer size also influences the mammalian immune response to chitin (183, 184). Since appropriately sized chitin fragments could result from chitin digestion by Chit1, we used heterogeneous-length chitin and highly purified chitin heptamers to understand the effect of Chit1-associated degradation of chitin on Th2 cell accumulation. Although treatment with heterogeneous-length chitin augmented Th2 cell induction in wildtype animals infected with *gpr4Δgpr5Δ* cells **(Fig. 5F)**, it did not increase Th2 cell numbers in Chit1-/- mice **(Fig. 6G)**. Conversely, inoculation with mass equivalent amounts of chitin heptamers boosted the Th2 cell response in *C. neoformans*-infected animals with Chit1

deficiency **(Fig. 6G),** revealing the requirement for Chit1 in chitin polymer recognition can be bypassed by providing exogenous chitin fragments. Therefore, our data demonstrate a role for Chit1 in the chitin cleavage pathway that leads to Th2 cell accumulation.

We next examined how chitin fragments influence the upstream pathway of Th2 cell induction. To test the hypothesis that DC interact directly with chitin fragments, we cultured primary pulmonary leukocytes from infected mice in the presence of R-phycoerithrin-fluorophore conjugated chitin heptamers (RPE-GN7) or unbound REP-streptavidin (RPE-SA). While RPE-GN7 labeled a subset of B cells that have been shown to bind chitin (160), RPE-GN7 did not adhere to conventional CD11b+ DC **(S9A Fig.)**. Thus, we did not detect direct binding of chitin heptamers to the conventional DC. Furthermore, conventional CD11b+ DC stimulated *ex vivo* with PMA + ionomycin produced an important Th2 cell differentiation cytokine, IL-4, yet this DC subset did not express IL-4 upon stimulation with chitin heptamers (GN7) **(S9B Fig.)**. Combined, these data suggest the CD11b+ conventional dendritic cells may not sense chitin levels directly.

Pulmonary epithelial cells respond to chitin (101) and secrete several Th2-inducing alarmins, thymic-stromal lymphopoietin (TSLP), IL-25, and IL-33 (69, 185, 186). As a result, alarmin receptors on DC could potentially mediate the indirect recognition of chitin, leading to Th2 cell polarization during pulmonary fungal infection. We found CD11b+ conventional DC from the lungs of fungal infected mice expressed high levels of TSLP receptor, but not receptors for IL-25 or IL-33 **(S9C&D Fig.)**, indicating this DC subset is capable of sensing TSLP generated by epithelial cells. Taken together, our data suggest Th2 cell induction by conventional CD11b+ DC appears to involve an indirect recognition of chitin oligomers.

Chitotriosidase activity correlates with cryptococcal infection in humans.

The importance of Chit1 in promoting Th2 cell-mediated disease in an experimental model of cryptococcosis prompted us to investigate the relevance of chitotriosidase activity in human fungal disease. Blood samples were collected from human donors: 46 Ugandan patients presenting at the hospital for the first time with

AIDS and 38 similar AIDS patients experiencing acute cryptococcal disease **(S1 Table)**. We analyzed chitotriosidase and AMCase enzymatic activity in plasma from each group as described for the mouse lung homogenates. Chitin substrate cleavage at pH=5 was significantly elevated in plasma from AIDS patients with cryptococcal infection when compared to AIDS patients without cryptococcal infection **(Fig. 6H)**. Comparatively low levels of enzymatic activity were detected at pH=2 for each group, indicating that chitotriosidase and not acidic mammalian chitinase is the predominate chitinase produced by humans with cryptococcal infection **(Fig. 6H)**.

To determine if the difference in chitotriosidase activity was due to an inherent propensity or deficiency in chitotriosidase expression, we used cryptococcal lysate antigens to stimulate chitinase production in whole blood samples from the human donors. Stimulation of whole blood from all patients induced robust chitotriosidase activity relative to unstimulated samples, and chitinase activity did not differ between the groups **(Fig. 6H)**, indicating all human donors had equivalent capacity to produce chitotriosidase. Chitinase activity was not detectable in pure cryptococcal culture supernatants or cryptococcal lysate antigens (**S10 Fig.**), and as a result, the chitinase activity detected in the assays with human samples was not due to *Cryptococcus*-derived chitinases. Taken together, we conclude that fungal antigen induces chitotriosidase activity in humans experiencing cryptococcosis.

DISCUSSION

An association between pulmonary fungal exposure and allergic Th2 inflammation is well established (53, 75). Fungal proteases (99) and fungal chitin (187) impact the innate immune responses underlying allergic inflammation, but elements of Th2 cell induction are enigmatic. Using an experimental model of pulmonary cryptococcosis, we demonstrated that inhalation of *C. neoformans* establishes a robust pulmonary infection, and the potent antigen-specific Th2 cell accumulation required lung resident CD11b+ conventional DC. Since these CD11b+ conventional DC can stimulate Th2 or Th17 cell differentiation in response to *C. neoformans* and *Aspergillus fumigatus* exposure respectively (176), these DC must interpret specific features of the infection to direct Th2 cell fate. To this end, we found cryptococcal chitin and exogenous administration of chitin particles correlated with increased Th2 cell accumulation. We further showed that chitotriosidase activity was highest in mice and humans infected with *C. neoformans*, and Chit1 was necessary for efficient Th2 cell induction and disease in our murine model of cryptococcosis. Taken together, these data indicate the host response to fungal chitin is an important factor that enhances Th2 cell production during pulmonary fungal infection.

Our findings narrow an important gap in the mechanism of pattern recognition of fungal chitin in the lungs **(Fig. 7)**. We have shown Chit1 functions as a "gatekeeper" in making chitin fragments available to host surveillance, thereby promoting Th2 cell accumulation and disease. Additionally, the use of pharmaceutical grade chitin heptamers to augment Th2 cell responses establishes a new minimum component for chitin recognition in vertebrates. While we did not detect direct interactions between the CD11b+ conventional DC and labeled chitin *ex vivo*, other systems have shown chitin binding to the mannose receptor and subsequent recognition by TLR9 and/or NOD2 (188). Alternatively, pulmonary allergy models demonstrate that lung epithelial cells recognize chitin fragments and produce the necessary alarmins for Th2 cell induction: TSLP, IL-25, and IL-33 (185, 186, 189). In our model, CD11b+ conventional DC express high levels of TSLPR. Finally, natural IgM has been shown to bind fungal carbohydrates,

including chitin, and facilitate the interaction of DC and fungal carbohydrates (160). Signals, such as alarmins or antibody-chitin complexes, could be received by CD11b+ conventional DC to direct Th2 cell differentiation via IL-4 or another novel pathway.

A major impediment in understanding Th cell responses to pulmonary fungal infection has been the lack of reagents to detect antigen-specific Th cells. Antigen-specific reagents are particularly important when examining Th2 responses, because Th2 cells can be induced by the wounding that occurs during infection. Our ability to track endogenously derived, antigen-specific Th cells with pMHCII tetramers (190) allowed us to present for the first time that Th2 cells produced in response to fungal pathogens are not part of a generalized wound healing response but are fungal-antigen specific. Unlike T cell receptor transgenic approaches, pMHCII tetramers permitted us to monitor the population of infection-specific Th cells in the polyclonal repertoire, while maintaining physiologic precursor frequency and clonal expansion. Thus, we are able to examine the Th cell response during the natural course of infection and keep all other variables constant. The availability of these pMHCII tetramers will undoubtedly empower cryptococcal researchers and accelerate the field of fungal immunology.

The use of IL-2 complexes allowed us to conveniently and reliably augment the Th2 cell response to further understand unappreciated elements underlying Th2-mediated disease. This strategy is amenable to any host or microbial genetic model, which facilitates direct comparisons. Also, this gain-of-function approach permitted us to test the sufficiency of Th2 cells to exacerbate disease. These data, combined with loss-of-function studies by other groups (62, 191), alter the longstanding paradigm that susceptibility to lethal fungal disease is traditionally viewed as a breakdown in protective immunity. This paradigm is supported by the higher prevalence of invasive fungal disease in immunosuppressed individuals, including people living with HIV/AIDS, cancer patients undergoing chemotherapy, and solid organ transplant recipients. However, we propose that in addition to the lack of a protective response, an independent development of a harmful Th2 cell response further exacerbates disease. This is particularly important in the the case of human cryptococcocosis were a compromised immune system not only lacks sufficient quantities of lymphocytes to resolve the fungal

infection, but the residual Th cell repertoire is plastic and detrimentally influenced by the microbe (6, 57, 58, 148).

A subset of innate lymphoid cells (ILC) produce the Th2 cytokines, IL-5 and IL-13 (192), and these so-called ILC2 have been shown to contribute to allergic airway disease (97). While IL-2 complex treatment dramatically increases Th2 cell accumulation and enhances pulmonary disease, ILC numbers are not affected by IL-2 complex treatment in our model. Likewise, CD25+ ILC2 exist in the lungs under homeostatic conditions (193), yet uninfected mice exhibit no ill effects of IL-2 complex treatment. However, the developmental relationship of ILC2 to lymphocytes, combined with the lack of lineage markers expressed by ILC, make it challenging to separate the relative effects of Th2 cells and ILC2 in driving immunopathology. Thus, our conclusion that Th2 cells are vital mediators of disease does not categorically exclude the participation of ILC2 in this process.

CD11b+ conventional DC are an ontologically distinct mononuclear phagocyte subset that require IRF4 for maturation (156). Although it has been suggested that this subset is also functionally unique in programing specific Th cell differentiation, building evidence seems to indicate a plastic role of these cells in Th cell induction. CD11b+ conventional IRF4-dependent DC have been shown to coordinate Th2 cell priming following protease inoculation and worm infection in the skin (194), as well as house dust mite extract installation in the lungs (195). However, several research groups have found the same DC subset, using identical host genetic systems, can control Th17 cell differentiation in the gut under homeostatic conditions (196) and the lungs after fungal infection (176). While these observations infer that CD11b+ conventional DC are plastic, these cells may have different functions in the skin and gut compared to the lungs that could explain their role in priming Th17 and Th2 cell responses. Our findings showing Th2 priming by *C. neoformans*, combined with work by Schlitzer et al. showing IRF4-dependent DC are capable of priming Th17 cells in response to *A. fumigatus* to pulmonary fungal infection, highlight a fatal flaw in the notion that DC subsets are inherently specialized to control Th cell lineage fate. As a result, we explored an

alternative hypothesis that higher order signals (e.g. chitin recognition) are required for pulmonary CD11b+ conventional DC to promote Th2 cell priming to fungal infection.

Gene deletions in microbes can cause pleiotropic phenotypes, as seen in the *rim101Δ* strain (35) that can complicate interpretation of the effects of these mutations on host responses. However, the data obtained from the mutants utilized in this study support the conclusion that fungal chitin promotes Th2-mediated disease for several reasons. First, equivalent fungal burden in the lungs at 14 days post-infection indicates these mutations do not confer an inherent survival advantage or disadvantage for the fungus, and any effect the mutants have on leukocyte accumulation or disease is not simply driven by antigen load. Second, Rim101 transcriptionally controls many elements associated with cryptococcal virulence, including pH responses, encapsulation, cell enlargement, and iron sequestration (37). While individual mutations in each of these pathways should result in a loss of virulence, the *rim101Δ* mutants paradoxically exhibit equivalent or accelerated disease (179). Altered expression of cell wall synthesis genes combined with unmasking of the cell wall has been posited (179, 180), and in particular, our data implicate cell wall chitin in enhancing fungal pathogenesis associated with *rim101* deficiency. More importantly, we view *rim101Δ* as an essential control for the effect cryptococcal cell size has on Th2 cell formation more than an independent test of the hypothesis that fungal chitin drives Th2 cell priming. Thus, we needed a strain of *C. neoformans* that produces mostly small cells but retained elevated chitin density to offset the loss of elevated chitin density with titan cell deficiency. At a minimum, these data prove that large cryptococcal cell size is not driving robust Th2 cell accumulation. Finally, due to the structural similarities, as well as the interdependent synthetic pathways, it is extremely challenging to decouple how chitin and chitosan separately impact a complex biological system. Although we cannot rule out immunomodulatory effects of chitosan in our experiments with *C. neoformans* mutants, we have confirmed chitin alone, when provided as an adjuvant, is sufficient to augment Th2 cell accumulation. Interpretation of the *Cryptococcus* chitin mutant data in the context of our additional data regarding host recognition of exogenous chitin builds a compelling argument that fungal chitin promotes detrimental Th2 cell induction.

Acidic mammalian chitinase has been previously implicated in innate type-2 responses (197). However, a head-to-head comparison of the effect of both mammalian chitinases, chitotriosidase and acidic mammalian chitinase, has never been performed in any model, much less in the context of Th2 cell responses to fungal infection. Surprisingly, chitotriosidase, and not acidic mammalian chitinase, influenced Th2 cell accumulation and disease during pulmonary fungal infection. While no direct explanation exists, the different patterns of expression of AMCase and Chit1 could explain our results. AMCase is produced by a number of cells including several leukocyte subsets and pulmonary epithelial cells, whereas Chit1 expression is restricted to mononuclear phagocytes, including DC (181, 198). Since these DC are the main coordinators of antigen presentation to CD4+ T cells, the close proximity of chitin degradation and recognition likely allows the DC to efficiently influence the fate of CD4+ T cells during pulmonary fungal infection. Furthermore, the varying pH-dependent enzymatic activity of Chit1 and AMCase suggest these enzymes may function in disparate anatomical and subcellular compartments that may bias their participation in response to pulmonary fungal infection.

Considering Th2 cell responses likely evolved to resist parasitic infection (161), the asymmetric global distribution of *CHIT1* alleles (199) combined with the data presented herein offers a unique perspective on why individuals from tropical regions with endemic parasites tend to experience frequent and severe mycosis (8, 200-203). Ethnic groups historically residing in regions with highly prevalent parasites like *Strongyloides* tend to maintain functional *CHIT1*, whereas populations from more temperate climates with lower endemic parasitic burdens frequently possess enzymatically inactive *CHIT1* alleles (199). Perhaps continuous fungal exposure in the absence of parasitic encounters provides sufficient negative selection pressure to eliminate functional *CHIT1* alleles from these populations (e.g. Europe). Conversely, ethnic groups historically residing in tropical areas (e.g. Africa) that maintain functional *CHIT1* alleles may have enhanced protection against common parasitic exposures, while these same individuals experience exacerbation of Th2-mediated fungal disease (8, 202, 203).

In conclusion, we elucidated a novel mechanism of Th2 cell induction during fungal infection. CD11b+ DC, and importantly recognition of chitin via Chit1, drives the generation of deleterious Th2 cells responding to pulmonary fungal infection. Next generation anti-fungal treatments should not only block fungal growth, but should also target the host immune response. A recent trial used IFNγ in combination with traditional anti-fungal therapy to promote beneficial immune responses. This treatment improved cryptococcal clearance, yet it had no significant impact on patient survival (55). Our study suggests treatments that additionally aim to suppress the pathologic Th2 response, perhaps through chitotriosidase inhibition, may be necessary to improve clinical outcomes. Ultimately, the coordinated efforts of microbiologists, immunologists and infectious disease physicians will enable personalized medicine approaches that effectively combat lethal fungal infections by inhibiting fungal growth, promoting beneficial host responses, and dampening pathologic inflammation.

MATERIALS AND METHODS

Ethics Statement. This study was approved by the institutional review boards of the University of Minnesota, Makerere University, and the Uganda National Council of Science and Technology. Written informed consent was obtained from all human participants prior to inclusion in the sutdy, and all data were de-identified (204). All animal experiments were done in concordance with the Animal Welfare Act, U.S. federal law, and NIH guidelines. Mice were handled in accordance with guidelines defined by the University of Minnesota Institutional Animal Care and Use Committee (IACUC) protocol numbers 1010A91133 and 1207A17286 and University of Massachuesets IACUC protocol number A-1802.

Mice. All mice used in this study were derived from a C57BL/6 background. C57BL/6J, LysM-cre (B6.129P2-*Lyz2*$^{tm1(cre)Ifo}$/J), CD11c-cre (B6.Cg-Tg (Itgax-cre) 1-1Reiz/J), MHCII *loxP* (B6.129X1-*H2-Ab1*^{tm1Koni}/J), Batf3 -/- (B6.129S(C)-*Batf3*$^{tm1Kmm/J}$), CCR2 -/- (B6.129(Cg)-*Ccr2*$^{tm2.1Ifc/J}$), B6.129(Cg)-*Foxp3*$^{tm3(DTR/GFP)Ayr}$/J) mice were purchased from Jackson Laboratories (Bar Harbor, ME) and Flt3L -/- (C57BL/6-$_{flt3L}$*tm1Imx*) were purchased from Taconic (Hudson, NY). Crosses were performed when necessary to generate the mouse strains used in this study, as indicated in **S2 Table**. Chit1 -/- (205) mice were infected and processed in the laboratory of Kirsten Nielsen. AMCase -/- (206) mice were infected and processed in the laboratory of Stuart Levitz per MTA stipulations. All mice were housed in specific pathogen–free conditions.

Cryptococcus. *Cryptococcus neoformans* var. *grubii* strains were streaked on yeast peptone dextrose (YPD) agar plates and incubated for 2 days at 30°C. YPD broth was inoculated with colonies from the aforementioned plate and incubated for 16 hours at 30°C with gentle agitation. The inoculum was prepared by pelleting the culture, washing 3 times with phosphate buffered saline (PBS), and resuspending in PBS at a concentration of $2x10^6$ cells/mL. All strains used in this study were on a KN99α genetic background, and the complemented strains have wildtype phenotypes (35, 38, 167).

Infection. A well established intranasal pulmonary aspiration model of cryptococcosis was used for this study (207). 6-8 week old, sex-matched mice were anesthetized with pentobarbitol or isoflurane. $5x10^4$ cryptococcal cells in 25 μL of PBS was placed on the nares of each mouse, and the mice aspirated the inoculum into the lower respiratory tract. Finally, the mice were suspended by their incisors for 5 minutes and subsequently placed upright in their cage until regaining consciousness. For survival studies, ten mice per group were infected as described above. Animals were monitored for morbidity and sacrificed when endpoint criteria were reached. Endpoint criteria were defined as 20% total body weight loss, loss of 2 grams of weight in 2 days, or symptoms of neurological disease.

Tetramer Production. Nine amino acid peptides from Cda2 were selected using a MHCII loading algorithm (208). pMHCII tetramers were produced as previously described (209). In short, biotinylated pMHCII monomers were expressed in *Drosophila melanogaster* S2 cells and isolated from culture supernatants by affinity chromatography. Streptavidin-Phycoerythrin (Prozyme) was added to pMHCII monomers at a 4:1 molar ratio. Finally, tetramer formation was assessed by western blot analysis.

Pulmonary Leukocyte Preparation. Lung leukocytes were isolated as previously described (210). Briefly, lungs were excised and minced to generate approximately 1 mm^3 pieces. The lung mince was incubated in HBSS (Invitrogen, Grand Island, NY) + 1.3 mM EDTA solution for 30 min at 37°C with agitation, and then transferred to RPMI-1640 (Invitrogen) medium supplemented with 5% Fetal Bovine Serum (FBS) (Invitrogen) and 150 U/ml type I collagenase (Invitrogen) and incubated for 1 h at 37°C with agitation. The cells were passed through a 70 μm filter, pelleted, and resuspended in 44% Percoll-RPMI medium (GE Life Sciences, Pittsburgh, PA). A Percoll density gradient was created (44% top, 67% bottom), and the samples were centrifuged for 20 min at 650 x *g*. The leukocytes at the interface were removed, washed 2 times with RPMI medium, and resuspended in PBS + FBS at a concentration of 10^7 cells/ml. CD4+ T cells were enriched using a Dynabeads CD4+ T Cell Negative Isolation Kit (Life

Technologies, Grand Island, NY) per manufacture's instructions. After enrichment, ~10^6 cells were suspended in 200 μL of restimulation buffer (RPMI + 10% FBS + 1% Penicillin/Streptomycin + 5 μg Brefeldin A) with (stimulated) or without (unstimulated) 10 ng phorbol myristate acetate (PMA) and 50 ng ionomycin. After 6 hours, the cells were washed and immediately prepared for flow cytometry.

IL-2 Complexes. 5 μg of murine IL-2 cytokine (Biolegend) and 25 μg of clone JES6-1A12 anti-IL-2 antibody (Bio X Cell, West Lebanon, NH) were added to 100 μL of PBS at room temperature. Each mouse received intraperitoneal injections of IL-2 complexes every other day beginning at 5 days post-infection.

Flow Cytometry. Samples were incubated for 5 minutes with CD16/32 antibody (Biolegend) to block the Fc receptor and prevent nonspecific antibody binding. 25nM Cda2-tetramer was added to the sample and incubated at 25°C for 1 hour in the dark. Samples were surface-stained at 4°C for 30 minutes with the following antibodies (see gating **S1 Fig.**): CD4 (RM4-5, BV605, Biolegend), CD8 (53-6.7, APC-eFluor 780, eBioscience, San Diego, CA), CD11b (M1/70, PE-Cy5, eBioscience), CD11c (N418, PE-Cy5, eBioscience), B220 (RA3-6B2, PE-Cy5, eBioscience), and CD44 (IM7, Alexa Fluor 700, Biolegend). The cells were then incubated in Foxp3 Transcription Factor Buffer (eBioscience) at 4°C for 30 minutes. The cells were labeled with antibodes against the following intracellular antigens: Foxp3 (FJK-16s, FITC, eBioscience), IL-5 (TRFK5, APC, Biolegend), IL-13 (eBio13A, eFluor 450, eBioscience), IL-17A (TC11-18H10.1, BV650, Biolegend), and IFNγ (XMG1.2, PE-Cy7, eBioscience). 1:200 antibody concentrations were used for surface staining, and 1:100 antibody concentrations were used for intracelluar staining. For data acquisition, events from the entire sample (500,000-1,000,000) were collected on a BD FACSCanto II flow cytometer (BD Biosciences, San Jose, CA), and the data were analyzed with FlowJo X (Tree Star Inc., Ashland, OR).

To account for cell loss during CD4+ T cell enrichment and mitogen restimulation, several calculations were performed. Total leukocyte numbers were

determined by hemacytometer count after Percoll density gradient separation. 2.5% of the sample was stained with the following antibodies: Ly6G (RB6-8C5, APC-eFluor 780, eBioscience), Ly6C (HK1.4, eFluor 450, eBioscience), CD11b (M1/70, BV650, Biolegend), CD11c (N418, BV605, Biolegend), NK1.1 (PK136, AF700, Biolegend), CD3 (17A2, PE-Cy5, Biolegend), CD4 (RM4-5, FITC, Biolegend), CD19 (6D5, PE-Cy7, Biolegend), Sca1 (D7, APC, Biolegend), and Siglec F (E50-2440, PE, BD Biosciences). Cells were identified as the following (see gating **S2 Fig.**): Th cells = CD11b- CD3+ CD4+. Eosinophils = CD11b+ CD11c- Siglec F+. Innate lymphoid cells = lineage- Sca1+. Dendritic cells and macrophages = CD11b+ CD11c+ Siglec F-. B cells = Siglec F- CD11b- CD11c- CD19+. Natural killer cells = Siglec F- CD11c- NK1.1+. Neutrophils = CD11b+ CD11c- Ly6G+. Monocytes = CD11b+ Ly6C+ Siglec F-. CD8+ T cells = Siglec F- CD11b- CD3+ CD4-. The proportion of CD4+ T cells was determined by flow cytometry, and this percentage was multiplied by the total number of lung leukocytes to calculate the number of CD4+ T cells per pair of lungs. The number of CD4+ T cells in the unstimulated, CD4+ T cell enriched sample was calculated after flow cytometric analysis, as described in the previous paragraph. The number of CD4+ T cells recovered in the unstimulated, enriched sample was divided by the total number of CD4+ T cells to calculate the CD4+ T cell isolation efficiency. Cell death due to mitogen restimulation was calculated by dividing the number of CD4+ T cells recovered in the stimulated sample by the number of CD4+ T cells recovered in the unstimulated sample. The number of Cda2+ Th2 cells was determined by dividing the number of Cda2+ IL-5 and/or IL-13+ positive cells by the CD4+ enrichment and cell viability indices.

Dendritic cell subsets were determined using the following antibodies and gating strategy. CD3 (17A2, PE-Cy5, Biolegend), CD19 (6D5, PE-Cy5, Biolegend), Siglec F (E50-2440, APC, BD Biosciences), CD64 (X54-5/7.1, PE, Biolegend), MHCII (M5/114.15.2, AF700, Biolegend), CD11c (N418, BV605, Biolegend), CD11b (M1/70, BV650, Biolegend), CD103 (2E7, e450, eBioscience), FcεRI (MAR-1, PE-Cy7, Biolegend), TSLPR (PE, R&D Systems), IL-25R (9B10, PE, Biolegend), IL-33Rα (DIH9, PE, Biolegend), IL-4 (BVD6-24G2), PE, Biolegend), and GN7-PE (211). See gating **S5B Fig.** Dump = CD3+, CD19+, Siglec F+. Monocyte-derived DC = Dump-,

CD64+, CD11c+, MHCII+, CD11b+, CD103-, FcεRI+. CD103+ cDC = Dump-, CD64-, CD11c+, MHCII+, CD103+, CD11b-. CD11b+ cDC = Dump-, CD64-, CD11c+, MHCII+, CD11b+, CD103-. While CD103, CD11b, FcεRI, and CD64 surface markers allow convenient detection of each DC subset, it is unclear whether other developmentally and/or functionally unrelated cells can express similar markers. Consequently, genetic blockade in the developmental pathways of each DC subset were assumed to be completely penetrant, notwithstanding the persistence of cells expressing surrogate markers for each ontological subset.

Lung Cytokines. Lungs from mice 14-days post-infection were excised, snap frozen in liquid nitrogen, and homogenized in 3 mL of T-PER (Thermo Fisher Scientific) with Complete Protease Inhibitor Cocktail (Roche, Indianapolis, IN). The lung homogenate was pelleted, and the supernatant was collected and stored at -80°C until analysis. Samples were diluted 1:4 in assay buffer immediately before processing. Cytokines were quantified using Luminex technology according to manufacturer instructions (Bio-Rad, Hercules, CA).

Lung Histology. Lungs were removed from mice 14 days post-infection, perfused via the right ventricle with cold PBS, inflated with 10% formalin (Thermo Fisher Scientific, Rockford, IL), and placed in a container of 10% formalin. Tissues were dried with organic solvent, embedded in parafin, sectioned, and stained with hematoxylin and eosin, before images were captured.

Fungal Chitin/Chitosan Quantification. Cryptococcal cells were isolated from the lungs after enzymatic digestion and density gradient separation, as described above. Cells were fixed with 3.7% formaldehyde and stored at 4°C until analyzed. The cells were standardized to $1x10^6$ cells/mL and stained for 2 minutes at 25°C with 1 μg/mL of Calcofluor White (Sigma Aldrich, St. Louis, MO) (212). Cells were washed and immediately processed with an epifluorescence microscope (Axio Imager M1, 40X/0.6 lens, Zeiss Filter Set 02, Axio Cam MRc5, Axiovision 4.8; Carl Zeiss, Inc., Munich,

Germany). ImageJ software (NIH.gov) was used to calculate fluorescence intesity per pixel. For flow cytometry, large and typical sized cells were first gated by forward scatter properties to distinguish size. Chitin/chitosan content was then determined by 405 nm laser excitation and fluorescence detection at ~450 nm.

Biochemical chitin/chitosan quantification was adapted from Banks et al. (178). Purified titan cell (>15 μm) and typical sized cell (<15 μm) samples collected from infected mice were each divided into two aliquots: one treated with acetic anhydride to fully acetylate the chitin/chitosan polymer and the other was left untreated. 5 μl of purified *Streptomyces griseus* chitinase (5 mg/ml in PBS) was added to hydrolyze chitin to *N*-acetylglucosamine (GlcNAc) and samples were incubated for 3 days at 37°C. For colorimetric determination of GlcNAc, the Morgan-Elson method was adapted for microplate readers. Chitinase-treated samples were incubated with 0.27 M sodium borate (pH 9.0) and heated at 99.9°C for 10 minutes. Immediately upon cooling to room temperature, freshly diluted 10X DMAB solution (10 g p-dimethylaminobenzaldehyde in 12.5 ml concentrated HCl and 87.5 ml glacial acetic acid) was added, followed by incubation at 37°C for 20 minutes. Absorbance at 585 nm was recorded for each sample. Standard curves were prepared from stocks of 0.2 to 2.0 mM of GlcNAc (Sigma). The amount of GlcNAc was calculated as mol/g cells (dry weight). The acetylated samples contained chitin plus chitosan, and the untreated sample contained chitin. The difference between the two measurements estimated the amount of chitosan.

Exogenous Chitin. Chitin was prepared as previously published (101). Chitin from shrimp shells (Sigma Aldrich) was pulverized with a mortar and pestle. 12.5N HCl was added, and the slurry was incubated at 40°C for 30 minutes. Chilled 10N NaOH was added until a neutral pH was attained. The sample was centrifuged at $2x10^4$ *g* for 5 minutes, the supernatant was decanted, and the sample was suspended in deionized water (dH_2O). This step was repeated 3 times followed by a wash in ethanol. The sample was pelleted, suspended in dH_2O, and filtered through a 10μm membrane (EMD Millipore, Billerica, MA). The solution containing <10 μm chitin was dried with a SpeedVac (Thermo Scientific, West Palm Beach, FL). The powder was weighed and resuspended in

PBS to make a concentration of 50 mg/mL (i.e. 10X). Endotoxin was measured by Limulus amebocyte lysate assay (Associates of Cape Cod, East Falmouth, MA) and was found to be less than 0.03 EU/mL. Chitin heptamers were purchased from Carbosynth (Berkshire, UK). Mice were anesthetized and allowed to aspirate 125 μg of chitin suspended in 25 μL of PBS into the lungs at 0, 5, and 10 d.p.i. Pulmonary leukocytes from wildtype mice 14 days post-infection with KN99α were cultured and stimulated *ex vivo* for 5 hours with PMA + ionomycin (as previously described for Th cells) + 125 μg of chitin heptamers + golgi stop, or golgi stop alone (unstimulated) before processing by flow cytometry.

Chitinase Activity. CycLex Acidic Mammalian Chitinase (AMCase) and Chitotriosidase (Chit1) Fluorometric Assays (MBL International, Woburn, MA) were used to detect chitinase activity. In brief, each of the following were added to pH 2 and pH 5 buffers containing 4-Methylumbelliferyl Chitotriose: 25 ng of recombinant AMCase, 25 ng recombinant Chit1, 10 μL of mouse lung homogenate, 10 μL of human plasma, 10 μL of lysate antigen, or 10 μL of culture supernatant of KN99α grown in YPD. The samples were incubated at 37°C in a Synergy H1 Microplate Reader (Biotek, Winooski, VT) and 360 nm excitation/450 nm emission readings were obtained every 2 minutes. The relative fluorescent units (RFU) at 1 hour of incubation were compared to the RFU of serial dilutions of 4MU standard, and the molar concentration of cleaved chitin was calculated.

Antigen Stimulation of Whole Blood. The assay was performed as previously described (6). Cell wall antigens were prepared from *Cryptococcus neoformans*, strain KN99α. The cells were flash frozen in liquid nitrogen, combined with glass beads, and vortexed vigorously for 2 hours at 4°C to disrupt the cells. The insoluble fraction (i.e., cell wall) was analyzed for protein concentrations (bicinchoninic acid protein assay; Thermo Fisher Scientific, Rockford, IL). Endotoxin levels in all antigen preparations were undetectable (<0.06 U/ml) by *Limulus* amebocyte lysate assay (Associates of Cape Cod, East Falmouth, MA). Whole-blood samples were obtained from AIDS patients at screening for the *Cryptococcus* Optimal Timing of Anti-retroviral Therapy Trial in Sub-Saharan

Africa (204). Peripheral blood samples from each subject were drawn into lithium heparin tubes, diluted 2-fold with PBS, and dispensed into a tissue culture plate. Cell wall antigens containing 5 μg of protein were added to the wells, and PBS was used as the "unstimulated" control. The plates were incubated at 37°C in 5% CO_2 for 20 hours. After incubation, the plasma was separated from the cells and stored at 4°C until chitinase activity analysis.

Statistics. *P*-values for pairwise comparisions were by Mann-Whitney *U* with Bonferroni adjustments for multiple comparisons. Global tests were by Kruskal-Wallis ANOVA. Surival curves were compared with Mann-Whitney tests. Power calculations were performed to assess appropriate sample size for all experiments. *P*-values ≤ 0.05 were considered statistically significant. All statistics and graphs were processed with Prism 6 (GraphPad Software, La Jolla, CA).

ACKNOWLEDGEMENTS

We thank Jon Linehan and Jennifer Walter for technical assistance with tetramer development, the University of Minnesota Flow Cytometry Core Facility for instrumentation, and the University of North Carolina Lineberger Comprehensive Cancer Center Animal Histopathology Core Facility. AMCase deficient mice were kindly provided by Lori Fitz (Pfizer) and Thomas Wynn (NIAID).

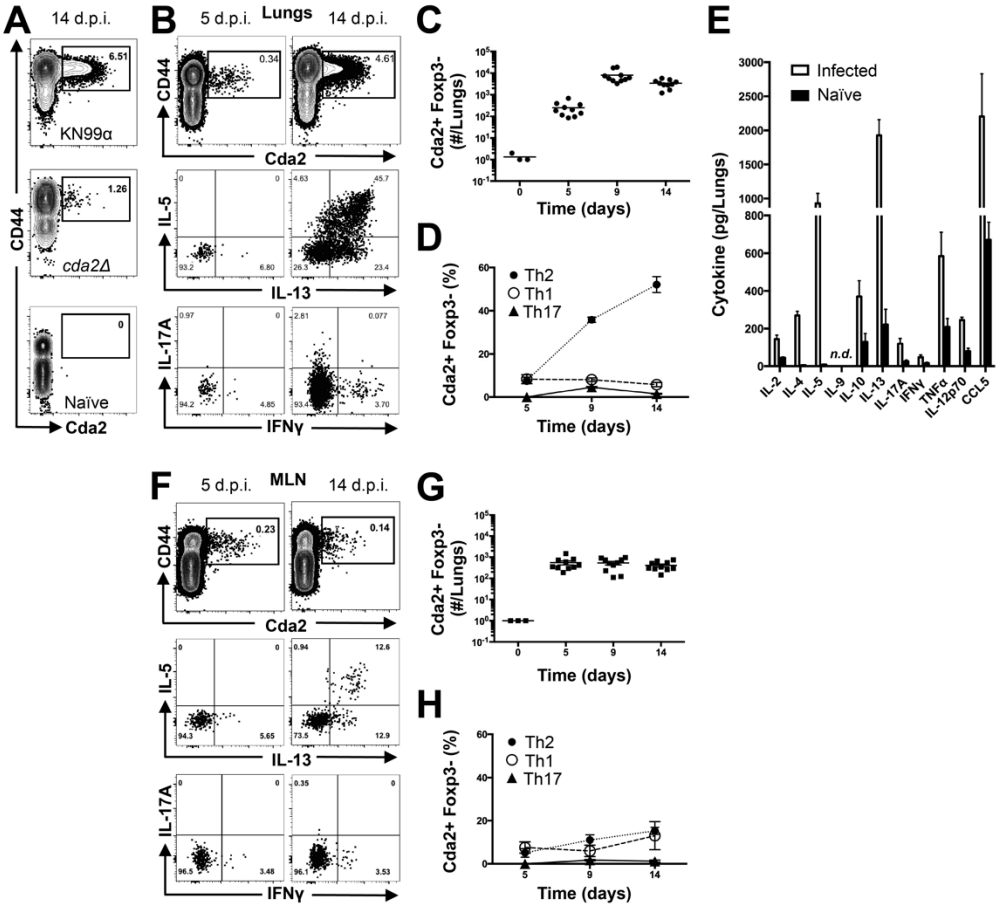

Figure 1. Type-2 Helper T Cells Accumulate in the Lungs of Mice Infected with *C. neoformans*. (**A**) Cda2-MHCII tetramer identifies *C. neoformans*-specific helper T (Th) cells from mice 14 days post-infection with strain KN99α, *cda2Δ*, or age-matched, naïve mice. Flow cytometry plot (**B**) or graphs (**C&D**) from lung digests showing CD4+, Foxp3-, CD44+ Cda2+ Th cells expressing Th1 (IFNγ), Th2 (IL-5 & IL-13), or Th17 (IL-17A) cytokines. (**E**) Cytokines from lung homogenates 14 days post-infection with KN99α or age-matched, naïve mice. Flow cytometry plot (**F**) and graphs (**G&H**) from mediastinal lymph node suspensions of Th cells expressing Th1, Th2, or Th17 cytokines. Data are presented as mean +/- standard error with 2 independent experiments of at least 5 mice per group. Cda = Chitin deacetylase, CCL = chemokine ligand, IFN = interferon, IL = interleukin, MLN = mediastinal lymph node, TNF = tumor necrosis factor

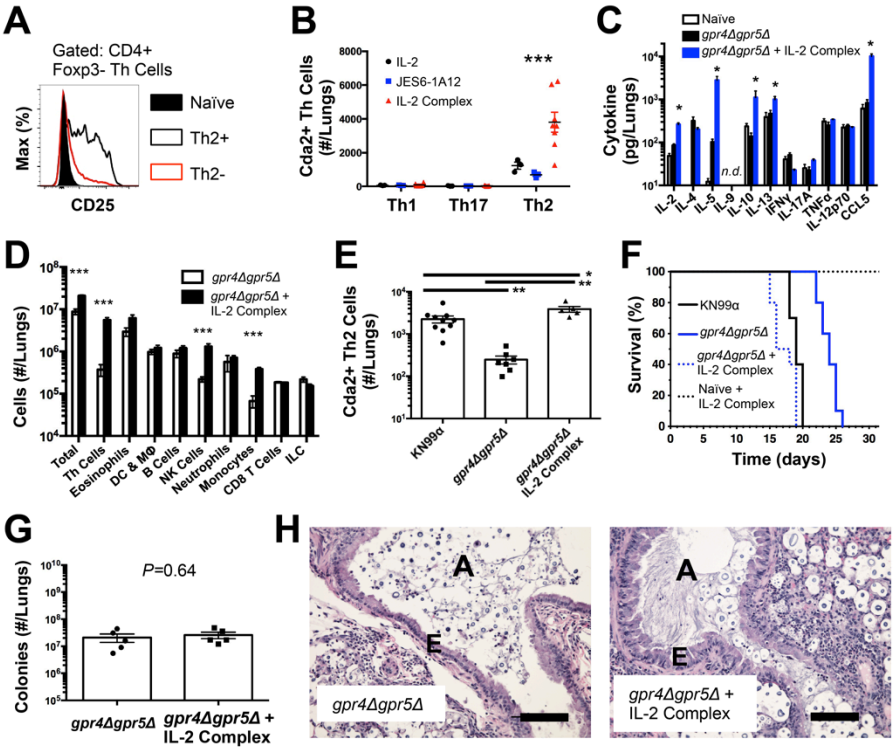

Figure 2. IL-2 Complexes Augment Type-2 Helper T Cells and Enhance Fungal Disease. (**A**) CD25 expression by naïve (CD4+, CD44-), Th2- (CD4+, CD44+, IL-5-, IL-13-), and Th2+ (CD4+, CD44+, IL-5+, IL-13+) cells. (**B**) Cda+ Th cell numbers in the lungs of *gpr4Δgpr5Δ* infected mice treated with 5 µg IL-2, 25 µg anti-IL-2 antibody (JES6-1A12), or both (IL-2 Complex). Th1, Th17, and Th2 cells were identified by production of IFNγ, IL-17A, and IL-5/13, respectively. (**C**) Cytokines from lung homogenates of mice infected with *gpr4Δgpr5Δ* or age-matched naïve animals, with or without IL-2 complex treatment. (**D**) Pulmonary leukocytes from mice infected with *gpr4Δgpr5Δ*, with or without IL-2 complex treatment. (**E**) Cda2+ Th2 cells from lungs of mice infected with fully virulent KN99α, attenuated *gpr4Δgpr5Δ*, or mice infected with *gpr4Δgpr5Δ* and treated with IL-2 complex. (**F**) Survival of naïve mice or mice infected with *gpr4Δgpr5Δ* either with or without IL-2 complex treatment. *P*-value represents log-rank test comparing each survival curve with 10 mice per group to: *gpr4Δgpr5Δ* vs. *gpr4Δgpr5Δ* + IL-2 complex, $P<0.0005$; *gpr4Δgpr5Δ* vs. KN99α, $P<0.0005$; *gpr4Δgpr5Δ* + IL-2 complex vs. KN99α, $P=0.23$. (**G**) Fungal burden within lungs of mice with or

without IL-2 complex 14 days post-infection with *gpr4Δgpr5Δ*. (**H**) Hematoxylin and eosin staining of lungs from mice infected with *gpr4Δgpr5Δ* or similarly infected and treated with IL-2 complexes. A = brochial airway, E = epithelial cell layer. Data are presented as the mean +/- standard error with at least 2 independent experiments per group. * = $P < 0.05$, ** = $P < 0.005$, *** = $P < 0.0005$ by Mann-Whitney *U*. Cda = chitin deacetylase, CCL = chemokine ligand, DC = Dendritic Cells, IFN = interferon, IL = interleukin, ILC = Innate Lymphoid Cells, MΦ = Macrophages, NK = Natural Killer. TNF = tumor necrosis factor.

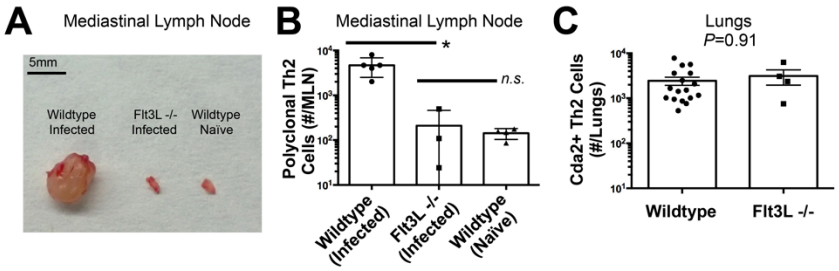

Figure 3. Lymphoid Priming is Dispensable for Pulmonary Th2 Cell Induction during Cryptococcal Infection. (**A**) Lymphadenopathy of mediastinal lymph nodes (MLN) after 14 days post-infection with strain KN99α. (**B**) Quantification of IL-5+ IL-13+ polyclonal Th2 cells from the MLN in wild-type and Flt3L-/- mice. (**C**) Quantification of IL-5+ IL-13+ antigen-specific Th2 cells contained in the lungs of wild-type and Flt3L-/- mice.

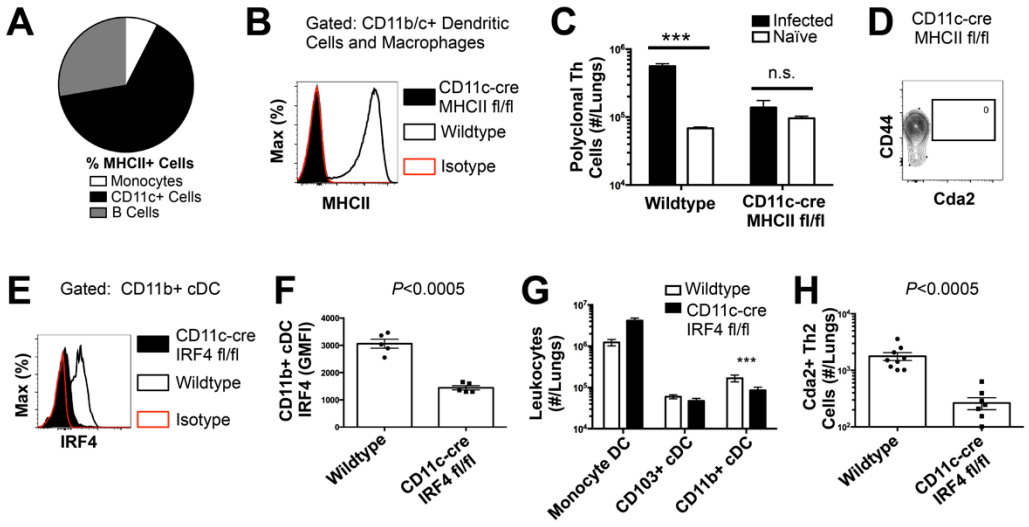

Figure 4. Interferon Regulatory Factor 4-Dependent Conventional Dendritic Cells Coordinate Th2 Cell Induction. (**A**) Antigen-presenting cells as a proportion of total MHCII+ cells in the lungs of infected mice. (**B**) MHCII expression by CD11b/c+ cells from mice 14 days post-infection with KN99α. Isotype refers to CD11b/c+ cells from wildtype mice stained with a rat IgG2b antibody of irrelevant specificity. (**C**) Quantification of pulmonary CD4+ Foxp3- CD44+ pulmonary Th cells. (**D**) Biexponential plot of CD4+ Foxp3- cells, indicating the absence of antigen-specific (CD44-, Cda2-) cells in the lungs of CD11c-cre MHCII mice infected with KN99α. (**E**) IRF4 expression by CD11b+ cDC from lungs of CD11cre IRF4 fl/fl or wildtype mice 14 days post-infection with KN99α. Isotype refers to CD11b+ cDC from wildtype mice stained with a rat IgG1 antibody of irrelevant specificity. (**F**) Geometric mean fluorescence intensity of CD11b+ cDC in from the lungs of infected CD11c-re IRF4 fl/fl mice. (**G**) Quantification of monocytes and dendritic cell subsets from the lungs of mutant or wildtype mice infected with KN99α. (**H**) Quantification of IL-5+ IL-13+ antigen-specific Th2 cells contained in the lungs of mutant or wildtype mice 14 days post-infection with KN99α. Data are presented as mean +/- standard error. * = $P < 0.05$, *** = $P < 0.0005$, and n.s. = not significant by Mann-Whitney *U*. Cda = chitin deacetylase, Flt3L = fms-like tyrosine kinase 3 ligand, MHC = major histocompatibility complex, cDC = conventional dendritic cells, IRF4 = interferon regulatory factor 4.

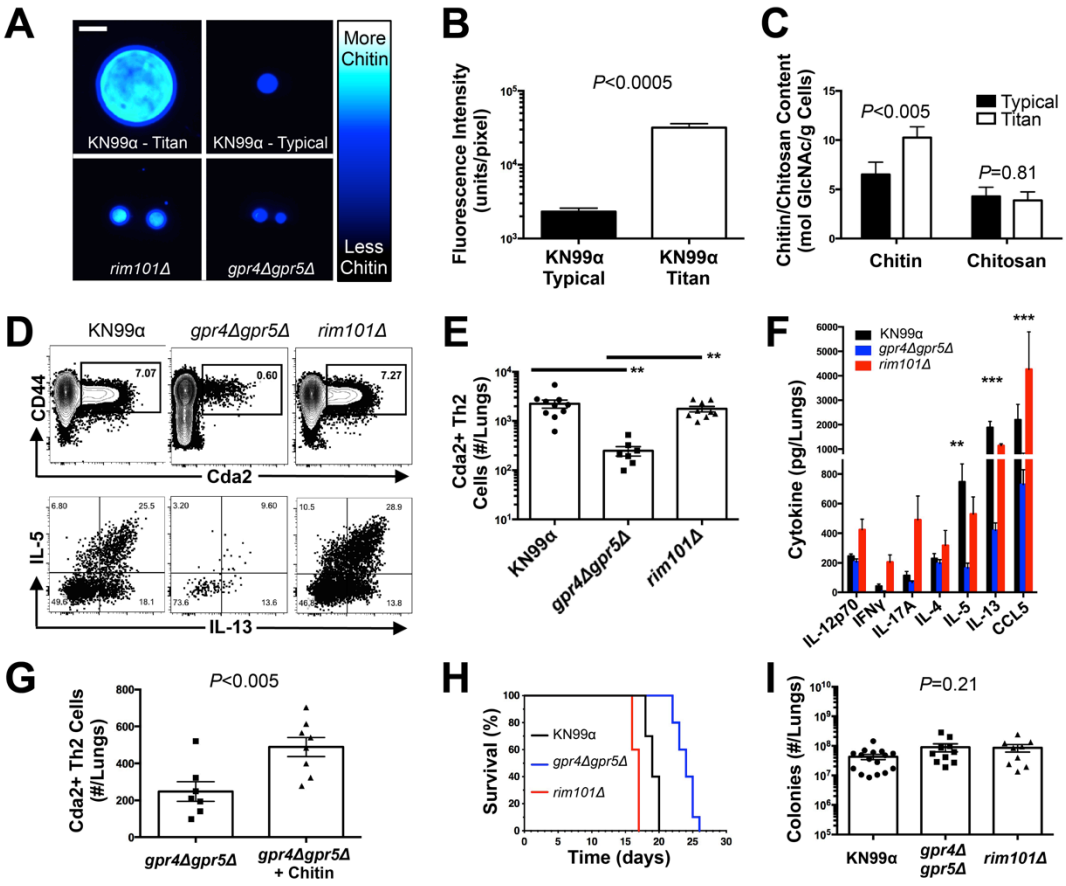

Figure 5. *C. neoformans* Chitin Correlates with Type-2 Helper T Cell Response and Subsequent Disease. (**A&B**) Cryptococcal cells isolated from lungs at 14 days post-infection and stained with Calcofluor White. Cells were either imaged with epifluorescence microscopy (**A**) or analyzed by flow cytometry with fluorescence intensity calculated per pixel to determine chitin density within the cell wall (**B**). **(C)** Total chitin and chitosan content normalized to dry weight of cryptococccal cells. (**D**) Flow cytometry plots of CD4+, Foxp3-, CD44+ Cda2+ Th cells expressing Th2 cytokines, IL-5 & IL-13, at 14 days post-infection and (**E**) the quantification of these plots. (**F**) Cytokines from lung homogenates of mice 14 days post-infection. (**G**) IL-5+ IL-13+ antigen-specific Th2 cells from lungs of mice 14 days post-infection without and with intranasal chitin particle treatment. (**H**) *P*-value represents log-rank test comparing each survival curve with 10 mice per group to: *gpr4Δgpr5Δ* vs. KN99α, P<0.0005;

gpr4Δgpr5Δ vs. *rim101Δ*, $P<0.0005$; KN99α vs. *rim101Δ*, $P<0.0005$. (**I**) Fungal burden in the lungs at 14 days post-infection. Data are presented as the mean +/- standard error with at least 2 independent experiments per group. ** = $P < 0.005$, *** = $P < 0.0005$ by Mann-Whitney *U* or Kruskal Wallis ANOVA. Cda = chitin deacetylase, CCL = chemokine ligand, GlcNAc = *N*-acetylglucosamine, IFN = interferon, IL = interleukin.

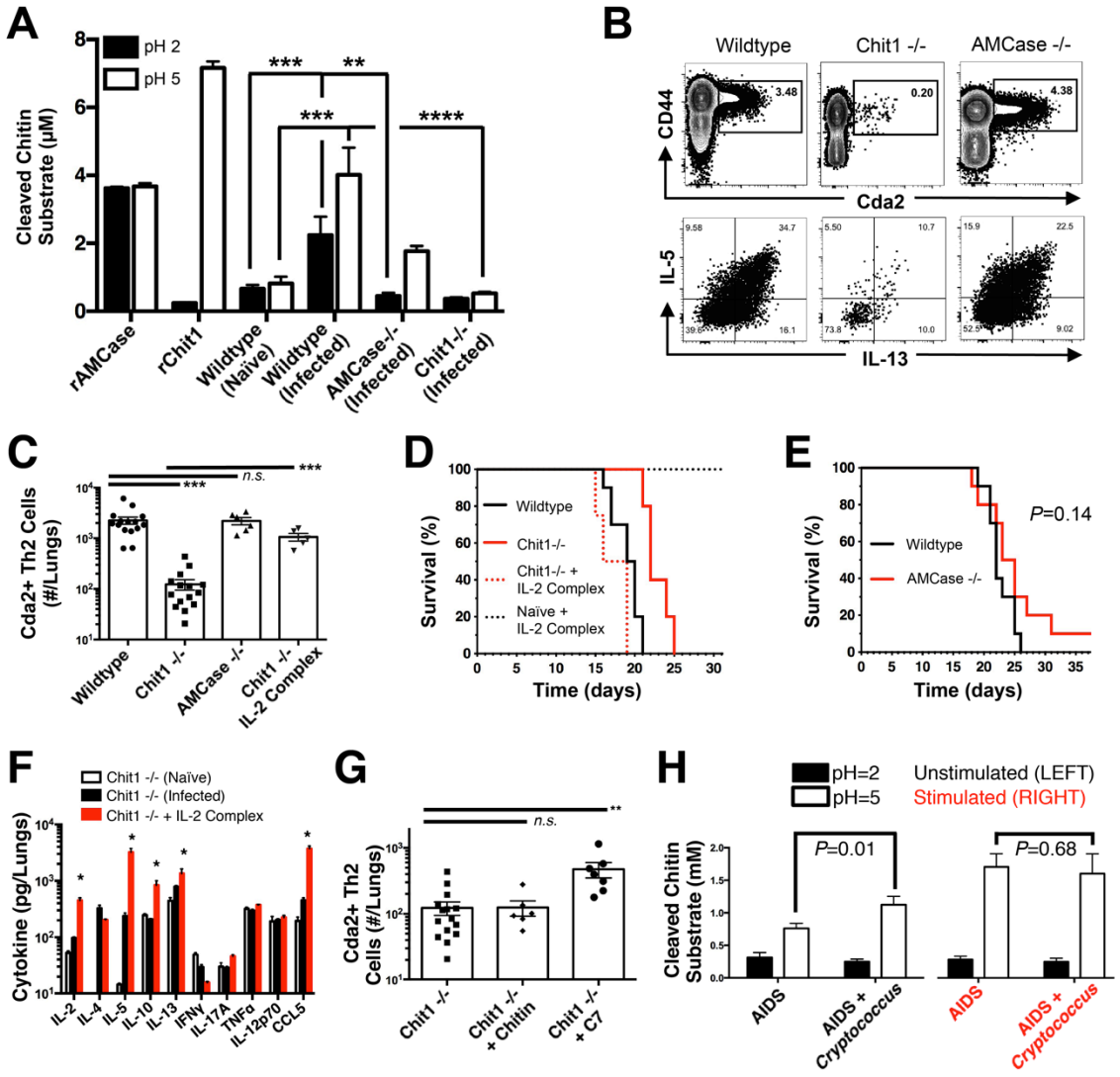

Figure 6. Chitotriosidase Promotes Chitin Recognition and Th2 Cell-mediated Disease. (**A**) Chitinase enzyme activity of recombinant enzymes or lung homogenates from 14 days post-infected or naïve mice. (**B**) Flow cytometry plots of CD4+, Foxp3-, CD44+ Cda2+ Th cells expressing Th2 cytokines, IL-5 & IL-13, at 14 days post-infection and (**C**) the quantification of these plots. (**D&E**) Survival of mutant or wildtype mice infected with KN99α either with or without IL-2 complex treatment. Logrank test comparing each survival curve relative with 10 mice for each group to: Chit1 -/- vs. wildtype, $P<0.005$; Chit1 -/- vs. Chit1 -/- + IL-2 complex, $P<0.0005$; Chit1 -/- + IL-2 complex vs. wildtype, $P=0.07$. (**F**) Cytokines from lung homogenates of naïve or

wildtype and Chit1-/- mice 14 days post-infection with KN99α or age-matched, naïve Chit1-/- mice. (**G**) IL-5+ IL-13+ antigen-specific Th2 cells from lungs of Chit1-/- mice 14 days post-infection and mice treated with intranasal chitin particles or chitin heptamer fragments (C7). (**H**) Chitinase enzyme activity of human plasma without (LEFT) or with (RIGHT) cryptococcal lysate antigen stimulation. Data are presented as the mean +/- standard error with at least 2 independent experiments per group. * = $P < 0.05$, ** = $P < 0.005$, *** = $P < 0.0005$ by Mann-Whitney *U* or Kruskal Wallis ANOVA. AMCase = Acidic Mammalian Chitinase, C7 = chitin heptamer, CCL = chemokine ligand, Cda = chitin deacetylase, Chit1 = Chitotriosidase, IFN = interferon, IL = interleukin, TNF = tumor necrosis factor.

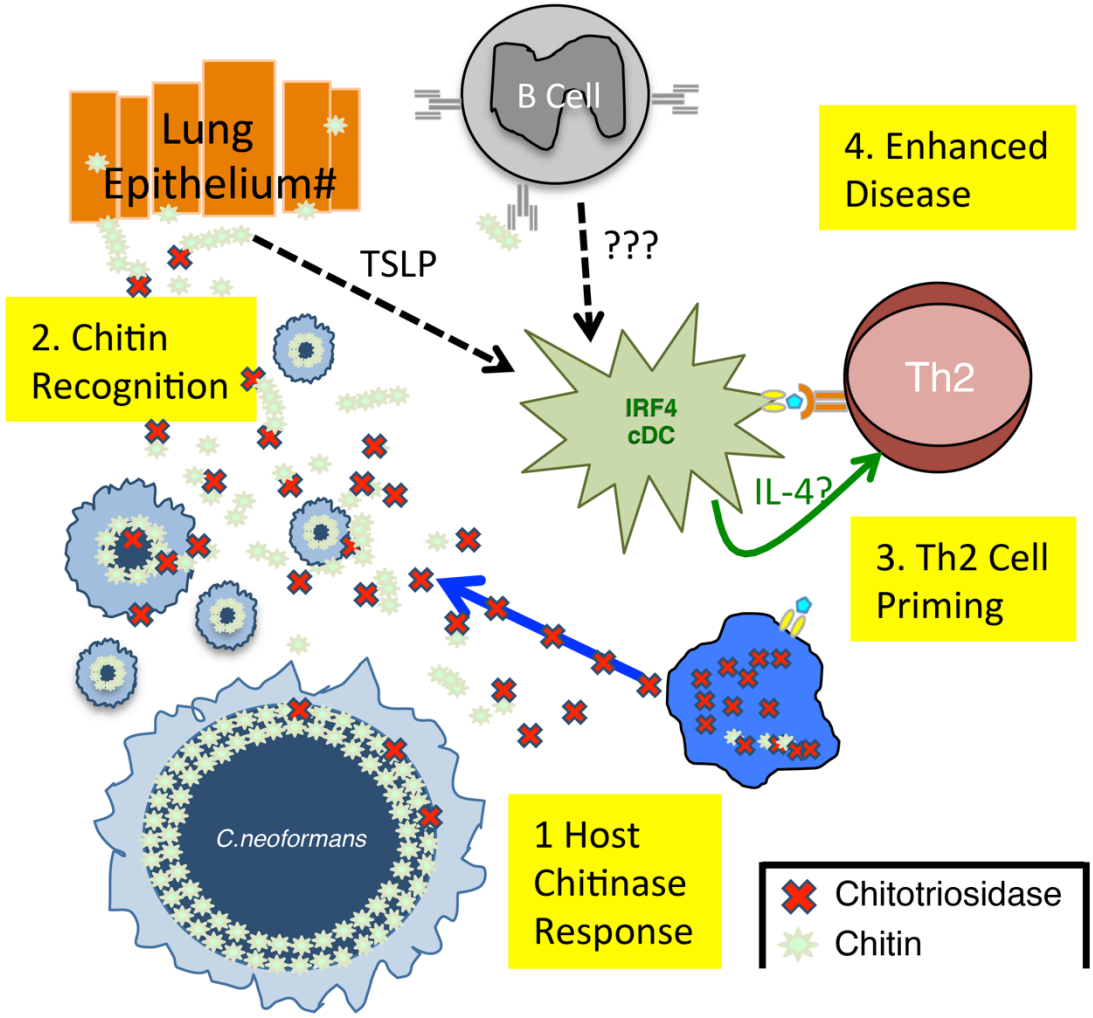

Figure 7. Model of Th2 Cell-mediated Disease during Pulmonary Fungal Infection. (**1**) Chitotriosidase is released by the host and degrades fungal chitin to generate small chitin fragments, such as chitin heptamers. (**2**) Chitin recognition occurs by an unknown mechanism that could involve either epithelial cell production of alarmins, such as thymic stromal lymphopoietin (TLSP) [9] or antibodies that bind chitin (160). (**3**) These chitin-based signals are recognized by lung-resident CD11b+ conventional dendritic cells that are capable of producing IL-4, an essential Th2 cell differentiation factor. (**4**) The adaptive Th2 cell response results in enhanced disease in the absence of significant changes in pulmonary fungal burden.

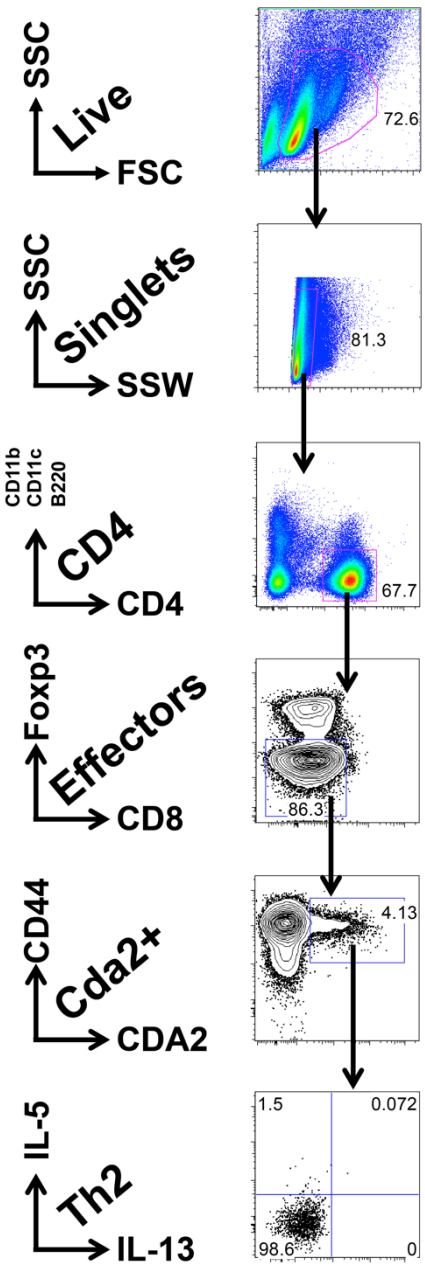

Supplemental Figure 1. Helper T Cell Flow Cytometry Gating Strategy. Single cell suspension isolated from lungs of wildtype mice 14 days post-infection with strain KN99α. Red or blue gate contains the entirety of the the subsequent plot below. "Th2" gate is drawn based on sample not incubated with PMA + ionomycin.

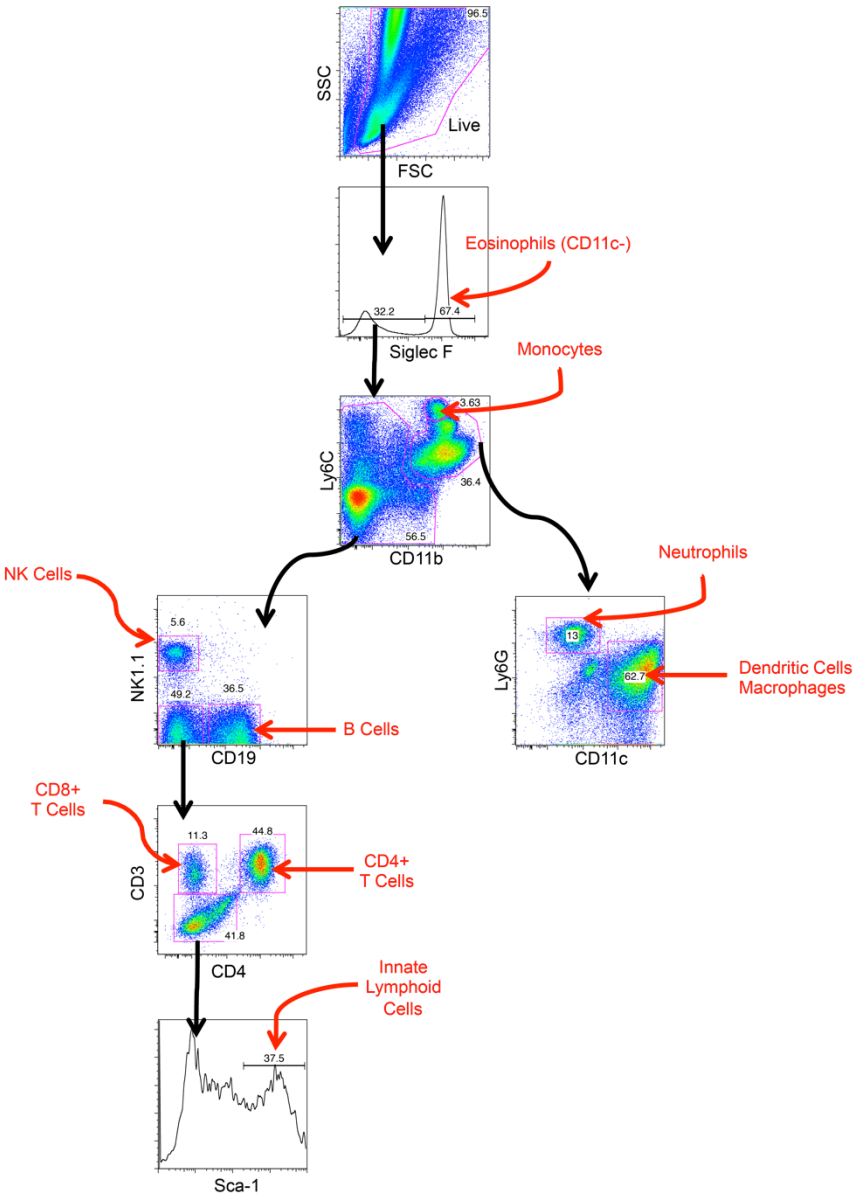

Supplemental Figure 2. Bulk Leukocyte Flow Cytometry Gating Strategy. Single cell suspension isolated from lungs of wildtype mice 14 days post-infection with strain KN99α. Red arrows and words indicate leukocyte subset.

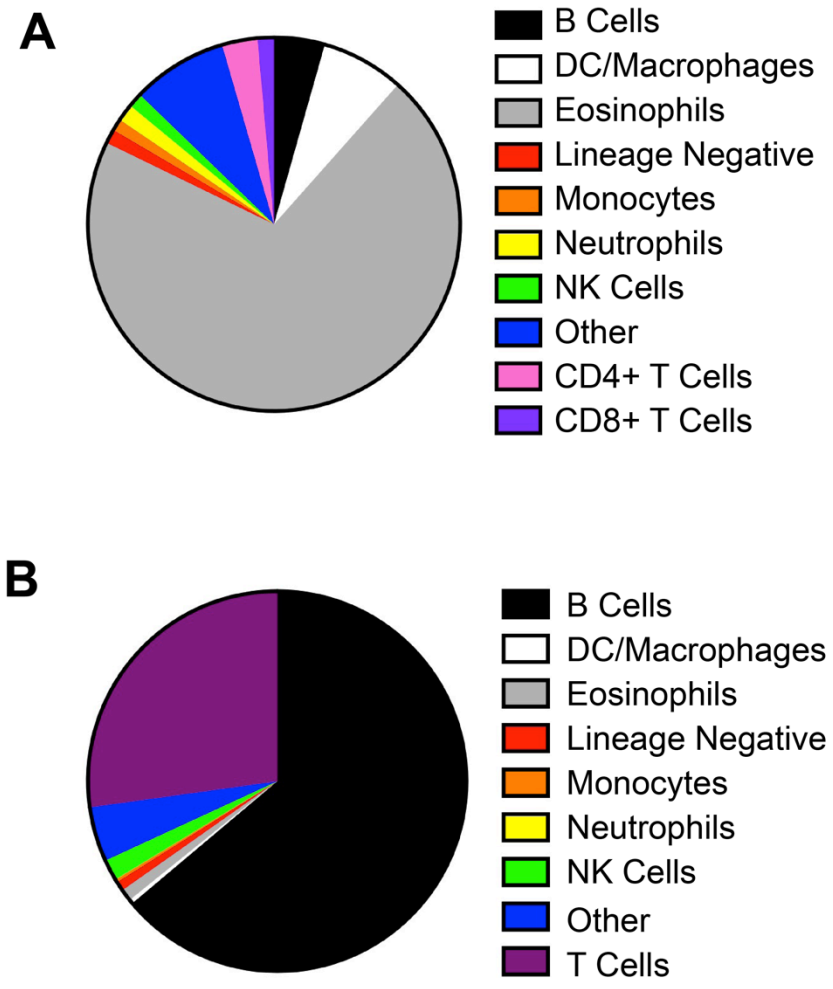

Supplemental Figure 3. Eosinophils Predominate in the Pulmonary Leukocyte Response to Cryptococcal Infection. Leukocytes harvested from (**A**) lungs or (**B**) mediastinal lymph nodes of mice 14 days post-infection with KN99α. Each subset is identified by non-redundant gating per Supplementary Figure 2.

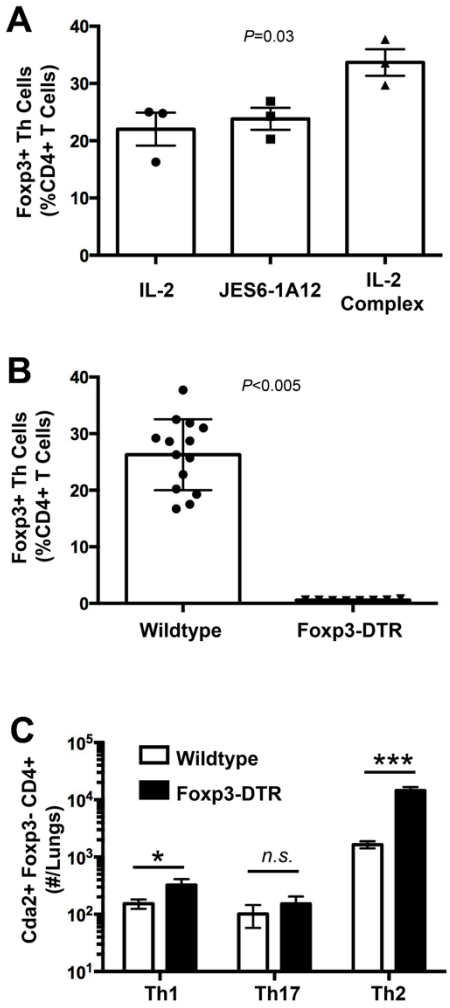

Supplemental Figure 4. Foxp3+ Regulatory T Cells Specifically Suppress Type-2 Helper T Cells During Pulmonary Fungal Infection. (**A**) Proportion of Th cells that express Foxp3 in wildtype mice infected and treated with IL-2, IL-2 antibody (JES6-1A12), or IL-2 complex. (**B-C**) Foxp3-*Diptheria* Toxin (DT) Receptor mice received DT every other day beginning at 5 days post-infection. Single cell suspensions isolated from lungs of wildtype and Foxp3-DTR mice at 14 days post-infection with KN99α were analyzed as the proportion of CD4+ cells expressing Foxp3 to monitor Treg depletion (**B**), or CD4+, Foxp3-, CD44+ Cda2+ Th cells expressing Th1 (IFNγ), Th2 (IL-5 & IL-13), or Th17 (IL-17A) cytokines to determine effector T cell differentiaion (**C**). Data are presented as mean ± standard error of the mean. * $P < 0.05$ and *** $P < 0.0005$ by Mann-Whitney *U*.

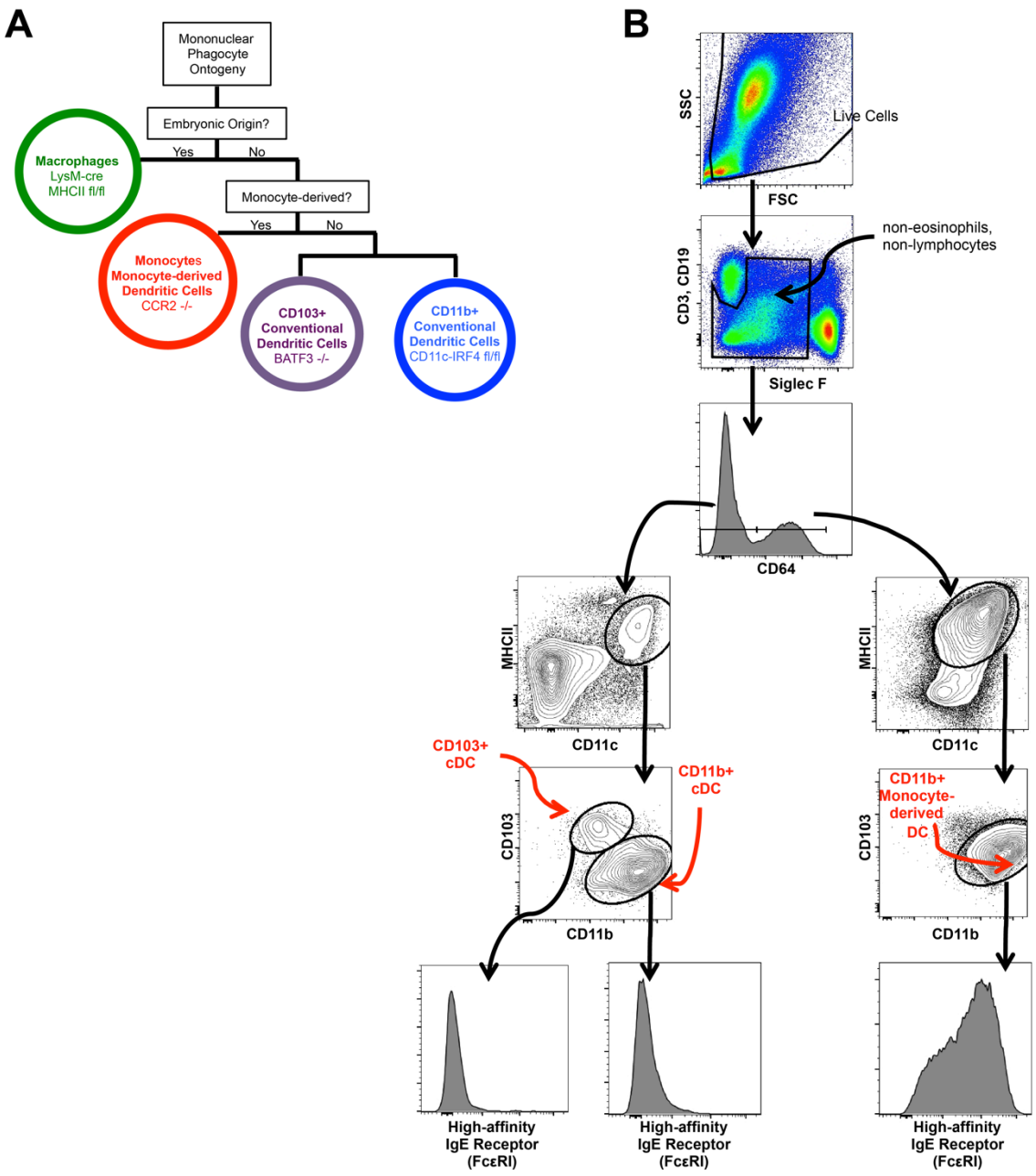

Supplemental Figure 5. Analysis of CD11c+ Cell Subsets. (**A**) Diagram depicting the relationship between various CD11c+ cell subsets and mice used to delete/inhibit the subsets [5]. (**B**) Flow cytometry gating gtrategy. Single cell suspension isolated from lungs of wildtype or mutant mice 14 days post-infection with strain KN99α.

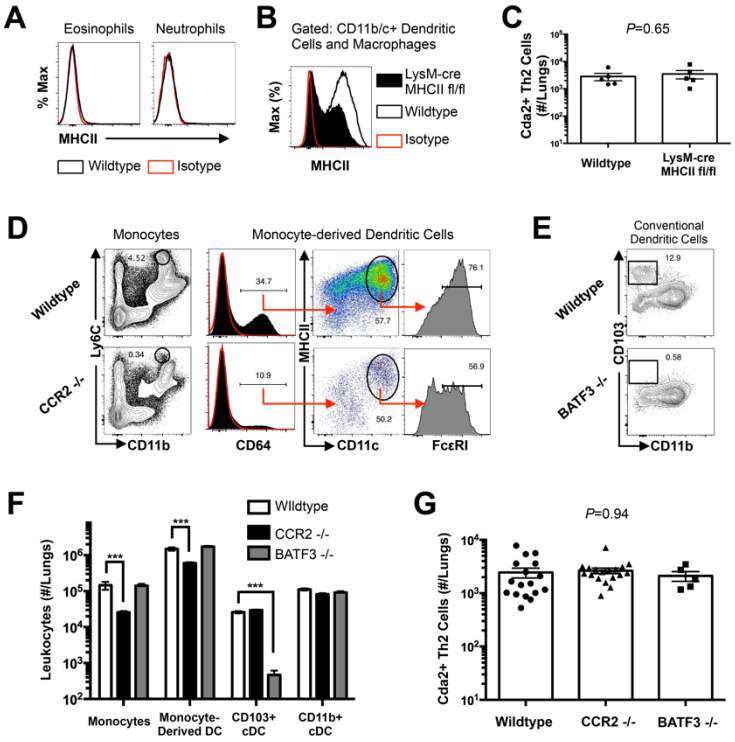

Supplemental Figure 6. Macrophages, granulocytes, CD103+ Conventional Dendritic Cells, Monocytes, and Monocyte-derived Dendritic Cells are Dispensable for Th2 Cell Priming. **(A)** Eosinophils and neutrophils do not express MHCII during Cryptococcal infection. MHCII expression in eosinophils or neutrophils from lungs of mice 14 days post-infection with strain KN99α. Isotype refers to similar cells stained with a rat IgG2b antibody of irrelevant specificity. (**B-G**) Cells from wild-type, LysM-cre MHC fl/fl, CCR2-/-, or BATF3-/- mice 14 days post-infection with KN99α. (**B**) Representivive biexponential flow cytometry plot indicating the loss of macrophages in the lungs of LysM-cre MHCII fl/fl mice. (**C**) Quantification of antigen-specific Th2 cells in LysM-cre MHCII fl/fl infected mice. (**D**) Representative biexponential flow cytometry plot indicating the loss of monocytes (Ly6C+, CD11b+) and monocyte-derived DC (CD64+, CD11c+, MHCII+, FcεRI+) in the lungs of CCR2 -/- mice. (**E**) Representative biexponential flow cytometry plot indicating the loss of CD103+ conventional dendritic cells in BATF3-/- mice. (**F**) Quantification of monocytes and dendritic cell subsets from the lungs of mutant or wildtype mice. (**G**) Quantification of antigen-specific Th2 cells in wild-type, CCR2-/-, and BATF3-/- infected mice.

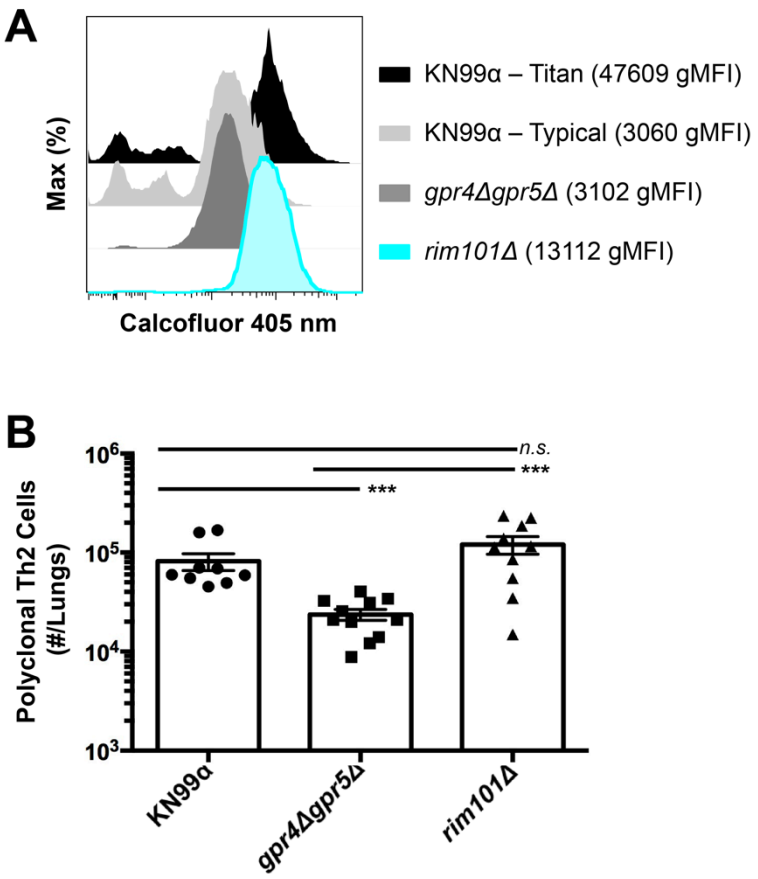

Supplemental Figure 7. Cryptococcal Chitin Promotes Polyclonal Type-2 Helper T Cell Accumulation. **(A)** Cryptococcal cells isolated from lungs at 14 days post-infection. Cryptococcal cells stained with Calcofluor White, and analyzed with flow cytometry. **(B)** CD4+ Foxp3- IL-5+ IL-13+ polyclonal Th2 cells in the lungs of mice infected with high chitin (KN99α, *rim101Δ*) or low chitin (*gpr4Δgpr5Δ*) cryptococcal strains. Data are presented as the mean +/- standard error with at least 2 independent experiments per group. *** = $P < 0.0005$ by Mann-Whitney *U*.

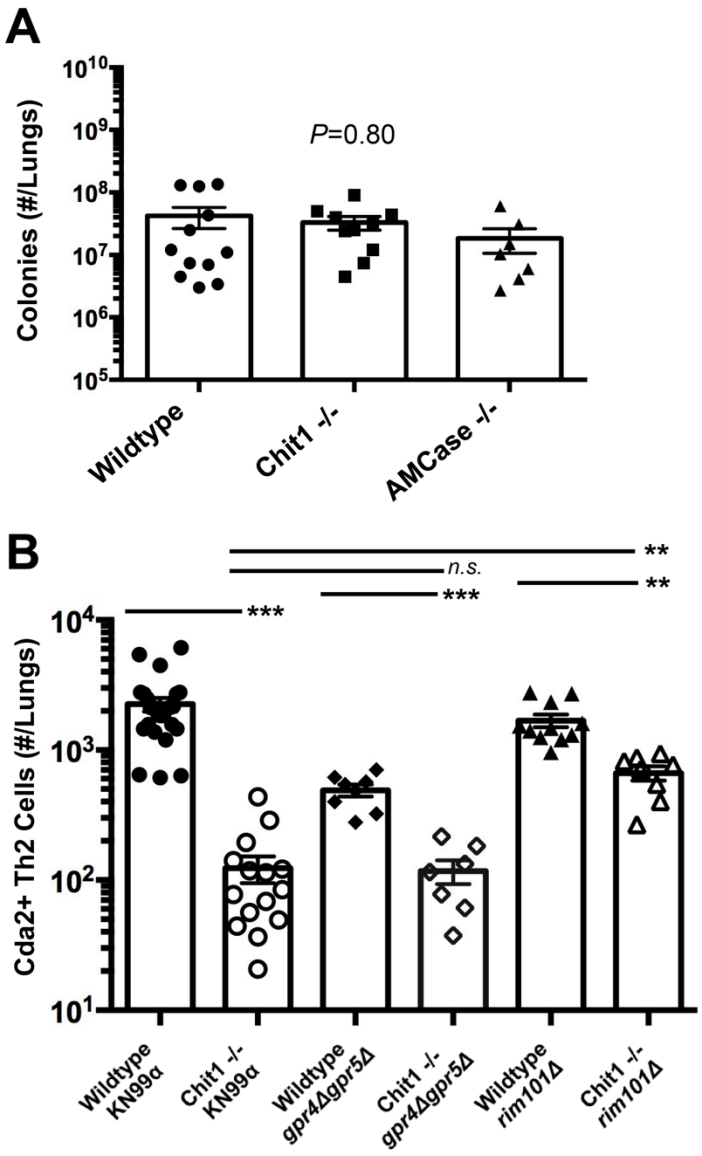

Supplemental Figure 8. Chitotriosidase Promotes Th2 Cell Accumulation without Altering Fungal Burden. (**A**) Fungal burden in the lungs of wildtype, Chit1-/-, and AMCase-/- mice 14 days post-infection. (**B**) IL-5+ IL-13+ antigen-specific Th2 cells from lungs of mice 14 days post-infection. Data are presented as the mean +/- standard error with at least 2 independent experiments per group. ** = $P < 0.005$, *** = $P < 0.0005$ by Mann-Whitney *U* or Kruskal Wallis ANOVA.

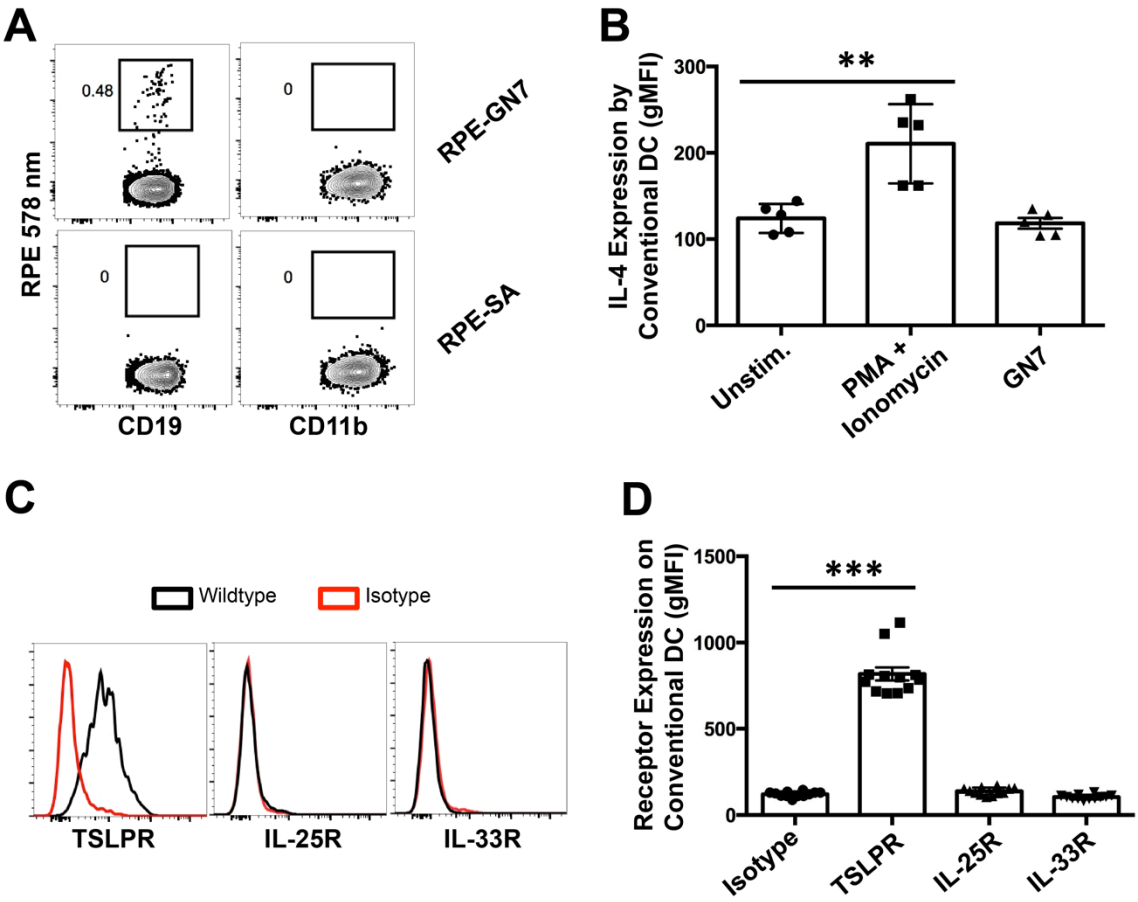

Supplemental Figure 9. CD11b+ Conventional Dendritic Cells Respond to Chitin Indirectly. Pulmonary leukocytes from wildtype mice 14 days post-infection with KN99 α. (**A**) CD19 (B cells) or CD11c (dendritic cells) co-labeled with R-phycoerithrin conjugated to streptavidin with biotinylated chitin heptamers (RPE-GN7) or without biotinylated chitin heptamers (RPE-SA). (**B**) IL-4 expression of CD11b+ conventional dendritic cells after 5 hours of stimulation with PMA + ionomycin, 125 μg of chitin heptamers (GN7) or left unstimulated. Histogram (**C**) and quantification of alarmin receptor expression (**D**) by CD11b+ conventional dendritic cells. Data are presented as the mean +/- standard error with at least 2 independent experiments per group. ** = $P < 0.005$, *** = $P < 0.0005$ by Mann-Whitney U. gMFI = geometric mean fluorescence intesity, TSLP = thymic stromal lymphopoietin.

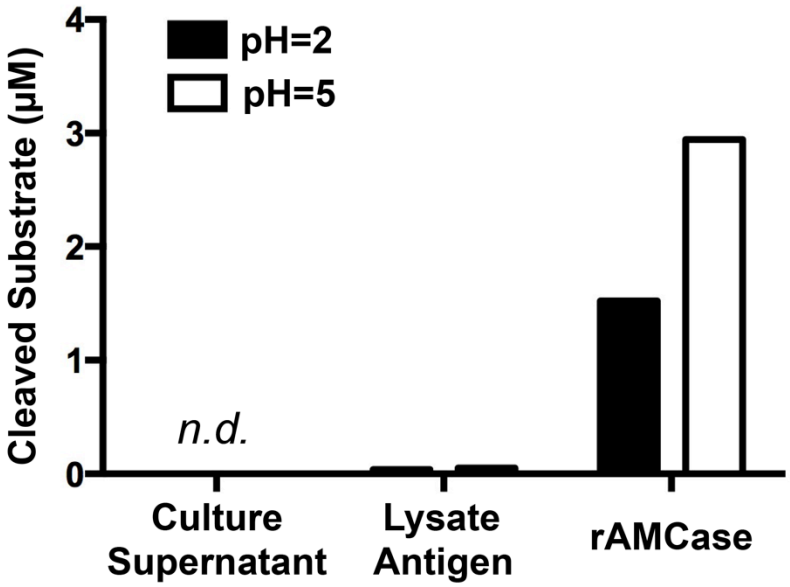

Supplemental Figure 10. *Cryptococcus* Antigens and Culture Supernatants Do Not Possess Chitinase Activity. Chitinase activity at pH=2 and pH=5 as measured in *Cryptococcus* lysate antigens and YPD supernatant from overnight cultures.

Table 1. CD4+ T Cell Cda2-MHCII Tetramer Peptide Sequence and Putative Cross Reactive Peptides from Other *C. neoformans* Chitin Deacetylases.

Gene	Amino Acid Sequence[a]	MHCII Score[b]
cda1	WSHP**ALTTLTNEE**IVAELG	36
cda2[c]	WSHQ**YMTALSNEV**VFAELY	74
cda3	WSHP**YMTTLTNEQ**VVGELG	56
fpd1	WSHA**DLTQLDESG**INDELS	13

The **bold** sequences indicate regions that align with the P1-P9 residues within the Cda2-MHCII tetramer core. The underlined sequences correspond to the total peptide included in the Cda2-MHCII tetramer.

[a] Homologous amino acid sequences within the catalytic domain of chitin deacetylases.

[b] Peptide loading score on MHCII I-A^B (74).

[c] Cda2-MHCII tetramer made from this gene and amino acid sequence.

Table 2. Differences in total chitin due to cell morphology

Strain	Proportion Titan Cells[a]	Chitin Per Cell (GMFI)[b]	Titan Cell Chitin (GMFI)	Typical Cell Chitin (GMFI)	Relative Total Chitin[c]
KN99α	20.4%	47609 (Titan) 3060 (Typical)	9712	2436	4.0
gpr4Δgpr5Δ	5.3%	43590 (Titan) 3102 (Typical)	2310	2938	1.7
rim101Δ	0.5%	45708 (Titan) 13112 (Typical)	2235	12456	4.8

[a] Proportion of cryptococcal titan cells in the lungs, as reported by Okagaki et al. 2011(35).

[b] Mean fluorescence intesity of calcofluor white in size-fractionated cryptococcal cells analyzed by flow cytometry. GMFI = geometric mean fluorescence intensity

[c] Estimated total chitin calculated uising the folowing equation: Relative Total Chitin = [(Proportion Titan Cells × Titan GMFI) + (Proportion Typical Cells × Typical GMFI)]/KN99α Typical Cell GMFI

CHAPTER 3

Regulatory T Cell Induction and Retention in the Lungs Drives Suppression of Detrimental Type-2 Helper T Cells During Pulmonary Cryptococcal Infection.

SUMMARY

Lethal disease caused by the fungus, *Cryptococcus neoformans*, is a consequence of the combined failure to control pulmonary fungal replication and immunopathology caused by induced type-2 helper T (Th2) cell responses. In order to gain insight into immune regulatory networks, we examined the role of regulatory T (Treg) cell suppression of Th2 cells, using a mouse model of experimental cryptococcosis. Upon pulmonary infection with *Cryptococcus*, Treg cells accumulated in the lung parenchyma independently of priming in the draining lymph node. Using peptide-MHCII molecules to identify *Cryptococcus*-specific Treg cells combined with genetic fate-mapping, we noted that a majority of the Treg cells found in the lungs were induced during the infection. Additionally, we found that Treg cells utilized the transcription factor, Interferon Regulatory Factor 4 (IRF4), to dampen harmful Th2 cell responses, as well as mediate chemokine retention of Treg cells in the lungs. Taken together, induction and IRF4-dependent localization of Treg cells in the lungs allow Treg cells to suppress the deleterious effects of Th2 cells during cryptococcal infection.

INTRODUCTION

Cryptococcosis is an emerging infectious disease of humans caused by the fungus, *Cryptococcus neoformans* (8). Yeasts or spores are inhaled from the environment and enter the lower respiratory tract. Robust CD4+ helper T (Th) cell-mediated immunity controls this initial pulmonary infection, and as a result, immune replete individuals rarely experience overt disease. However, Th cell deficiencies associated with solid organ transplantation, cancer chemotherapy, and HIV/AIDS dramatically increases susceptibility to invasive cryptococcosis. In the absence of immune control, *C. neoformans* emigrates from the lung, enters the bloodstream, and traverses the blood-brain barrier to cause cryptococcal meningitis. Despite access to standard antifungal and antiretroviral therapies, patients receiving treatment for cryptococcal meningitis exhibit a wide range of adverse clinical outcomes, including: infection relapse, immune reconstitution inflammatory syndrome (IRIS) due to excessive reaction to persistent antigen, and/or death (148). The reasons why some individuals recover without experiencing complications and others perish remains enigmatic.

Differences in the quality of the impaired Th cell responses in HIV patients stratify the spectrum of clinical outcomes (58, 213, 214). Interferon-γ production by Type-1 helper T (Th1) cells defends against invasive cryptococcal disease and promotes fungal clearance (55, 215, 216). Dysregulated reconstitution of protective immunity in patients with recent cryptococcosis can also cause harmful inflammation (204). In addition, *C. neoformans* (serotype A) subverts protective immunity and exacerbates disease by driving Th2 cell production of interleukin (IL)-4, IL-5, and IL-13 (217, 218). Therefore, therapies that dampen detrimental Th cell responses could be used to ameliorate disease.

One mechanism the immune system uses to dampen Th cell responses is by employing regulatory T (Treg) cells. Treg cells are a distinct subset of Th cells that uniquely express the transcription factor forkhead box P3 (Foxp3), which stabilizes the suppressive function of Treg cells. Genetic aberrations in Foxp3 (i.e. IPEX syndrome) cause fatal Th cell-driven autoimmunity in humans, highlighting the importance of Foxp3

in immune homeostasis (219). Treg cells also inhibit effector Th cell responses to microbial infections (220). In particular, conditional depletion of Foxp3+ Treg cells in mice infected with *C. neoformans* increases Th2 cell abundance in the lungs, indicating Treg cells limit the proliferation of Th2 cells primed by cryptococcal infection (221, 222). Beyond these initial observations, little is known about the mechanism of Th2 cell suppression by Treg cells during cryptococcal infection.

Since Treg cell suppression of effector Th cells is contact dependent (223), Treg cells must colocalize with effector cells in order to function in tissues such as the lung (224). To accomplish this, Treg cells express chemokine receptors (CCR) and integrins that allow them to home to and to be retained at sites of inflammation (225). Separate evidence indicates Treg cells that restrain mucosal Th cell responses exhibit highly specialized control of distinct Th cell subsets by expressing the same lineage-defining transcription factors as their effector Th cell counterpart (226-228). In particular, interferon regulatory factor 4 (IRF4) expression by Treg cells has been implicated in the suppression of Th2-driven autoimmunity (228).

Here, we utilized a mouse model of experimental cryptococcosis to investigate Treg cell responses to pulmonary fungal infection. Specifically, we explored the hypothesis that Treg cells utilize IRF4 and chemokine receptors to colocalize with Th2 cells in the lungs. While in proximity with Th2 cells, Treg cells are able to inhibit the expansion of deleterious Th2 cell responses to cryptococcal infection.

RESULTS

Regulatory and effector Th cells coexist in the lung parenchyma.

Upon pulmonary infection with the pathogenic fungus, *Cryptococcus neoformans* (KN99α), mice develop lethal disease that results from a combination of unabated fungal replication and Th2-driven immunopathology. Importantly, these detrimental Th2 cells are primed and accumulate in the lungs (222). Since Treg cell suppression of effector cells requires these cells to be in close proximity (223), we hypothesized that Treg/effector cells colocalize within *Cryptococcus*-infected lungs.

Th cells are highly heterogeneous with respect to their T cell receptor and cognate functions. Thus, the use of *Cryptococcus*-specific reagents to track antigen-specific Th cells within a polyclonal repertoire facilitates direct comparisons of Th cell subsets responding to infection. We used a peptide from chitin deacetylase 2 (Cda2), an immunogenic cryptococcal protein (166), to construct a recombinant peptide-MHCII tetramer to track *Cryptococcus*-specific Th cells by flow cytometry (222). The Cda2-MHCII tetramer not only identified Cda2+ Foxp3- effector Th cells in the lungs of infected mice, but the tetramer also labeled a sizable population of Cda2+ Foxp3+ Treg cells **(Figure 1A)**.

The lung consists of three physically separate compartments that may contain Th cells: blood vessels, airways, and lung parenchyma. To determine whether the lung Treg/effector cells were circulating in the blood vasculature or residing in the airways/lung parenchyma, we performed intravital antibody staining. Anti-CD45 antibody administered intravenously (IV) was used to label polyclonal Foxp3+ Treg cells and Foxp3- effector Th cells retrieved from the peripheral blood **(Figure 1B)**. The complete labeling of all Foxp3+ and Foxp3- cells in the blood indicates that the antibody completely penetrated the entirety of the blood vasculature (**Figure 1B, left**). Cells collected from whole lung digests had a mixture of IV stained and unstained cells, showing the lung was composed of circulating and lung-resident Treg/effector Th cells **(Figure 1B, middle)**. In contrast, nearly all antigen-specific cells were unstained, indicating that infection-induced Th cells resided outside of the blood vasculature

(Figure 1B, right). To distinguish Treg/effector Th cells in the lungs from the airways, we sedated infected mice and instilled fluorescent-coupled antibodies into the nares. A majority of polyclonal and antigen-specific Treg/effector Th cells obtained from lung digests did not stain with this inhaled antibody **(Figure 1C)**, thus most of the Treg/effector Th cells were not resident in the airways. These data collectively indicate that Treg and effector Th cells responding to infection coexist in the lung parenchyma.

Treg cell induction does not depend on lymphoid priming.

We next sought to determine the location of Treg cell induction. The mediastinal lymph node (MLN) is the principle origin of Th cell priming to most microbes that breech the airway mucosa. However, we previously showed that effector Th cells gather in the lungs in the absence of dendritic cell trafficking and subsequent T cell activation in the lung-draining lymph node (222). Thus, we compared the presence of Treg cells at the location of traditional Th cell priming in the MLN and the site of *C. neoformans* infection in the lungs. Foxp3-expressing Treg cells increased as a proportion of total CD4+ Th cells in the lungs throughout the course of infection **(Figure 2A)**. Yet, Treg cell proportions remained unchanged, if not slightly reduced, in the MLN **(Figure 2A)**.

The relatively small Treg cell response in the MLN suggests that either Treg cells immediately migrate after activation in the lymph node to the site of infection or Treg cell induction occurs autonomously in the lungs. We used CCR7 -/- mice to answer this question. CCR7 is required for naïve T cell entry into lymph nodes, thus CCR7 deficiency expectedly inhibited naïve Th cells (i.e. CD44 low) from accumulating in the MLN **(Figure 2B)**. Likewise, the MLN of infected CCR7 -/- mice exhibited decreased swelling compared to wildtype mice **(Figure 2C)**, further indicating dysfunctional Th cell priming in the MLN of CCR7-deficient mice. Despite the aberrant MLN response, Treg cells accumulated in the lungs of CCR7 -/- mice similar to levels in wildtype mice after *C. neoformans* infection **(Figure 2D)**. Thus, Treg cell induction and accumulation in the lungs does not require mediastinal lymph node priming during pulmonary cryptoccocal infection.

Cryptococcus-specific Treg cells are induced in the lungs upon pulmonary infection.

Treg cells develop along two ontologically distinct lineages: "peripheral" Treg (pTreg) cells and "thymic" Treg (tTreg) cells. Upon receiving secondary cues of excessive inflammation, naïve Th cells can differentiate in the periphery into pTreg cells. Conversely, tTreg cells become regulatory cells during thymic selection based on T cell receptor affinity for self-antigens (229). Of note, tTreg cells emigrate from the thymus with full suppressive potency and do not need to undergo further activation in lymphoid tissues (230). Therefore, we asked whether the Treg cells in cryptococcal infected lungs are tTreg cells that populate the lungs independently of lymph node priming or pTreg cells autonomously induced in the lungs.

Cryptococcus-specific tTreg cells must exist in the pre-immune, naïve Th cell repertoire, if these cells are the dominant source of Treg cells in the lungs of infected mice. Therefore, we examined the thymus or secondary lymphoid organs of uninfected mice for the presence of Cda2+ Foxp3+ Treg cells. Cda2-specific Treg cells were present in the pre-immune repertoire contained in the thymus or secondary lymphoid organs, albeit at lower Treg/effector proportions compared with polyclonal Th cells **(Figure 3A)**. Therefore, a small number of *Cryptococcus*-specific tTreg cells can be found in uninfected mice, and these cells could migrate to the lung and proliferate in response to cryptococcal infection.

To further address the question of whether the Treg cells accumulating in lungs of infected mice migrated from the thymus or were induced in the lungs, we developed a genetic fate-mapping system to distinguish where these cells developed. Mice containing a Foxp3-cre Estrogen Receptor 2 (ERT2) transgene were crossed with mice that had a Rosa26 stop codon-floxed tdTomato allele to make Foxp3-i-cre tdTomato mice. Effectively, the combination of these transgenes allows for inducible fluorescent marking *in vivo* of Treg cells and all of the progeny of these cells. Similarly, when tamoxifen is removed, Treg cells produced *de novo* will not have any detectable fluorescence reporter activity. Ultimately, this allowed us to label tTreg cells (and all cells derived from this progenitor) within the pre-immune repertoire, halt new reporter induction by stopping tamoxifen administration, and determine whether the lung-resident Treg cell progenitors

existed prior to infection (i.e. tdTomato+) or were produced post-infection (i.e. tdTomato-) **(Figure 3B)**. Less than 1% of Treg cells from Foxp3-i-cre tdTomato mice that did not receive tamoxifen were fluorescent **(Figure 3B)**, and tamoxifen administered during the peak Th cell response, 9-14 days post-infection, induced fluorescence in more than 90% of the Treg cells **(Figure 3B)**. Thus, the genetic fate-mapping system is not leaky and suitably penetrant. When tamoxifen was given 12-7 days prior to infection to label the pre-immune Treg cells, a minor fraction of Treg cells retained fluorescence when harvested at 14 days post-infection **(Figure 3B)**. Therefore, a small proportion of Treg cells in the lungs came from tTreg cells in the pre-immune repertoire, and instead, the majority were pTreg cells that acquire a regulatory phenotype as a consequence of fungal infection.

Interferon Regulatory Factor 4 expression by Treg cells is required to efficiently suppress the pathologic Th2 cell response to pulmonary fungal infection.

Treg cells generated during cryptococcal infection are poised to uniquely suppress Th2 cells (221, 222). Additionally, our data indicating that Treg cells are induced and reside in the lungs of infected mice led us to investigate features consistent with Treg cells that develop extrathymically, accumulate at mucosal surfaces, and target Th2 cells for suppression (231-233). A prominent feature of pTreg cells that suppress distinct Th cell subsets in mucosal tissues is the expression of transcription factors that mirror the lineage of the effector Th cell populations targeted for suppression (226, 228). Therefore, we examined the expression kinetics of the Th2 cell transcription factor, IRF4, by both antigen-specific Foxp3+ Treg cells and cognate Foxp3- effector Th2 cells from mice infected with *C. neoformans*. As hypothesized, IRF4 expression increased in Treg cells and effector Th cells throughout the course of infection **(Figure 4A).** This raised the possibility that IRF4 is utilized by Treg cells to suppress the Th2 cell response to pulmonary fungal infection.

To test whether IRF4 expression by Tregs was important for Th2 suppression, we bred Foxp3-cre mice with IRF4 floxed mice to generate mice with a conditional IRF4 gene deletion in Treg cells (Foxp3-cre IFR4 fl/fl) **(Figure 4B)**. *Cryptococcus*-specific

Th2 cells increased >5-fold in the lungs of Foxp3-cre IRF4 fl/fl mice, and this impaired suppression of Th2 cells resembled the situation observed with complete Treg abrogation **(Figure 4C&D).** Consistent with the increase in Th2 cell numbers, Foxp3-cre IRF4 fl/fl mice also had significantly elevated amounts of IL-5 and IL-13 from infected lung homogenates compared with both wildtype animals and Treg cell depleted mice **(Figure 4E)**.

The failure to efficiently suppress Th2 cell proliferation and effector function in mice with IRF4-deficient Treg cells also correlated with exacerbation of Th2-mediated disease. IRF4-deficiency in Treg cells enhanced pulmonary accumulation of macrophages, multinucleate giant cells, and polymorphonuclear cells **(Figure 4F)**, as well as accelerated lethal cryptococcal disease **(Figure 4G)**. While lethal disease onset appeared to be accelerated in Foxp3-DTR mice relative to Foxp3-cre IRF4 fl/fl mice, naïve Foxp3-DTR mice receiving DT experienced fatal autoimmunity **(Fig. 4G)**. DT treatment also negatively impacted the survival of infected wildtype mice independently of Treg cell ablation **(Fig. 4G)**. Thus, DT treatment and autoimmunity additionally contributed to the more rapid disease experienced by Foxp3-DTR mice. Taken together, IRF4-deficient Treg cells exhibited a profound Th2 suppression defect that was comparable to complete Treg cell deficiency.

Interferon Regulatory Factor 4 is needed for localization of Treg cells in cryptococcal infected lungs.

How Treg cells utilize IRF4 to suppress Th2 cells remains incompletely understood. Existing evidence suggests that IRF4 may dictate expression of suppressive factors employed by Treg cells. For example, IRF4 interacts with Blimp-1 to mediate transcription of the suppressive cytokine, IL-10 (234). Chromatin immunoprecipitation of IRF4 confirms that IRF4 binds to the IL-10 locus, and IRF4 has been shown to mediate IL-10 production by Th2 cells (235, 236). However, IL-10 in lung homogenates of cryptococcal infected mice was unaffected by IRF4-deficiency in Treg cells and actually increased in mice with complete Treg cell abrogation **(Figure S1A)**. Furthermore, blockade with substantial quantities (i.e. 2 mg/mouse over the course of 9 days) of anti-

IL-10R antibody did not alter Th2 cell production **(Figure S1B)** or IL-5 and IL-13 secretion in lungs of infected mice **(Figure S1C)**. Finally, in other systems, IRF4-deficient Treg cells still suppress effector Th cells in an *in vitro* assay, indicating that IRF4 is dispensable for the direct suppression of effector Th cells by Treg cells (228).

An alternative hypothesis is IRF4 promotes the retention of Treg cells at the site of inflammation. Although IRF4-deficiency in Treg cells did not alter the proportion of Foxp3+ Treg cells among total CD4+ Th cells in the spleen and MLN **(Figure S2)**, it significantly decreased Treg cell proportions in the lungs of infected mice **(Figure 5A)**. Furthermore, Foxp3-cre IRF4 fl/fl mice had substantially fewer antigen-specific Treg cells in the lungs in comparison to wildtype mice **(Figure 5B)**. However, these studies could not determine whether the decreased Treg cell proportions were due to biased effector Th cell accumulation or defective Treg cell retention in the lungs.

To directly test the hypothesis that IRF4 promotes Treg cell localization in the lungs, we performed a set of adoptive transfers. Naïve CD4+ Th cells from Foxp3-cre IRF4 fl/fl mice were transferred into congenic wildtype recipients, as well as the reciprocal transfer of wildtype Th cells into Foxp3-cre IRF4 fl/fl mice. After resting in infected mice for 5 days (9-14 days post-infection of recipient), the donor cells were identified using the congenic markers. Transferred Th cells from Foxp3-cre IRF4 and wildtype mice parked equivalently in the lungs of their respective hosts **(Figure 5C)**. However, the proportion of Foxp3-cre IRF4 fl/fl Th cells that expressed Foxp3 was significantly lower than similarly transferred wildtype cells **(Figure 5C)**, indicating Treg cells lacking IRF4 were inefficiently retained in the lungs. Finally, Treg cells from Foxp3-cre IRF4 fl/fl mice were over-represented in the blood vasculature of infected lungs **(Figure 5D)**, correlating the decrease in pulmonary retention of Treg cells with the diffusion of these cells into the local bloodstream. These data demonstrate that IRF4 intrinsically regulates Treg cell localization in the lungs of cryptococcal infected mice.

Treg cell accumulation in the lungs is dependent on Chemokine Receptor 5.

Th cells follow chemokine gradients to traffic to the site of inflammation (225). Therefore, we investigated chemotactic signals that may influence pulmonary localization

of Treg cells. Chemokine ligands (CCL)3, CCL4, and CCL5 are involved in type-2 immunity (237), and these chemokines increased 5-100-fold in the lungs of infected mice compared with naïve controls **(Figure 6A)**. To determine if the Treg cells could recognize these chemokines, we examined expression of the cognate chemokine receptors by Treg cells in the lungs of infected mice **(Figure 6B)**. CCR4 and CCR5 were highly expressed by Treg cells, and expression of these receptors decreased in IRF4-deficient Treg cells **(Figure 6B)**. In contrast, CCR3 was minimally expressed by Treg cells **(Figure 6B)**, and instead appeared to be associated with eosinophils in the blood and lungs of infected mice **(Figure S3)**. Thus, CCL3, CCL4, and CCL5 were highly abundant in the lungs of infected mice, and the ability to detect these chemokine signals by Treg cells would require IRF4-dependent expression of CCR4 and CCR5.

Due to the elevated expression of CCR5, abundance of cognate chemokine ligands, and the high dependence of CCR5 on IRF4, we tested the causal relationship between CCR5 and pulmonary retention of Treg cells during fungal infection. Maraviroc is a selective inhibitor of CCR5 that is used in HIV patients to block CCR5-mediated entry of HIV into leukocytes (238). Mice that received 500 micrograms of maraviroc every day from 9 days to 14 days post-infection had significantly reduced accumulation of pulmonary Treg cells compared to similarly infected, vehicle treated controls **(Figure 6C)**. To further test the requirement of CCR5 for Treg localization in the lungs. CD45.1/CD90.2 congenic Foxp3-DTR mice were infected, and Treg cells were eliminated at 7 days post-infection by administering DT. 1 million naïve CD4+ Th cells from uninfected CD45.2/CD90.1 wildtype and CD45.2/CD90.2 CCR5 -/- mice were transferred into the Foxp3-DTR mice. At 14 days post-infection the lungs were harvested and analyzed for Treg accumulation in the lungs. Strikingly, while wildtype Tregs readily accumulated in the lungs, the Tregs transferred from CCR5 -/-, mice were absent from the lungs of infected mice (**Figure 6D**). Thus, Treg cell induction and retention in the lungs requires CCR5.

DISCUSSION

Th cells are central to immunity and immunopathology associated with cryptococcal infection. While Th1 cells correlate with protection, Th2 cells exacerbate cryptococcal disease. Therefore, a deeper understanding of how the diseased host regulates Th cell responses could lead to development of interventions that ameliorate disease in predisposed individuals. One promising target of immune modulation is the Foxp3+ Treg cell population. Previously, Treg cells were found to counterbalance pathologic Th2 cell inflammation following pulmonary cryptococcal infection (221, 222). Yet, the mechanism behind this suppression was largely unexplored. Herein, we tracked *Cryptococcus*-specific Th cell responses with multi-parameter flow cytometry and manipulated host immune responses to unravel the mechanism of Treg-mediated suppression of Th2 cells during cryptococcal infection. We showed that Treg cells are induced in the tissues and utilize CCR5 and IRF4 to colocalize with and suppress Th2 effector cells in the lung parenchyma.

Many fungal pathogens elicit Treg cell responses. In most cases, Treg cells control the axis of Th17 cell responses and fungal clearance (239-242). In contrast, the primary function of Treg cells generated during cryptococcal infection is Th2 cell suppression. This clearly benefits the host, as disease is enhanced when Tregs fail to adequately control Th2 cell proliferation. The signals the host uses to detect host damage and elicit Treg cell induction are unknown in the case of pulmonary cryptococcal infection. Additional insight into these processes could lead to the identification of potent biomarkers to predict immune dysfunction in patients stricken with cryptococcal disease. Furthermore, therapeutic targeting of these pathways could be used to prompt the host to dampen harmful Th2 cell production.

Collectively, our data unify several emerging concepts regarding Treg cell suppression of Th2 cells. Peripherally induced Treg cells inhibit Th2 cells at mucosal surfaces (233), and Treg cells utilize effector cell programs like IRF4 to mediate specific suppression of Th2 cells (228). IRF4 functions as a rheostat for T cell receptor signaling (243), and TCR signaling is required to maintain a portion of the suppressive program of

Treg cells (244). Additionally, chemokines promote the migration and retention of Treg cells in inflamed tissues (225), and CCR5 is important for Treg cells to suppress Th cell responses to pulmonary fungal infections (245). In our model, Treg cells were induced in the periphery and IRF4 expression by Treg cells was required for efficient Th2 suppression. Treg cells in the lungs of cryptococcal infected mice expressed high levels of CCR5, and the few remaining IRF4-deficient Treg cells in the lungs had significantly decreased expression of CCR5. IRF4 does not directly interact with the promoter region of CCR5 (236) and does not likely influence CCR5 gene transcription. Thus, we favor a model where diminished T cell receptor signaling in Treg cells due to IRF4 deficiency reduces CCR5 expression. This prevents Treg/effector cell colocalization and hinders Treg suppression of Th2 cells. Thus, our data provide a logical connection between the hitherto disjointed observations of extrathymically induced Treg cells, IRF4-dependent suppression, chemokine-mediated localization, and Th2-specific inhibition.

Skewed type-2 cytokine responses in the peripheral blood and cerebral spinal fluid of patients with cryptococcal meningitis are associated with early mortality and onset of immune reconstitution inflammatory syndrome (57, 58). CCR5+ T cells are recruited to the CSF of patients experiencing cryptococcal meningitis and increased presence of CCR5+ T cells is associated with poor clinical outcome (246). HIV infects and lyses CCR5+ and CXCR4+ Th cells equally (247), and the *in vivo* evolution of CXCR4-tropic virus is assisted by efficient elimination of CCR5+ Th cells (248). Moreover, maraviroc treatment selectively eliminates Treg cells in HIV patients (249). Taken together with our findings that Treg cells require CCR5 to colocalize and suppress detrimental Th2 cell responses, these findings unveil a novel potential etiology of cryptococcal pathogenesis. Perhaps, HIV-directed lysis of CCR5+ Treg cells and/or therapeutic targeting of CCR5 in patients could exacerbate Th2-driven disease.

MATERIALS AND METHODS

Host. All mice used in this study were derived from a C57BL/6 background. B6.129P2(C)-*Ccr7*^{tm1Rfor}/J, B6.129P2-*Ccr5*^{tm1Kuz}/J, B6.Cg-*Foxp3*^{tm2Tch}/J, B6.129(Cg)-*Foxp3*$^{tm3(DTR/GFP)Ayr}$/J, *Foxp3*$^{tm9(EGFP/cre/ERT2)Ayr}$/J, B6.129S1-*Irf4*^{tm1Rdf}/J, B6.Cg-*Gt(ROSA)26Sor*$^{tm14(CAG-tdTomato)Hze}$/J, B6.PL-*Thy1*^{a}/CyJ mice were purchased from Jackson Laboratories (Bar Harbor, ME). Foxp3-cre/GFP mice were a kind gift from Calvin Williams. Foxp3-eGFP mice were crossed with Thy1.1 mice to generate congenic marked mice for transfer experiements. Foxp3-cre ERT2 mice were crossed with tdTomato mice for Treg fate-mapping studies. All mice were housed in specific pathogen–free conditions.

Pathogen. *Cryptococcus neoformans* var. *grubii* strain KN99α was streaked on yeast peptone dextrose (YPD) agar plates and incubated for 2 days at 30°C. YPD broth was inoculated with colonies from the aforementioned plate and incubated for 16 hours at 30°C with gentle agitation. The inoculum was prepared by pelleting the culture, washing 3 times with phosphate buffered saline (PBS), and resuspending in PBS at a concentration of $2x10^6$ cells/mL.

Infection. 6-8 week old, sex-matched mice were anesthetized with pentobarbitol. $5x10^4$ cryptococcal cells in 25 μL of PBS was placed on the nares of each mouse, and the mice aspirated the inoculum into the lower respiratory tract. Finally, the mice were suspended by their incisors for 5 minutes and subsequently placed upright in their cage until regaining consciousness. For survival studies, ten mice per group were infected as described above. Animals were monitored for morbidity and sacrificed when endpoint criteria were reached. Endpoint criteria were defined as 20% total body weight loss, loss of 2 grams of weight in 2 days, or symptoms of neurological disease.

Treatments. For intravital staining, 3 micrograms of anti-CD45.2 (104, BV421, Biolegend) was injected into the tail vein of mice or placed on the nares of sedated mice

(250). Foxp3-cre ERT2 tdTomato mice received 2mg/day tamoxifen IP for five consecutive days to induce endogenous fluorescence for Treg cell fate-mapping. For transfer studies, $1x10^6$ negatively-selected CD4+ Th cells from naïve mice were injected via tail vein into congenic mice infected 7 days previously, and lungs were harvested at 14 days post-infection for leukocyte isolation and flow cytometric analysis. For CCR5 blockade experiments, mice were treated IP with 500 μg/day maraviroc (R&D Systems, Minneapolis, MN) from 9-14 days post-infection. Lastly, wildtype mice were treated 5 and 10 days post-infection with 1 mg of IL-10R antibody (1B1-3A, Bio-X-Cell) to block IL-10 signaling.

Pulmonary Leukocyte Preparation. Lung leukocytes were isolated as previously described (210). Briefly, lungs were excised and minced to generate approximately 1 mm^3 pieces. The lung mince was incubated in HBSS (Invitrogen, Grand Island, NY) + 1.3 mM EDTA solution for 30 min at 37 °C with agitation, and then transferred to RPMI-1640 (Invitrogen) medium supplemented with 5% Fetal Bovine Serum (FBS) (Invitrogen) and 150 U/ml type I collagenase (Invitrogen) and incubated for 1 h at 37 °C with agitation. The cells were passed through a 70 μm filter, pelleted, and resuspended in 44% Percoll-RPMI medium (GE Life Sciences, Pittsburgh, PA). A percoll density gradient was created (44% top, 67% bottom), and the samples were centrifuged for 20 min at 650X *g*. The leukocytes at the interface were removed, washed 2 times with RPMI medium, and resuspended in PBS + FBS at a concentration of 10^7 cells/ml. CD4+ T cells were enriched using a Dynabeads CD4+ T Cell Negative Isolation Kit (Life Technologies, Grand Island, NY) per manufacture's instructions. For intracellular cytokine analysis, ~10^6 CD4+ T cells were suspended in 200 μL of restimulation buffer (RPMI + 10% FBS + 1% penicillin/streptomycin + 5 μg brefeldin A) without (unstimulated) or with (stimulated) 10 ng phorbol myristate acetate (PMA) and 50 ng ionomycin. After 5 hours, the cells were washed and immediately prepared for flow cytometry.

Flow Cytometry. Samples were incubated for 5 minutes with CD16/32 antibody (Biolegend) and LIVE/DEAD Fixable Far Red stain (Invitrogen) to prevent nonspecific antibody binding, as well as mark dead cells. 25nM Cda2-tetramer was added to the sample and incubated at 25°C for 1 hour in the dark. CCR3 (J07E35, PE, Biolegend), CCR4 (2G12, PE, Biolegend), and CCR5 (HM-CCR5, PE, Biolegend) were added 1:50 during tetramer staining when appropriate. Samples were surface-stained at 4°C for 30 minutes with the following antibodies: CD4 (RM4-5, BV605, Biolegend), CD11b (M1/70, PE-Cy5, eBioscience, San Diego, CA), CD11c (N418, PE-Cy5, eBioscience), B220 (RA3-6B2, PE-Cy5, eBioscience), CD25 (3C7, BV650, Biolegend), CD44 (IM7, Alexa Fluor 700, Biolegend) and/or Siglec F (E50-2440, PE, BD Biosciences). When applicable, the cells were then incubated in Foxp3 Transcription Factor Buffer (eBioscience) at 4°C for 30 minutes. The cells were labeled with antibodes against the following intracellular antigens: Foxp3 (FJK-16s, FITC, eBioscience), IL-5 (TRFK5, APC, Biolegend), IL-13 (eBio13A, eFluor 450, eBioscience), GATA3 (L50-823, PE-Cy7, BD Biosciences), and/or IRF4 (3E4, eFluor 450, eBioscience). 1:200 antibody concentrations were used for most surface staining, and 1:100 antibody concentrations were used for intracelluar staining. For data acquisition, events from the entire sample (500,000-1,000,000) were collected on a BD FACSCanto II flow cytometer (BD Biosciences, San Jose, CA), and the data were analyzed with FlowJo X (Tree Star Inc., Ashland, OR).

Naïve Th cell Enrichment. Analysis of antigen-specific Th cells within the pre-immune repertoire was performed, as previously published (209). Briefly, thymi and secondary lymphoid organs were collected from uninfected Foxp3-GFP mice. Cell suspensions were labeled with Cda2-tetramer and enriched using anti-PE MACS cell isolation kits (Miltenyi, San Diego, CA). Flow cytometry was performed as described above.

Lung Cytokines. Lungs from naïve mice or mice 14-days post-infection were excised, snap frozen in liquid nitrogen, and homogenized in 3 mL of T-PER (Thermo Fisher Scientific) with Complete Protease Inhibitor Cocktail (Roche, Indianapolis, IN). The lung

homogenate was pelleted, and the supernatant was collected and stored at -80°C until analysis. Samples were diluted 1:4 in assay buffer immediately before processing. Cytokines were quantified using Luminex technology according to manufacturer instructions (Bio-Rad, Hercules, CA).

Lung Histology. Lungs were removed from mice 14 days post-infection, perfused via the right ventricle with cold PBS, inflated with 10% formalin (Thermo Fisher Scientific, Rockford, IL), and placed in a container of 10% formalin. Tissues were dried with organic solvent, embedded in parafin, sectioned, and stained with hematoxylin and eosin, before images were captured.

Statistics. *P*-values for pairwise comparisions were by Mann-Whitney *U* with Bonferroni adjustments for multiple comparisons. Global tests were by Kruskal-Wallis ANOVA. Surival curves were compared with log-rank tests. Power calculations were performed to assess appropriate sample size for all experiments. *P*-values ≤ 0.05 were considered statistically significant. All statistics and graphs were processed with Prism 6 (GraphPad Software, La Jolla, CA).

Study Aproval. All animal experiments were done in concordance with the Animal Welfare Act, U.S. federal law, and NIH guidelines. Mice were handled in accordance with guidelines defined by the University of Minnesota Institutional Animal Care and Use Committee (IACUC) protocol numbers 1010A91133 and 1207A17286.

ACKNOWLEDGEMENTS:

We thank Dr. Calvin Williams (Medical College of Wisconsin) for kindly providing Foxp3-cre mice, as well as Dr. Marc Jenkins for helpful discussions. We are also grateful to the University of Minnesota Flow Cytometry Core Facility for instrumentation, and the University of North Carolina Lineberger Comprehensive Cancer Center Animal Histopathology Core Facility. This work was supported by NIH grant AI080275 to KN.

DLW received support from NIH T32 training grant AI007313, University of Minnesota Doctoral Dissertation Fellowship, and Dennis W. Watson Fellowship.

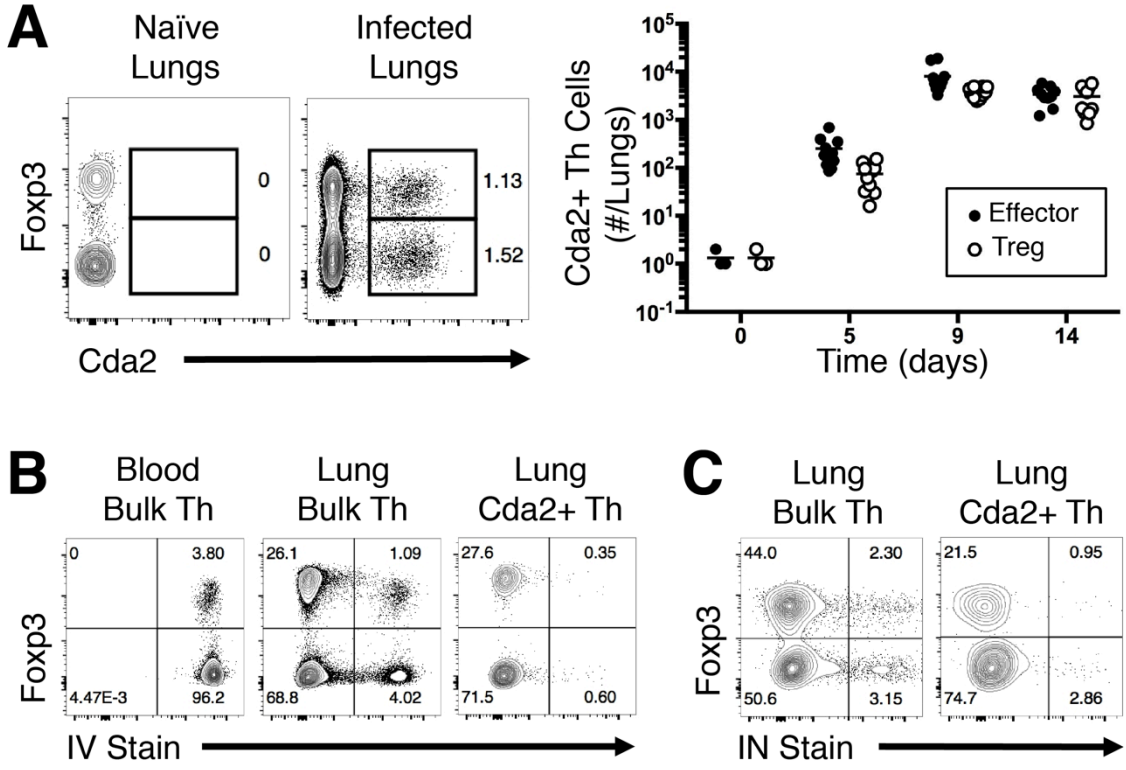

Figure 1. Antigen-specific Treg and effector Th cells colocalize in the lung parenchyma. (**A**) Flow plots (*left*) and composite graph (*right*) of antigen-specific Cda2+ CD4+ Treg and effector Th cells in naïve and infected mice. (**B**) Cytometry plots of CD4+ Th cells in peripheral blood (*left*) or whole lung (*center*), and antigen-specific CD4+ Th cells in whole lungs (*right*) all treated with intravital/intravenous (IV) fluorescent CD45 antibody. (**C**) Cytometry plots of CD4+ polyclonal Th cells (*left*) and antigen-specific Th cells (*right*) from whole lung digests after intravital/intranasal (IN) instillation of fluorescent CD45 antibody. Plots are representative of 2 independent experiments.

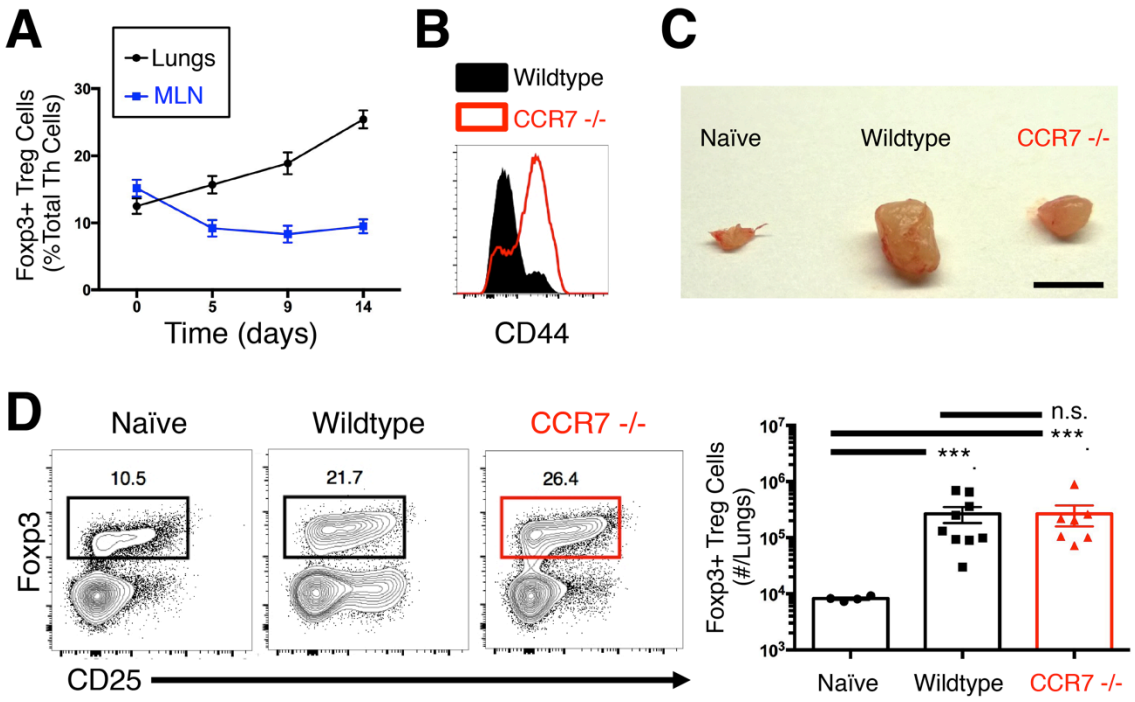

Figure 2. Lymph node priming is dispensable for Treg cell accumulation in the lungs. (**A**) Foxp3+ Treg cells as a proportion of total CD4+ Th cells in the lungs and mediastinal lymph nodes (MLN). (**B**) Histogram of CD44 expression by CD4+ Th cells from lymph nodes of wildtype and CCR7 -/- mice 14 days post-infection. (**C**) MLN of naïve wildtype, as well as 14 days post-infection wildtype and chemokine receptor 7 (CCR7) deficient mice Scale bar = 2 mm. (**D**) Cytometry plot (*left*) and composite graph (*right*) of Foxp3+ Treg cells from lungs of naïve wildtype and 14 days post-infection wildtype and CCR7 -/- mice. Pairwise comparisons were made by Man-Whitney U with Bonferoni adjustments for multiple comparisons. *** = $P<0.0005$, *n.s.* = non-significant. All data are presented as the mean +/- standard error of the mean and represent 2 independent experiments.

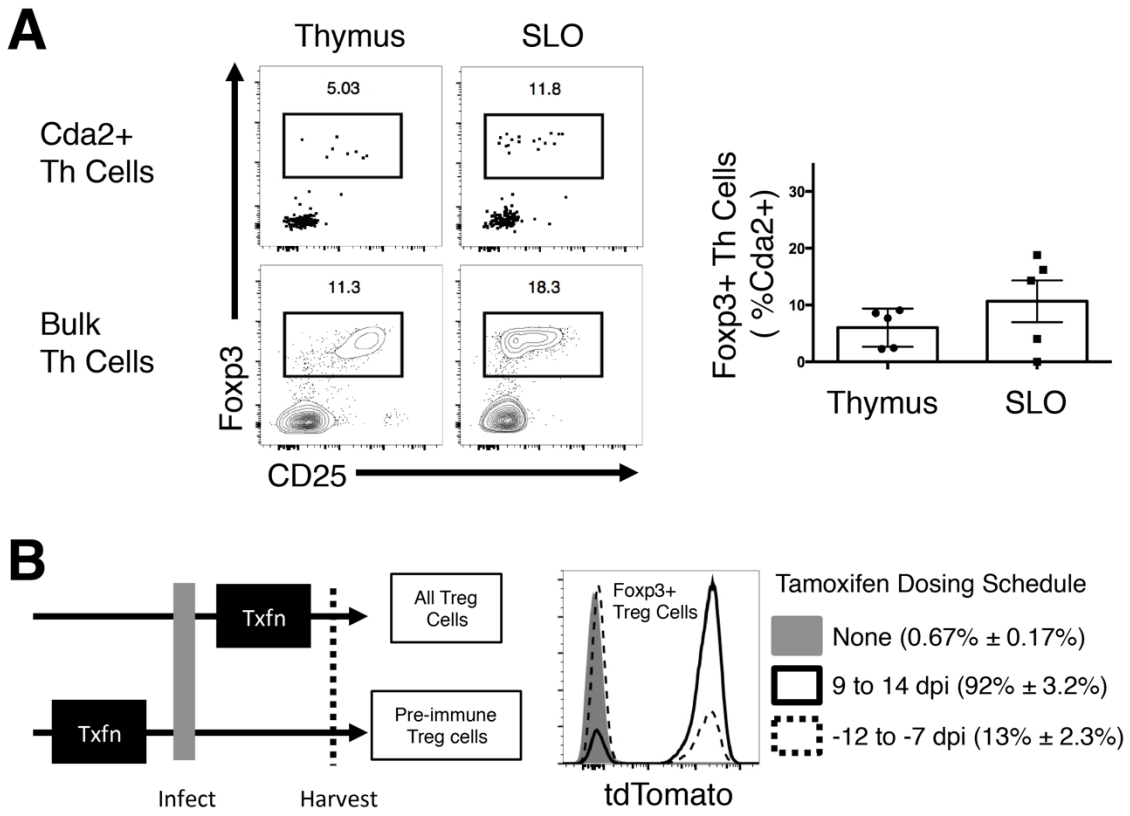

Figure 3. Treg cells in the preimmune repertoire are not the dominant source of Treg cells that accumulate in the lungs of fungal infected mice. (**A**). Foxp3+ Treg cells as a proportion of Th cells in the thymus or secondary lymphoid tissue of naïve mice. Representative cytometry plots of polyclonal and antigen-specific Th cells (*left*) and composite graph of antigen-specific Th cells (*right*). (**B**) *In vivo* genetic fate-mapping strategy of Treg cells using Foxp3-cre ERT2 x Rosa26 stop-floxed tdTomato mice (*left*). Cytometry plots of fluorescent reporter activity in antigen-specific Treg cells from lungs with or without tamoxifen (Txfn) (*right*). All data are presented as the mean ± standard error of the mean and represent 2 independent experiments.

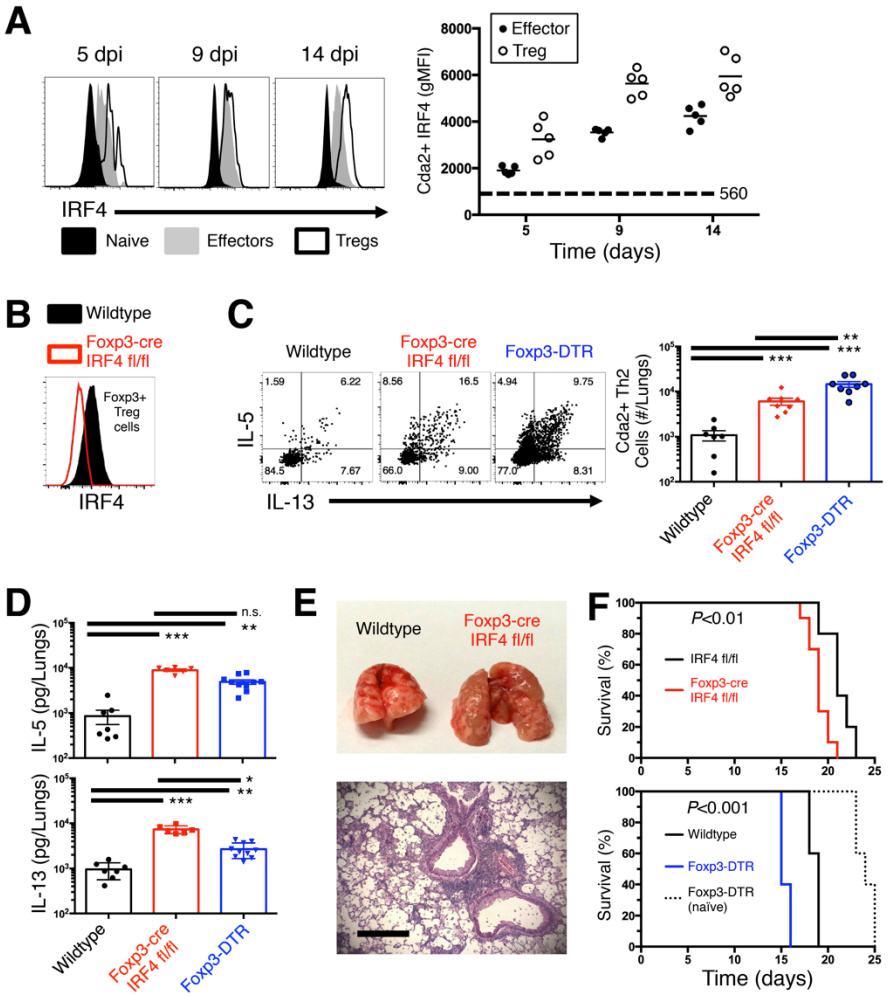

Figure 4. IRF4 is required by Treg cells to efficiently suppress the detrimental Th2 cell response to pulmonary cryptococcal infection. (**A**) Flow cytometry histogram (*left*) and composite graphs (*right*) of Interferon Regulatory Factor 4 (IRF4) expression in CD44 low naïve, Cda2+ Foxp3+ Treg, Cda2+ Foxp3- effector cells collected from the lungs of mice. (**B**) Histogram of IRF4 expression by lung Treg cells in wildtype and Foxp3-cre IRF4 fl/fl mice 14 days post infection. (**C**) Antigen-specific Th2 cells producing interleukin-5 (IL-5) and/or IL-13 in the lungs of wildtype, Foxp3-cre, and Foxp3-DTR mice 14 days post-infection. (**D**) Total IL-5 and IL-13 secreted in lung homogenates from wildtype, Foxp3-cre, and Foxp3-DTR mice 14 days post-infection.

(**E**) Photograph of gross-level pathology of lungs from mice infected 14 days previously (*top*). Hematoxylin and eosin staining of lung sections from Foxp3-cre mice 14 days post-infection (*bottom*). Bar = 200 μm. (**F**) Survival curve of IRF4 fl/fl and Foxp3-cre IRF4 fl/fl infected mice (*top*). Survival curves of naïve Foxp3-DTR, as well as infected wildtype and Foxp3-DTR mice – all groups treated every other day with 200 ng DT beginning at 5 days post-infection (*bottom*). Survival curves include 10 mice per group, and *P*-values calculated by log rank test. Pairwise comparisons were made by Man-Whitney U with Bonferoni adjustments for multiple comparisons. *** = $P<0.0005$, ** = $P<0.005$, * = $P<0.05$, *n.s.* = non-significant. All data are presented as the mean ± standard error of the mean and represent 2 independent experiments.

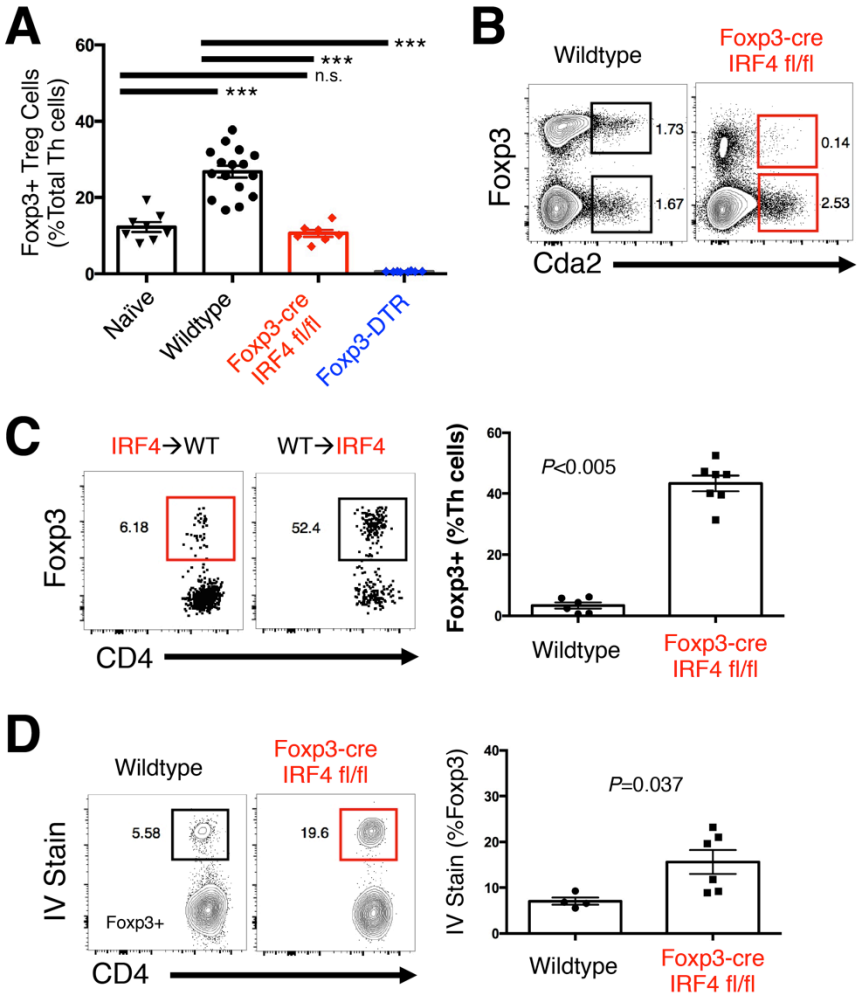

Figure 5. Pulmonary retention of Treg cells is maintained by IRF4. (**A**) Frequency of Foxp3+ Treg cells in the lungs of naïve wildtype mice and wildtype, Foxp3-cre, and Foxp3-DTR mice 14 days post-infection. (**B**) (**C**) Flow cytometry plots and composite graphs of Foxp3-IRF4 fl/fl or widltype donor Th cells collected from lungs of wildtype or Foxp3-cre IRF4 mismatched recipients at 14 days post-infection. (**D**) Flow plots and composite graphs of pulmonary Treg cells from wildtype and Foxp3-cre IRF4 mice infected 14 days previously and treated with intravenous anti-CD45 antibody. Pairwise comparisons were made by Man-Whitney U with Bonferoni adjustments for multiple comparisons. *** = $P<0.0005$, *n.s.* = non-significant. All data are presented as the mean ± standard error of the mean and represent 3 independent experiments.

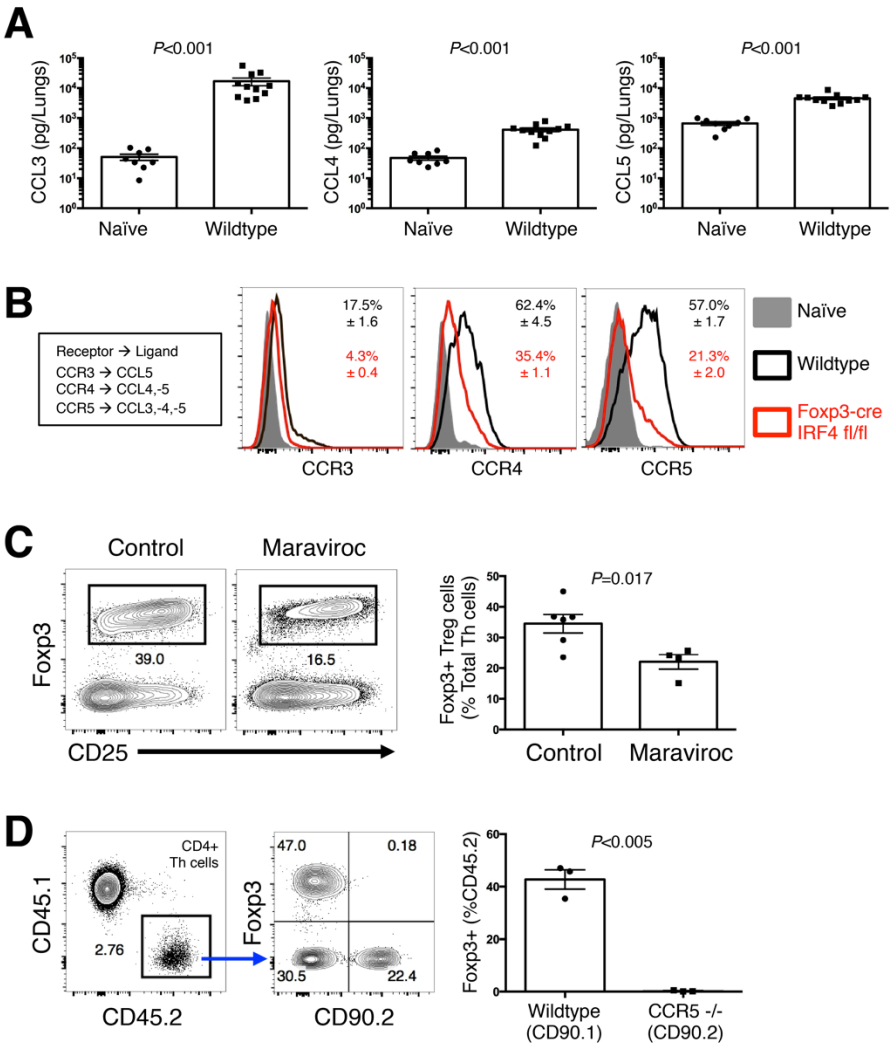

Figure 6. Treg cell accumulation is mediated by CCR5 via IRF4. (**A**) Chemokine Ligands (CCL) measured in lung homogenates from wildtype mice 14 days post-infection. (**B**) Cytometry histograms of Chemokine Receptor (CCR) expression on CD44 low naïve cells, as well as Treg cells from wildtype and Foxp3-cre IRF4 fl/fl mice 14 days post-infection. (**C**) Flow plots (*left*) and composite graphs (*right*) of Treg cells in the lungs of mice 14 days post-infection with and without maraviroc treatment. (**D**) CD45.2/CD90.1 wildtype and CD45.2/CD90.2 CCR5 -/- naïve Th cells transferred into a CD45.1/ CD90.2 Foxp3-DTR mouse infected and Treg cell-depleted 7 days previously. Pairwise comparisons were made by Man-Whitney U. All data are presented as the mean ± standard error of the mean and represent 2 independent experiments.

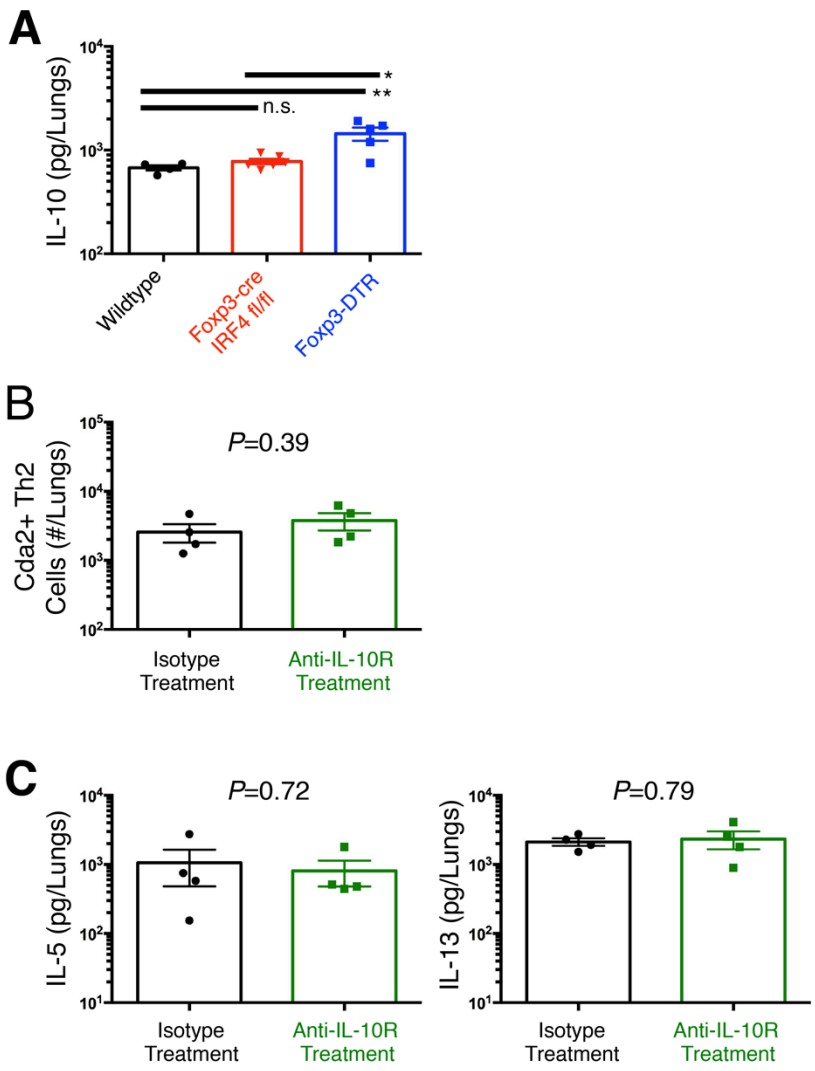

Figure S1. IL-10 is dispensable for suppression of Th2 cells produced in response to pulmonary cryptococcal infection. (**A**) Interleukin (IL)-10 measured in lung homogenates from wildtype, Foxp3-IRF4 fl/fl, and Foxp3-DTR mice 14 days post-infection. (**B**) Cda2+ Th2 cells quantified in the lungs of infected mice treated with IL-10 receptor blocking antibody or isotype control. (**C**). IL-5 (*left*) and IL-13 (*right*) measured in lung homogenates from infected mice treated with IL-10 receptor blocking antibody or isotype control. Pairwise comparisons were made by Man-Whitney U with Bonferoni adjustments for multiple comparisons. All data are presented as the mean ± standard error of the mean.

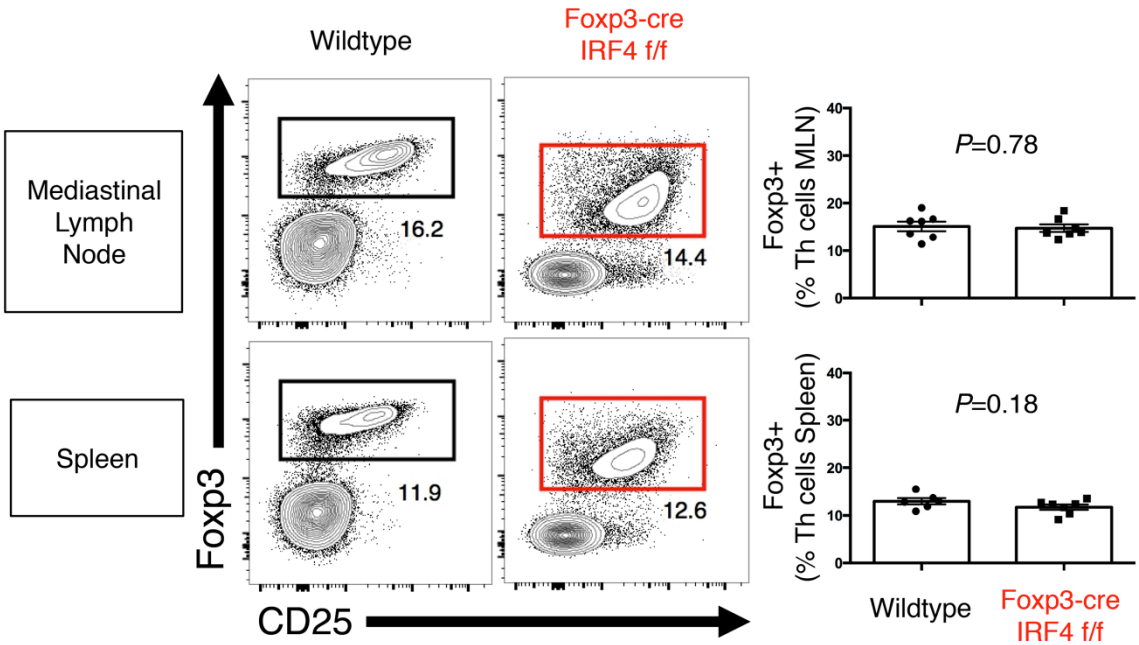

Figure S2. IRF4-deficient Treg cells differentiate normally in secondary lymphoid tissues. Flow cytometry plots and composite graphs of Th cells of mediastinal lymph nodes (MLN) and spleens from wildtype and Foxp3-cre IRF4 fl/fl mice infected 14 days prior. Plots are representative of 2 independent experiments.

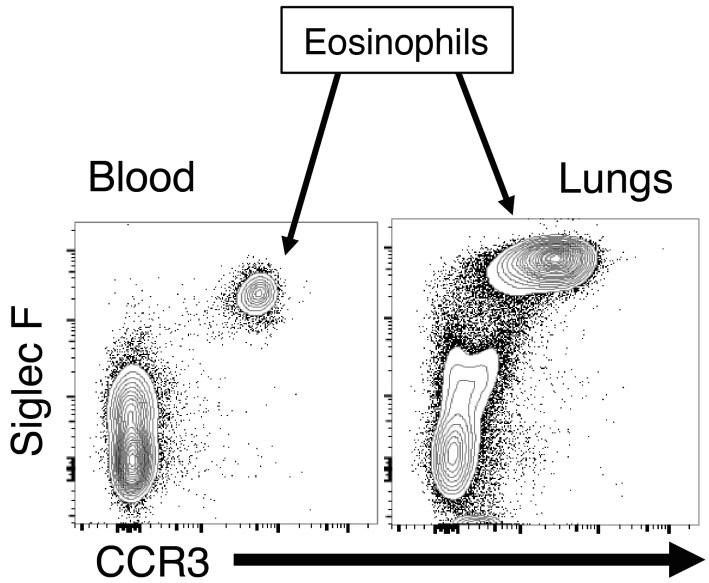

Figure S3. Anti-CCR3 (J07E35) readily detects eosinophils in the blood and lungs of cryptococcal infected mice. Flow plots of total leukocytes in blood (*left*) and lungs (*right*) 14 days post-infection. Siglec F+, CCR3 + cells are eosinophils. Plots are representative of 2 independent experiments.

CHAPTER 4

Lymphocyte Competition Determines Granulocyte Responses to Pulmonary Fungal Infection.

SUMMARY

Immunity to pulmonary fungal infection often involves a complex orchestration of an array of lymphocytes that instruct eosinophil and neutrophil differentiation. Interleukin-5 production by type-2 innate lymphoid cells and CD4+ T cells induces and sustains eosinophilia. Type-3 innate lymphoid cells, CD4+ T cells, CD8+ T cells, and γδ T cells coordinate neutrophil accumulation via secretion of interleukin-17. However, the relative contribution of each lymphocyte subset that ultimately determines a dichotomous eosinophil or neutrophil response remains enigmatic. Here, we use a murine model of pulmonary fungal infection to show that distinct lymphocyte lineages engage in competition to direct eosinophil or neutrophil responses, and we further establish a hierarchical relationship between these lymphocytes based on their ability to organize granulocytes in the lungs. Finally, we show that lymphocyte-derived IL-5 functions to promote eosinophilia, as well as intrinsically suppress neutrophil accumulation. Our data collectively address a fundamental question of lymphocyte regulation. We demonstrate that competition between lymphocyte subsets can determine the functional consequences of an immune response, leading to eosinophilia or neutrophilia and exacerbated disease.

INTRODUCTION

Fungi belong to a unique class of pathogens where the host both relies on lymphocytes to confer protection from disease, as well as suffers the unfortunate consequence of lymphocyte-mediated pathology. A selective elimination of T cells due to HIV infection results in more frequent and severe mycosis, revealing a potent, beneficial role for lymphocytes in preventing invasive disease (53). Conversely, most cases of allergic asthma in otherwise healthy individuals directly result from inappropriate lymphocyte responses to fungal exposure (90). This dichotomy highlights the heterogeneity among lymphocytes responding to fungal infection, and further draws attention to the delicate balance of immune homeostasis. Thus, pulmonary fungal infections are an optimal model to study lymphocyte regulation.

Eosinophils and neutrophils are granulocyte subsets that originate from the same myeloblast progenitor in the bone marrow. IL-5 is a key regulator of eosinophil maturation, whereas IL-17/IL-22 leads to systemic release of G-CSF and neutrophil differentiation (251, 252). Upon differentiating into eosinophils or neutrophils, each of these granulocytes acquires unique functional capabilities. Eosinophils expel toxic products from granules into the inflammatory milieu (253). While this is an effective strategy to ward off parasitism, it causes host damage and when dysregulated, contributes to allergic airway disease (254). Neutrophils also produce toxic granules, yet the additional ability to produce extracellular traps and phagocytose microbes make neutrophils particularly useful in immunity to some fungal and bacterial pathogens (255, 256).

Among other important functions, lymphocytes secrete cytokines that coordinate eosinophil and neutrophil responses. Type-2 CD4+ T (Th2) cells along with type-2 innate lymphoid cells produce interleukin (IL)-5 that sustains and induces eosinophil production under homeostatic and inflammatory conditions (97, 193). Additionally Th17 cells, CD8+ T (Tc17) cells, γδ T cells, and ILC3 promote neutrophil maturation through secretion of IL-17 and/or IL-22 (257-259). Some pulmonary pathogens elicit neutrophilic responses (260, 261) while other pulmonary pathogens prompt eosinophil responses (262,

263). Moreover, a mixture of these responses is most advantageous for protection against parasitic and fungal infections (264, 265). Finally, the loss of eosinophils often accompanies neutrophil accumulation and *vice versa* (69, 70, 266). Thus, a dynamic interaction between the host and microbe can fundamentally influence the immune response. This spurs the question of how is downstream granulopoiesis regulated by a complex mixture of lymphocytes.

To investigate lymphocyte and granulocyte responses, we utilized a well-established murine model of experimental cryptococcosis. A highly virulent strain of the fungus, *Cryptococcus neoformans* (KN99α), was instilled into the lungs of C57BL6/J mice. We analyzed lymphocyte and granulocyte composition in the bone marrow, blood, and lungs with flow cytometry at regular intervals following infection. Genetic deficiencies in lymphocyte subsets revealed an intricate competition among lymphocytes that had polarizing effects on the downstream eosinophil and neutrophil responses. Through these genetic manipulations we were able to define a hierarchy of lymphocytes regarding their ability to determine neutrophil or granulocyte accumulation in the lungs. Furthermore, we uncovered a duality in the role of IL-5; IL-5 functions to positively regulate eosinophilia, as well as inhibit neutrophil accumulation. Taken, together these findings offer unique insights into the dynamic regulation of lymphocyte and granulocyte responses to pulmonary fungal infection that have profound impacts on disease.

RESULTS

We used flow cytometry to identify eosinophils and neutrophils in the bone marrow, blood, and lungs. Siglec F is expressed by eosinophils upon commitment to the eosinophil lineage (272). Chemokine receptor 3 (CCR3) binds to eotaxin, and this interaction is required for eosinophil chemotaxis from the bone marrow to the tissues (273). Thus, mature eosinophils are defined by the expression of CCR3 and Siglec F in the bone marrow and blood. However, in the lungs, eosinophils and alveolar macrophages express CCR3 and Siglec F, yet only alveolar macrophages have CD11c on their surface (**Figure 1**). Consequently, lung eosinophils are denoted as Siglec F+ CD11c- cells. Neutrophils are uniquely identified as Ly6G+ CD11b+ in the bone marrow, blood, and lungs (274).

Progressive production of granulocytes in response to cryptococcal infection

Eosinophils and neutrophils develop in the bone marrow, travel through the blood stream, and enter the tissues (267, 268). More specifically, granulocytes can arrive at a site of insult along two trajectories. First, mature granulocytes are distributed throughout the body in vascular pools, and upon "emergency" response, the granulocytes can be acutely recruited to the inflamed tissues in a process known as demargination (269-271). Alternatively, immature granulocytes in the bone marrow can receive cytokine and chemokine cues from lymphocytes and other cells in the tissues that lead to *de novo* eosinophil and neutrophil differentiation and recruitment (251). The kinetics of the granulocyte response is a key difference between these pathways. Demargination occurs on the order of hours to a day, while lymphocyte-induced production of granulocytes occurs over the course of days to weeks.

To understand whether granulocytes accumulated in the lungs due to demargination or a lymphocyte-mediated process, we measured eosinophils and neutrophils throughout the course of pulmonary infection with *C. neoformans*. CCR3+ Siglec F+ eosinophils progressively increased in the bone marrow (**Figure 2A**), and these cells were steadily released into the bloodstream (**Figure 2B**). Siglec F+ CD11c-

eosinophils accumulated in the lungs and accounted for an overwhelming majority of the pulmonary leukocytes at later time points of infection (**Figure 2C**). Ly6G+ CD11b+ neutrophils were continuously produced in the bone marrow (**Figure 2A**) and represented a large, increasing population in the blood (**Figure 2B**). However, neutrophils stayed a minor proportion of leukocytes in the lungs of infected mice (**Figure 2C**). Thus, both granulocyte types were produced upon infection, but predominantly eosinophils accumulated in the lungs. The long duration and progressive nature of granulocyte responses to pulmonary fungal infection also suggested that granulocytes are induced by a lymphocyte-dependent process, not demargination.

Lung-resident lymphocytes fully govern eosinophil responses and partially influence neutrophil responses to pulmonary fungal infection

Lymph nodes are conventional locations for lymphocyte priming. However, *C. neoformans* elicits a Th2 cell response that is not dependent on lymph node responses (222). Therefore, we tested the hypothesis that granulocyte recruitment does not require lymphocyte induction in the mediastinal lymph node. FMS-like tyrosine kinase 3 ligand (Flt3L) is required for dendritic cell maturation (275), and CCR7 mediates lymphocyte entry into lymph nodes (276). Thus, genetic deficiency in each of these molecules significantly impairs lymph node responses. Eosinophil and neutrophil recruitment to the lungs were not decreased by Flt3L or CCR7 ablation (**Figure 3**), indicating the mediastinal lymph node is not a primary location for priming of granulocyte-inducing lymphocytes in this model. This finding prompted us to focus our attention on lymphocytes in the lungs.

To identify which lymphocytes induce eosinophils, we screened an array of lymphocyte-deficient mice and monitored the effect this had on eosinophil accumulation in the lungs upon infection. Lymphocytes were identified as lineage- (CD19, CD11b, CD11c, CD49b, CD161, F4/80, FcεRIα, B220) and CD90.2+. Lymphocytes increased >25-fold in infected wildtype mice at an intermediate time point of infection (i.e. 14 days) compared to naïve controls **(Figure 4A**). Two lineages of lymphocytes are known to be involved in eosinophil recruitment: Th2 cells and ILC2. Only Th cells are major

histocompatibility complex II (MHCII) restricted. Therefore, MHCII-deficiency inhibits the development and function of Th cells, but not other lymphocytes. As predicted, MHCII -/- mice had a defective TCRβ+ CD4+ Th cell response (**Figure 4A**). The loss of Th cells through MHCII-deficiency also abrogated pulmonary eosinophil accumulation (**Figure 4B**). Notably, eosinophil production was evident in the bone marrow, blood, and lungs early in the response (<5 days) of infected MHCII -/- mice, but eosinophil production subsided at the onset of the adaptive immune phase (>9 days) (**Figure 5A-C**). Recombination-activating gene 2 (Rag2) knockout mice have ILC but no peripheral T cells (i.e. TCRβ+ CD4+ Th cells, TCRβ+ CD8+ T cells, or γδ T cells) (**Figure 4A**). In striking contrast to the MHCII -/- response, Rag2 -/- mice experienced robust eosinophilia in the lungs (**Figure 4B**). To assess whether eosinophil recruitment is limited to lymphocytes, we utilized Rag2 -/- IL-2Rγ -/- mice that have a complete lymphocyte deficiency (**Figure 4B**). These mice exhibited a dramatic reduction of lung eosinophils (**Figure 2B**), and as a result, pulmonary lymphocytes govern eosinophil responses to fungal infection. Taken together, Th cells are the main drivers of eosinophil recruitment during fungal infection, and ILC are only sufficient to drive eosinophilia early in the response or in the absence of T lymphocytes.

With specific elimination of Th cells in MHCII knockout mice, we observed a dramatic increase in CD8 T cells upon cryptococcal infection (**Figure 4A**). This correlated with a massive accumulation of neutrophils in the lungs (**Figure 4B**). Conversely, T lymphocyte-deficient Rag2 -/- mice did not exhibit a compensatory neutrophilic response (**Figure 4B**). Finally, total lymphocyte-lacking Rag2 -/- IL-2Rγ -/- mice recruited fewer neutrophils to the lungs than infected wildtype mice, yet the loss of lymphocytes in these mice did not completely abrogate neutrophil recruitment (**Figure 4B**). Therefore, lymphocytes influence neutrophil recruitment in response to pulmonary fungal infection, especially with a dearth of Th cells. However, lymphocytes are not completely required for neutrophil accumulation.

Lymphocyte-derived cytokines regulate granulocyte responses

Next, we investigated the regulation of granulocytes by lymphocyte cytokines. Increased quantities of IL-5, eotaxin, granulocyte-colony stimulating factor (G-CSF), and to a lesser extent, IL-17A were found in lung homogenates of infected wildtype mice compared to naïve controls (**Figure 6A**). IL-5, eotaxin, and G-CSF were also abundant in the plasma of infected mice (**Figure 6A**). Thus, these cytokines were released into the bloodstream where they can instigate bone marrow granulopoiesis. IL-5 secretion, but not eotaxin, in Th cell-deficient MHCII -/- mice was knocked down to near naïve levels in the lungs and plasma. Instead, local IL-17A and G-CSF, as well as peripheral G-CSF, dramatically increased in fungal infected MHCII -/- mice compared to wildtype counterparts (**Figure 6A**). Thus, Th2 cells are required for IL-5 production. Eotaxin is produced by a Th cell-independent source and eotaxin is not sufficient to drive eosinophil accumulation in the lungs. Finally, local IL-17A and G-CSF, as well as systemic G-CSF, increase in the absence of Th cells and this correlates with the neutrophilia experienced by infected MHCII -/- mice.

IL-5 signaling is a canonical pathway of eosinopoiesis with no known role in neutrophil development (251, 277). The observations that neutrophils increase in the absence of IL-5 or IL-17-producing lymphocytes, led us to test the hypothesis that IL-5 promotes eosinophil responses while simultaneously inhibiting neutrophils. Mepolizumab (GlaxoSmithKline) is an anti-IL-5 antibody therapy that recently concluded clinical trials for the treatment of eosinophilic asthma in humans (278, 279). The drug functions by blocking IL-5 binding to the alpha chain of the IL-5 receptor (IL-5Rα) (280). Treatment of infected wildtype mice with a murine equivalent anti-IL-5 antibody (TRFK5) reciprocally decreased eosinophils and increased neutrophils (**Figure 6B**). Infected IL-17Rα -/- mice experienced a reduced, though incomplete elimination of neutrophil accumulation (**Figure 6B**), which is consistent with the lymphocyte-independent neutrophil production previously observed in Rag2 -/- IL-2Rγ -/- mice (**Figure 2**). Thus, abrogation of IL-5 enhances neutrophil accumulation.

Lymphocytes do not express IL-5Rα (**Figure 6C**), which rules out the possibility that IL-5 directly cues lymphocytes to coordinate indirect suppression of neutrophil

recruitment. In contrast, neutrophils are the highest IL-5α-expressing hematopoietic cells in bone marrow, blood, and lungs of infected mice (**Figure 6C**). This raises the possibility that IL-5 signals intrinsically on neutrophils. In support of this idea, exogenous IL-5 treatment of mice incapable of producing IL-5+ Th2 cells (MHCII -/- mice) inhibited neutrophils in a dose-dependent manner (**Figure 6D**). Taken together, IL-5 mediates intrinsic suppression of neutrophils.

Lymphocyte competition determines eosinophil or neutrophil polarity and impacts lethal fungal disease

The unexpected lymphocyte compensation observed in the preceding experiments prompted us to dissect the hierarchy of lymphocytes in coordinating granulocyte recruitment. Infection of wildtype mice elicited production of IL-5 by both Th2 cells and ILC2 (**Figure 7, Table 1**). However, the specific loss of Th cells in MHCII -/- mice concomitantly reduced IL-5+ lymphocytes and eliminated eosinophilia (**Figure 7, Table 1**). Thus, ILC2 are either impotent without Th2 cells or Th2 cells are the main determinant of the eosinophil response.

Next, we evaluated the position of IL-17+ lymphocytes in the hierarchy. Signal transducer and activator 6 (STAT6) is a regulator of the type-2 effector phenotype (281), and STAT6 -/- mice had a defective Th2 cell and ILC2 response to fungal infection (**Figure 7**). Accordingly, a potent neutrophil response coincided with Th17 cells that outnumbered Tc17 cells, γδ T cells, and ILC3 in STAT6 -/- mice (**Figure 7&8, Table 1**). Upon anti-CD4 treatment of infected STAT6 -/- mice, Tc17 cells compensated for the loss of Th17 cells (**Figure 7, Table 1**), establishing Tc17 cells as subordinate to Th17 cells but dominant to γδ T cells and ILC3.

We next isolated γδ T cells and ILC using TCRα -/- mice that have CD4+ and CD8+ T cell deficiencies. γδ T cells outpaced the ILC subsets to drive a neutrophilic response in infected TCRα -/- mice (**Figure 7&8, Table 1**). Finally, T lymphocyte-deficient Rag2 -/- mice experienced eosinophilia instigated by a large population of ILC2 (**Figure 7&8, Table 1**). In summary, Th2 cells command the eosinophil response seen in mice with a full complement of lymphocytes. In their absence, an expansion of IL-17A+

lymphocytes correlates with a neutrophilic switch. Within these IL-17A+ lymphocytes, Th17 cells are the main inducers of neutrophil recruitment, followed in order by Tc17 cells and γδ T cells. Finally, without T lymphocyte participation, ILC2 outcompete ILC3 to incite eosinophilia.

Balanced eosinophil and neutrophil responses are more beneficial than strongly polarized responses to some fungal and parasitic infections (264, 265). Consequently, we sought to determine how extreme eosinophil or neutrophil polarization would affect lethal cryptococcal disease compared to the mildly balanced wildtype granulocyte response. IL-2/IL-2 antibody complex treatment strongly amplifies type-2 responses, and this significantly exacerbates disease in wildtype mice (222). Conversely, STAT6 -/- mice experienced neutrophilia (**Figure 8**), and this shift in neutrophil response correlated with significantly accelerated disease. Thus, eosinophil or neutrophil polarization is detrimental during pulmonary fungal infection.

DISCUSSION

Herein, we aimed to dissect the complex regulation of lymphocytes with regard to their ability to coordinate pulmonary granulocyte accumulation. CD4+ Th cells were long believed to be the main coordinators of granulopoiesis through production of IL-5 and IL-17A (282). However, the realization that other lymphocyte subsets, like Tc17 cells, γδ T cells and ILC, could perform similar functions challenges this understanding (283, 284). Thus, a systematic evaluation of the potency of each subset in determining downstream responses (e.g. granulocytes) is warranted.

We showed through systematic elimination of lymphocyte subsets that lymphocytes engage in fierce competition to guide granulocyte induction (**Figure 10**). Fei and colleagues observed a similar phenomenon where BALB/c or C57BL/6 mice mounted disparate neutrophil or eosinophil responses to repeated exposure to *Aspergillus* conidia, and the loss of TNFα in *Aspergillus* treated BALB/c mice caused a neutrophil-to-eosinophil transition (266). This granulocyte switch observation was further corroborated in a model system of pulmonary inoculation with purified chitin (69). Chitin is a polysaccharide that elicts a CD4/8 T cell-independent, ILC2 allergic response (100), and depletion of IL-5+ ILC2 in chitin treated mice resulted in a compensatory increase in γδ T cell-driven neutrophil recruitment (69). Methodical examination of lymphocyte responses to bacterial and viral infections could reveal an equally interesting lymphocyte dynamic.

In recent years, ILC have emerged as main players in a variety of processes, including maintenance of tissue homeostasis, inflammation, and tissue damage repair (284). The standard model for investigating the sufficiency of ILC to coordinate these processes involves the use a RAG -/- mouse and examination of the effect CD90 antibody depletion or use of Rag -/- IL-2Rγ -/- mice has on a defined outcome (69, 285-287). In the case of pulmonary cryptococcal infection, T cells, not ILC, are the main propagators of granulocyte responses. The inclusion of MHCII -/- mice in our comparisons revealed that T cells reign supreme. Perhaps, a lack of competition with other lymphocytes for shared growth factors, like IL-2 and IL-7, exaggerates the effect of ILC2 on driving

eosinophilia in Rag2 -/- models. With the emergence of methods to specifically ablate ILC (189, 288), a more accurate description of the roles ILC have to play in inflammation may follow.

Eosinophil and neutrophil responses are traditionally thought be induced by distinct IL-5 and IL-17 modules. While IL-5 is clearly required for eosinophilia, neutrophil responses are only partially dependent on IL-17. Additionally, the reciprocal switch from eosinophil dominated response to one dominated by neutrophils when IL-5-producing lymphocytes were removed from the system led us to test the hypothesis that IL-5 also negatively regulates neutrophils. This hypothesis is supported by the observation of IL-5 receptor expression on neutrophils, as well as the IL-5 dose-dependent loss of neutrophils in Th2 cell deficient infected mice. However, the definitive test of the hypothesis will come from studies using IL-5Rα -/- (289); wildtype mixed bone marrow chimeras to determine the cell-intrinsic effect of IL-5 on neutrophil inhibition.

Allergic asthma is traditionally viewed as a type-2-driven eosinophilic disorder. However, neutrophils have an underappreciated role in allergic airway disease (290). IL-17-induced neutrophil responses are paradigmatically credited for protection against fungal infections (52). While true in some cases, as evidenced by enhanced susceptibility to mucocutaneous candidiasis in humans with IL-17-deficiencies (291), there are instances where IL-17 responses to fungal infection are deleterious, particularly in the lungs (292). As a result, the protection afforded by IL-17 against some pathogens should be weighed in the context of IL-17-associated immunopathology.

Next generation therapies will simultaneously utilize antimicrobials and immune modulators (104, 293). As a result, understanding the individual contributions of lymphocyte subsets informs important targets, predicts problematic compensation, and thereby, affords rational design of clinical interventions that modulate lymphocyte-dependent granulocyte responses. Moreover, IL-5 blockade with FDA approved therapies raises the exciting possibility of shunting detrimental IL-5/eosinophilia towards more beneficial, balanced IL-17/neutrophil responses to pulmonary fungal infections.

MATERIAL AND METHODS:

Host. All mice used in this study were derived from a C57BL/6 background. B6.129P2(C)-*Ccr7*^{tm1Rfor}/J, B6.PL-*Thy1*^{a}/CyJ, B6.129S2-*H2d*$^{lAb1\text{-}Ea}$/J, B6.129S7-*Rag1*^{tm1Mom}/J, B6.129S2(C)-*Stat6*^{tm1Gru}/J, and B6.129S2-*Tcra*^{tm1Mom}/J mice were purchased from Jackson Laboratories (Bar Harbor, ME). C57BL/6-*flt3*^{Ltm1Imx} and B10;B6-*Rag2*^{tm1Fwa} *Il2rg*^{tm1Wjl} mice were purchased from Taconic. IL-17Rα -/- were provided by Amgen. Mice were housed in specific pathogen–free conditions and were fed *ad labitum*.

Infection. 6-8 week old, sex-matched mice were anesthetized with pentobarbitol. $5x10^4$ *Cryptococcus neoformans* var. *grubii* (KN99α) cells in 25 μL of PBS were placed on the nares of each mouse, and the mice aspirated the inoculum into the lower respiratory tract.

Treatments. Mice received 1 mg anti-IL-5 (TRFK5, Bio X Cell, West Lebanon, NH) or 500 μg anti-CD4 (GK1.5, Bio X Cell) injected into the peritoneal cavity on -1, 5, and 10 days post-infection.

Leukocyte Preparation. Leukocytes were isolated from lung digests as previously described (222). For bone marrow cells, femurs were harvested from euthanized mice, pulverized in RPMI. ~250 μL of blood was collected from anesthetized mice via retro-obrital bleeding. Red blood cells were lysed in whole blood and bone marrow by incubating the samples in ACK buffer for 15 minutes at room temperature. Cell solutions were filtered, washed several times, and resuspended in PBS staining buffer at $5x10^6$ cells/mL. For intracellular cytokine analysis, ~10^6 CD4+ T cells were suspended in 200 μL of restimulation buffer (RPMI + 10% FBS + 1% penicillin/streptomycin + 5 μg brefeldin A) without (unstimulated) or with (stimulated) 10 ng phorbol myristate acetate (PMA) and 50 ng ionomycin. After 5 hours, the cells were washed and immediately prepared for flow cytometry.

Flow Cytometry. Samples were incubated for 15 minutes with CD16/32 antibody (Biolegend) and LIVE/DEAD Fixable Near Infrared stain (Invitrogen) to prevent nonspecific antibody binding, as well as mark dead cells. Samples were surface-stained at 4°C for 30 minutes with the following antibodies: Granulocytes – CCR3 (J07E35, PE, Biolegend, San Diego, CA), Ly6G (1A8, PE-Cy7, Biolegend), CD11b (M1/70, BV650, eBioscience, San Diego, CA), CD11c (N418, PE-Cy5, eBioscience), Siglec F (E50-2440, PE, BD Biosciences, San Jose, CA), IL-5Rα (T21, FITC, BD Biosciences), CD45 (30-F11, AF700, Biolegend), and Erithroid Cells (TER-119, Percp-Cy5.5, Biolegend); Lymphocytes – CD90.2 (30-H12, APC, Biolegend), CD4 (RM4-5, e450, eBioscience), CD8 (BV650, Biolegend), TCRβ (H57-597, PE-Cy7, Biolegend), TCRγδ (GL3, AF488, Biolegend), CD11b (M1/70, Percp-Cy5.5, Biolegend), CD11c (N418, Percp-Cy5.5, Biolegend), F4/80 (BM8, Percp-Cy5.5, Biolegend), CD49b (DX5, Percp-Cy5.5, Biolegend), Ly6G (1A8, Percp-Cy5.5, Biolegend), CD19 (6D5, Percp-Cy5.5, Biolegend), FcεRIα (MAR1, Percp-Cy5.5, Biolegend), CD161 (PK136, Percp-Cy5.5, eBioscience), and B220 (RA3-6B2, Percp-Cy5.5, eBioscience). When applicable, the cells were then incubated in Foxp3 Transcription Factor Buffer (eBioscience) at 4°C for 30 minutes. The cells were labeled with antibodes against the following intracellular antigens: IL-5 (TRFK5, PE, Biolegend) and IL-17A (BL168, BV605, Biolegend). For data acquisition, events from the entire sample (500,000-1,000,000) were collected on a BD FACSCanto II flow cytometer (BD Biosciences), and the data were analyzed with FlowJo X (Tree Star Inc., Ashland, OR).

Lung Cytokines. Lungs from naïve mice or mice 14-days post-infection were excised, snap frozen in liquid nitrogen, and homogenized in 3 mL of T-PER (Thermo Fisher Scientific) with Complete Protease Inhibitor Cocktail (Roche, Indianapolis, IN). Cytokines were quantified using Luminex technology according to manufacturer instructions (Bio-Rad, Hercules, CA).

Statistics. *P*-values for pairwise comparisions were by Mann-Whitney *U* with Bonferroni adjustments for multiple comparisons. Global tests were by Kruskal-Wallis

ANOVA. Power calculations were performed to assess appropriate sample size for all experiments. *P*-values ≤ 0.05 were considered statistically significant. All statistics and graphs were processed with Prism 6 (GraphPad Software, La Jolla, CA).

Study Aproval. All animal experiments were done in concordance with the Animal Welfare Act, U.S. federal law, and NIH guidelines. Mice were handled in accordance with guidelines defined by the University of Minnesota Institutional Animal Care and Use Committee (IACUC) protocol numbers 1010A91133 and 1207A17286.

AUTHOR CONTRIBUTIONS:

DLW conceived and performed experiments and wrote the manuscript. KDS performed experiments and edited the manuscript. PRB and KN helped conceive experiments and edited the manuscript.

ACKNOWLEDGEMENTS:

We thank Amgen for kindly providing IL-17Rα -/- mice, as well as Bryce Binstadt and Daniel Mueller for also sharing mice. We additionally thank Marc Jenkins for helpful discussions. We are grateful to the University of Minnesota Flow Cytometry Core Facility for instrumentation. This work was supported by NIH grant AI080275 to KN. DLW received support from NIH T32 training grant AI007313, University of Minnesota Doctoral Dissertation Fellowship, and Dennis W. Watson Fellowship.

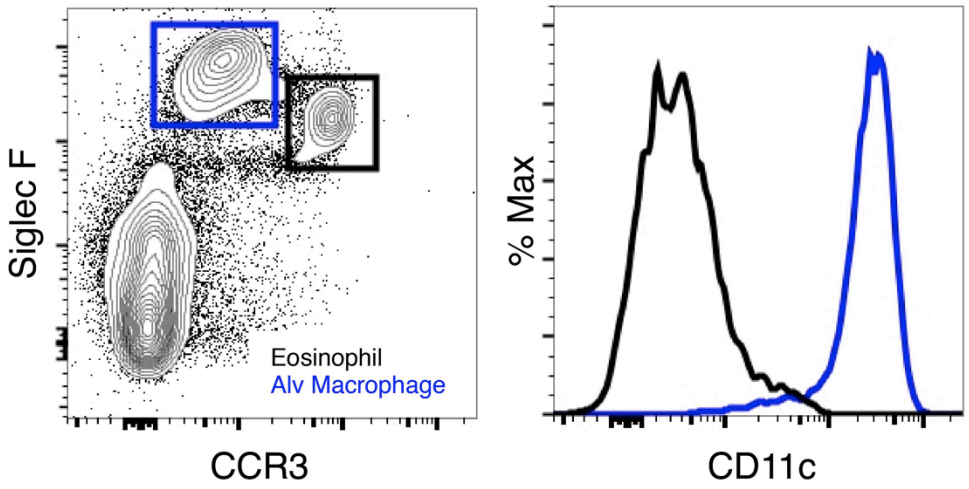

Figure 1. Eosinophils express Siglec F and CCR3, not CD11c in the lungs. Leukocyte suspension collected from lung digests of uninfected C57BL6/J mice. Flow cytometric analysis showing alveolar macrophages (blue) or eosinophils (black) as a proportion of CD45+ TER119+ hematopoietic cells. Alv = alveolar, CCR3 = chemokine receptor 3.

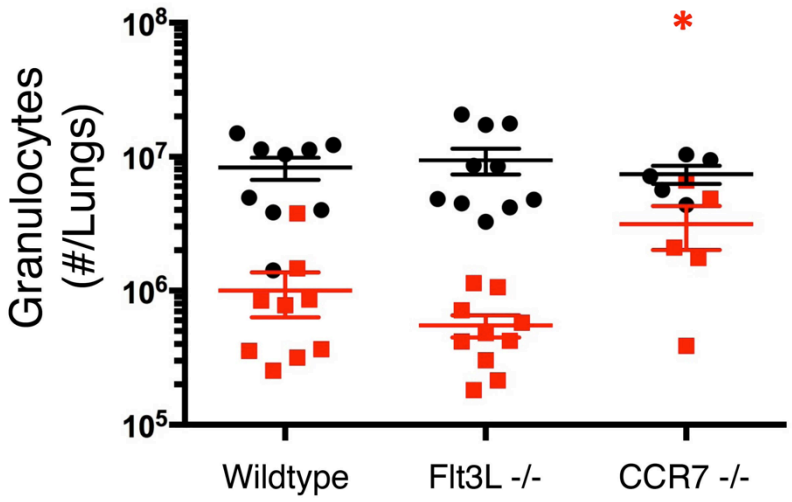

Figure 2. Pulmonary eosinophil accumulation does not require lymph node priming. Wildtype, Fms-related tyrosine kinase 3 ligand (Flt3L) -/-, and chemokine receptor 7 (CCR7) -/- mice were analyzed 14 days post-infection with *Cryptococcus neoformans*. Composite graph of eosinophil (black) and neutrophil (red) numbers from the lungs of infected mice. Pairwise comparisons were made by Man-Whitney U with Bonferoni adjustments for multiple comparisons. * = $P<0.05$ relative to wildtype. All data are presented as the mean ± standard error of the mean and represent 2 independent experiments.

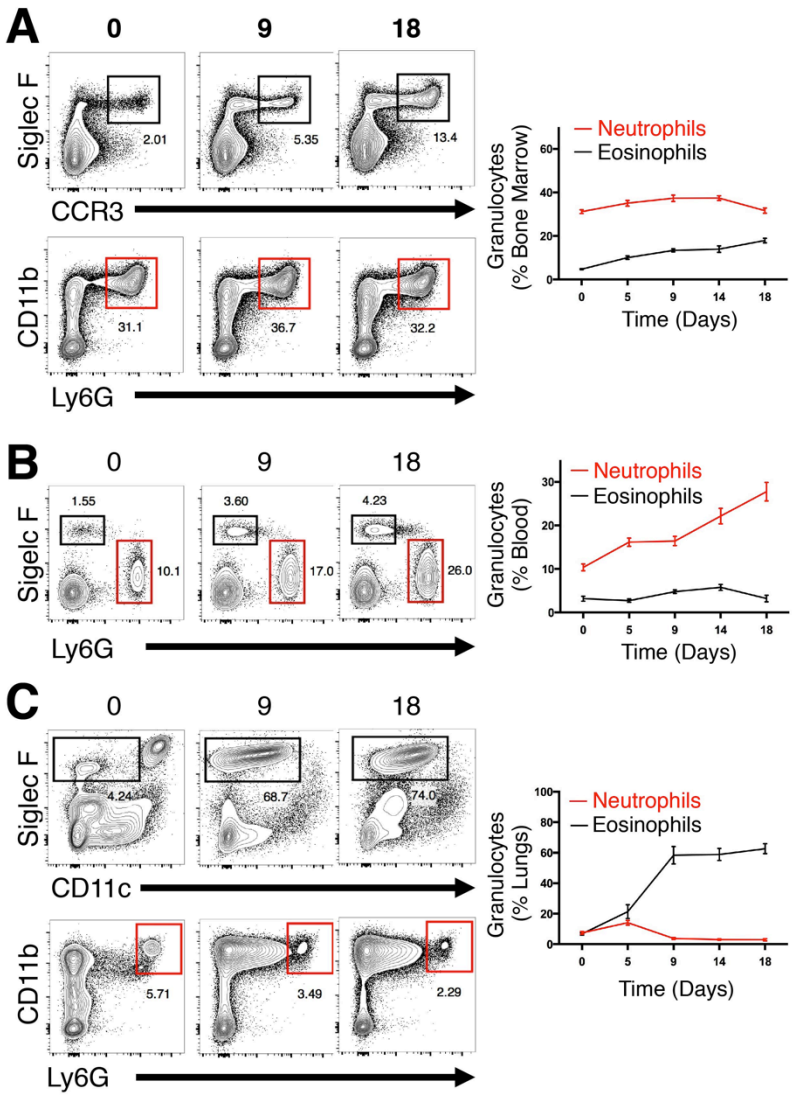

Figure 3. Granulocyte Response to Pulmonary Fungal Infection. C57BL6/J mice 0-18 days post-infection with *Cryptococcus neoformans*. Flow cytometric analysis (left) and composite graphs (right) showing granulocytes as a proportion of CD45+ TER119+ hematopoietic cells. (**A**) Siglec F+ CCR3+ eosinophils and CD11b+ Ly6G+ neutrophils contained in the bone marrow. (**B**) Siglec F+ eosinophils and Ly6G+ neutrophils from peripheral blood. (**C**) Siglec F+ CD11c- eosinophils and CD11b+ Ly6G+ neutrophils collected from lung digests. All data are presented as the mean ± standard error of the mean and represent 2 independent experiments.

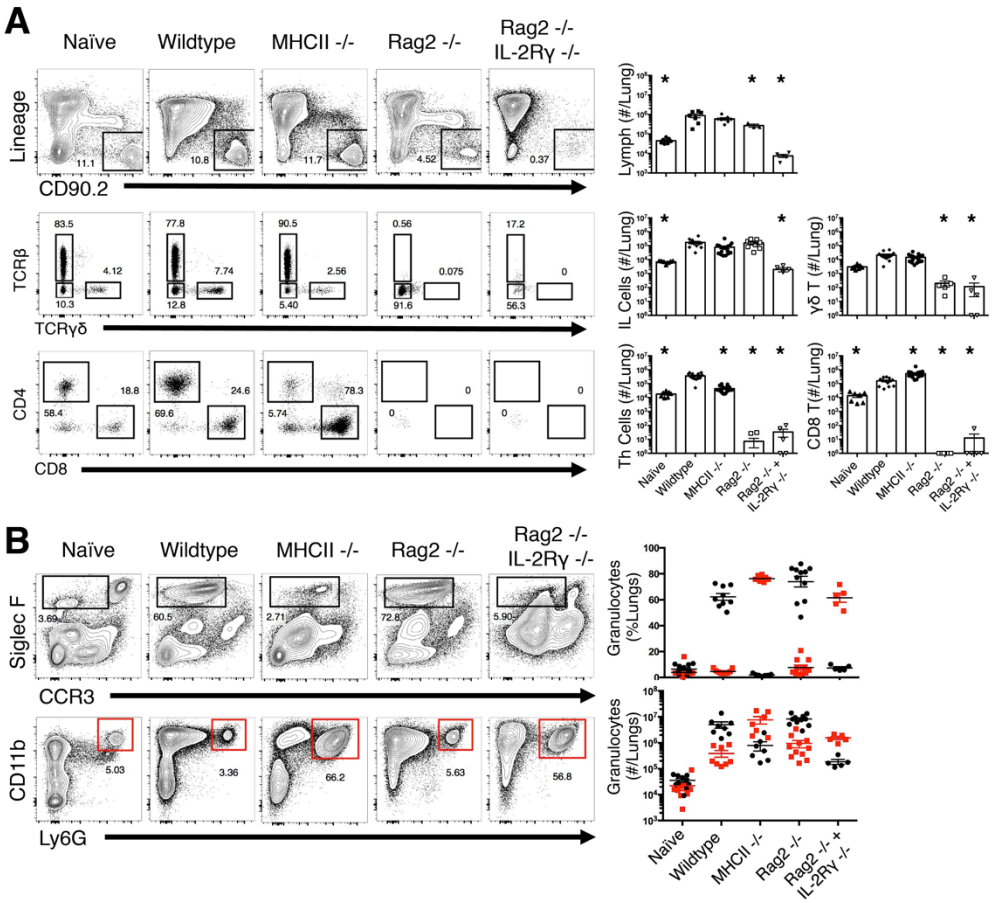

Figure 4. Lymphocytes mediate eosinophil and neutrophil accumulation. Wildtype, Major histocompatibility (MHCII) -/-, Recombinase activating gene 2 (Rag2) -/-, or Rag2 -/- Interelukin-2 receptor γ (IL-2Rγ) -/- mice 0 or 14 days post-infection with *Cryptococcus neoformans*. Flow cytometric analysis (left) and composite graphs (right) showing (**A**) CD90+ Lineage - lymphocytes. T cell receptor (TCR)β+ CD4+ helper T (Th) cell, TCRβ+ CD8+ T cells, γδ T cells, and TCRγδ- TCRβ- innate lymphoid cells (ILC) (**B**) Siglec F+ CD11c- eosinophils and CD11b+ Ly6G+ neutrophils as a proportion of CD45+ TER119+ hematopoietic cells collected from lung digests. Pairwise comparisons were made by Man-Whitney U with Bonferoni adjustments for multiple comparisons. * = P<0.05 relative to wildtype. All data are presented as the mean ± standard error of the mean and represent 2 independent experiments. Lineage = B220, CD11b, CD11c, CD19, CD49b, CD161, F4/80, FcεRIα.

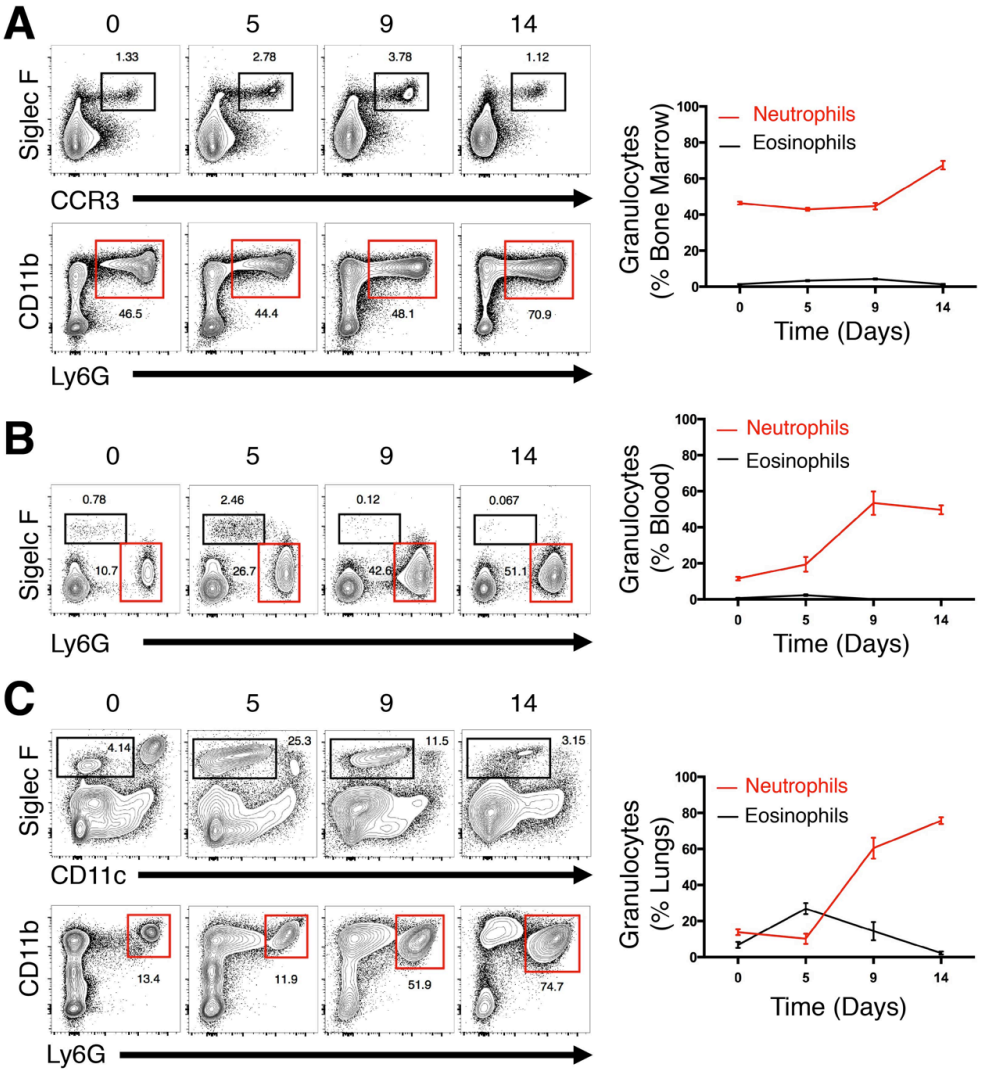

Figure 5. Eosinophils are produced early, not late, in MHCII -/- infected mice. MHCII -/- mice 0-14 days post-infection with *Cryptococcus neoformans*. Flow cytometric analysis (left) and composite graphs (right) showing granulocytes as a proportion of CD45+ TER119+ hematopoietic cells. (**A**) Siglec F+ CCR3+ eosinophils and CD11b+ Ly6G+ neutrophils contained in the bone marrow. (**B**) Siglec F+ eosinophils and Ly6G+ neutrophils from peripheral blood. (**C**) Siglec F+ CD11c- eosinophils and CD11b+ Ly6G+ neutrophils collected from lung digests All data are presented as the mean ± standard error of the mean and represent 2 independent experiments.

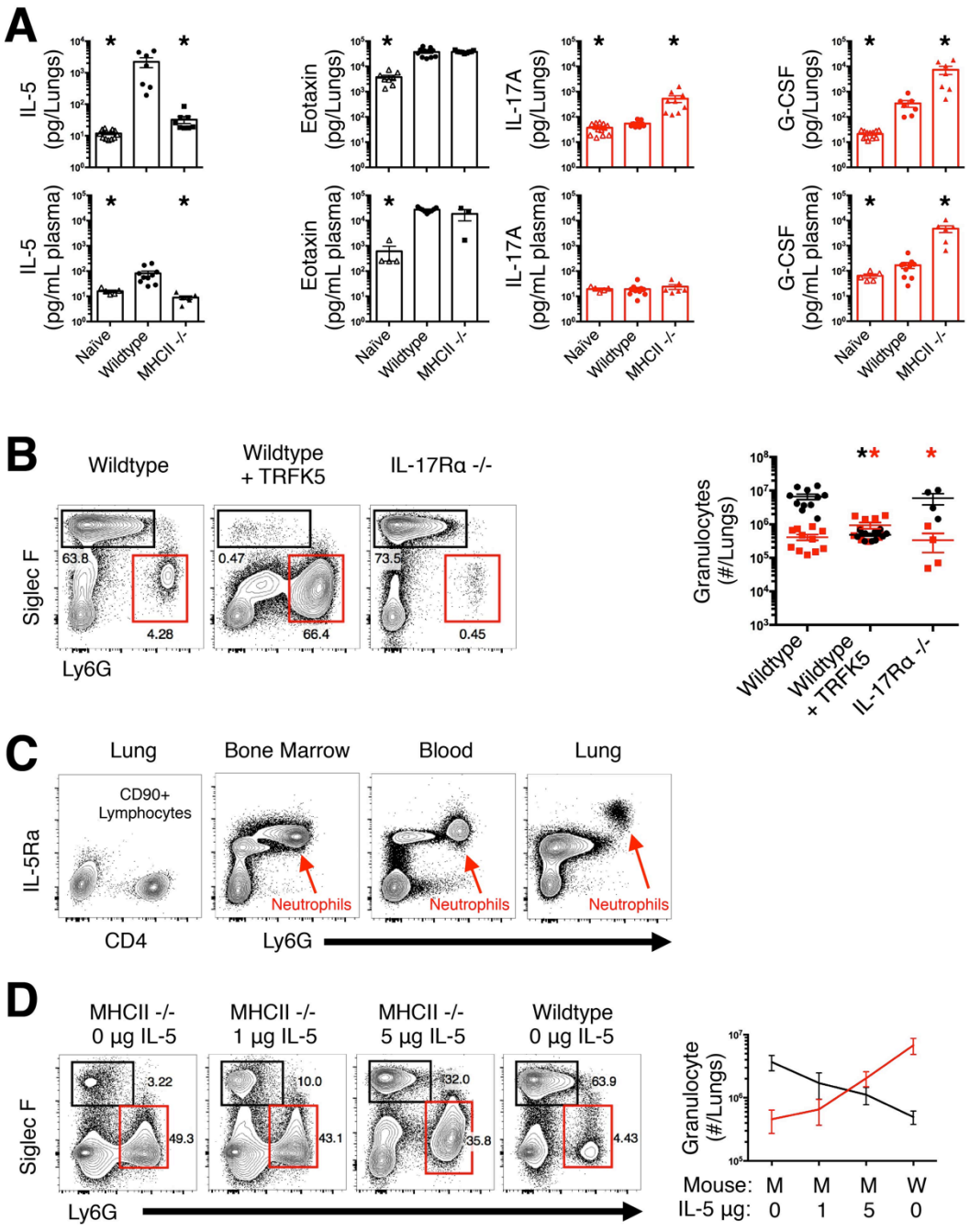

Figure 6. IL-5 positively regulates eosinophils and inhibits neutrophils. Wildtype, Major Histocompatibility Class II (MHCII) -/-, and Interleukin-17 receptor α (IL-17α) -/- mice were left unifected (naïve) or infected with *Cryptococcus neoformans*. Lungs were harvested 14 days post-infection and analyzed. (**A**) Cytokines measured in naïve wildtype

mice, as well as infected wildtype and MHCII -/- mice. (**B**) Eosinophils (black) and neutrophils (red) from wildtype mice, wildtype mice treated with anti-IL-5 antibody (TRFK), and IL-17Rα -/- mice. (**C**) IL-5Rα expression on pulmonary CD90+ Lineage- lymphocytes or neutrophils in the bone marrow, blood, and lungs. (**D**) Eosinophils (black) and neutrophils (red) quantified from IL-5 treated MHCII -/- , as wells as untreated wildtype and MHCII -/- mice. Pairwise comparisons were made by Man-Whitney U with Bonferoni adjustments for multiple comparisons. * = $P<0.05$ relative to wildtype. All data are presented as the mean ± standard error of the mean and represent 2 independent experiments. G-CSF = granulocyte-colony stimulating factor.

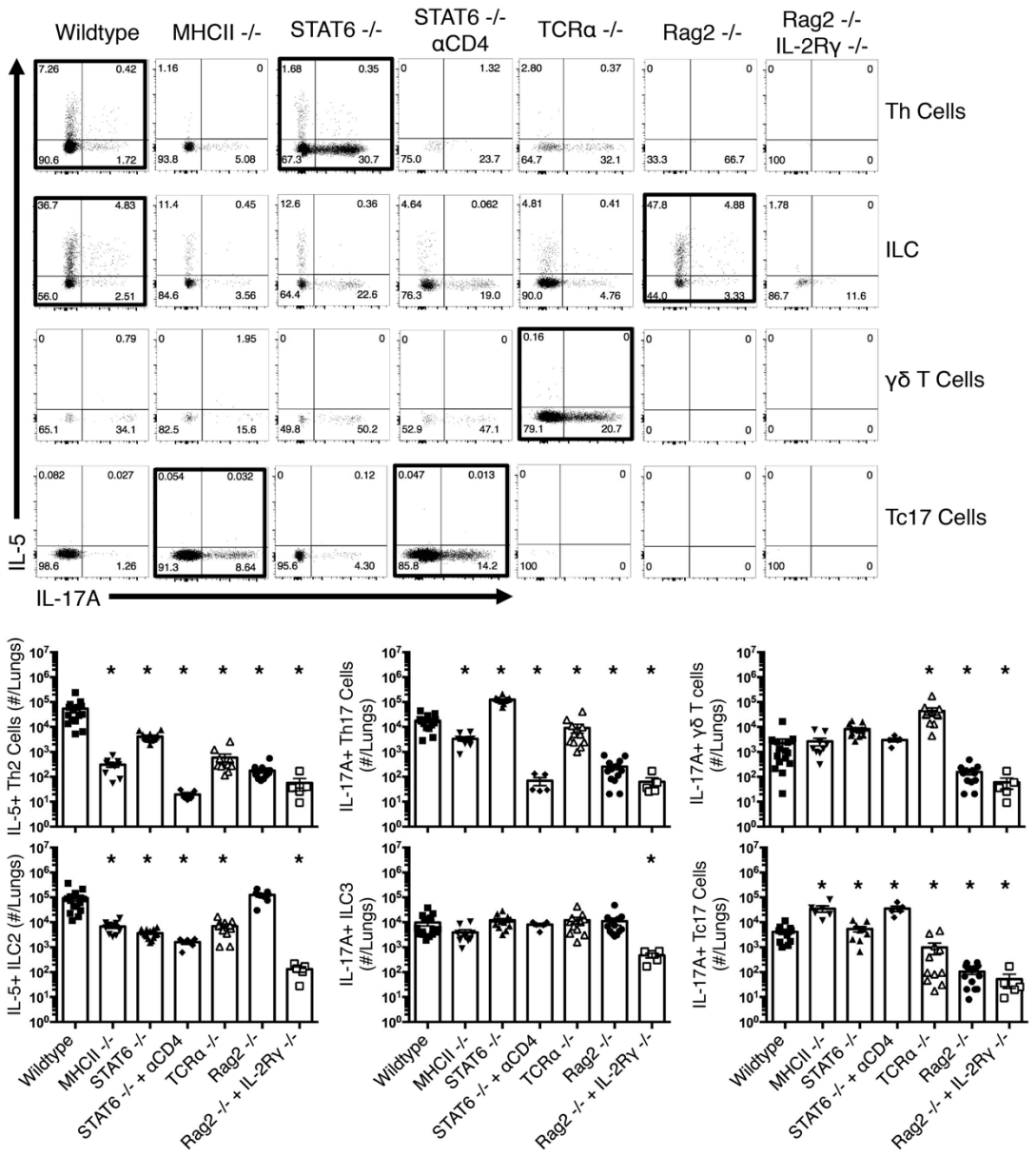

Figure 7. Lymphocyte subset definition by intracellular cytokine detection.

Wildtype, Major histocompatibility (MHCII) -/-, Signal transducer and activator 6 (STAT6) -/-, T cell receptor α (TCRα) -/-, Recombinase activating gene 2 (Rag2) -/-, or Rag2 -/- Interelukin-2 receptor γ (IL-2Rγ) -/- mice 14 days post-infection with *Cryptococcus neoformans*. Flow cytometric analysis (top) and composite graphs (bottom) showing interleuking (IL)-5 or IL-17A production by CD90+ Lineage – lymphocytes:

TCRβ+ CD4+ helper T (Th) cell, TCRβ+ CD8+ T cells, γδ T cells, and TCRγδ- TCRβ- innate lymphoid cells (ILC). Pairwise comparisons were made by Man-Whitney U with Bonferoni adjustments for multiple comparisons. * = $P<0.05$ relative to wildtype. All data are presented as the mean ± standard error of the mean and represent 2 independent experiments. Lineage = B220, CD11b, CD11c, CD19, CD49b, CD161, F4/80, FcεRIα. αCD4 indicates anti-CD4 antibody (GK1.5) treatment.

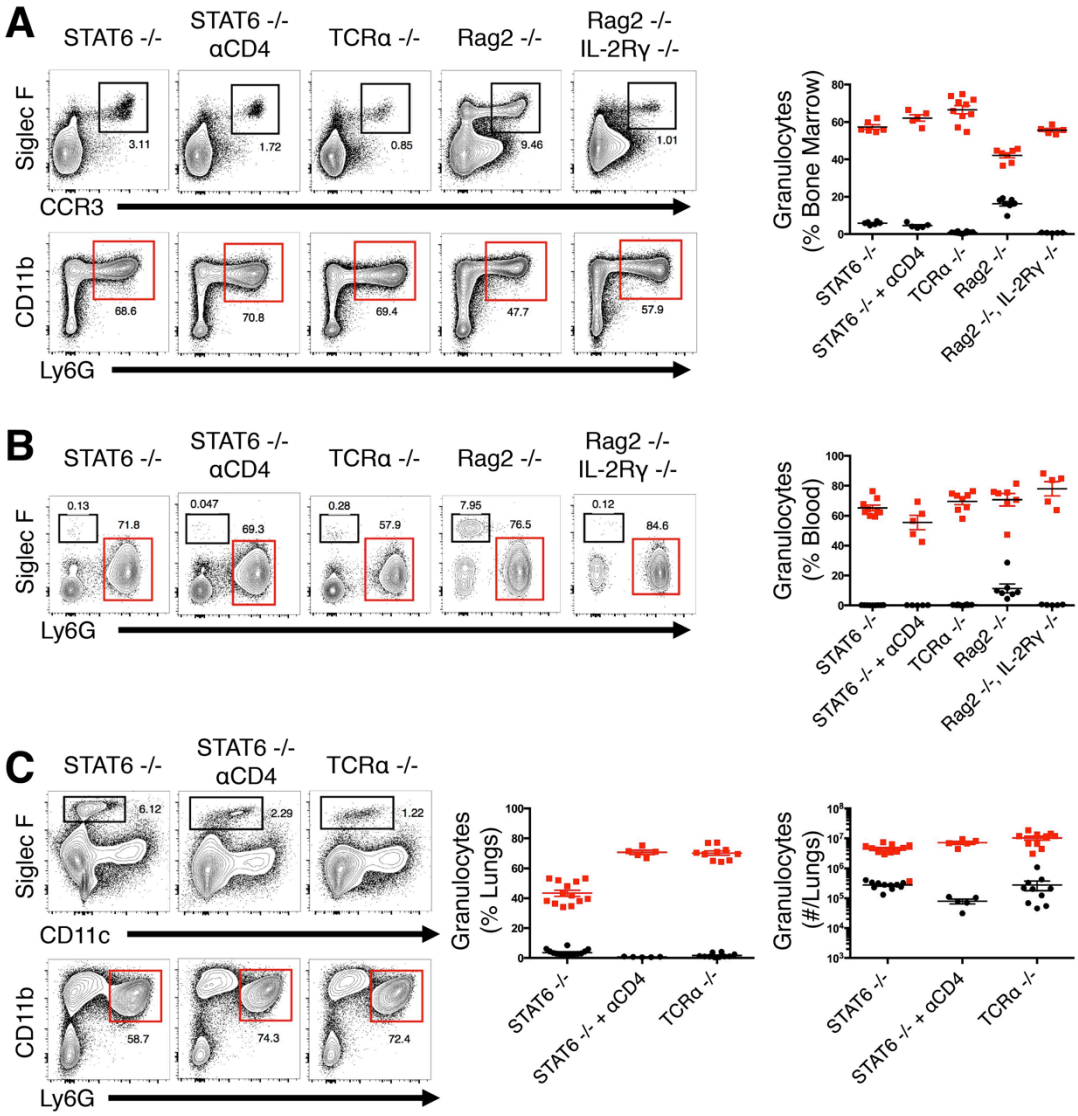

Figure 8. Granulocyte responses detected in lymphocyte deficient mice. Signal transducer and activator 6 (STAT6) -/-, T cell receptor α (TCRα) -/-, Recombinase activating gene 2 (Rag2) -/-, or Rag2 -/- Interelukin-2 receptor γ (IL-2Rγ) -/- mice 14 days post-infection with *Cryptococcus neoformans*. Flow cytometric analysis (left) and composite graphs (right) showing granulocytes as a proportion of CD45+ TER119+ hematopoietic cells. (**A**) Siglec F+ CCR3+ eosinophils and CD11b+ Ly6G+ neutrophils contained in the bone marrow. (**B**) Siglec F+ eosinophils and Ly6G+ neutrophils from peripheral blood. (**C**) Siglec F+ CD11c- eosinophils and CD11b+ Ly6G+ neutrophils collected from lung digests. αCD4 indicates anti-CD4 antibody (GK1.5) treatment.

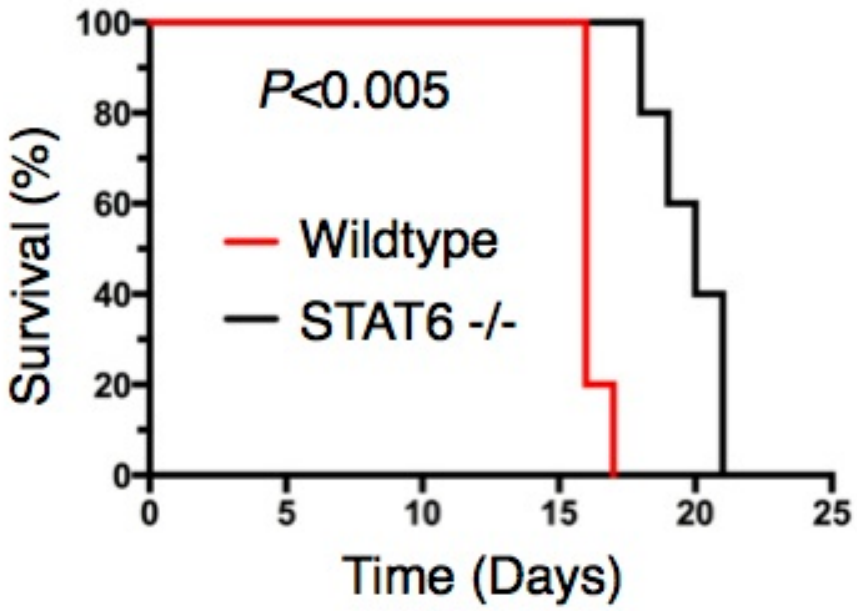

Figure 9. Neutrophil polarization is detrimental. Survival curve includes 10 mice per group. *P*-value calculated by log rank test. STAT6 = signal transducer and activator 6.

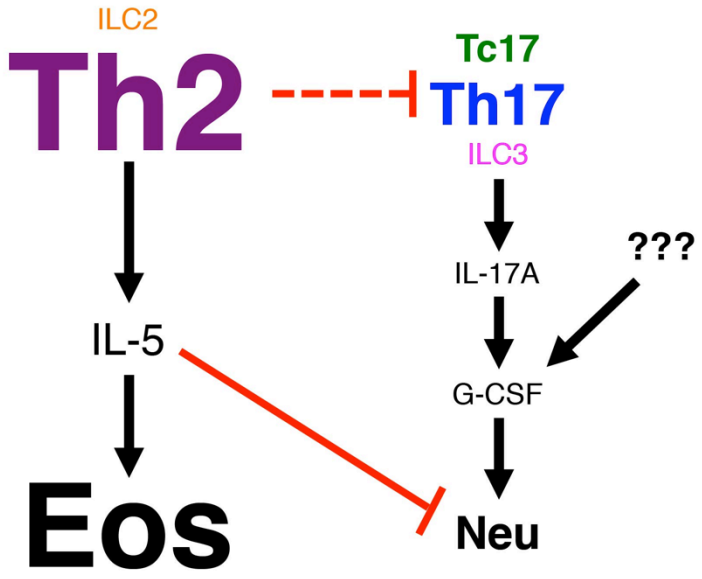

Figure 10. Model of lymphocyte competition and granulocyte regulation. Eos = eosinophil, G-CSF = granulocyte-colony stimulating factor, IL = interleukin, ILC = innate lymphoid cell, Neu = neutrophil, Tc = CD8+ T cell, Th = helper T cell.

Table 1. Summary of Lymphocyte and Granulocyte Responses to Pulmonary Fungal Infection.

	T_H2	ILC2	T_H17	ILC3	Tc17	γδ T	Outcome
WT	+(***)	+ (**)	+ (*)	+ (*)	+ (*)	+ (*)	Eos
MHCII -/-	−	+ (*)	−	+ (*)	+(***)	+ (*)	Neu
STAT6 -/-	−	−	+(***)	+ (*)	+ (*)	+ (*)	Neu
STAT6 -/- + αCD4[i]	−	−	−	+ (*)	+(***)	+ (*)	Neu
TCRα -/-	−	+ (*)	−	+ (*)	−	+(***)	Neu
Rag1 -/-	−	+(***)	−	+ (*)	−	−	Eos
Rag2 -/- IL-2Rγ -/-	−	−	−	−	−	−	Neu

+/- = present/absent
*<*** = relative amount of lymphocyte subset
[i] αCD4 = antibody depletion of CD4+ Th cells
Eos = eosinophil, Neu = neutrophil

CONCLUDING REMARKS

Research Summary

Cryptococcus neoformans is a fungal pathogen that infects greater than one million people per annum and is the most common cause of lethal meningitis worldwide. Upon inhalation, *C. neoformans* establishes a pulmonary infection that eventually disseminates to the central nervous system to cause cryptococcal meningitis. Persons with CD4 T cell deficiencies are at high risk of developing cryptococcal meningitis. However, not all immunodeficient individuals with pulmonary cryptococcosis acquire cryptococcal meningits. Moreover, people with infections that progress to meningitis exhibit a wide range of clinical outcomes after effective antifungal therapies. These include full recovery, relapse infection, paradoxical reaction to latent antigen, or death. The varying quality of the CD4 T cell response is a likely explanation, but the exact cause of this clinical heterogeneity is currently unknown. In this dissertation, I provide a comprehensive investigation of fungal intrinsic factors and host determinants that influence the induction, suppression, and downstream consequences of Th2-mediated fungal disease (**Figure 1**).

I investigated the association between cryptococcal strain genotype and virulence of isolates collected from a cohort of HIV/AIDS patients with cryptococcal meningitis. Using multilocus sequence typing, I demonstrated that patients infected with evolutionarily related strains were shown to have similar disease presentation and outcome. I developed an ex vivo assay using cryptococcal antigens and found that virulent genotypes elicited type-2 characteristic immune responses. Contrary to the dogma that the genetics of the host determines their response to infection, these data show that the genotype (and subsequent phenotype) of the infecting cryptococcal strain also has profound affects on the host response to infection and ultimately outcome of disease. Thus, endogenous (host) and exogenous (pathogen) factors contribute concurrently to disease and need to be taken into account during disease treatment.

I used a mouse model of pulmonary infection with the fungal pathogen *C. neoformans* to better understand lymphocyte responses to fungal infection. Upon

inhalation, *C. neoformans* establishes a robust lung infection that disseminates and ultimately leads to mortality. To differentiate T cell responses to the *C. neoformans* infection from non-specific T cell responses, I created a reagent that enables identification of T cells with *C. neoformans*-specific receptors. Infection with *C. neoformans* resulted in a progressive accumulation of antigen-specific T cells in the lungs that produced molecules associated with Th2 cells, but not Th1 or Th17 cells**.** To understand whether these Th2 cells responding to pulmonary fungal infection are a cause or consequence of disease severity, I specifically induced expansion of the Th2 cells. Mice with increased numbers of Th2 cells had greatly reduced survival time compared to control infections or uninfected mice. These data show that Th2 cells directly cause fungal disease.

My findings alter a longstanding paradigm, where susceptibility to lethal fungal disease is traditionally viewed as a breakdown in protective immunity. This idea is supported by the higher prevalence of invasive fungal disease in immunosuppressed individuals, including people living with HIV/AIDS, cancer patients undergoing chemotherapy, and solid organ transplant recipients. However, I propose that in addition to the lack of a protective immune response, independent development of a harmful Th2 cell response further exacerbates disease.

While pathologic Th2 cells are generated during fungal infection, how Th2 cells are induced remained unknown. One aim of my thesis project was to delineate the pathway of Th2 cell induction during pulmonary fungal infection. A forward genetic screen in mice allowed me to identify a specific subset of lung resident dendritic cells (DC) as the dominant antigen-presenting cell for Th2 cell induction. Existing evidence shows that these lung resident DC are capable of inducing both Th17 and Th2 cell responses; therefore, this DC subset is not inherently programmed to specify a single Th cell lineage during pulmonary fungal infection. Consequently, determination of Th2 cell fate by lung resident DC requires higher order detection of specific features of the infection (e.g. pattern recognition).

Since parasites and fungi elicit Th2 cell responses, I hypothesized that chitin, a molecule produced by both organisms, leads to Th2 cell production. To explore the role

of chitin in Th2 cell production, I exploited a natural property of *C. neoformans* based on previous descriptions of thickened cell walls in titan cells. Since chitin is a prominent component of the fungal cell wall, I compared chitin content of typical sized cells and titan cells. In fact, titan cells had more chitin, at a higher density, in the cell wall. Using various *C. neoformans* mutants, I found chitin abundance, not cell size influenced Th2 cell accumulation and disease severity. Next, I tested whether purified chitin was sufficient to increase Th2 cells. I treated infected mice with chitin particles, and this expanded the Th2 cell response. Therefore, chitin promotes Th2 cell accumulation during fungal infection. Chitin is a defining structural feature of all fungal cells , thus this mechanism of chitin-induced inflammation could potentially explain disease associated with an entire kingdom of pathogens.

I next investigated how the host responds to chitin and influences detrimental Th2 cell responses to fungal infection. Chitin is found deep within the fungal cell wall, thus chitin is not readily available to host surveillance. Enzymes that degrade chitin, termed chitinases, are a pivotal component of host recognition of chitin-containing organisms. Mammals encode two functional chitinases, chitotriosidase-1 (Chit1) and acidic mammalian chitinase. I determined that both enzymes are abundantly produced in response to pulmonary fungal infection. However, infection of mice with separate genetic deletions in each of these enzymes revealed that only Chit1 was necessary during cryptococcal infection for Th2 cell induction and subsequent disease. Furthermore, I used chitin particles and highly purified chitin fragments to understand the effect of Chit1-mediated enzyme degradation of chitin on Th2 cell accumulation. Though Chit1-deficient mice were resistant to the effects of chitin particles, the mice had a robust increase of Th2 cells in response to small chitin fragments. Therefore, Chit1 degradation of chitin is an early step in the host response, resulting in the production of chitin fragments that promote Th2 cell development.

My thesis also addressed whether the host has evolved ways to counterbalance the detrimental Th2 cell response. One suppressive mechanism could be Treg cells. I determined that Treg cells represent a large proportion of the T cell repertoire in the lungs of mice infected with *C. neoformans*. I further showed that Treg cell induction occurs

outside the thymus and Treg cells accumulate in proximity to Th2 effector cells in the lung parenchyma. I additionally demonstrated that Treg cells utilize a Th2 transcription factor to drive expression of chemokine receptors, which allows the Treg cells to colocalize with and suppress detrimental Th2 effector cells. Collectively, these data provide a logical connection between the hitherto disjointed observations of extrathymically induced Treg cells, chemokine-mediated localization, and Th2-specific inhibition.

Eosinophils are normally associated with allergic airway disease, and neutrophils assist in protection against fungal infections like candidiasis and aspergillosis. The immune response to cryptococcal infection elicits a striking accumulation of eosinophils in the lungs of infected mice. The last chapter of my thesis focused on lymphocyte regulation of eosinophil and neutrophil responses to pulmonary cryptococcal infection with the goal of understanding how this eosinophil response could be diminished. I showed lymphocytes are required for the IL-5 production that stimulates eosinophil differentiation in the bone marrow and recruitment to the lung. Furthermore, Th2 cells were the dominant source of IL-5, and ILC2 could only produce sufficient IL-5 to induce eosinophilia in the absence of other lymphocyte subsets. Th17 cells, IL-17-producing CD8+ T cells, γδ T cells, and ILC3 produced IL-17A in situations where Th2 cells were lacking, and lymphocyte expression of IL-17A correlated with neutrophilia in cryptococcal infected mice. Although neutrophils were dependent on IL-17A, IL-17A was not fully required for neutrophils to accumulate in the lungs. The eosinophil-to-neutrophil switch in the absence of IL-5 and the abundant expression of IL-5R on neutrophils led to the hypothesis that IL-5 negatively regulates neutrophils. Treatment of mice experiencing neutrophilia with exogenous IL-5 caused a dose-dependent reduction in neutrophils in the lungs, which affirmed the hypothesis. Taken together, a complex network of lymphocytes governs eosinophil and neutrophil accumulation in the lungs of infected mice through the production of IL-5 and IL-17A.

In conclusion, I have elucidated a complete mechanism for how fungal pathogens and host immune responses both contribute to cause disease. Upon fungal exposure, mammalian chitinases enzymatically digest full-length fungal chitin to produce chitin

fragments, and this leads to potent induction of pathologic Th2 cells. Furthermore, the host attempts to mitigate these detrimental effects by producing Treg cells that are induced and retained in the lungs. Finally, Th2 cells and other lymphocytes engage in fierce competition to drive eosinophil or neutrophil accumulation in the lungs.

Future Directions

Chitin receptor – I have identified chitin as an important fungal PAMP that is recognized by mammalian immune system. Moreover, my work and others showed that chitin promotes type-2 immunity (100). Yet, I failed to determine how this signal can be recognized by the host. Identification of the chitin receptor in mammals could go a long way in targeted therapies aimed at alleviating the allergic responses associated with chitin exposure.

Plants and animals are similarly confronted with the challenge of preventing fungal infection. Fungal diseases in plants affect millions of people and cost hundreds of billions of dollars per year due to famine and crop loss (294). As a result, plant pathologists have intensely investigated host-pathogen interactions between plants and fungi. The outer surface of microbes often contains the first exogenous molecules that contact immune recognition components. The fungal cell wall contains mannans, glucans, and chitin (295). Each of these molecules is recognized by the plant immune system as a pathogen/microbe-associated molecular pattern (296). The pathways describing mannan and glucan recognition are well understood in both plants and animals (297). However, mammalian immunologists can learn from decades of plant research on mechanisms for host recognition of chitin.

The chitin receptor is known in plants (298, 299). Chitin-elicitor binding protein (CERK1) is composed of a Lysin motif (LysM) and a receptor-like kinase domain (RLK). Upon ligation with a chitin oligomer, CERK1 forms a homodimer (182). The dimerization initiates a signaling cascade and results in anti-fungal immunity. The RLK domain is unique among plants so comparative genome searches do not identify a homologous receptor in mammals. However, the LysM ectodomain is highly conserved

across kingdoms (300). A mammalian chitin receptor could have several components in common with the plant chitin receptor. Systematic and reductionist approaches could be used to identify the elusive mammalian receptor for chitin.

Non-lymph node priming in BALT - I observed that Treg and Th2 cells are induced in substantial quantities during cryptococcal infection, even in the absence of CCR7-mediated entry of naïve Th cells into the MLN or Flt3L-dependent dendritic cell priming in lymph nodes (222). This begs the question as to the precise location of T cell priming during cryptococcal infection. Bronchus-associate lymphoid tissue (BALT) is comprised of stochastically distributed clusters of lymphocytes in proximity to high endothelial venules and tissue-resident dendritic cells (301). These structures exist under homeostatic conditions and readily increase in size and number (known as "inducible" BALT) in individuals with chronic inflammatory conditions (302, 303).

BALT sufficiently supports T cell priming in the absence of canonical lymphoid responses (304, 305). It is plausible that the BALT is responsible for T cell priming to cryptococcal infection. Fungi may not freely diffuse through the lymphatics to reach the lymph nodes due to the relatively large size of individual fungal cells. Consequently, during early cryptococcal infection in mice, an overwhelming majority of antigen is contained in the lungs. The lung is a high blood flow organ so circulating naïve Th cells have consistent access to the depot of cryptococcal antigen. Naïve Th cells could be coaxed into the lungs via high endothelial venules in a chemokine/integrin-mediated process, and the BALT could direct naïve Th cell activation, proliferation, and differentiation.

Mechanism of Treg cell suppression by IL-2 starvation – Treg cells are required for the suppression of Th2 cells in this model of pulmonary cryptococcal infection. However, the mechanism of Treg cell-mediated suppression is unknown. IL-10 production by Treg cells is a well-known pathway by which Treg cells inhibit pulmonary Th cell responses (306). IL-10 signaling reduces the proliferative potential of Th cells (307), as well as amplifies the suppressive potency of Treg cells (308). However, IL-10 blockade had

minimal impact on Th2 cell responses to cryptococcal infection. Previous studies have shown IL-10-independent Treg cell suppression of effector Th cells involves close contact (309). Thus, mechanistically, the colocalization of Treg cells with effector Th2 cells during cryptococcal infection is an important observation, and the ability of Treg cells to inhibit effector Th cell niches affords unique functional opportunities.

Perhaps, the most interesting regulatory pathway concerns the potential ability of Treg cells to mediate suppression by starving Th cells of local growth factors. In particular, Treg cells scavenge IL-2 via their high affinity IL-2 receptor (310). This competition limits IL-2 growth factor availability and restricts Th cell proliferation (311). There is some evidence to suggest this might occur in the context of pulmonary cryptococcal infection. First, IL-2 complexes administered to infected mice massively augment Th2 cell accumulation (222). Thus, IL-2 is not only an important signal for Th2 cell proliferation, but IL-2 is also recognized as a limited resource in this setting. Additionally, Signal Transducer and Activator 6 (STAT6) and IRF4 are each individually required for Th2 cell generation during cryptococcal infection (unpublished observations). However, the requirement for these transcription factors can be bypassed by treating infected knockout mice with IL-2 complexes (unpublished observations). Local IL-2 starvation by Treg cells leading to Th2 cell suppression is an intriguing, but still untested hypothesis in this model of pulmonary fungal infection.

Significance

Pulmonary fungal diseases are an enormous economic burden and global health threat. Chronic and subclinical infections, as well as repeated, low level exposures of environmental fungi evoke asthma and allergy in a multitude of otherwise healthy individuals. In addition, billions of dollars are spent annually to prevent or treat invasive fungal infections that affect millions of immunosuppressed people. Combined, most people worldwide are susceptible to mycoses. Current therapies and prophylaxes are expensive, ineffective, and consequently, unsustainable. Improvement of these remedies

is limited by our incomplete understanding of the how host responses to pulmonary fungal pathogens trigger type-2 immune responses.

CD4+ Helper T (Th) cells are central mediators of the host response to fungal exposure. Th cell subsets coordinate both protective and detrimental responses to fungal pathogens. Th1 and Th17 responses protect against fungal disease, yet many fungi elicit pathologic Th2 responses that cause asthma/allergy. The cellular and molecular mechanisms underlying this Th2 cell polarization during pulmonary fungal exposure are not well defined.

My investigations of Th2 cell responses to cryptococcal infection aim to overcome this critical gap in fundamental knowledge. Moreover, my findings suggest that blocking chitin recognition, promoting Treg suppression of Th2 cells, and manipulating lymphocyte subsets to balance eosinophil and neutrophil responses could be fruitful avenues of therapeutic intervention in patients experiencing fungal disease. Collectively, this information could guide the development of novel treatment strategies that attempt to reduce Th2 cell-mediated disease in response to fungal encounters.

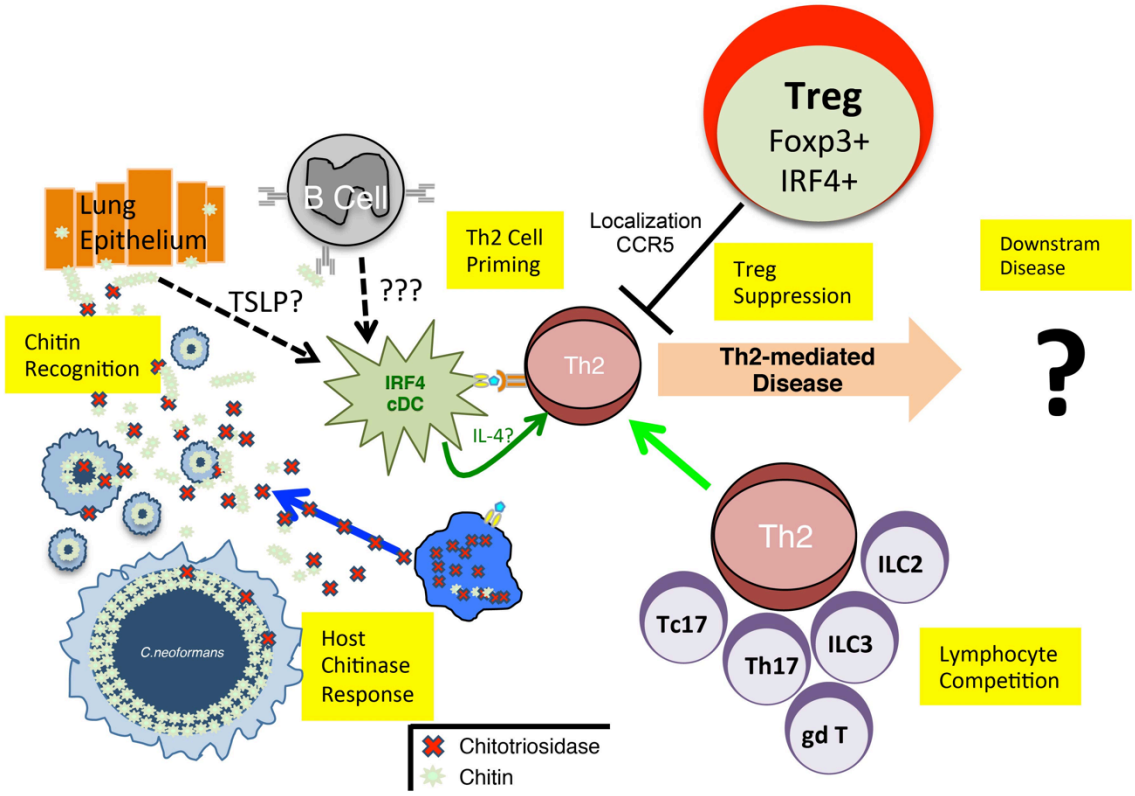

Figure 1. Model of Th2-mediated Cryptococcal Disease. CCR, chemokine receptor; cDC, classical dendritic cell; Foxp3, forkhead box P3; gd T cell, gamma delta T cell; ILC, innate lymphoid cell; IRF4, interferon regulatory factor 4; IL, interleukin; Treg, regulatory T cell; Tc17, CD8+ IL-17A+ T cell; Th, helper T cell; TSLP, thymic stromal lymphopoietin;

REFERENCES

1. Kidd SE, Chow Y, Mak S, Bach PJ, Chen H, Hingston AO, Kronstad JW, and Bartlett KH. Characterization of environmental sources of the human and animal pathogen Cryptococcus gattii in British Columbia, Canada, and the Pacific Northwest of the United States. *Applied and environmental microbiology.* 2007;73(5):1433-43.

2. Litvintseva AP, Kestenbaum L, Vilgalys R, and Mitchell TG. Comparative analysis of environmental and clinical populations of Cryptococcus neoformans. *Journal of clinical microbiology.* 2005;43(2):556-64.

3. Currie BP, Freundlich LF, and Casadevall A. Restriction fragment length polymorphism analysis of Cryptococcus neoformans isolates from environmental (pigeon excreta) and clinical sources in New York City. *Journal of clinical microbiology.* 1994;32(5):1188-92.

4. Hagen F, Khayhan K, Theelen B, Kolecka A, Polacheck I, Sionov E, Falk R, Parnmen S, Lumbsch HT, and Boekhout T. Recognition of seven species in the Cryptococcus gattii/Cryptococcus neoformans species complex. *Fungal genetics and biology : FG & B.* 2015.

5. Goldman DL, Khine H, Abadi J, Lindenberg DJ, Pirofski L, Niang R, and Casadevall A. Serologic evidence for Cryptococcus neoformans infection in early childhood. *Pediatrics.* 2001;107(5):E66.

6. Wiesner DL, Moskalenko O, Corcoran JM, McDonald T, Rolfes MA, Meya DB, Kajumbula H, Kambugu A, Bohjanen PR, Knight JF, et al. Cryptococcal genotype influences immunologic response and human clinical outcome after meningitis. *mBio.* 2012;3(5).

7. Sabiiti W, Robertson E, Beale MA, Johnston SA, Brouwer AE, Loyse A, Jarvis JN, Gilbert AS, Fisher MC, Harrison TS, et al. Efficient phagocytosis and laccase activity affect the outcome of HIV-associated cryptococcosis. *The Journal of clinical investigation.* 2014;124(5):2000-8.

8. Park BJ, Wannemuehler KA, Marston BJ, Govender N, Pappas PG, and Chiller TM. Estimation of the current global burden of cryptococcal meningitis among persons living with HIV/AIDS. *Aids.* 2009;23(4):525-30.

9. Chen SC, Slavin MA, Heath CH, Playford EG, Byth K, Marriott D, Kidd SE, Bak N, Currie B, Hajkowicz K, et al. Clinical manifestations of Cryptococcus gattii infection: determinants of neurological sequelae and death. *Clinical infectious diseases : an official publication of the Infectious Diseases Society of America.* 2012;55(6):789-98.

10. Galanis E, Macdougall L, Kidd S, Morshed M, and British Columbia Cryptococcus gattii Working G. Epidemiology of Cryptococcus gattii, British Columbia, Canada, 1999-2007. *Emerging infectious diseases.* 2010;16(2):251-7.

11. Mylonakis E, Ausubel FM, Perfect JR, Heitman J, and Calderwood SB. Killing of Caenorhabditis elegans by Cryptococcus neoformans as a model of yeast pathogenesis. *Proceedings of the National Academy of Sciences of the United States of America.* 2002;99(24):15675-80.

12. Mylonakis E, Moreno R, El Khoury JB, Idnurm A, Heitman J, Calderwood SB, Ausubel FM, and Diener A. Galleria mellonella as a model system to study Cryptococcus neoformans pathogenesis. *Infection and immunity.* 2005;73(7):3842-50.

13. Steenbergen JN, Shuman HA, and Casadevall A. Cryptococcus neoformans interactions with amoebae suggest an explanation for its virulence and intracellular pathogenic strategy in macrophages. *Proceedings of the National Academy of Sciences of the United States of America.* 2001;98(26):15245-50.

14. Aksenov SI, Babyeva IP, and Golubev VI. On the mechanism of adaptation of micro-organisms to conditions of extreme low humidity. *Life sciences and space research.* 1973;11(55-61.

15. Zaragoza O, Chrisman CJ, Castelli MV, Frases S, Cuenca-Estrella M, Rodriguez-Tudela JL, and Casadevall A. Capsule enlargement in Cryptococcus neoformans confers resistance to oxidative stress suggesting a mechanism for intracellular survival. *Cellular microbiology.* 2008;10(10):2043-57.

16. Wang Y, and Casadevall A. Decreased susceptibility of melanized Cryptococcus neoformans to UV light. *Applied and environmental microbiology.* 1994;60(10):3864-6.

17. Wang Y, Aisen P, and Casadevall A. Cryptococcus neoformans melanin and virulence: mechanism of action. *Infection and immunity.* 1995;63(8):3131-6.

18. Qiu Y, Davis MJ, Dayrit JK, Hadd Z, Meister DL, Osterholzer JJ, Williamson PR, and Olszewski MA. Immune modulation mediated by cryptococcal laccase promotes pulmonary growth and brain dissemination of virulent Cryptococcus neoformans in mice. *PloS one.* 2012;7(10):e47853.

19. Cox GM, McDade HC, Chen SC, Tucker SC, Gottfredsson M, Wright LC, Sorrell TC, Leidich SD, Casadevall A, Ghannoum MA, et al. Extracellular phospholipase activity is a virulence factor for Cryptococcus neoformans. *Molecular microbiology.* 2001;39(1):166-75.

20. Xu CY, Zhu HM, Wu JH, Wen H, and Liu CJ. Increased permeability of blood-brain barrier is mediated by serine protease during Cryptococcus meningitis. *The Journal of international medical research.* 2014;42(1):85-92.

21. Olszewski MA, Noverr MC, Chen GH, Toews GB, Cox GM, Perfect JR, and Huffnagle GB. Urease expression by Cryptococcus neoformans promotes microvascular sequestration, thereby enhancing central nervous system invasion. *The American journal of pathology.* 2004;164(5):1761-71.

22. Bartlett KH, Cheng PY, Duncan C, Galanis E, Hoang L, Kidd S, Lee MK, Lester S, MacDougall L, Mak S, et al. A decade of experience: Cryptococcus gattii in British Columbia. *Mycopathologia.* 2012;173(5-6):311-9.

23. Byrnes EJ, 3rd, Bartlett KH, Perfect JR, and Heitman J. Cryptococcus gattii: an emerging fungal pathogen infecting humans and animals. *Microbes and infection / Institut Pasteur.* 2011;13(11):895-907.

24. Marr KA. Cryptococcus gattii as an important fungal pathogen of western North America. *Expert review of anti-infective therapy.* 2012;10(6):637-43.

25. Voelz K, and May RC. Cryptococcal interactions with the host immune system. *Eukaryotic cell.* 2010;9(6):835-46.

26. Olszewski MA, Zhang Y, and Huffnagle GB. Mechanisms of cryptococcal virulence and persistence. *Future microbiology.* 2010;5(8):1269-88.

27. Giles SS, Dagenais TR, Botts MR, Keller NP, and Hull CM. Elucidating the pathogenesis of spores from the human fungal pathogen Cryptococcus neoformans. *Infection and immunity.* 2009;77(8):3491-500.

28. Velagapudi R, Hsueh YP, Geunes-Boyer S, Wright JR, and Heitman J. Spores as infectious propagules of Cryptococcus neoformans. *Infection and immunity.* 2009;77(10):4345-55.

29. Botts MR, and Hull CM. Dueling in the lung: how Cryptococcus spores race the host for survival. *Current opinion in microbiology.* 2010;13(4):437-42.

30. Feldmesser M, Kress Y, and Casadevall A. Dynamic changes in the morphology of Cryptococcus neoformans during murine pulmonary infection. *Microbiology.* 2001;147(Pt 8):2355-65.

31. Cruickshank JG, Cavill R, and Jelbert M. Cryptococcus neoformans of unusual morphology. *Applied microbiology.* 1973;25(2):309-12.

32. Zaragoza O, and Nielsen K. Titan cells in *Cryptococcus neoformans*: cells with a giant impact. *Curr Opin Microbiol.* 2013;16(4):409-13.

33. Zaragoza O, Garcia-Rodas R, Nosanchuk JD, Cuenca-Estrella M, Rodriguez-Tudela JL, and Casadevall A. Fungal cell gigantism during mammalian infection. *PLoS Pathog.* 2010;6(6):e1000945.

34. Okagaki LH, Strain AK, Nielsen JN, Charlier C, Baltes NJ, Chretien F, Heitman J, Dromer F, and Nielsen K. Cryptococcal cell morphology affects host cell interactions and pathogenicity. *PLoS Pathog.* 2010;6(6):e1000953.

35. Okagaki LH, Wang Y, Ballou ER, O'Meara TR, Bahn YS, Alspaugh JA, Xue C, and Nielsen K. Cryptococcal titan cell formation is regulated by G-protein signaling in response to multiple stimuli. *Eukaryotic cell.* 2011;10(10):1306-16.

36. Rutherford ST, and Bassler BL. Bacterial quorum sensing: its role in virulence and possibilities for its control. *Cold Spring Harbor perspectives in medicine.* 2012;2(11).

37. Kronstad JW, Hu G, and Jung WH. An encapsulation of iron homeostasis and virulence in Cryptococcus neoformans. *Trends in microbiology.* 2013;21(9):457-65.

38. O'Meara TR, Norton D, Price MS, Hay C, Clements MF, Nichols CB, and Alspaugh JA. Interaction of Cryptococcus neoformans Rim101 and protein kinase A regulates capsule. *PLoS pathogens.* 2010;6(2):e1000776.

39. Crabtree JN, Okagaki LH, Wiesner DL, Strain AK, Nielsen JN, and Nielsen K. Titan cell production enhances the virulence of Cryptococcus neoformans. *Infection and immunity.* 2012;80(11):3776-85.

40. Bulmer GS, and Tacker JR. Phagocytosis of Cryptococcus neoformans by alveolar macrophages. *Infection and immunity.* 1975;11(1):73-9.

41. Osterholzer JJ, Chen GH, Olszewski MA, Zhang YM, Curtis JL, Huffnagle GB, and Toews GB. Chemokine receptor 2-mediated accumulation of fungicidal exudate macrophages in mice that clear cryptococcal lung infection. *The American journal of pathology.* 2011;178(1):198-211.

42. Diamond RD, and Erickson NF, 3rd. Chemotaxis of human neutrophils and monocytes induced by Cryptococcus neoformans. *Infection and immunity.* 1982;38(1):380-2.

43. Sorrell TC, and Chen SC. Fungal-derived immune modulating molecules. *Advances in experimental medicine and biology.* 2009;666(108-20.

44. Kozel TR, Wilson MA, Pfrommer GS, and Schlageter AM. Activation and binding of opsonic fragments of C3 on encapsulated Cryptococcus neoformans by using an alternative complement pathway reconstituted from six isolated proteins. *Infection and immunity.* 1989;57(7):1922-7.

45. Vecchiarelli A, Pietrella D, Lupo P, Bistoni F, McFadden DC, and Casadevall A. The polysaccharide capsule of Cryptococcus neoformans interferes with human dendritic cell maturation and activation. *Journal of leukocyte biology.* 2003;74(3):370-8.

46. Luberto C, Martinez-Marino B, Taraskiewicz D, Bolanos B, Chitano P, Toffaletti DL, Cox GM, Perfect JR, Hannun YA, Balish E, et al. Identification of App1 as a regulator of phagocytosis and virulence of Cryptococcus neoformans. *The Journal of clinical investigation.* 2003;112(7):1080-94.

47. Romagnani S. The Th1/Th2 paradigm. *Immunol Today.* 1997;18(6):263-6.

48. Dardalhon V, Awasthi A, Kwon H, Galileos G, Gao W, Sobel RA, Mitsdoerffer M, Strom TB, Elyaman W, Ho IC, et al. IL-4 inhibits TGF-beta-induced Foxp3+ T cells and, together with TGF-beta, generates IL-9+ IL-10+ Foxp3(-) effector T cells. *Nat Immunol.* 2008;9(12):1347-55.

49. Fontenot JD, Gavin MA, and Rudensky AY. Foxp3 programs the development and function of CD4+CD25+ regulatory T cells. *Nat Immunol.* 2003;4(4):330-6.

50. Korn T, Bettelli E, Oukka M, and Kuchroo VK. IL-17 and Th17 Cells. *Annu Rev Immunol.* 2009;27(485-517.

51. Veldhoen M, Uyttenhove C, van Snick J, Helmby H, Westendorf A, Buer J, Martin B, Wilhelm C, and Stockinger B. Transforming growth factor-beta 'reprograms' the differentiation of T helper 2 cells and promotes an interleukin 9-producing subset. *Nat Immunol.* 2008;9(12):1341-6.

52. Zhu J, and Paul WE. CD4 T cells: fates, functions, and faults. *Blood.* 2008;112(5):1557-69.

53. Romani L. Immunity to fungal infections. *Nature reviews Immunology.* 2011;11(4):275-88.

54. Zhang Y, Wang F, Tompkins KC, McNamara A, Jain AV, Moore BB, Toews GB, Huffnagle GB, and Olszewski MA. Robust Th1 and Th17 immunity supports pulmonary clearance but cannot prevent systemic dissemination of highly virulent Cryptococcus neoformans H99. *Am J Pathol.* 2009;175(6):2489-500.

55. Jarvis JN, Meintjes G, Rebe K, Williams GN, Bicanic T, Williams A, Schutz C, Bekker LG, Wood R, and Harrison TS. Adjunctive interferon-gamma immunotherapy for the treatment of HIV-associated cryptococcal meningitis: a randomized controlled trial. *AIDS.* 2012;26(9):1105-13.

56. Pappas PG, Bustamante B, Ticona E, Hamill RJ, Johnson PC, Reboli A, Aberg J, Hasbun R, and Hsu HH. Recombinant interferon- gamma 1b as adjunctive therapy for AIDS-related acute cryptococcal meningitis. *J Infect Dis.* 2004;189(12):2185-91.

57. Boulware DR, Bonham SC, Meya DB, Wiesner DL, Park GS, Kambugu A, Janoff EN, and Bohjanen PR. Paucity of initial cerebrospinal fluid inflammation in cryptococcal meningitis is associated with subsequent immune reconstitution inflammatory syndrome. *The Journal of infectious diseases.* 2010;202(6):962-70.

58. Boulware DR, Meya DB, Bergemann TL, Wiesner DL, Rhein J, Musubire A, Lee SJ, Kambugu A, Janoff EN, and Bohjanen PR. Clinical features and serum biomarkers in HIV immune reconstitution inflammatory syndrome after cryptococcal meningitis: a prospective cohort study. *PLoS medicine.* 2010;7(12):e1000384.

59. Kawakami K, Hossain Qureshi M, Zhang T, Koguchi Y, Xie Q, Kurimoto M, and Saito A. Interleukin-4 weakens host resistance to pulmonary and disseminated cryptococcal infection caused by combined treatment with interferon-gamma-inducing cytokines. *Cell Immunol.* 1999;197(1):55-61.

60. Hernandez Y, Arora S, Erb-Downward JR, McDonald RA, Toews GB, and Huffnagle GB. Distinct roles for IL-4 and IL-10 in regulating T2 immunity during allergic bronchopulmonary mycosis. *J Immunol.* 2005;174(2):1027-36.

61. Stenzel W, Muller U, Kohler G, Heppner FL, Blessing M, McKenzie AN, Brombacher F, and Alber G. IL-4/IL-13-dependent alternative activation of macrophages but not microglial cells is associated with uncontrolled cerebral cryptococcosis. *Am J Pathol.* 2009;174(2):486-96.

62. Jain AV, Zhang Y, Fields WB, McNamara DA, Choe MY, Chen GH, Erb-Downward J, Osterholzer JJ, Toews GB, Huffnagle GB, et al. Th2 but not Th1 immune bias results in altered lung functions in a murine model of pulmonary *Cryptococcus neoformans* infection. *Infect Immun.* 2009;77(12):5389-99.

63. Davis MJ, Tsang TM, Qiu Y, Dayrit JK, Freij JB, Huffnagle GB, and Olszewski MA. Macrophage M1/M2 polarization dynamically adapts to changes in cytokine microenvironments in Cryptococcus neoformans infection. *mBio.* 2013;4(3):e00264-13.

64. Holmer SM, Evans KS, Asfaw YG, Saini D, Schell WA, Ledford JG, Frothingham R, Wright JR, Sempowski GD, and Perfect JR. Impact of surfactant protein D, interleukin-5, and eosinophilia on Cryptococcosis. *Infection and immunity.* 2014;82(2):683-93.

65. Huffnagle GB, Boyd MB, Street NE, and Lipscomb MF. IL-5 is required for eosinophil recruitment, crystal deposition, and mononuclear cell recruitment during a pulmonary Cryptococcus neoformans infection in genetically susceptible mice (C57BL/6). *Journal of immunology.* 1998;160(5):2393-400.

66. Piehler D, Stenzel W, Grahnert A, Held J, Richter L, Kohler G, Richter T, Eschke M, Alber G, and Muller U. Eosinophils contribute to IL-4 production and shape the T-

helper cytokine profile and inflammatory response in pulmonary cryptococcosis. *The American journal of pathology.* 2011;179(2):733-44.

67. Wozniak KL, Kolls JK, and Wormley FL, Jr. Depletion of neutrophils in a protective model of pulmonary cryptococcosis results in increased IL-17A production by gammadelta T cells. *BMC immunology.* 2012;13(65.

68. Wozniak KL, Hardison SE, Kolls JK, and Wormley FL. Role of IL-17A on resolution of pulmonary C. neoformans infection. *PloS one.* 2011;6(2):e17204.

69. Van Dyken SJ, Mohapatra A, Nussbaum JC, Molofsky AB, Thornton EE, Ziegler SF, McKenzie AN, Krummel MF, Liang HE, and Locksley RM. Chitin activates parallel immune modules that direct distinct inflammatory responses via innate lymphoid type 2 and gammadelta T cells. *Immunity.* 2014;40(3):414-24.

70. Choy DF, Hart KM, Borthwick LA, Shikotra A, Nagarkar DR, Siddiqui S, Jia G, Ohri CM, Doran E, Vannella KM, et al. TH2 and TH17 inflammatory pathways are reciprocally regulated in asthma. *Science translational medicine.* 2015;7(301):301ra129.

71. Teixeira PA, Penha LL, Mendonca-Previato L, and Previato JO. Mannoprotein MP84 mediates the adhesion of Cryptococcus neoformans to epithelial lung cells. *Frontiers in cellular and infection microbiology.* 2014;4(106.

72. Chen SC, Wright LC, Golding JC, and Sorrell TC. Purification and characterization of secretory phospholipase B, lysophospholipase and lysophospholipase/transacylase from a virulent strain of the pathogenic fungus Cryptococcus neoformans. *The Biochemical journal.* 2000;347(Pt 2):431-9.

73. Santangelo RT, Nouri-Sorkhabi MH, Sorrell TC, Cagney M, Chen SC, Kuchel PW, and Wright LC. Biochemical and functional characterisation of secreted phospholipase activities from Cryptococcus neoformans in their naturally occurring state. *Journal of medical microbiology.* 1999;48(8):731-40.

74. Rutherford JC. The emerging role of urease as a general microbial virulence factor. *PLoS pathogens.* 2014;10(5):e1004062.

75. Brown GD, Denning DW, Gow NA, Levitz SM, Netea MG, and White TC. Hidden killers: human fungal infections. *Science translational medicine.* 2012;4(165):165rv13.

76. Carson MJ, Doose JM, Melchior B, Schmid CD, and Ploix CC. CNS immune privilege: hiding in plain sight. *Immunological reviews.* 2006;213(48-65.

77. Liu WY, Wang ZB, Zhang LC, Wei X, and Li L. Tight junction in blood-brain barrier: an overview of structure, regulation, and regulator substances. *CNS neuroscience & therapeutics.* 2012;18(8):609-15.

78. Vu K, Tham R, Uhrig JP, Thompson GR, 3rd, Na Pombejra S, Jamklang M, Bautos JM, and Gelli A. Invasion of the central nervous system by Cryptococcus neoformans requires a secreted fungal metalloprotease. *mBio.* 2014;5(3):e01101-14.

79. Shi M, Li SS, Zheng C, Jones GJ, Kim KS, Zhou H, Kubes P, and Mody CH. Real-time imaging of trapping and urease-dependent transmigration of Cryptococcus neoformans in mouse brain. *The Journal of clinical investigation.* 2010;120(5):1683-93.

80. Chang YC, Stins MF, McCaffery MJ, Miller GF, Pare DR, Dam T, Paul-Satyaseela M, Kim KS, and Kwon-Chung KJ. Cryptococcal yeast cells invade the central nervous system via transcellular penetration of the blood-brain barrier. *Infection and immunity.* 2004;72(9):4985-95.

81. Jong A, Wu CH, Prasadarao NV, Kwon-Chung KJ, Chang YC, Ouyang Y, Shackleford GM, and Huang SH. Invasion of Cryptococcus neoformans into human brain microvascular endothelial cells requires protein kinase C-alpha activation. *Cellular microbiology.* 2008;10(9):1854-65.

82. Jong A, Wu CH, Shackleford GM, Kwon-Chung KJ, Chang YC, Chen HM, Ouyang Y, and Huang SH. Involvement of human CD44 during Cryptococcus neoformans infection of brain microvascular endothelial cells. *Cellular microbiology.* 2008;10(6):1313-26.

83. Liu TB, Kim JC, Wang Y, Toffaletti DL, Eugenin E, Perfect JR, Kim KJ, and Xue C. Brain inositol is a novel stimulator for promoting Cryptococcus penetration of the blood-brain barrier. *PLoS pathogens.* 2013;9(4):e1003247.

84. Kechichian TB, Shea J, and Del Poeta M. Depletion of alveolar macrophages decreases the dissemination of a glucosylceramide-deficient mutant of Cryptococcus neoformans in immunodeficient mice. *Infection and immunity.* 2007;75(10):4792-8.

85. Charlier C, Nielsen K, Daou S, Brigitte M, Chretien F, and Dromer F. Evidence of a role for monocytes in dissemination and brain invasion by Cryptococcus neoformans. *Infection and immunity.* 2009;77(1):120-7.

86. Chen Y, Toffaletti DL, Tenor JL, Litvintseva AP, Fang C, Mitchell TG, McDonald TR, Nielsen K, Boulware DR, Bicanic T, et al. The Cryptococcus neoformans transcriptome at the site of human meningitis. *mBio.* 2014;5(1):e01087-13.

87. Bicanic T, and Harrison TS. Cryptococcal meningitis. *British medical bulletin.* 2004;72(99-118.

88. Macsween KF, Bicanic T, Brouwer AE, Marsh H, Macallan DC, and Harrison TS. Lumbar drainage for control of raised cerebrospinal fluid pressure in cryptococcal meningitis: case report and review. *The Journal of infection.* 2005;51(4):e221-4.

89. Meya DB, Manabe YC, Castelnuovo B, Cook BA, Elbireer AM, Kambugu A, Kamya MR, Bohjanen PR, and Boulware DR. Cost-effectiveness of serum cryptococcal antigen screening to prevent deaths among HIV-infected persons with a CD4+ cell count < or = 100 cells/microL who start HIV therapy in resource-limited settings. *Clinical infectious diseases : an official publication of the Infectious Diseases Society of America.* 2010;51(4):448-55.

90. Denning DW, O'Driscoll BR, Hogaboam CM, Bowyer P, and Niven RM. The link between fungi and severe asthma: a summary of the evidence. *The European respiratory journal.* 2006;27(3):615-26.

91. Denning DW, Pleuvry A, and Cole DC. Global burden of allergic bronchopulmonary aspergillosis with asthma and its complication chronic pulmonary aspergillosis in adults. *Med Mycol.* 2012.

92. Hogan C, and Denning DW. Allergic bronchopulmonary aspergillosis and related allergic syndromes. *Semin Respir Crit Care Med.* 2011;32(6):682-92.

93. Worldwide variation in prevalence of symptoms of asthma, allergic rhinoconjunctivitis, and atopic eczema: ISAAC. The International Study of Asthma and Allergies in Childhood (ISAAC) Steering Committee. *Lancet.* 1998;351(9111):1225-32.

94. Dall'Igna C, Palombini BC, Anselmi F, Araujo E, and Dall'Igna DP. Fungal rhinosinusitis in patients with chronic sinusal disease. *Braz J Otorhinolaryngol.* 2005;71(6):712-20.

95. Blaiss MS. Allergic rhinitis: Direct and indirect costs. *Allergy Asthma Proc.* 2010;31(5):375-80.

96. Romani L. The T cell response against fungal infections. *Curr Opin Immunol.* 1997;9(4):484-90.

97. Licona-Limon P, Kim LK, Palm NW, and Flavell RA. TH2, allergy and group 2 innate lymphoid cells. *Nature immunology.* 2013;14(6):536-42.

98. Zhu Z, Zheng T, Homer RJ, Kim YK, Chen NY, Cohn L, Hamid Q, and Elias JA. Acidic mammalian chitinase in asthmatic Th2 inflammation and IL-13 pathway activation. *Science.* 2004;304(5677):1678-82.

99. Millien VO, Lu W, Shaw J, Yuan X, Mak G, Roberts L, Song LZ, Knight JM, Creighton CJ, Luong A, et al. Cleavage of fibrinogen by proteinases elicits allergic responses through Toll-like receptor 4. *Science.* 2013;341(6147):792-6.

100. Reese TA, Liang HE, Tager AM, Luster AD, Van Rooijen N, Voehringer D, and Locksley RM. Chitin induces accumulation in tissue of innate immune cells associated with allergy. *Nature.* 2007;447(7140):92-6.

101. Roy RM, Wuthrich M, and Klein BS. Chitin elicits CCL2 from airway epithelial cells and induces CCR2-dependent innate allergic inflammation in the lung. *J Immunol.* 2012;189(5):2545-52.

102. Mari A, Schneider P, Wally V, Breitenbach M, and Simon-Nobbe B. Sensitization to fungi: epidemiology, comparative skin tests, and IgE reactivity of fungal extracts. *Clin Exp Allergy.* 2003;33(10):1429-38.

103. Pikman R, and Ben-Ami R. Immune modulators as adjuncts for the prevention and treatment of invasive fungal infections. *Immunotherapy.* 2012;4(12):1869-82.

104. Casadevall A, and Pirofski LA. Adjunctive immune therapy for fungal infections. *Clinical infectious diseases : an official publication of the Infectious Diseases Society of America.* 2001;33(7):1048-56.

105. UNAIDS. World AIDS Day Report 2011.

106. Bicanic T, Meintjes G, Rebe K, Williams A, Loyse A, Wood R, Hayes M, Jaffar S, and Harrison T. Immune reconstitution inflammatory syndrome in HIV-associated cryptococcal meningitis: a prospective study. *J Acquir Immune Defic Syndr.* 2009;51(2):130-4.

107. Perfect JR. Cryptococcus neoformans: a sugar-coated killer with designer genes. *FEMS Immunol Med Microbiol.* 2005;45(3):395-404.

108. Vecchiarelli A. Immunoregulation by capsular components of Cryptococcus neoformans. *Med Mycol.* 2000;38(6):407-17.

109. Kozel TR, and Gotschlich EC. The capsule of *Cryptococcus neoformans* passively inhibits phagocytosis of the yeast by macrophages. *J Immunol.* 1982;129(4):1675-80.

110. Beenhouwer DO, Shapiro S, Feldmesser M, Casadevall A, and Scharff MD. Both Th1 and Th2 cytokines affect the ability of monoclonal antibodies to protect mice against *Cryptococcus neoformans*. *Infect Immun.* 2001;69(10):6445-55.

111. Siddiqui AA, Brouwer AE, Wuthiekanun V, Jaffar S, Shattock R, Irving D, Sheldon J, Chierakul W, Peacock S, Day N, et al. IFN-gamma at the site of infection

determines rate of clearance of infection in cryptococcal meningitis. *J Immunol.* 2005;174(3):1746-50.

112. Murphy K. *Janeway's Immunobiology.* New York and London: Garland Science; 2011.

113. Retini C, Kozel TR, Pietrella D, Monari C, Bistoni F, and Vecchiarelli A. Interdependency of interleukin-10 and interleukin-12 in regulation of T-cell differentiation and effector function of monocytes in response to stimulation with Cryptococcus neoformans. *Infect Immun.* 2001;69(10):6064-73.

114. Nallapareddy SR, Wenxiang H, Weinstock GM, and Murray BE. Molecular characterization of a widespread, pathogenic, and antibiotic resistance-receptive Enterococcus faecalis lineage and dissemination of its putative pathogenicity island. *J Bacteriol.* 2005;187(16):5709-18.

115. Ruiz-Garbajosa P, Bonten MJ, Robinson DA, Top J, Nallapareddy SR, Torres C, Coque TM, Canton R, Baquero F, Murray BE, et al. Multilocus sequence typing scheme for Enterococcus faecalis reveals hospital-adapted genetic complexes in a background of high rates of recombination. *J Clin Microbiol.* 2006;44(6):2220-8.

116. Dagerhamn J, Blomberg C, Browall S, Sjostrom K, Morfeldt E, and Henriques-Normark B. Determination of accessory gene patterns predicts the same relatedness among strains of Streptococcus pneumoniae as sequencing of housekeeping genes does and represents a novel approach in molecular epidemiology. *J Clin Microbiol.* 2008;46(3):863-8.

117. Chang GH, Lin L, Luo YJ, Cai LJ, Wu XY, Xu HM, and Zhu QY. Sequence analysis of six enterovirus 71 strains with different virulences in humans. *Virus Res.* 2010;151(1):66-73.

118. Ngamskulrungroj P, Serena C, Gilgado F, Malik R, and Meyer W. Global VGIIa isolates are of comparable virulence to the major fatal Cryptococcus gattii Vancouver Island outbreak genotype. *Clin Microbiol Infect.* 2010.

119. Casadevall A, and Perfect JR. *Cryptococcus neoformans.* Amer Society for Microbiology; 1998.

120. Heitman J, Kozel, T.R., Kwon-Chung, K.J., Perfect, J.R., and Casadevall, A. *Cryptococcus: From human pathogen to model yeast.* Washington, D.C.: ASM Press; 2011.

121. Meyer W, Aanensen DM, Boekhout T, Cogliati M, Diaz MR, Esposto MC, Fisher M, Gilgado F, Hagen F, Kaocharoen S, et al. Consensus multi-locus sequence typing scheme for Cryptococcus neoformans and Cryptococcus gattii. *Med Mycol.* 2009;47(6):561-70.

122. Litvintseva AP, Thakur R, Vilgalys R, and Mitchell TG. Multilocus sequence typing reveals three genetic subpopulations of Cryptococcus neoformans var. grubii (serotype A), including a unique population in Botswana. *Genetics.* 2006;172(4):2223-38.

123. Desnos-Ollivier M, Patel S, Spaulding AR, Charlier C, Garcia-Hermoso D, Nielsen K, and Dromer F. Mixed infections and In Vivo evolution in the human fungal pathogen Cryptococcus neoformans. *MBio.* 2010;1(1).

124. Feil EJ, Li BC, Aanensen DM, Hanage WP, and Spratt BG. eBURST: inferring patterns of evolutionary descent among clusters of related bacterial genotypes from multilocus sequence typing data. *J Bacteriol.* 2004;186(5):1518-30.

125. Staib F, and Bethauser G. [Demonstration of Cryptococcus neoformans in the dust of a dovectoe]. *Mykosen.* 1968;11(9):619-24.

126. Miglia KJ, Govender NP, Rossouw J, Meiring S, Mitchell TG, Group for Enteric R, and Meningeal Disease Surveillance in South A. Analyses of pediatric isolates of Cryptococcus neoformans from South Africa. *J Clin Microbiol.* 2011;49(1):307-14.

127. Litvintseva AP, Carbone I, Rossouw J, Thakur R, Govender NP, and Mitchell TG. Evidence that the human pathogenic fungus Cryptococcus neoformans var. grubii may have evolved in Africa. *PLoS One.* 2011;6(5):e19688.

128. Mandal P, Banerjee U, Casadevall A, and Nosanchuk JD. Dual infections with pigmented and albino strains of Cryptococcus neoformans in patients with or without human immunodeficiency virus infection in India. *J Clin Microbiol.* 2005;43(9):4766-72.

129. Haynes KA, Sullivan DJ, Coleman DC, Clarke JC, Emilianus R, Atkinson C, and Cann KJ. Involvement of multiple Cryptococcus neoformans strains in a single episode of cryptococcosis and reinfection with novel strains in recurrent infection demonstrated by random amplification of polymorphic DNA and DNA fingerprinting. *J Clin Microbiol.* 1995;33(1):99-102.

130. Litvintseva AP, Marra RE, Nielsen K, Heitman J, Vilgalys R, and Mitchell TG. Evidence of sexual recombination among Cryptococcus neoformans serotype A isolates in sub-Saharan Africa. *Eukaryot Cell.* 2003;2(6):1162-8.

131. Lin X, Nielsen K, Patel S, and Heitman J. Impact of mating type, serotype, and ploidy on the virulence of Cryptococcus neoformans. *Infect Immun.* 2008;76(7):2923-38.

132. Huffnagle GB, Toews GB, Burdick MD, Boyd MB, McAllister KS, McDonald RA, Kunkel SL, and Strieter RM. Afferent phase production of TNF-alpha is required

for the development of protective T cell immunity to Cryptococcus neoformans. *J Immunol.* 1996;157(10):4529-36.

133. Olszewski MA, Huffnagle GB, McDonald RA, Lindell DM, Moore BB, Cook DN, and Toews GB. The role of macrophage inflammatory protein-1 alpha/CCL3 in regulation of T cell-mediated immunity to Cryptococcus neoformans infection. *J Immunol.* 2000;165(11):6429-36.

134. Kawakami K, Tohyama M, Xie Q, and Saito A. IL-12 protects mice against pulmonary and disseminated infection caused by Cryptococcus neoformans. *Clin Exp Immunol.* 1996;104(2):208-14.

135. Huffnagle GB, Yates JL, and Lipscomb MF. Immunity to a pulmonary Cryptococcus neoformans infection requires both CD4+ and CD8+ T cells. *J Exp Med.* 1991;173(4):793-800.

136. Flesch IE, Schwamberger G, and Kaufmann SH. Fungicidal activity of IFN-gamma-activated macrophages. Extracellular killing of Cryptococcus neoformans. *J Immunol.* 1989;142(9):3219-24.

137. Hoag KA, Lipscomb MF, Izzo AA, and Street NE. IL-12 and IFN-gamma are required for initiating the protective Th1 response to pulmonary cryptococcosis in resistant C.B-17 mice. *Am J Respir Cell Mol Biol.* 1997;17(6):733-9.

138. Hardison SE, Ravi S, Wozniak KL, Young ML, Olszewski MA, and Wormley FL. Pulmonary Infection with an Interferon-γ-Producing Cryptococcus neoformans Strain Results in Classical Macrophage Activation and Protection. *The American Journal of Pathology.* 2010;176(2):774-85.

139. Koguchi Y, and Kawakami K. Cryptococcal infection and Th1-Th2 cytokine balance. *Int Rev Immunol.* 2002;21(4-5):423-38.

140. Chayakulkeeree M, and Perfect JR. Cryptococcosis. *Infect Dis Clin North Am.* 2006;20(3):507-44, v-vi.

141. Kozel TR, and Mastroianni RP. Inhibition of phagocytosis by cryptococcal polysaccharide: dissociation of the attachment and ingestion phases of phagocytosis. *Infect Immun.* 1976;14(1):62-7.

142. Mitchell TG, and Friedman L. In vitro phagocytosis and intracellular fate of variously encapsulated strains of Cryptococcus neoformans. *Infect Immun.* 1972;5(4):491-8.

143. Bulmer GS, and Sans MD. Cryptococcus neoformans. 3. Inhibition of phagocytosis. *J Bacteriol.* 1968;95(1):5-8.

144. Yauch LE, Lam JS, and Levitz SM. Direct inhibition of T-cell responses by the Cryptococcus capsular polysaccharide glucuronoxylomannan. *PLoS Pathog.* 2006;2(11):e120.

145. Retini C, Vecchiarelli A, Monari C, Bistoni F, and Kozel TR. Encapsulation of Cryptococcus neoformans with glucuronoxylomannan inhibits the antigen-presenting capacity of monocytes. *Infect Immun.* 1998;66(2):664-9.

146. Mariano Andrade R, Monteiro Almeida G, Alexandre DosReis G, and Alves Melo Bento C. Glucuronoxylomannan of Cryptococcus neoformans exacerbates in vitro yeast cell growth by interleukin 10-dependent inhibition of CD4+ T lymphocyte responses. *Cellular Immunology.* 2003;222(2):116-25.

147. Muller U, Piehler D, Stenzel W, Kohler G, Frey O, Held J, Grahnert A, Richter T, Eschke M, Kamradt T, et al. Lack of IL-4 receptor expression on T helper cells reduces T helper 2 cell polyfunctionality and confers resistance in allergic bronchopulmonary mycosis. *Mucosal Immunol.* 2012.

148. Wiesner DL, and Boulware DR. *Cryptococcus*-Related Immune Reconstitution Inflammatory Syndrome(IRIS): Pathogenesis and Its Clinical Implications. *Current fungal infection reports.* 2011;5(4):252-61.

149. Kambugu A, Meya DB, Rhein J, O'Brien M, Janoff EN, Ronald AR, Kamya MR, Mayanja-Kizza H, Sande MA, Bohjanen PR, et al. Outcomes of cryptococcal meningitis in Uganda before and after the availability of highly active antiretroviral therapy. *Clin Infect Dis.* 2008;46(11):1694-701.

150. Christensen WB. Urea Decomposition as a Means of Differentiating Proteus and Paracolon Cultures from Each Other and from Salmonella and Shigella Types. *J Bacteriol.* 1946;52(4):461-6.

151. Klein KR, Hall L, Deml SM, Rysavy JM, Wohlfiel SL, and Wengenack NL. Identification of Cryptococcus gattii by use of L-canavanine glycine bromothymol blue medium and DNA sequencing. *J Clin Microbiol.* 2009;47(11):3669-72.

152. Liu D, Coloe S, Baird R, and Pederson J. Rapid mini-preparation of fungal DNA for PCR. *J Clin Microbiol.* 2000;38(1):471.

153. Thompson JD, Higgins DG, and Gibson TJ. CLUSTAL W: improving the sensitivity of progressive multiple sequence alignment through sequence weighting, position-specific gap penalties and weight matrix choice. *Nucleic Acids Res.* 1994;22(22):4673-80.

154. Swofford DL. PAUP4.0b10 Phylogenetic Analysis Using Parsimony (*and Other Methods). Version 4. *Sinauer Associates, Sunderland, Massachusetts.* 2003.

155. Lengeler KB, Cox GM, and Heitman J. Serotype AD strains of Cryptococcus neoformans are diploid or aneuploid and are heterozygous at the mating-type locus. *Infect Immun.* 2001;69(1):115-22.

156. Guilliams M, Ginhoux F, Jakubzick C, Naik SH, Onai N, Schraml BU, Segura E, Tussiwand R, and Yona S. Dendritic cells, monocytes and macrophages: a unified nomenclature based on ontogeny. *Nat Rev Immunol.* 2014;14(8):571-8.

157. Pulendran B, and Artis D. New paradigms in type 2 immunity. *Science.* 2012;337(6093):431-5.

158. Burton OT, and Zaccone P. The potential role of chitin in allergic reactions. *Trends Immunol.* 2007;28(10):419-22.

159. Bueter CL, Specht CA, and Levitz SM. Innate sensing of chitin and chitosan. *PLoS Pathog.* 2013;9(1):e1003080.

160. Rapaka RR, Ricks DM, Alcorn JF, Chen K, Khader SA, Zheng M, Plevy S, Bengten E, and Kolls JK. Conserved natural IgM antibodies mediate innate and adaptive immunity against the opportunistic fungus *Pneumocystis murina*. *J Exp Med.* 2010;207(13):2907-19.

161. Anthony RM, Rutitzky LI, Urban JF, Jr., Stadecker MJ, and Gause WC. Protective immune mechanisms in helminth infection. *Nat Rev Immunol.* 2007;7(12):975-87.

162. Lee CG, Da Silva CA, Lee JY, Hartl D, and Elias JA. Chitin regulation of immune responses: an old molecule with new roles. *Curr Opin Immunol.* 2008;20(6):684-9.

163. Gordon-Thomson C, Kumari A, Tomkins L, Holford P, Djordjevic JT, Wright LC, Sorrell TC, and Moore GP. Chitotriosidase and gene therapy for fungal infections. *Cell Mol Life Sci.* 2009;66(6):1116-25.

164. Boot RG, Renkema GH, Verhoek M, Strijland A, Bliek J, de Meulemeester TM, Mannens MM, and Aerts JM. The human chitotriosidase gene. Nature of inherited enzyme deficiency. *J Biol Chem.* 1998;273(40):25680-5.

165. Choi EH, Zimmerman PA, Foster CB, Zhu S, Kumaraswami V, Nutman TB, and Chanock SJ. Genetic polymorphisms in molecules of innate immunity and susceptibility to infection with *Wuchereria bancrofti* in South India. *Genes Immun.* 2001;2(5):248-53.

166. Levitz SM, Nong S, Mansour MK, Huang C, and Specht CA. Molecular characterization of a mannoprotein with homology to chitin deacetylases that

stimulates T cell responses to *Cryptococcus neoformans*. *Proc Natl Acad Sci U S A.* 2001;98(18):10422-7.

167. Baker LG, Specht CA, Donlin MJ, and Lodge JK. Chitosan, the deacetylated form of chitin, is necessary for cell wall integrity in *Cryptococcus neoformans*. *Eukaryot Cell.* 2007;6(5):855-67.

168. Gause WC, Wynn TA, and Allen JE. Type 2 immunity and wound healing: evolutionary refinement of adaptive immunity by helminths. *Nat Rev Immunol.* 2013;13(8):607-14.

169. Boyman O, Kovar M, Rubinstein MP, Surh CD, and Sprent J. Selective stimulation of T cell subsets with antibody-cytokine immune complexes. *Science.* 2006;311(5769):1924-7.

170. Webster KE, Walters S, Kohler RE, Mrkvan T, Boyman O, Surh CD, Grey ST, and Sprent J. In vivo expansion of T reg cells with IL-2-mAb complexes: induction of resistance to EAE and long-term acceptance of islet allografts without immunosuppression. *J Exp Med.* 2009;206(4):751-60.

171. Schulze B, Piehler D, Eschke M, von Buttlar H, Kohler G, Sparwasser T, and Alber G. CD4 FoxP3 regulatory T cells suppress fatal T helper 2 cell immunity during pulmonary fungal infection. *Eur J Immunol.* 2014.

172. McKenna HJ, Stocking KL, Miller RE, Brasel K, De Smedt T, Maraskovsky E, Maliszewski CR, Lynch DH, Smith J, Pulendran B, et al. Mice lacking flt3 ligand have deficient hematopoiesis affecting hematopoietic progenitor cells, dendritic cells, and natural killer cells. *Blood.* 2000;95(11):3489-97.

173. GeurtsvanKessel CH, and Lambrecht BN. Division of labor between dendritic cell subsets of the lung. *Mucosal Immunol.* 2008;1(6):442-50.

174. Clausen BE, Burkhardt C, Reith W, Renkawitz R, and Forster I. Conditional gene targeting in macrophages and granulocytes using LysMcre mice. *Transgenic Res.* 1999;8(4):265-77.

175. Plantinga M, Guilliams M, Vanheerswynghels M, Deswarte K, Branco-Madeira F, Toussaint W, Vanhoutte L, Neyt K, Killeen N, Malissen B, et al. Conventional and monocyte-derived CD11b(+) dendritic cells initiate and maintain T helper 2 cell-mediated immunity to house dust mite allergen. *Immunity.* 2013;38(2):322-35.

176. Schlitzer A, McGovern N, Teo P, Zelante T, Atarashi K, Low D, Ho AW, See P, Shin A, Wasan PS, et al. IRF4 transcription factor-dependent CD11b+ dendritic cells in human and mouse control mucosal IL-17 cytokine responses. *Immunity.* 2013;38(5):970-83.

177. Lenardon MD, Munro CA, and Gow NA. Chitin synthesis and fungal pathogenesis. *Curr Opin Microbiol.* 2010;13(4):416-23.

178. Banks IR, Specht CA, Donlin MJ, Gerik KJ, Levitz SM, and Lodge JK. A chitin synthase and its regulator protein are critical for chitosan production and growth of the fungal pathogen *Cryptococcus neoformans*. *Eukaryot Cell.* 2005;4(11):1902-12.

179. O'Meara TR, Holmer SM, Selvig K, Dietrich F, and Alspaugh JA. *Cryptococcus neoformans* Rim101 is associated with cell wall remodeling and evasion of the host immune responses. *MBio.* 2013;4(1).

180. O'Meara TR, Xu W, Selvig KM, O'Meara MJ, Mitchell AP, and Alspaugh JA. The *Cryptococcus neoformans* Rim101 transcription factor directly regulates genes required for adaptation to the host. *Mol Cell Biol.* 2014;34(4):673-84.

181. Boot RG, Blommaart EF, Swart E, Ghauharali-van der Vlugt K, Bijl N, Moe C, Place A, and Aerts JM. Identification of a novel acidic mammalian chitinase distinct from chitotriosidase. *J Biol Chem.* 2001;276(9):6770-8.

182. Liu T, Liu Z, Song C, Hu Y, Han Z, She J, Fan F, Wang J, Jin C, Chang J, et al. Chitin-induced dimerization activates a plant immune receptor. *Science.* 2012;336(6085):1160-4.

183. Da Silva CA, Chalouni C, Williams A, Hartl D, Lee CG, and Elias JA. Chitin is a size-dependent regulator of macrophage TNF and IL-10 production. *J Immunol.* 2009;182(6):3573-82.

184. Kogiso M, Nishiyama A, Shinohara T, Nakamura M, Mizoguchi E, Misawa Y, Guinet E, Nouri-Shirazi M, Dorey CK, Henriksen RA, et al. Chitin particles induce size-dependent but carbohydrate-independent innate eosinophilia. *J Leukoc Biol.* 2011;90(1):167-76.

185. Ito T, Wang YH, Duramad O, Hori T, Delespesse GJ, Watanabe N, Qin FX, Yao Z, Cao W, and Liu YJ. TSLP-activated dendritic cells induce an inflammatory T helper type 2 cell response through OX40 ligand. *J Exp Med.* 2005;202(9):1213-23.

186. Paul WE, and Zhu J. How are T(H)2-type immune responses initiated and amplified? *Nat Rev Immunol.* 2010;10(4):225-35.

187. Van Dyken SJ, Garcia D, Porter P, Huang X, Quinlan PJ, Blanc PD, Corry DB, and Locksley RM. Fungal chitin from asthma-associated home environments induces eosinophilic lung infiltration. *J Immunol.* 2011;187(5):2261-7.

188. Wagener J, Malireddi RK, Lenardon MD, Koberle M, Vautier S, MacCallum DM, Biedermann T, Schaller M, Netea MG, Kanneganti TD, et al. Fungal chitin

dampens inflammation through IL-10 induction mediated by NOD2 and TLR9 activation. *PLoS Pathog.* 2014;10(4):e1004050.

189. Halim TY, Steer CA, Matha L, Gold MJ, Martinez-Gonzalez I, McNagny KM, McKenzie AN, and Takei F. Group 2 innate lymphoid cells are critical for the initiation of adaptive T helper 2 cell-mediated allergic lung inflammation. *Immunity.* 2014;40(3):425-35.

190. Moon JJ, Chu HH, Hataye J, Pagan AJ, Pepper M, McLachlan JB, Zell T, and Jenkins MK. Tracking epitope-specific T cells. *Nat Protoc.* 2009;4(4):565-81.

191. Muller U, Piehler D, Stenzel W, Kohler G, Frey O, Held J, Grahnert A, Richter T, Eschke M, Kamradt T, et al. Lack of IL-4 receptor expression on T helper cells reduces T helper 2 cell polyfunctionality and confers resistance in allergic bronchopulmonary mycosis. *Mucosal Immunol.* 2012;5(3):299-310.

192. Spits H, Artis D, Colonna M, Diefenbach A, Di Santo JP, Eberl G, Koyasu S, Locksley RM, McKenzie AN, Mebius RE, et al. Innate lymphoid cells--a proposal for uniform nomenclature. *Nat Rev Immunol.* 2013;13(2):145-9.

193. Nussbaum JC, Van Dyken SJ, von Moltke J, Cheng LE, Mohapatra A, Molofsky AB, Thornton EE, Krummel MF, Chawla A, Liang HE, et al. Type 2 innate lymphoid cells control eosinophil homeostasis. *Nature.* 2013;502(7470):245-8.

194. Gao Y, Nish SA, Jiang R, Hou L, Licona-Limon P, Weinstein JS, Zhao H, and Medzhitov R. Control of T helper 2 responses by transcription factor IRF4-dependent dendritic cells. *Immunity.* 2013;39(4):722-32.

195. Williams JW, Tjota MY, Clay BS, Vander Lugt B, Bandukwala HS, Hrusch CL, Decker DC, Blaine KM, Fixsen BR, Singh H, et al. Transcription factor IRF4 drives dendritic cells to promote Th2 differentiation. *Nat Commun.* 2013;4(2990.

196. Persson EK, Uronen-Hansson H, Semmrich M, Rivollier A, Hagerbrand K, Marsal J, Gudjonsson S, Hakansson U, Reizis B, Kotarsky K, et al. IRF4 transcription-factor-dependent CD103(+)CD11b(+) dendritic cells drive mucosal T helper 17 cell differentiation. *Immunity.* 2013;38(5):958-69.

197. Sutherland TE, Maizels RM, and Allen JE. Chitinases and chitinase-like proteins: potential therapeutic targets for the treatment of T-helper type 2 allergies. *Clin Exp Allergy.* 2009;39(7):943-55.

198. Boot RG, Renkema GH, Strijland A, van Zonneveld AJ, and Aerts JM. Cloning of a cDNA encoding chitotriosidase, a human chitinase produced by macrophages. *J Biol Chem.* 1995;270(44):26252-6.

199. Malaguarnera L, Simpore J, Prodi DA, Angius A, Sassu A, Persico I, Barone R, and Musumeci S. A 24-bp duplication in exon 10 of human chitotriosidase gene from the sub-Saharan to the Mediterranean area: role of parasitic diseases and environmental conditions. *Genes Immun.* 2003;4(8):570-4.

200. Ustianowski AP, Sieu TP, and Day JN. *Penicillium marneffei* infection in HIV. *Curr Opin Infect Dis.* 2008;21(1):31-6.

201. Kenyon C, Bonorchis K, Corcoran C, Meintjes G, Locketz M, Lehloenya R, Vismer HF, Naicker P, Prozesky H, van Wyk M, et al. A dimorphic fungus causing disseminated infection in South Africa. *N Engl J Med.* 2013;369(15):1416-24.

202. Couppie P, Sobesky M, Aznar C, Bichat S, Clyti E, Bissuel F, El Guedj M, Alvarez F, Demar M, Louvel D, et al. Histoplasmosis and acquired immunodeficiency syndrome: a study of prognostic factors. *Clin Infect Dis.* 2004;38(1):134-8.

203. Lowe DM, Rangaka MX, Gordon F, James CD, and Miller RF. *Pneumocystis jirovecii* pneumonia in tropical and low and middle income countries: a systematic review and meta-regression. *PLoS One.* 2013;8(8):e69969.

204. Boulware DR, Meya DB, Muzoora C, Rolfes MA, Huppler Hullsiek K, Musubire A, Taseera K, Nabeta HW, Schutz C, Williams DA, et al. Timing of antiretroviral therapy after diagnosis of cryptococcal meningitis. *N Engl J Med.* 2014;370(26):2487-98.

205. Lee CG, Herzog EL, Ahangari F, Zhou Y, Gulati M, Lee CM, Peng X, Feghali-Bostwick C, Jimenez SA, Varga J, et al. Chitinase 1 is a biomarker for and therapeutic target in scleroderma-associated interstitial lung disease that augments TGF-beta1 signaling. *J Immunol.* 2012;189(5):2635-44.

206. Fitz LJ, DeClercq C, Brooks J, Kuang W, Bates B, Demers D, Winkler A, Nocka K, Jiao A, Greco RM, et al. Acidic mammalian chitinase is not a critical target for allergic airway disease. *Am J Respir Cell Mol Biol.* 2012;46(1):71-9.

207. Sabiiti W, May RC, and Pursall ER. Experimental models of cryptococcosis. *Int J Microbiol.* 2012;2012(626745.

208. Zhu Y, Rudensky AY, Corper AL, Teyton L, and Wilson IA. Crystal structure of MHC class II I-Ab in complex with a human CLIP peptide: prediction of an I-Ab peptide-binding motif. *J Mol Biol.* 2003;326(4):1157-74.

209. Moon JJ, Chu HH, Pepper M, McSorley SJ, Jameson SC, Kedl RM, and Jenkins MK. Naive CD4(+) T cell frequency varies for different epitopes and predicts repertoire diversity and response magnitude. *Immunity.* 2007;27(2):203-13.

210. Zhang J, Dong Z, Zhou R, Luo D, Wei H, and Tian Z. Isolation of lymphocytes and their innate immune characterizations from liver, intestine, lung and uterus. *Cell Mol Immunol.* 2005;2(4):271-80.

211. Shinya T, Osada T, Desaki Y, Hatamoto M, Yamanaka Y, Hirano H, Takai R, Che FS, Kaku H, and Shibuya N. Characterization of receptor proteins using affinity cross-linking with biotinylated ligands. *Plant & cell physiology.* 2010;51(2):262-70.

212. Monheit JE, Cowan DF, and Moore DG. Rapid detection of fungi in tissues using calcofluor white and fluorescence microscopy. *Arch Pathol Lab Med.* 1984;108(8):616-8.

213. Bicanic T, Meintjes G, Wood R, Hayes M, Rebe K, Bekker LG, and Harrison T. Fungal burden, early fungicidal activity, and outcome in cryptococcal meningitis in antiretroviral-naive or antiretroviral-experienced patients treated with amphotericin B or fluconazole. *Clin Infect Dis.* 2007;45(1):76-80.

214. French N, Gray K, Watera C, Nakiyingi J, Lugada E, Moore M, Lalloo D, Whitworth JA, and Gilks CF. Cryptococcal infection in a cohort of HIV-1-infected Ugandan adults. *AIDS.* 2002;16(7):1031-8.

215. Decken K, Kohler G, Palmer-Lehmann K, Wunderlin A, Mattner F, Magram J, Gately MK, and Alber G. Interleukin-12 is essential for a protective Th1 response in mice infected with Cryptococcus neoformans. *Infection and immunity.* 1998;66(10):4994-5000.

216. Wormley FL, Jr., Perfect JR, Steele C, and Cox GM. Protection against cryptococcosis by using a murine gamma interferon-producing Cryptococcus neoformans strain. *Infection and immunity.* 2007;75(3):1453-62.

217. Muller U, Stenzel W, Kohler G, Polte T, Blessing M, Mann A, Piehler D, Brombacher F, and Alber G. A gene-dosage effect for interleukin-4 receptor alpha-chain expression has an impact on Th2-mediated allergic inflammation during bronchopulmonary mycosis. *The Journal of infectious diseases.* 2008;198(11):1714-21.

218. Osterholzer JJ, Surana R, Milam JE, Montano GT, Chen GH, Sonstein J, Curtis JL, Huffnagle GB, Toews GB, and Olszewski MA. Cryptococcal urease promotes the accumulation of immature dendritic cells and a non-protective T2 immune response within the lung. *The American journal of pathology.* 2009;174(3):932-43.

219. Verbsky JW, and Chatila TA. Immune dysregulation, polyendocrinopathy, enteropathy, X-linked (IPEX) and IPEX-related disorders: an evolving web of heritable autoimmune diseases. *Current opinion in pediatrics.* 2013;25(6):708-14.

220. Rowe JH, Ertelt JM, and Way SS. Foxp3(+) regulatory T cells, immune stimulation and host defence against infection. *Immunology.* 2012;136(1):1-10.

221. Schulze B, Piehler D, Eschke M, von Buttlar H, Kohler G, Sparwasser T, and Alber G. CD4(+) FoxP3(+) regulatory T cells suppress fatal T helper 2 cell immunity during pulmonary fungal infection. *European journal of immunology.* 2014;44(12):3596-604.

222. Wiesner DL, Specht CA, Lee CK, Smith KD, Mukaremera L, Lee ST, Lee CG, Elias JA, Nielsen JN, Boulware DR, et al. Chitin recognition via chitotriosidase promotes pathologic type-2 helper T cell responses to cryptococcal infection. *PLoS pathogens.* 2015;11(3):e1004701.

223. Sakaguchi S, Wing K, Onishi Y, Prieto-Martin P, and Yamaguchi T. Regulatory T cells: how do they suppress immune responses? *International immunology.* 2009;21(10):1105-11.

224. Burzyn D, Benoist C, and Mathis D. Regulatory T cells in nonlymphoid tissues. *Nature immunology.* 2013;14(10):1007-13.

225. Campbell DJ, and Koch MA. Phenotypical and functional specialization of FOXP3+ regulatory T cells. *Nature reviews Immunology.* 2011;11(2):119-30.

226. Chaudhry A, Rudra D, Treuting P, Samstein RM, Liang Y, Kas A, and Rudensky AY. CD4+ regulatory T cells control TH17 responses in a Stat3-dependent manner. *Science.* 2009;326(5955):986-91.

227. Koch MA, Tucker-Heard G, Perdue NR, Killebrew JR, Urdahl KB, and Campbell DJ. The transcription factor T-bet controls regulatory T cell homeostasis and function during type 1 inflammation. *Nature immunology.* 2009;10(6):595-602.

228. Zheng Y, Chaudhry A, Kas A, deRoos P, Kim JM, Chu TT, Corcoran L, Treuting P, Klein U, and Rudensky AY. Regulatory T-cell suppressor program co-opts transcription factor IRF4 to control T(H)2 responses. *Nature.* 2009;458(7236):351-6.

229. Moran AE, Holzapfel KL, Xing Y, Cunningham NR, Maltzman JS, Punt J, and Hogquist KA. T cell receptor signal strength in Treg and iNKT cell development demonstrated by a novel fluorescent reporter mouse. *The Journal of experimental medicine.* 2011;208(6):1279-89.

230. Li X, and Zheng Y. Regulatory T cell identity: formation and maintenance. *Trends in immunology.* 2015;36(6):344-53.

231. Cretney E, Kallies A, and Nutt SL. Differentiation and function of Foxp3(+) effector regulatory T cells. *Trends in immunology.* 2013;34(2):74-80.

232. Vasanthakumar A, Moro K, Xin A, Liao Y, Gloury R, Kawamoto S, Fagarasan S, Mielke LA, Afshar-Sterle S, Masters SL, et al. The transcriptional regulators IRF4, BATF and IL-33 orchestrate development and maintenance of adipose tissue-resident regulatory T cells. *Nature immunology.* 2015;16(3):276-85.

233. Josefowicz SZ, Niec RE, Kim HY, Treuting P, Chinen T, Zheng Y, Umetsu DT, and Rudensky AY. Extrathymically generated regulatory T cells control mucosal TH2 inflammation. *Nature.* 2012;482(7385):395-9.

234. Cretney E, Xin A, Shi W, Minnich M, Masson F, Miasari M, Belz GT, Smyth GK, Busslinger M, Nutt SL, et al. The transcription factors Blimp-1 and IRF4 jointly control the differentiation and function of effector regulatory T cells. *Nature immunology.* 2011;12(4):304-11.

235. Ahyi AN, Chang HC, Dent AL, Nutt SL, and Kaplan MH. IFN regulatory factor 4 regulates the expression of a subset of Th2 cytokines. *Journal of immunology.* 2009;183(3):1598-606.

236. Kwon H, Thierry-Mieg D, Thierry-Mieg J, Kim HP, Oh J, Tunyaplin C, Carotta S, Donovan CE, Goldman ML, Tailor P, et al. Analysis of interleukin-21-induced Prdm1 gene regulation reveals functional cooperation of STAT3 and IRF4 transcription factors. *Immunity.* 2009;31(6):941-52.

237. Sallusto F, Lanzavecchia A, and Mackay CR. Chemokines and chemokine receptors in T-cell priming and Th1/Th2-mediated responses. *Immunology today.* 1998;19(12):568-74.

238. Dorr P, Westby M, Dobbs S, Griffin P, Irvine B, Macartney M, Mori J, Rickett G, Smith-Burchnell C, Napier C, et al. Maraviroc (UK-427,857), a potent, orally bioavailable, and selective small-molecule inhibitor of chemokine receptor CCR5 with broad-spectrum anti-human immunodeficiency virus type 1 activity. *Antimicrobial agents and chemotherapy.* 2005;49(11):4721-32.

239. Kroetz DN, and Deepe GS, Jr. CCR5 dictates the equilibrium of proinflammatory IL-17+ and regulatory Foxp3+ T cells in fungal infection. *Journal of immunology.* 2010;184(9):5224-31.

240. McKinley L, Logar AJ, McAllister F, Zheng M, Steele C, and Kolls JK. Regulatory T cells dampen pulmonary inflammation and lung injury in an animal model of pneumocystis pneumonia. *Journal of immunology.* 2006;177(9):6215-26.

241. Netea MG, Sutmuller R, Hermann C, Van der Graaf CA, Van der Meer JW, van Krieken JH, Hartung T, Adema G, and Kullberg BJ. Toll-like receptor 2 suppresses immunity against Candida albicans through induction of IL-10 and regulatory T cells. *Journal of immunology.* 2004;172(6):3712-8.

242. Pandiyan P, Conti HR, Zheng L, Peterson AC, Mathern DR, Hernandez-Santos N, Edgerton M, Gaffen SL, and Lenardo MJ. CD4(+)CD25(+)Foxp3(+) regulatory T cells promote Th17 cells in vitro and enhance host resistance in mouse Candida albicans Th17 cell infection model. *Immunity.* 2011;34(3):422-34.

243. Man K, Miasari M, Shi W, Xin A, Henstridge DC, Preston S, Pellegrini M, Belz GT, Smyth GK, Febbraio MA, et al. The transcription factor IRF4 is essential for TCR affinity-mediated metabolic programming and clonal expansion of T cells. *Nature immunology.* 2013;14(11):1155-65.

244. Levine AG, Arvey A, Jin W, and Rudensky AY. Continuous requirement for the TCR in regulatory T cell function. *Nature immunology.* 2014;15(11):1070-8.

245. Moreira AP, Cavassani KA, Massafera Tristao FS, Campanelli AP, Martinez R, Rossi MA, and Silva JS. CCR5-dependent regulatory T cell migration mediates fungal survival and severe immunosuppression. *Journal of immunology.* 2008;180(5):3049-56.

246. Chang CC, Omarjee S, Lim A, Spelman T, Gosnell BI, Carr WH, Elliott JH, Moosa MY, Ndung'u T, French MA, et al. Chemokine levels and chemokine receptor expression in the blood and the cerebrospinal fluid of HIV-infected patients with cryptococcal meningitis and cryptococcosis-associated immune reconstitution inflammatory syndrome. *The Journal of infectious diseases.* 2013;208(10):1604-12.

247. Grivel JC, and Margolis LB. CCR5- and CXCR4-tropic HIV-1 are equally cytopathic for their T-cell targets in human lymphoid tissue. *Nature medicine.* 1999;5(3):344-6.

248. Scarlatti G, Tresoldi E, Bjorndal A, Fredriksson R, Colognesi C, Deng HK, Malnati MS, Plebani A, Siccardi AG, Littman DR, et al. In vivo evolution of HIV-1 co-receptor usage and sensitivity to chemokine-mediated suppression. *Nature medicine.* 1997;3(11):1259-65.

249. Pozo-Balado MM, Martinez-Bonet M, Rosado I, Ruiz-Mateos E, Mendez-Lagares G, Rodriguez-Mendez MM, Vidal F, Munoz-Fernandez MA, Pacheco YM, and Leal M. Maraviroc reduces the regulatory T-cell frequency in antiretroviral-naive HIV-infected subjects. *The Journal of infectious diseases.* 2014;210(6):890-8.

250. Anderson KG, Mayer-Barber K, Sung H, Beura L, James BR, Taylor JJ, Qunaj L, Griffith TS, Vezys V, Barber DL, et al. Intravascular staining for discrimination of vascular and tissue leukocytes. *Nature protocols.* 2014;9(1):209-22.

251. Kolaczkowska E, and Kubes P. Neutrophil recruitment and function in health and inflammation. *Nature reviews Immunology.* 2013;13(3):159-75.

252. Takatsu K, and Nakajima H. IL-5 and eosinophilia. *Current opinion in immunology.* 2008;20(3):288-94.

253. Acharya KR, and Ackerman SJ. Eosinophil granule proteins: form and function. *The Journal of biological chemistry.* 2014;289(25):17406-15.

254. Dombrowicz D, and Capron M. Eosinophils, allergy and parasites. *Current opinion in immunology.* 2001;13(6):716-20.

255. Brinkmann V, Reichard U, Goosmann C, Fauler B, Uhlemann Y, Weiss DS, Weinrauch Y, and Zychlinsky A. Neutrophil extracellular traps kill bacteria. *Science.* 2004;303(5663):1532-5.

256. Nathan C. Neutrophils and immunity: challenges and opportunities. *Nature reviews Immunology.* 2006;6(3):173-82.

257. Eyerich S, Eyerich K, Cavani A, and Schmidt-Weber C. IL-17 and IL-22: siblings, not twins. *Trends in immunology.* 2010;31(9):354-61.

258. Zheng Y, Danilenko DM, Valdez P, Kasman I, Eastham-Anderson J, Wu J, and Ouyang W. Interleukin-22, a T(H)17 cytokine, mediates IL-23-induced dermal inflammation and acanthosis. *Nature.* 2007;445(7128):648-51.

259. Shibata K, Yamada H, Hara H, Kishihara K, and Yoshikai Y. Resident Vdelta1+ gammadelta T cells control early infiltration of neutrophils after Escherichia coli infection via IL-17 production. *Journal of immunology.* 2007;178(7):4466-72.

260. Mircescu MM, Lipuma L, van Rooijen N, Pamer EG, and Hohl TM. Essential role for neutrophils but not alveolar macrophages at early time points following Aspergillus fumigatus infection. *The Journal of infectious diseases.* 2009;200(4):647-56.

261. Schaffner A, Davis CE, Schaffner T, Markert M, Douglas H, and Braude AI. In vitro susceptibility of fungi to killing by neutrophil granulocytes discriminates between primary pathogenicity and opportunism. *The Journal of clinical investigation.* 1986;78(2):511-24.

262. Feldmesser M, Casadevall A, Kress Y, Spira G, and Orlofsky A. Eosinophil-Cryptococcus neoformans interactions in vivo and in vitro. *Infection and immunity.* 1997;65(5):1899-907.

263. Fleury-Feith J, Van Nhieu JT, Picard C, Escudier E, and Bernaudin JF. Bronchoalveolar lavage eosinophilia associated with Pneumocystis carinii pneumonitis in AIDS patients. Comparative study with non-AIDS patients. *Chest.* 1989;95(6):1198-201.

264. Lilly LM, Scopel M, Nelson MP, Burg AR, Dunaway CW, and Steele C. Eosinophil deficiency compromises lung defense against Aspergillus fumigatus. *Infection and immunity.* 2014;82(3):1315-25.

265. Galioto AM, Hess JA, Nolan TJ, Schad GA, Lee JJ, and Abraham D. Role of eosinophils and neutrophils in innate and adaptive protective immunity to larval strongyloides stercoralis in mice. *Infection and immunity.* 2006;74(10):5730-8.

266. Fei M, Bhatia S, Oriss TB, Yarlagadda M, Khare A, Akira S, Saijo S, Iwakura Y, Fallert Junecko BA, Reinhart TA, et al. TNF-alpha from inflammatory dendritic cells (DCs) regulates lung IL-17A/IL-5 levels and neutrophilia versus eosinophilia during persistent fungal infection. *Proceedings of the National Academy of Sciences of the United States of America.* 2011;108(13):5360-5.

267. Borregaard N. Neutrophils, from marrow to microbes. *Immunity.* 2010;33(5):657-70.

268. Voehringer D, van Rooijen N, and Locksley RM. Eosinophils develop in distinct stages and are recruited to peripheral sites by alternatively activated macrophages. *Journal of leukocyte biology.* 2007;81(6):1434-44.

269. Nakagawa M, Terashima T, D'Yachkova Y, Bondy GP, Hogg JC, and van Eeden SF. Glucocorticoid-induced granulocytosis: contribution of marrow release and demargination of intravascular granulocytes. *Circulation.* 1998;98(21):2307-13.

270. Mukae H, Zamfir D, English D, Hogg JC, and van Eeden SF. Polymorphonuclear leukocytes released from the bone marrow by granulocyte colony-stimulating factor: intravascular behavior. *The hematology journal : the official journal of the European Haematology Association / EHA.* 2000;1(3):159-71.

271. Manz MG, and Boettcher S. Emergency granulopoiesis. *Nature reviews Immunology.* 2014;14(5):302-14.

272. Zhang M, Angata T, Cho JY, Miller M, Broide DH, and Varki A. Defining the in vivo function of Siglec-F, a CD33-related Siglec expressed on mouse eosinophils. *Blood.* 2007;109(10):4280-7.

273. Pope SM, Zimmermann N, Stringer KF, Karow ML, and Rothenberg ME. The eotaxin chemokines and CCR3 are fundamental regulators of allergen-induced pulmonary eosinophilia. *Journal of immunology.* 2005;175(8):5341-50.

274. Fleming TJ, Fleming ML, and Malek TR. Selective expression of Ly-6G on myeloid lineage cells in mouse bone marrow. RB6-8C5 mAb to granulocyte-differentiation antigen (Gr-1) detects members of the Ly-6 family. *Journal of immunology.* 1993;151(5):2399-408.

275. Karsunky H, Merad M, Cozzio A, Weissman IL, and Manz MG. Flt3 ligand regulates dendritic cell development from Flt3+ lymphoid and myeloid-committed progenitors to Flt3+ dendritic cells in vivo. *The Journal of experimental medicine.* 2003;198(2):305-13.

276. Lira SA. A passport into the lymph node. *Nature immunology.* 2005;6(9):866-8.

277. Martinez-Moczygemba M, and Huston DP. Biology of common beta receptor-signaling cytokines: IL-3, IL-5, and GM-CSF. *The Journal of allergy and clinical immunology.* 2003;112(4):653-65; quiz 66.

278. Bel EH, Wenzel SE, Thompson PJ, Prazma CM, Keene ON, Yancey SW, Ortega HG, Pavord ID, and Investigators S. Oral glucocorticoid-sparing effect of mepolizumab in eosinophilic asthma. *The New England journal of medicine.* 2014;371(13):1189-97.

279. Ortega HG, Liu MC, Pavord ID, Brusselle GG, FitzGerald JM, Chetta A, Humbert M, Katz LE, Keene ON, Yancey SW, et al. Mepolizumab treatment in patients with severe eosinophilic asthma. *The New England journal of medicine.* 2014;371(13):1198-207.

280. Zia-Amirhosseini P, Minthorn E, Benincosa LJ, Hart TK, Hottenstein CS, Tobia LA, and Davis CB. Pharmacokinetics and pharmacodynamics of SB-240563, a humanized monoclonal antibody directed to human interleukin-5, in monkeys. *The Journal of pharmacology and experimental therapeutics.* 1999;291(3):1060-7.

281. Wynn TA. Type 2 cytokines: mechanisms and therapeutic strategies. *Nature reviews Immunology.* 2015;15(5):271-82.

282. Zhu J, Yamane H, and Paul WE. Differentiation of effector CD4 T cell populations (*). *Annual review of immunology.* 2010;28(445-89.

283. Hamada H, Garcia-Hernandez Mde L, Reome JB, Misra SK, Strutt TM, McKinstry KK, Cooper AM, Swain SL, and Dutton RW. Tc17, a unique subset of CD8 T cells that can protect against lethal influenza challenge. *Journal of immunology.* 2009;182(6):3469-81.

284. Sonnenberg GF, and Artis D. Innate lymphoid cells in the initiation, regulation and resolution of inflammation. *Nature medicine.* 2015;21(7):698-708.

285. Gladiator A, Wangler N, Trautwein-Weidner K, and LeibundGut-Landmann S. Cutting edge: IL-17-secreting innate lymphoid cells are essential for host defense against fungal infection. *Journal of immunology.* 2013;190(2):521-5.

286. Sonnenberg GF, Monticelli LA, Alenghat T, Fung TC, Hutnick NA, Kunisawa J, Shibata N, Grunberg S, Sinha R, Zahm AM, et al. Innate lymphoid cells promote

anatomical containment of lymphoid-resident commensal bacteria. *Science.* 2012;336(6086):1321-5.

287. Brestoff JR, Kim BS, Saenz SA, Stine RR, Monticelli LA, Sonnenberg GF, Thome JJ, Farber DL, Lutfy K, Seale P, et al. Group 2 innate lymphoid cells promote beiging of white adipose tissue and limit obesity. *Nature.* 2015;519(7542):242-6.

288. Yu Y, Wang C, Clare S, Wang J, Lee SC, Brandt C, Burke S, Lu L, He D, Jenkins NA, et al. The transcription factor Bcl11b is specifically expressed in group 2 innate lymphoid cells and is essential for their development. *The Journal of experimental medicine.* 2015;212(6):865-74.

289. Yoshida T, Ikuta K, Sugaya H, Maki K, Takagi M, Kanazawa H, Sunaga S, Kinashi T, Yoshimura K, Miyazaki J, et al. Defective B-1 cell development and impaired immunity against Angiostrongylus cantonensis in IL-5R alpha-deficient mice. *Immunity.* 1996;4(5):483-94.

290. Macdowell AL, and Peters SP. Neutrophils in asthma. *Current allergy and asthma reports.* 2007;7(6):464-8.

291. Puel A, Cypowyj S, Bustamante J, Wright JF, Liu L, Lim HK, Migaud M, Israel L, Chrabieh M, Audry M, et al. Chronic mucocutaneous candidiasis in humans with inborn errors of interleukin-17 immunity. *Science.* 2011;332(6025):65-8.

292. Zelante T, De Luca A, Bonifazi P, Montagnoli C, Bozza S, Moretti S, Belladonna ML, Vacca C, Conte C, Mosci P, et al. IL-23 and the Th17 pathway promote inflammation and impair antifungal immune resistance. *European journal of immunology.* 2007;37(10):2695-706.

293. Hancock RE, Nijnik A, and Philpott DJ. Modulating immunity as a therapy for bacterial infections. *Nature reviews Microbiology.* 2012;10(4):243-54.

294. Fisher MC, Henk DA, Briggs CJ, Brownstein JS, Madoff LC, McCraw SL, and Gurr SJ. Emerging fungal threats to animal, plant and ecosystem health. *Nature.* 2012;484(7393):186-94.

295. Bowman SM, and Free SJ. The structure and synthesis of the fungal cell wall. *BioEssays : news and reviews in molecular, cellular and developmental biology.* 2006;28(8):799-808.

296. Newman MA, Sundelin T, Nielsen JT, and Erbs G. MAMP (microbe-associated molecular pattern) triggered immunity in plants. *Frontiers in plant science.* 2013;4(139.

297. Nurnberger T, Brunner F, Kemmerling B, and Piater L. Innate immunity in plants and animals: striking similarities and obvious differences. *Immunological reviews.* 2004;198(249-66.

298. Kaku H, Nishizawa Y, Ishii-Minami N, Akimoto-Tomiyama C, Dohmae N, Takio K, Minami E, and Shibuya N. Plant cells recognize chitin fragments for defense signaling through a plasma membrane receptor. *Proc Natl Acad Sci U S A.* 2006;103(29):11086-91.

299. Petutschnig EK, Jones AM, Serazetdinova L, Lipka U, and Lipka V. The lysin motif receptor-like kinase (LysM-RLK) CERK1 is a major chitin-binding protein in Arabidopsis thaliana and subject to chitin-induced phosphorylation. *J Biol Chem.* 2010;285(37):28902-11.

300. Buist G, Steen A, Kok J, and Kuipers OP. LysM, a widely distributed protein motif for binding to (peptido)glycans. *Mol Microbiol.* 2008;68(4):838-47.

301. Foo SY, and Phipps S. Regulation of inducible BALT formation and contribution to immunity and pathology. *Mucosal immunology.* 2010;3(6):537-44.

302. Richmond I, Pritchard GE, Ashcroft T, Avery A, Corris PA, and Walters EH. Bronchus associated lymphoid tissue (BALT) in human lung: its distribution in smokers and non-smokers. *Thorax.* 1993;48(11):1130-4.

303. Suda T, Chida K, Hayakawa H, Imokawa S, Iwata M, Nakamura H, and Sato A. Development of bronchus-associated lymphoid tissue in chronic hypersensitivity pneumonitis. *Chest.* 1999;115(2):357-63.

304. Halle S, Dujardin HC, Bakocevic N, Fleige H, Danzer H, Willenzon S, Suezer Y, Hammerling G, Garbi N, Sutter G, et al. Induced bronchus-associated lymphoid tissue serves as a general priming site for T cells and is maintained by dendritic cells. *The Journal of experimental medicine.* 2009;206(12):2593-601.

305. Moyron-Quiroz JE, Rangel-Moreno J, Kusser K, Hartson L, Sprague F, Goodrich S, Woodland DL, Lund FE, and Randall TD. Role of inducible bronchus associated lymphoid tissue (iBALT) in respiratory immunity. *Nature medicine.* 2004;10(9):927-34.

306. Rubtsov YP, Rasmussen JP, Chi EY, Fontenot J, Castelli L, Ye X, Treuting P, Siewe L, Roers A, Henderson WR, Jr., et al. Regulatory T cell-derived interleukin-10 limits inflammation at environmental interfaces. *Immunity.* 2008;28(4):546-58.

307. Taga K, and Tosato G. IL-10 inhibits human T cell proliferation and IL-2 production. *Journal of immunology.* 1992;148(4):1143-8.

308. Chaudhry A, Samstein RM, Treuting P, Liang Y, Pils MC, Heinrich JM, Jack RS, Wunderlich FT, Bruning JC, Muller W, et al. Interleukin-10 signaling in regulatory T cells is required for suppression of Th17 cell-mediated inflammation. *Immunity.* 2011;34(4):566-78.

309. O'Garra A, Vieira PL, Vieira P, and Goldfeld AE. IL-10-producing and naturally occurring CD4+ Tregs: limiting collateral damage. *The Journal of clinical investigation.* 2004;114(10):1372-8.

310. Sitrin J, Ring A, Garcia KC, Benoist C, and Mathis D. Regulatory T cells control NK cells in an insulitic lesion by depriving them of IL-2. *The Journal of experimental medicine.* 2013;210(6):1153-65.

311. Leon B, Bradley JE, Lund FE, Randall TD, and Ballesteros-Tato A. FoxP3+ regulatory T cells promote influenza-specific Tfh responses by controlling IL-2 availability. *Nature communications.* 2014;5(3495.

APPENDIX I

Cryptococcus

Tami McDonald, Darin L. Wiesner, and Kirsten Nielsen

Previously published in *Current Biology*. 2012 Jul 24;22(14):R554-5.

What is *Cryptococcus*?

Cryptococcus is a yeast that is surrounded by a thick coating of polysaccharides, called a capsule. For this reason *Cryptococcus* is often referred to as "the sugar yeast".

A sugar yeast?! Sounds great for making beer, bread and wine!

No, that's not *Cryptococcus*. "Yeast" is a catch-all term for any single-celled fungus, so many unrelated fungi can be called yeasts. The common kitchen yeast exploited by humankind for millennia to ferment the sugars in food into alcohol and CO_2 is actually *Saccharomyces cerevisiae*, an ascomycete. The *Cryptococcus* species were initially misclassified as *Saccharomyces* when two scientists independently discovered the fungus at the end of the 19th century. Sanfelice, a Sardinian, serendipitously isolated yeasts from aging peach juice. Yet his discovery was not the early precursor to the Bellini cocktail, because the German scientist Busse simultaneously isolated the encapsulated yeast from a patient presenting with an unknown mycosis. *Cryptococcus* is actually a basidiomycete yeast, more closely related to the mushrooms on your pizza than the yeast used to leaven the crust or to ferment the beer you drink with it. The early work by Busse suggesting that *Cryptococcus* could be a novel fungal pathogen were confirmed by subsequent animal pathogenesis experiments proving Koch's postulates that set the foundation for a century of productive research.

Thick hair, tanned flesh, buxom body, and a robust libido… a 21st century popular icon?

The above description is surprisingly not referring to the latest reality TV star. These traits in fact represent known virulence factors of *Cryptococcus*, such as: polysaccharide capsule, melanin, cell enlargement, and sexual reproduction. The thick sugary polysaccharide capsule allows the yeast to evade the host immune response by resisting

cellular uptake and subsequent degradation by phagocytes. Polysaccharide that has dissociated from the cell also inhibits T cell and cytokine responses, and this curious property has prompted investigation into using purified *Cryptococcus* capsule as a potential therapy for some forms of autoimmunity. Embedded in the cell wall directly below the sugar coat resides a pigment, melanin, that is capable of scavenging oxygen radicals deployed by host cells, thereby preventing oxidative damage and promoting survival inside phagocytes. The pigment can also bind to conventional fungicides and reduce drug efficacy. When the yeast is growing in the environment, melanin confers a fitness advantage by permitting the fungus to grow at wide temperature ranges, survive in high concentrations of toxic metals, and resist ionizing radiation. *Cryptococcus* also forms gigantic cells dubbed "titan cells" that are too large for phagocytes to engulf, are able to protect normal cryptococcal cells from the host immune response, and play a key role in establishment of disease. Finally, one of the sexes (the α mating type) is more prevalent in both the environment and the clinic. The α cells are bisexual – not only do they undergo heterosexual mating with the opposite mating type, but they are also homosexual, able to propagate by same-sex mating. These traits collectively distinguish *Cryptococcus* from other human pathogens.

Can *Cryptococcus* make you sick?

Yes and no. *Cryptococcus* is found in the environment, in and on things we are exposed to often. Been to a city park? You've probably been exposed to *Cryptococcus*. *Cryptococcus* can live in pigeon droppings, in soil, on trees, and in other environmental reservoirs not yet fully defined. Normally, your immune system fights the cryptococcal infection and you may never know you have been exposed. But… Cryptococcosis is recognized as an emerging infectious disease. *Cryptococcus gattii* is capable of infecting and causing disease in otherwise healthy individuals. More than 200 people have acquired *C. gattii* infections in the North American Pacific Northwest in an outbreak that is spreading south down the Pacific coast. In addition, *Cryptococcus neoformans* significantly burdens immunocompromised populations - mainly solid organs transplant

patients and persons living with HIV/AIDS. More than 1 million new cases of *C. neoformans* are reported annually in persons infected with HIV, and even with the availability of anti-retroviral and anti-fungal therapies, the rate of survival is less than 40%. Cryptococcal meningitis has surpassed tuberculosis as the most lethal opportunistic infection of AIDS patients in Africa. Roughly half the people that survive this meningitis are often confronted with additional complications during immune recovery. Patients can experience a clinical relapse of aseptic meningitis and non-central nervous system inflammation that can result in death. By and large, the general public need not fear infection, but cryptococcosis remains an important public health concern in specific regions of the world.

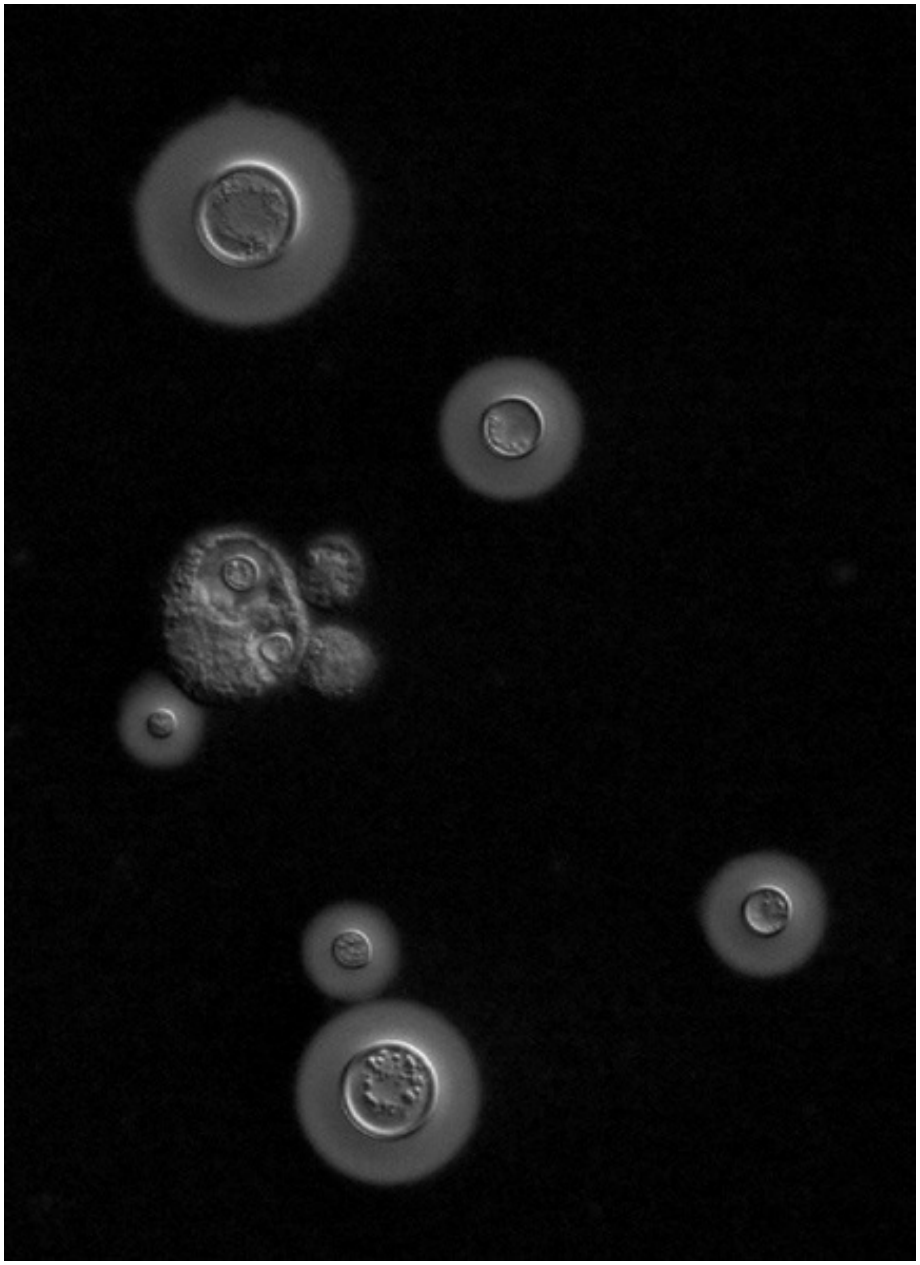

Figure 1. Micrograph of *Cryptococcus* cells stained with india ink. The polysaccharide capsule is visible as a zone of clearing around the cell body. Two normal sized cryptococcal cells have been phagocytosed by host cells. In contrast, the titan cells are too large to be phagocytosed.